Coupling between transfer RNA maturation and ribosomal RNA processing in Bacillus subtilis

Aude Trinquier

Université de Paris

Ecole doctorale Bio SPC – ED562

CNRS UMR8261 « Expression Génétique Microbienne »

Equipe Ciarán Condon – RNA Maturation and Degradation

Coupling between transfer RNA maturation and ribosomal RNA processing in *Bacillus subtilis*

Par Aude Trinquier

Thèse de doctorat de Microbiologie

Dirigée par Ciarán Condon
Et Frédérique Braun

Présentée et soutenue publiquement le 25 novembre 2019

Devant un jury composé de :

Président de jury :	Olivier Dussurget, Professeur, Institut Pasteur / Université de Paris
Rapporteurs :	Pascale Romby, Professeur, CNRS / Université de Strasbourg
	Jue D. Wang, Professeur, University of Wisconsin – Madison
Examinateur :	Isabelle Iost, Chercheur, INSERM / Université de Bordeaux
Directeur de thèse :	Ciarán Condon, Directeur de recherche, CNRS
Co-directeur de thèse :	Frédérique Braun, Maître de conférences, Université de Paris

Title: Coupling between transfer RNA maturation and ribosomal RNA processing in *B. subtilis.*

Abstract:

Cellular protein synthesis both requires functional ribosomes and mature transfer RNAs (tRNAs) as adapter molecules. The ribosomes are large essential ribonucleoprotein complexes whose biogenesis accounts for most of cellular transcription and consumes a major portion of the cell's energy. Ribosome biogenesis is therefore tightly adjusted to the cellular needs and actively surveilled to rapidly degrade defective particles that could interfere with translation. Interestingly, tRNAs and ribosomal RNAs (rRNAs) are both transcribed from longer primary transcripts and universally require processing to become functional for translation. In this thesis, I have characterized a coupling mechanism between tRNA processing and ribosome biogenesis in the Gram-positive model organism *Bacillus subtilis.* Accumulation of immature tRNAs during tRNA maturase depletion, specifically abolishes 16S rRNA 3' processing by the endonuclease YqfG/YbeY, the last step in small ribosomal subunit formation. We showed that this maturation deficiency resulted from a late small subunit (30S) assembly defect coinciding with changes in expression of several key 30S assembly cofactors, mediated by both transcriptional and post-transcriptional effects. Interestingly, our results indicate that accumulation of immature tRNAs is sensed by the stringent factor RelA and triggers (p)ppGpp production. We showed that (p)ppGpp synthesis and the accompanying decrease in GTP levels inhibits 16S rRNA 3' processing, most likely by affecting GTPases involved in ribosome assembly. The inhibition of 16S rRNA 3' processing is thought to further lead to degradation of partially assembled particles by RNase R. Thus, we propose a model where RelA senses temporary slow-downs in tRNA maturation and this leads to an appropriate readjustment of ribosome biogenesis. This coupling mechanism would maintain the physiological balance between tRNAs and rRNAs, the two major components of the translation machinery.

Keywords: tRNA maturation, rRNA maturation, ribosome biogenesis, (p)ppGpp, stringent response.

Titre : Couplage entre maturation des ARN de transfert et maturation de l'ARN ribosomique chez *B. subtilis*

Résumé :

La synthèse des protéines cellulaires requiert à la fois des ribosomes fonctionnels et des ARN de transfert (ARNt) matures comme molécules adaptatrices. Les ribosomes sont de larges complexes ribonucléoprotéiques dont la biogenèse représente la plupart de la transcription cellulaire et consomme une majeure partie de l'énergie de la cellule. Par conséquent, la biogenèse des ribosomes fait l'objet d'une régulation importante afin d'ajuster le nombre de ribosomes aux besoins de la cellule et de dégrader efficacement les particules défectueuses qui pourraient interférer avec la traduction. Les ARNs ribosomiques (ARNr) et les ARNt sont tous deux transcrits sous formes de précurseurs et sont universellement maturés pour devenir fonctionnels pour la traduction. Ce travail de thèse a permis de mettre en évidence un couplage entre la maturation des ARNt et la biogenèse des ribosomes chez la bactérie modèle à Gram positif *Bacillus subtilis.* Ainsi, l'accumulation d'ARNt immatures lors d'une déplétion en enzymes de maturation, abolit spécifiquement la maturation en 3' de l'ARNr 16S par l'endoribonucléase YqfG/YbeY, dernière étape dans la formation de la petite sous-unité ribosomique (30S). Nous avons mis en évidence que ce défaut de maturation résultait d'un défaut d'assemblage tardif du 30S coïncidant avec des changements d'expression de plusieurs facteurs d'assemblage du ribosome. Nous avons montré que cette modulation d'expression provenait d'effets transcriptionel et post-transcriptionel. De façon inédite, nos résultats indiquent que l'accumulation d'ARNt immatures est perçue par RelA (le facteur de la réponse stringente), déclenchant la production de (p)ppGpp. Nous avons observé que cette synthèse de (p)ppGpp et la baisse concomitante des niveaux de GTP cellulaire, inhibe la maturation de l'ARNr 16S en 3', probablement *via* un blocage des GTPases impliquées dans l'assemblage des ribosomes. L'inhibition de la maturation de l'ARNr 16S côté 3' est supposée conduire, par la suite, à une dégradation des particules partiellement assemblées par la RNase R. Ainsi, nos résultats supportent un modèle où RelA jouerait un rôle central ; en percevant une déficience de maturation des ARNt et en ajustant, en conséquence, la biogenèse des ribosomes *via* la production de (p)ppGpp. Ce mécanisme de couplage permettrait de maintenir un équilibre fonctionnel entre ARNt et ARNr, les deux composants majeurs de la machinerie de traduction.

Mots clefs : maturation des ARNt, maturation des ARNr, biogenèse des ribosomes, (p)ppGpp, réponse stringente.

Acknowledgments

Je tiens avant tout à remercier Frédérique et Ciarán pour m'avoir accueilli au sein du laboratoire lors de mon stage de M2 et pour avoir ensuite co-encadré cette thèse. Merci pour votre patience, votre disponibilité et votre soutien tout au long de ces années, j'ai énormément appris au laboratoire. Je vous suis également particulièrement reconnaissante de m'avoir permis de présenter mon travail de thèse à de nombreuses reprises dans des congrès en France et aux Etats-Unis. Ciarán, merci pour toutes les discussions scientifiques, les corrections de fautes d'anglais et pour n'avoir pas désespéré que je te tutoie avant la fin de ma thèse ! Frédérique, merci pour ta pédagogie et tes conseils. J'espère qu'un jour nos hologrammes pourront partager un trajet en capsule volante pour aller assister à un concert à la Philharmonie ; les discussions du « monde de Fred » vont me manquer ;) .

I would like to sincerely thank Pascale Romby and Jade Wang for accepting the extra load of work to review this thesis. A special thanks to Jade for giving me ppGpp^0 strains and advice during my PhD studies and for welcoming me to her lab next year. I also want to acknowledge Isabelle Iost and Olivier Dussurget for accepting with enthusiasm to be part of my thesis committee as examiner and president, respectively.

Je remercie aussi Lionel Bénard et Dominique Fourmy pour leurs conseils bienveillants pendant le comité de suivi de thèse.

Je remercie bien évidemment tous les membres de l'équipe RNA MAD pour m'avoir permis de travailler dans la bonne humeur (et avec des goûters réguliers ^^) : Sylvain, Anastasia, Gergana et Magali ; Kathrin pour sa gentillesse et pour toutes les discussions street art, voyage et (bien sur !) nourriture ; Olivier qui a vérifié (plusieurs fois par jour !) que j'étais bien en train d'écrire cette thèse ; Delphine qui est arrivée juste à temps pour égayer l'écriture de cette thèse (et faire le SAV sur Word). Pour finir, un énorme merci à Laëtitia pour m'avoir formé à de nombreuses manips et pour avoir été une super voisine de paillasse (tu vas me manquer !).

Je remercie également l'ensemble de l'UMR8261 « Expression Génétique Microbienne » pour l'entraide et la convivialité au sein de l'unité. Merci à Farès, Thomas et Grégory avec qui j'ai partagé les déboires des gradients de sucrose avec le (Bad) FRAC. Je remercie aussi Saravuth pour sa gentillesse et Anaïs pour ses conseils avisés d'ex-doctorante. Je tiens aussi à remercier les autres doctorants de l'institut pour leurs conseils et leur soutien, notamment Assia, Hilal, Maxence, Allegra, Nathalie, Héloïse et Sébastien (merci pour les déjeuners au jardin du Luxembourg, les papotages et les Haribo !).

I also want to thank Stuart MacNeill, Eammon Riley, Javier Lopez-Garrido and Kit Pogliano for teaching me so many things during my undergraduate internships in St Andrews and San Diego.

Merci à Julia, Aline et Laëtitia pour les sorties, les verres et les potins qui ont agréablement ponctué le magistère et cette thèse. Merci à Emma pour les papotages autour d'un thé à chaque fois qu'on a réussi à se trouver au même endroit au même moment ^^.

Je remercie tout particulièrement ma famille : mes parents et Jade pour m'avoir supporté (dans tous les sens du terme) tout au long de ces (nombreuses) années scolaires, mes grands-parents pour les bons petits plats de mon enfance (je sais d'où viens ma gourmandise !), mon oncle pour les vacances à la mer.

Et enfin, Franck, merci pour ton soutien indéfectible. On peut dire que tu as enchainé deux thèses haut la main ! À nos projets futurs. Je t'aime.

Table of contents

Figure index

Abbreviations

(p)ppGpp	Guanosine tetraphosphate and guanosine pentaphosphate
AaRS	Aminoacyl-tRNA synthetase
bp	Base pair
Cryo-EM	Cryo-electron microscopy
CTD	Carboxy-terminal domain
HD	Hydrolysis domain (for (p)ppGpp)
IC	Initiation Complex
iNTP	Initiator nucleotide
kb	kilobases
min	minute
mRNA	Messenger RNA
nt	Nucleotide
NTD	N-terminal domain
ORF	Open reading frame
pre-	Precursor
PROP	Protein-only RNase P
qMS	Quantitative Mass Spectrometry
RA-GTPase	Ribosome Assembly GTPase
RBS	Ribosome Binding Site
RHX	Arginine hydroxamate
RNase	Ribonuclease
rRNA	Ribosomal RNA
RSH	RelA/SpoT homolog
SAH	Small Alarmone Hydrolase
SAS	Small Alarmone Synthetase
SD	Shine Dalgarno
sRNA	Small RNA

SYNTH	Synthetase domain (for (p)ppGpp)
TLC	Thin layer chromatography
tRF	tRNA-derived fragments (or tRNA-derived small RNA)
tRNA	Transfer RNA
TSS	Transcription start site
WT	Wild type

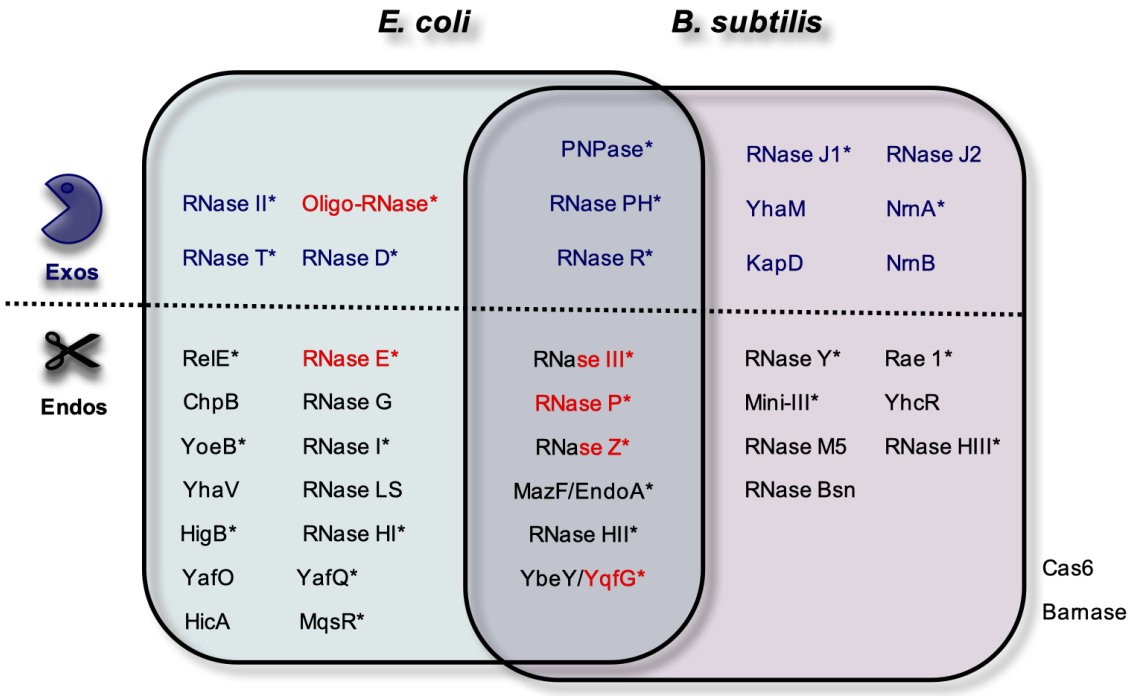

Figure 1: Venn diagram of ribonucleases identified in bacteria

Exoribonucleases (Exos) are above the horizontal dividing line, in blue type and represented by a "Pacman" symbol. Endoribonucleases (Endos) are below the dividing line, in black type and represented by a scissors symbol. Enzymes unique to *E. coli* are on the left side of the Venn diagram (light blue box), those unique to *B. subtilis* are on the right part of the diagram (purple box) and those in common are in the overlapping grey section. Essential enzymes are in red type. Shared enzymes essential to *B. subtilis*, but not *E. coli* are in black type on the *E. coli* side, and in red type on the *B. subtilis* side. Only two bacterial enzymes have so far been identified that are not present in either *E. coli* or *B. subtilis*, Barnase, found in some Gram-positive species, and Cas6, part of the CRISPR defense mechanism. Asterisks indicate enzymes for which a structure has been obtained.

Figure adapted from (Condon, 2009).

Introduction

I. RNA maturation and degradation in bacteria

Bacteria need to modulate their gene expression to adapt rapidly to ever changing environmental conditions. Post-transcriptional regulation allows modulation of gene expression in a timely manner by altering mRNA stability and/or translation. Ribonucleases (RNases), enzymes that break phosphodiester bonds in the RNA chain, are key players in these processes. RNases are divided into two main classes: exoribonucleases, which attack RNA from either its 5' or 3' end and endoribonucleases, which cleave the RNA internally. Exoribonucleases can be either processive, remaining attached to the same RNA molecule for many rounds of catalysis, or distributive, releasing the substrate with each nucleotide (nt) removed. Most RNases are hydrolytic, consuming a molecule of water upon the breaking of each phosphodiester bond, but some are phosphorolytic, using inorganic phosphate instead.

Historically, bacterial RNA maturation and decay pathways were studied in *Escherichia coli*. However, we now know that *Bacillus subtilis* and *E. coli* only share one quarter of the 40 ribonucleases identified in these two organisms so far (Figure 1), implying that strategies employed for RNA maturation and decay in those two bacteria can differ greatly.

1. Messenger RNA processing and decay

Modulation of mRNA stability is fundamentally important to control gene expression at the post-transcriptional level, both in *E. coli* and *B. subtilis* (Belasco, 2010). Upon changes in the environment, mRNA instability permits the rapid remodeling of the transcriptome and ensures the recycling of the cell's ribonucleotide pool. In *E. coli,* the median mRNA half-life is around 3 minutes in optimal growth conditions (Esquerré et al., 2014). Indeed, mRNA stabilities vary from a few seconds to around one hour, but mRNAs half-lives are generally significantly shorter than the cell's doubling time. On the contrary, rRNAs and tRNAs are designated as "stable RNAs" since – once processed to their mature form – they remain

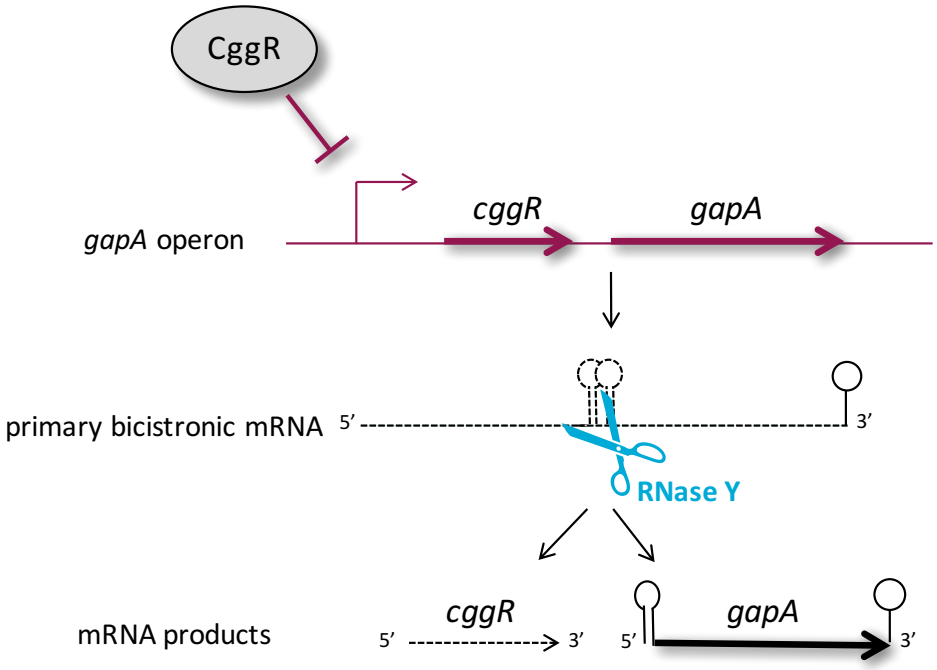

Figure 2: Differential expression of the bicistronic *cggR-gapA* transcript by RNase Y- mediated processing

The transcriptional regulator CggR and the glycolytic enzyme GapA are transcribed in a bicistronic operon in *B. subtilis*. Even though the genes are co-transcribed, the proteins are needed in different amounts to fulfill their cellular functions. One mechanism to achieve the different protein levels is the processing of the primary mRNA by an endoribonucleolytic cleavage. RNase Y cleaves upstream of *gapA* (between two stem-loop structures indicated as lollipops), producing two transcripts with different stabilities. While the *cggR* mRNA is very unstable, the *gapA* transcript is stabilized due to the presence of a stem-loop at the 5' end.

Figure adapted from (Lehnik-Habrink et al., 2012).

intact and functional for several generations. Moreover, modulation of mRNA stability allows, for example, the production of different stoichiometric amounts of different products from the same operon (DeLoughery et al., 2018). An example is the regulation of the bicistronic *cggR-gapA* operon in *B. subtilis* that encodes CggR, a transcriptional repressor specific for its own operon and a glycolytic enzyme GapA (Commichau et al., 2009). An RNase Y mediated processing event occurs between the two ORFs (open reading frames), in the middle of two stem-loop structures, producing two transcripts with different stabilities: the *cggR* transcript is very unstable whereas the *gapA* mRNA is stabilized by its 5' end stem-loop structure (Figure 2). This event leads to a differential expression of the two genes that fit the cellular needs, with an abundant production of the glycolytic enzyme and a lower level of the CggR repressor (Lehnik-Habrink et al., 2012). Processing/maturation and decay/degradation events thus permit the modulation of RNA half-lives by increasing or decreasing their stabilities, respectively (Arraiano et al., 2010).

a. Role of RNase E in mRNA decay

E. coli contains several endoribonucleases and 3'-5' exoribonucleases but so far lacks an identified 5'-3' exonuclease capable of degrading RNA from the 5' terminus. Moreover, the presence of a stem-loop structure at the 3' end corresponding to the Rho-independent transcription terminator, impedes degradation by 3'-5' exoribonucleases. Consequently, mRNA decay is generally initiated by endoribonucleolytic cleavage at one or more internal sites, in most cases by RNase E (Carpousis et al., 2009). This low-specificity endoribonuclease cleaves RNA in single-stranded AU-rich regions, typically with a key U-residue located two nts downstream of cleavage site (Chao et al., 2017). RNase E has two modes of action: the so-called 5' end dependent and direct entry pathways (Figure 3) (Mackie, 2013). In the first pathway, internal cleavage by RNase E is triggered by a prior event at the 5' end: the conversion of the 5'-terminal triphosphate to a monophosphate. This process is functionally similar to the decapping of eukaryotic mRNAs. Although this reaction can be performed by the RNA pyrophosphohydrolase RppH that preferentially acts on single-stranded 5' termini (Celesnik et al., 2007; Deana et al., 2008), recent evidence suggests that RppH prefers to act on a di-phosphorylated RNA intermediate generated by an enzyme that has yet to be identified (Luciano et al., 2018). The 5' monophosphate is bound by a specific

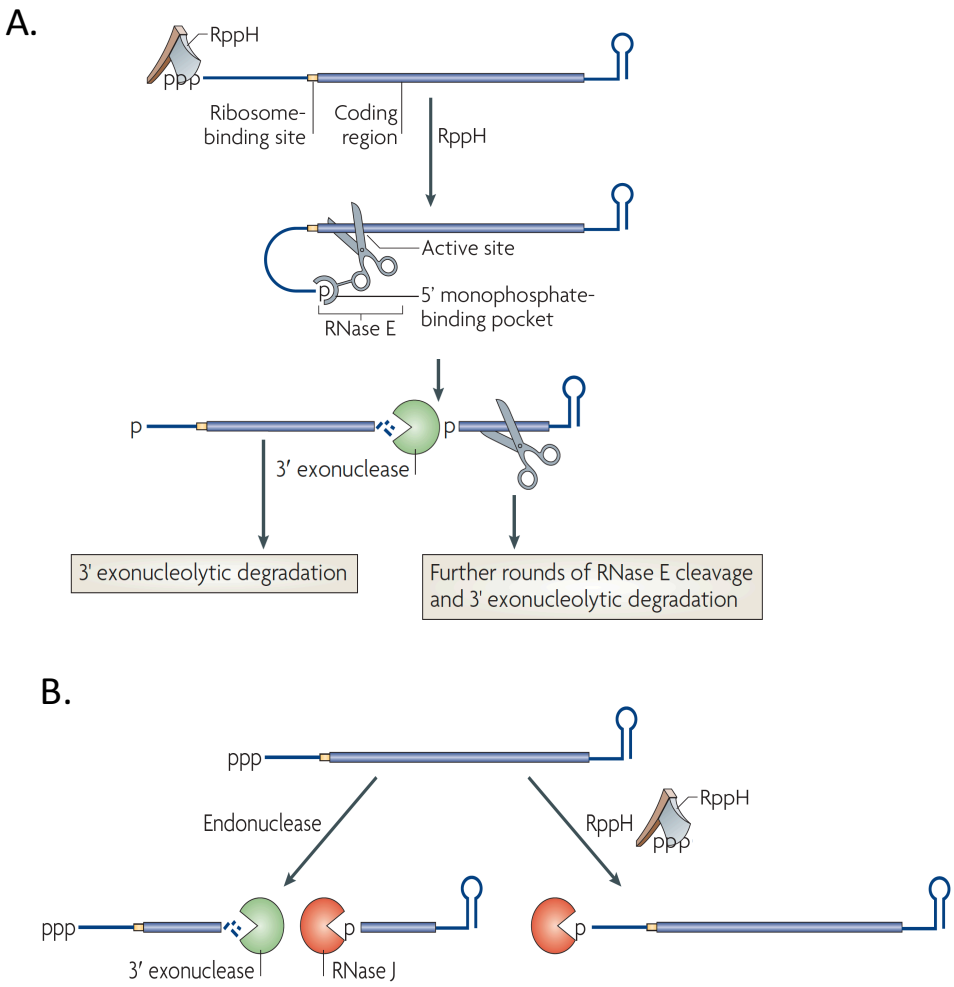

Figure 3: Messenger RNA degradation pathways in bacteria

A) mRNA decay in bacteria (such as *E. coli*) that contain the endoribonuclease RNase E or a homolog. Pyrophosphate removal by RppH generates a 5'-terminal monophosphate that binds to a discrete pocket on the surface of RNase E, facilitating mRNA cleavage at a downstream location. RNase E cleavage of primary transcripts can also occur by an alternative, 5' end-independent mechanism that does not require prior pyrophosphate removal. Serial internal cleavages by RNase E generate RNA fragments which lack protective structures at the 3' end. As a result, these degradation intermediates are susceptible to attack by the 3'-5' exoribonucleases.

B) 5' end dependent mRNA decay in bacteria that contain the 5'-3' exoribonuclease RNase J (such as *B. subtilis*). Internal cleavage by an endonuclease, such as RNase Y, generates a monophosphorylated intermediate that is susceptible to 5'-3' digestion by RNase J, whose exoribonucleolytic activity is impeded by a 5' triphosphate. Alternatively, 5'-3' exoribonucleolytic digestion by RNase J can be triggered by pyrophosphate removal from primary transcripts by RppH.

Figure adapted from (Belasco, 2010).

binding pocket in RNase E that stimulates its activity many fold (Callaghan et al., 2005; Koslover et al., 2008; Mackie, 1998). A recent report suggests that RNase E searches for cleavage sites by scanning linearly from the 5' mono-phosphorylated end and that its ability to cut is impeded by obstacles found along the way (Richards and Belasco, 2019). In the direct entry pathway, RNase E bypasses the 5' end sensing mechanism to cleave RNAs internally (Braun, 1998). Endoribonucleolytic mRNA cleavage by RNase E generates 5' mRNA fragments that are further degraded by 3'-5' exoribonucleases as they lack a protective 3' stem-loop, while 3' mRNA fragments undergo additional cycles of RNase E cleavage followed by exonucleolytic digestion (Figure 3). Four 3'-5' exoribonucleases are implicated in mRNA decay in *E. coli*: polynucleotide phosphorylase (PNPase), RNase II, RNase R and oligoribonuclease (Deutscher, 2006). Interestingly, RNase E has a C-terminal domain that permits both association with the inner membrane and interactions with other proteins, such as the RNA helicase RhlB, the glycolytic enzyme enolase and PNPase forming a complex known as the "degradosome" (Carpousis, 2007; Strahl et al., 2015). *E. coli* also possesses a non-essential paralog of the catalytic domain of RNase E, known as RNase G. RNase G has a similar cleavage specificity as RNase E, both having a marked preference for 5' mono-phosphorylated RNAs and for cleavage within AU-rich single stranded regions (Jiang and Belasco, 2004). RNase G overexpression was found to make viable a *rne* deletion strain, indicating that RNase G can achieve the essential action(s) of RNase E, even though the functions of those two RNases only partially overlap (Lee et al., 2002).

b. Another paradigm for mRNA decay: RNases J and Y in *B. subtilis*

Interestingly, many Gram-positive species do not possess RNase E or G homologs (Figure 4) (Condon and Putzer, 2002; Laalami and Putzer, 2011). Furthermore, several early experiments suggested that *B. subtilis,* the best studied of the Gram-positive bacteria might possess 5'-3' exoribonuclease activity: for example, a ribosome stalled on a transcript in *B. subtilis* can protect the entire downstream RNA segment (but not the upstream part) from degradation (Agaisse and Lereclus, 1996; Daou-Chabo et al., 2009; Hue and Bechhofer, 1991). It was discovered that, almost invariably, bacteria lacking RNase E instead contain the 5'-3' exoribonuclease RNase J and/or the endoribonuclease RNase Y (two enzymes absent from *E. coli*) (Figure 1). In *B. subtilis,* RNase J and RNase Y play important roles in mRNA

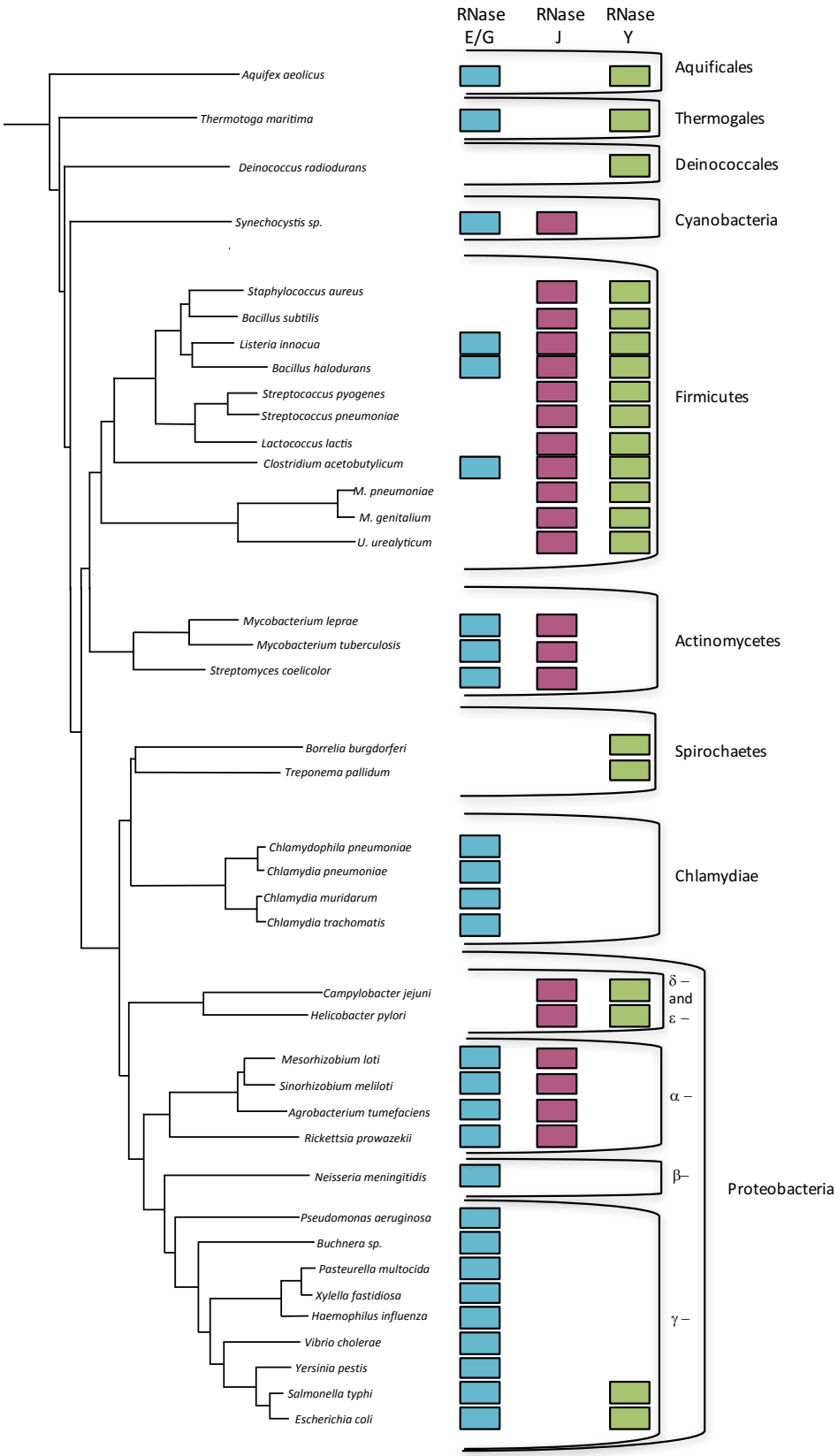

Figure 4: Simplified phylogeny of RNases in bacteria

Occurrence of RNases E/G (blue), J (purple) and Y(green) in different bacterial species.

Figure adapted from (Condon and Putzer, 2002; Condon et al., 2018)

turnover and although deletion of the gene encoding RNase J or RNase Y is viable, cells are quite sick and deletion of both is lethal (Durand et al., 2012a; Figaro et al., 2013). RNase J preferentially degrades RNA substrates with a mono-phosphorylated 5' end (Mathy et al., 2007; Shahbabian et al., 2009), generated either by a prior RNase Y endonucleolytic cleavage event or by the RNA pyrophosphohydrolase RppH (Figure 3) (Richards et al., 2011). *B. subtilis* contains two RNase J paralogues: RNase J1, which is primarily responsible for cell's 5'-3' exoribonucleolytic activity and RNase J2, whose main role appears to be the stabilization of RNase J1 by forming a complex with it (Linder et al., 2014). RNase J1 is responsible for both the degradation of multiple mRNAs and for 16S rRNA 5' maturation (Mathy et al., 2007). Like RNase E, *B. subtilis* RNase Y has a notable preference for cleavage in A/U rich regions and is membrane-associated (Lehnik-Habrink et al., 2011). Analysis of RNase Y cleavage sites in the transcriptome of *S. aureus* revealed a higher frequency of cleavage after guanosines (Khemici et al., 2015). RNase Y has also been suggested to be a scaffold for a degradosome-like network of transient interactions involving PNPase, the RNA helicase CshA and glycolytic enzymes (Lehnik-Habrink et al., 2011). Thus, despite a total lack of homology between the two enzymes, RNase Y is now accepted as the functional analog of RNase E in *B. subtilis.* Recently, RNase Y was shown to interact with a number of other proteins, including YmcA, YaaT and YlbF, forming the so-called Y-complex that has been recently suggested to be specifically involved in RNase Y processing of operon mRNA, leading to differential transcript stability and abundance (DeLoughery et al., 2018).

In contrast to *E. coli, B. subtilis* is able to degrade the two fragments resulting from RNase Y cleavage in both directions *via* its 5'-3' and 3'-5' exoribonucleolytic activities (Figure 3) (Belasco, 2010; Lehnik-Habrink et al., 2012). Therefore, the stability of the fragments resulting from endonucleolytic cleavage depends strongly on the structure of their 5' and 3' extremities: upstream fragments devoid of 3' protective stem-loop structures can be further degraded by 3'-5' exoribonucleases: PNPase, RNase PH, YhaM and RNase R (Deikus et al., 2004; Oussenko et al., 2005; Shahbabian et al., 2009). PNPase is a phosphorolytic enzyme and is considered as the main 3'-5' exoribonuclease involved in *B. subtilis* mRNA decay. Knowledge about the function of the other 3'-5' exoribonucleases in mRNA degradation remains limited, although a recent paper showed that YhaM shortens many transcripts by 2-3 nts in *S. pyogenes* (Lécrivain et al., 2018).

c. Role of RNA polyadenylation in bacteria

The post-transcriptional addition of poly(A) tails to the 3’ end of RNA occurs in all the three kingdoms of life, affecting the functionality and stability of these transcripts in different ways (Dreyfus and Régnier, 2002). In eukaryotes, poly(A) tail synthesis occurs in the nucleus coupled to cleavage of the pre-mRNA and transcription termination. This long poly(A) tail is then important for nuclear export, translation and stability of the mRNA (Proudfoot et al., 2002). Poly(A) tails in eukaryotes acts as a stabilizing element; poly(A) shortening initiates decay of cytoplasmic mRNAs as deadenylated mRNAs are decapped and then degraded by 5’-3’ exoribonucleases (such as XRN1 in yeast). In prokaryotes, the addition of poly(A) tails rather destabilizes RNAs and was shown to play a role in mRNA turnover and stable RNA quality control (see section on Transfer RNA maturation and turnover) (for review see (Hajnsdorf and Kaberdin, 2018; Mohanty and Kushner, 2011)). In *E. coli,* polyadenylation is mainly performed by PAP I (poly(A) polymerase I) encoded by the *pcnB* gene and PNPase that besides its 3’-5’ exoribonucleolytic activity can also function as a polymerase (Cao and Sarkar, 1992; Mohanty and Kushner, 2000). Poly(A) tails favor the decay of structured RNAs because they provide an entry for PNPase to degrade mRNAs ending with stable stem-loop structures that cannot be attacked in the absence of a single stranded stretch at the 3’ end (Blum et al., 1999). *B. subtilis* is devoid of identifiable PAP I homolog and thus PNPase is probably in charge of polyadenylation events. However, other enzymes may exist with PAP activity as a PNPase mutant still possesses poly(A) tails (Campos-Guillen et al., 2005). Note that, in eukaryotes, short poly(A) tails can also serve as degradation signals in nuclear RNA quality control pathways mediated by a complex known as TRAMP, mirroring the role of short poly(A) tails in bacteria (LaCava et al., 2005).

2. Stable RNA maturation and turnover

a. Transfer RNA maturation and turnover

Transfer RNA (tRNA) molecules are essential players in protein biosynthesis, functioning as adapter molecules to couple the presence of specific codons in mRNA to the incorporation of corresponding amino acids into polypeptides. The canonical tRNA is 76 nts in length ending with an NCCA sequence at the 3’ end, where N is the discriminator

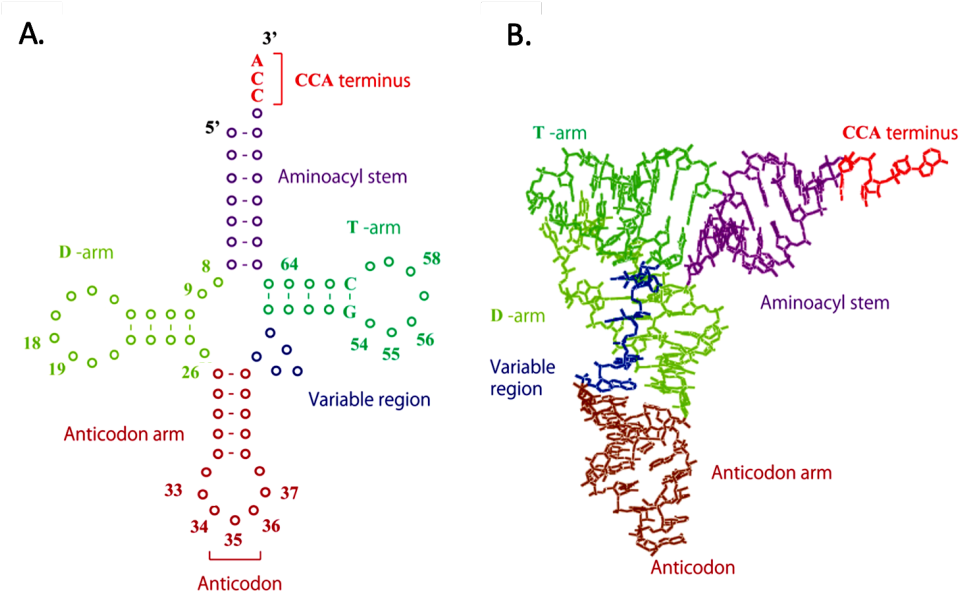

Figure 5: Transfer RNA (tRNA) secondary and tertiary structures

A) Representation of a classic tRNA secondary cloverleaf structure where domains are named and nucleotides are numbered according to conventional rules (Sprinzl et al., 1998). The variable region differs in size, ranging from 3 to more than 20 nucleotides (with additional nucleotides being referred to as 47:a, 47:b, etc).

B) Representation of L-shaped tRNA tertiary structure. The tRNA D- and T-arms interact by tertiary base pairs to form the L-shaped tRNA structure.

Figure adapted from (Hori, 2014)

nucleotide, recognized by many aminoacyl-tRNA synthetases (AaRS) for tRNA charging with their cognate amino acids (Giege et al., 1998). Transfer RNAs have a cloverleaf secondary structure with (from 5' to 3'): the acceptor stem, the D-arm (containing dihydrouridine), the anticodon arm that includes the anticodon loop, the T-arm (containing pseudouridine) and the unpaired NCCA 3' terminal sequence (Figure 5). Interactions between the D- and T-arms primarily, confer tRNAs with their characteristic L-shaped tertiary structure. Commonly, tRNAs are synthesized as precursor molecules that have to be processed on both ends to become functional for translation. *B. subtilis* encodes 86 tRNA genes organized in 21 transcription units (Hartmann et al., 2009). Indeed, tRNA genes can be found in many different contexts: as single transcription units, co-transcribed with other tRNAs (in tRNA gene clusters comprising up to 21 tRNA genes) or co-transcribed within rRNA operons. Transfer RNAs are also extensively post-transcriptionally modified: dedicated enzymes chemically modify tRNAs at specific positions with methylation and pseudouridylation, for example (Grosjean, 2013). Once fully mature, tRNA molecules are covalently linked to their cognate amino acid at their 3' extremity by AaRSs (Delarue, 1995).

i. Transfer RNA 5' end maturation by RNase P

All bacterial tRNAs are synthesized as precursor molecules with 5' and 3' extensions and the maturation of the 5' terminus of a pre-tRNA relies solely on the endonucleolytic activity of the ubiquitous and essential ribonuclease P (RNase P) (Willkomm and Hartmann, 2007). RNase P can be found as a ribozyme-powered ribonucleoprotein or as a protein-only form (PRORP) (Gobert et al., 2010; Gutmann et al., 2012). While RNA-based RNase P enzymes are found in all the three domains of life, protein-only forms (PRORPs) were originally only thought to exist in eukaryotes (Klemm et al., 2016). However, a bacterial protein only form, unrelated to eukaryotic PRORPs, was recently identified in *Aquifex aeolicus* and related species (Nickel et al., 2017). RNase P enzymes are found in nearly all species with the exception of the obligate symbiont *Nanoarchaeum equitans* that does not encode pre-tRNAs with 5' extensions and thus, can afford to lack an RNase P (Randau et al., 2008). The RNA-based form of RNase P might be a remnant of an ancient RNA-based RNA world (Evans et al., 2006).

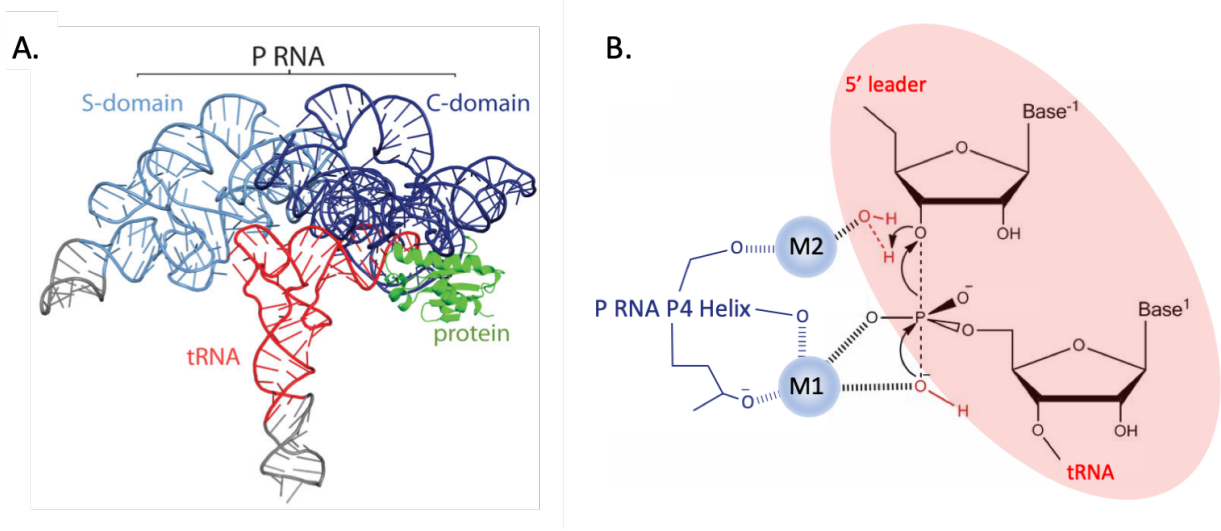

Figure 6: Structure and catalytic mechanism of bacterial RNase P.

A) Crystal structure of the bacterial RNase P holoenzyme (from *Thermotoga maritima*) in complex with tRNA. RNase P is composed of a large RNA subunit (in blue) and a small protein component (in green), in complex with $tRNA^{Phe}$ (in red). The RNA component serves as the primary biocatalyst in the reaction and contains two domains, termed the catalytic (C, dark blue) and specificity (S, light blue) domains. The RNase P protein binds the 5' leader region of the pre-tRNA substrate and assists in product release. Transfer RNA makes multiple interactions with the P RNA. Regions in grey denote additional RNA nucleotides required for crystallization.

B) Proposed mechanism of cleavage catalyzed by RNA-based RNase P. M1 and M2 represents the two bound metals required for the cleavage reaction. The P4 helix of the RNase P RNA (which is a component of the C-domain) is represented in dark blue. The pre-tRNA nucleotides are highlighted in light red, cleavage occurs between the 5'-leader and the mature tRNA sequence and results from the hydrolysis of a specific phosphodiester bond. Atoms involved in the hydrolysis reaction are represented in red.

Figure adapted from (Howard et al., 2012; Reiter et al., 2010).

The canonical bacterial RNase P is a ribozyme composed of two subunits that are both essential: a small basic protein (13kDa) encoded by the *rnpA* gene and a long catalytic RNA (350-400 nts) encoded by *rnpB* (Figure 6). The RNA subunit alone can cleave pre-tRNAs *in vitro,* showing that the main substrate-binding domain and active site are located in the RNA moiety (Guerrier-Takada et al., 1983). However, the two genes are essential. The protein subunit is indeed required as a cofactor for *in vivo* activity: RnpA enhances the affinity for pre-tRNA and metal ions (Klemm et al., 2016). Bacterial components of RNase P are functionally interchangeable: the RNA and protein subunits from one species can complement subunits from other species with variable reactivity (Gößringer and Hartmann, 2007; Wegscheid et al., 2006). Moreover, PRORP from the plant *Arabidopsis thaliana* can restore the viability of a *E. coli* strain depleted for RNase P, indicating that PROP maintains all the essential biological functions of the RNA-based RNase P (Weber et al., 2014).

RNase P recognizes pre-tRNA tertiary structure, interacting with the T-arm and acceptor stem of the precursor molecule (Figure 5 and Figure 6) (McClain et al., 1987; Reiter et al., 2010). The RnpA protein binds to a universally conserved structural module in *rnpB,* and interacts with the leader of pre-tRNA, but not with mature tRNA. The RNA moiety catalyzes a simple enzymatic reaction: the hydrolysis of a specific phosphodiester bond in pre-tRNAs to release the 5' precursor sequence and thereby generate tRNAs with a mature 5'-phosphate end (Figure 6). Catalysis by RNase P is dependent on divalent metal ions, notably Mg^{2+} and Mn^{2+}. Besides pre-tRNAs, the *B. subtilis* RNase P holoenzyme was shown to cleave and stabilize the adenine riboswitch upstream of the *pbuE* gene (encoding an adenine efflux pump) *in vivo*, probably by recognition of secondary structures (Seif and Altman, 2008). Interestingly, *B. subtilis* P RNA maturation is suggested to be at least partially autocatalytic (Loria and Pan, 2000). RNase P has been additionally implicated in the processing of the pre-transfer-messenger RNA (pre-tmRNA) both in *E. coli* and in *B. subtilis* (Gilet et al., 2015; Komine et al., 1994). *E. coli* RNase P is also known to process other non-tRNA substrates, in particular a few mRNA substrates (see (Klemm et al., 2016) for review) and the pre-4.5S RNA, belonging to the signal recognition particle ribonucleoprotein complex (Peck-Millert and Altman, 1991).

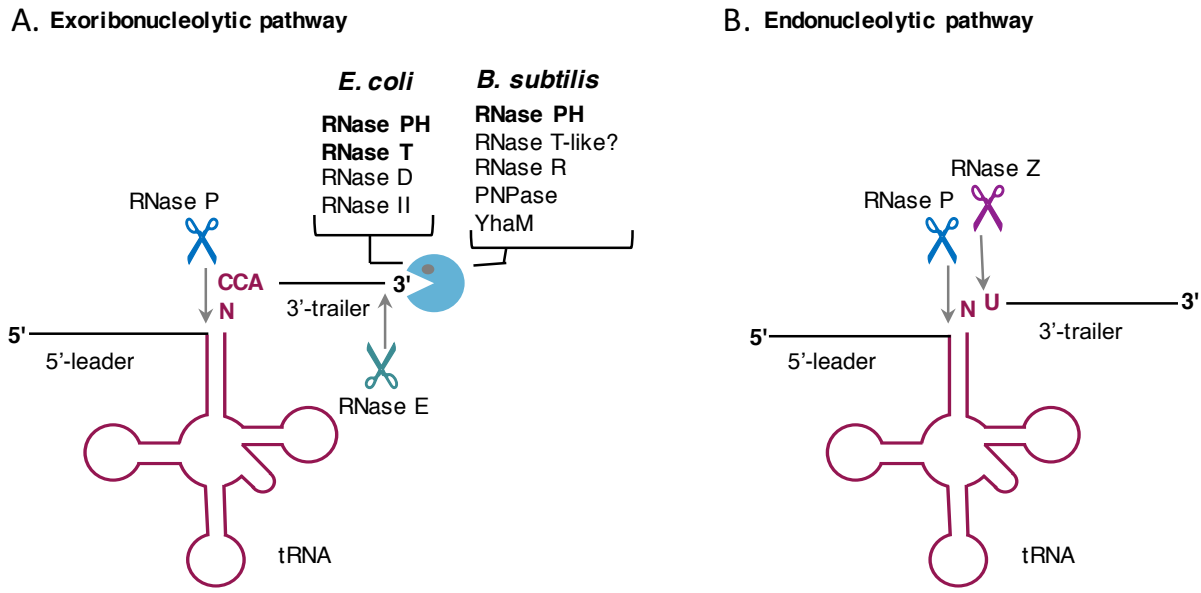

Figure 7: Transfer RNA (tRNA) maturation pathways in prokaryotes

A) The exoribonucleolytic pathway of tRNA 3'-end maturation in *E. coli* and *B. subtilis*. The 5'-leader and 3'-trailer sequences are indicated. The main exoribonucleases (Pacman symbol) identified so far are in bold type. In *E. coli*, this process is generally initiated by a downstream endoribonucleolytic cleavage reaction catalyzed by RNase E (green scissors).

B) The endoribonucleolytic pathway of tRNA 3'-end maturation. Endoribonucleolytic cleavages by RNase P and RNase Z are indicated by blue and purple scissors, respectively. RNase Z cleaves downstream of the discriminator nucleotide (N) of the precursor tRNA and is stimulated by the downstream uracil residue (U).

Figure adapted from (Redko et al., 2007).

ii. Transfer RNA 3’ end maturation pathways

Maturation of the tRNA 3’ extremity occurs *via* exoribonucleolytic or endoribonucleolytic processing, depending nominally on whether or not the CCA motif is encoded by the tRNA gene (Figure 7). As mentioned earlier, the CCA motif corresponds to the single-stranded sequence on the 3’ extremity of the acceptor stem to which the cognate amino acid is covalently attached by AaRSs (Delarue, 1995). In *E. coli,* all tRNA genes encode the CCA motif while, in *B. subtilis*, about one third of tRNA genes (26 out of 85) are devoid of the CCA (Hartmann et al., 2009).

The endoribonuclease RNase Z cleaves tRNA precursors lacking a CCA motif downstream of the discriminator nucleotide (Redko et al., 2007). The CCA motif is added after this 3’ processing by an enzyme called nucleotidyl transferase (Raynal et al., 1998). Indeed, to prevent futile cycles of CCA addition and removal, eukaryotic RNase Z discriminates against mature tRNAs bearing a CCA motif, with the first cytosine residue (C74) being the key antideterminant (Mohan et al., 1999). Resolution of the structure of *B. subtilis* RNase Z bound to a tRNA substrate showed that the enzyme has a specific pocket for binding a U74 residue, just downstream of the discriminator nucleotide. Thus, *B. subtilis* RNase Z doesn’t discriminate against a cytosine in position 74 but is instead stimulated about 200-fold by uracil in this location (Pellegrini et al., 2012). All the 26 CCA-less tRNAs in *B. subtilis* have evolved with a U-residue in position 74 (20 tRNAs), position 75 (5 tRNAs) or position 76 (1 tRNA). Endoribonucleolytic cleavage by RNase Z occurs immediately 5’ to the uracil residue in each case and, when necessary, is followed by trimming back to the discriminator base by the same enzyme in 3’-5’ exoribonucleolytic mode. In organisms encoding CCA-less tRNA precursors in their genomes, such as *B. subtilis*, RNase Z is an essential enzyme. Like RNase P, RNase Z recognizes the T-arm and acceptor stem of the tRNA (Sierra-Gallay et al., 2006). *E. coli* has a homolog of RNase Z (also called RNase BN) that was first identified has a host enzyme required for the maturation of phage T4-encoded tRNA precursors (which do not possess an encoded CCA triplet) (Asha et al., 1983). RNase BN was shown to have a minor redundant role in the maturation of *E. coli* tRNAs and has been suggested to be involved in turnover and repair of the CCA motif (Dutta and Deutscher, 2010).

All *E. coli* tRNAs and the 59 tRNAs in *B. subtilis* with an encoded CCA-motif are processed at their 3’ end by an exoribonucleolytic pathway (Figure 7). This pathway was first

discovered in *E. coli* where four redundant 3'-5' exoribonucleases are involved in this processing reaction: RNase II, RNase D, RNase PH and RNase T, with the last two being the most important (Figure 7) (Li and Deutscher, 1996). Damage caused to the CCA motif during 3' processing is repaired by the *E. coli* nucleotidyl transferase (Reuven and Deutscher, 1993). In absence of these four 3' exoribonucleases, RNase Z/RNase BN can achieve sufficient 3' tRNA maturation to maintain viability thanks to its 3'-5' exoribonuclease activity (Li and Deutscher, 1996). *E. coli* RNase Z/RNase BN 3'-5' exoribonucleolytic progression is halted by the CC residues of the CCA motif (Dutta and Deutscher, 2009).

Of the four 3'-5' tRNA exoribonucleases involved in tRNA maturation found in *E. coli,* only RNase PH is conserved in *B. subtilis.* Strains lacking RNase PH accumulate CCA-containing tRNA precursors that are 1-4 nts longer than the mature tRNA species (Wen et al., 2005). Therefore, RNase PH plays a key role in the removal of the last few nucleotides from the precursor 3' end. This distributive enzyme belongs to the PDX family of 3'-5' exoribonucleases that also includes PNPase (Zuo and Deutscher, 2001). Nonetheless, RNase PH null mutants still produce significant quantities (>50%) of accurately processed CCA-containing tRNAs. 3' exoribonucleolytic tRNA maturation can be achieved in *B. subtilis* by additional redundant RNases: PNPase, YhaM and RNase R. RNase R is a processive hydrolytic 3'-5' exoribonuclease, with an ability to degrade highly structured RNA. It is known to play a major role in rRNA degradation and in the decay of structured portions of mRNAs (Cheng and Deutscher, 2005). The primary substrates of YhaM in *B. subtilis* are unknown. However, as mentioned earlier, a recent *in vivo* study reported that YhaM has an intriguing behavior, trimming a few nucleotides from the 3' end of the majority of *Streptococcus pyogenes* mRNAs (Lécrivain et al., 2018). *S. pyogenes* YhaM was shown to target terminators as well as transcript 3' ends originating from endoribonucleolytic cleavage, but the implication of this broad ribonucleolytic activity for tRNA maturation remains to be determined. In the absence of other 3'-exonucleases in *B. subtilis,* YhaM can provide some back up in tRNA (Wen et al., 2005) and 23S rRNA (see below) 3' exoribonucleolytic maturation. A significant portion of CCA-containing tRNAs is still processed at their 3' ends in a strain deleted for the four known 3'- exoribonucleases in *B. subtilis* (Wen et al., 2005). Therefore, at least one other enzyme involved in 3'-exoribonucleolytic tRNA maturation in *B. subtilis* remains to be identified. This enzyme is predicted to have properties similar to *E. coli* RNase T, in that it can trim

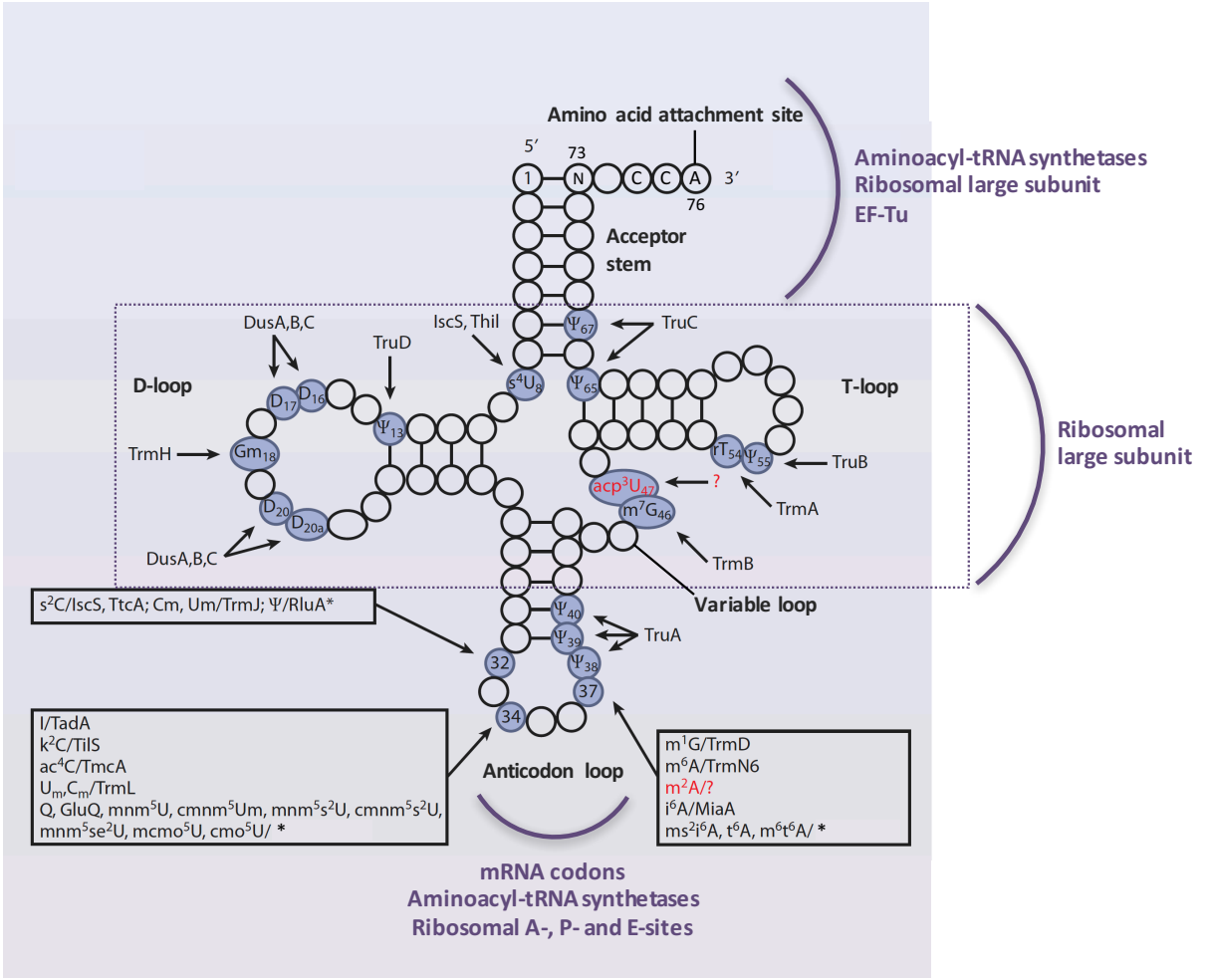

Figure 8: Post-transcriptional modifications of tRNA in *E. coli*

Transfer RNA molecules are post-transcriptionally modified with functional groups that confer structural stability and modulate codon-anticodon interactions. Structural domains are denoted in black, aminoacyl-tRNA synthetase and ribosomal subunit interaction sites are indicated in purple. Known modifications and modification enzymes are indicated. For the names of the enzymes responsible for the modifications denoted by asterisks refer to (El Yacoubi et al., 2012). The corresponding genes are still missing for the modifications in red. The N in position 73 corresponds to the discriminator nucleotide.

Figure adapted from (El Yacoubi et al., 2012; Koh and Sarin, 2018).

nucleotides close to the base of RNA secondary structures.

iii. Transfer RNA post-transcriptional modifications: chemical modifications and charging by aminoacyl-tRNA synthetases

Mature tRNAs have the highest density of post-transcriptional modifications among all RNAs, with numerous evolutionarily conserved modifications (Koh and Sarin, 2018). Many modifications are simple additions or substitutions of functional groups, such as methyl (CH_3), amine (NH_2), and thiol (S) groups, whereas others have more complex structures, whose biosynthesis requires the interplay of several enzymatic steps and pathways (El Yacoubi et al., 2012). These modifications are concentrated in two hotspots: the anticodon loop and the tRNA core region where the D- and T- loops interact with each other to stabilize the overall three-dimensional shape of the tRNA (Figure 8) (Lorenz et al., 2017). Modifications at or near the anticodon loop, in particular at the wobble position 34 (which is a universal hotspot for modification), are particularly important for efficient translation as they can modulate codon-anticodon interactions (for review, see (Koh and Sarin, 2018)). Transfer RNA modification levels can change significantly in response to growth rate and physiological stresses, altering translation in several ways. For example, tRNA hypomodification has been shown to lead to a translation slow-down in *S. cerevisiae* and *C. elegans* (Nedialkova and Leidel, 2015). These modifications have also been found to be involved in tRNA degradation (see below).

Following the tRNA maturation process, aminoacyl-tRNA synthetases (AaRS) are responsible for the accurate charging of tRNAs with their cognate amino acid (Ibba and Söll, 2000). Thus, the overall fidelity of protein synthesis is dependent not only on the accuracy of codon-anticodon recognition, but also on the accuracy of tRNA aminoacylation. Aminoacyl-tRNAs are produced by the 3'-esterification of tRNAs with the appropriate amino acids. tRNA aminoacylation is generally achieved in a two-step reaction: the amino acid is first activated by ATP and then transferred to the 3'OH of A76 at the 3' end of the tRNA. Despite their conserved mechanism of catalysis, AaRSs are divided into two unrelated classes (class I and class II) that differ in their active site topology (reflected by distinct sequence motifs) (Eriani et al., 1990). A single synthetase is generally responsible for specifically attaching an amino

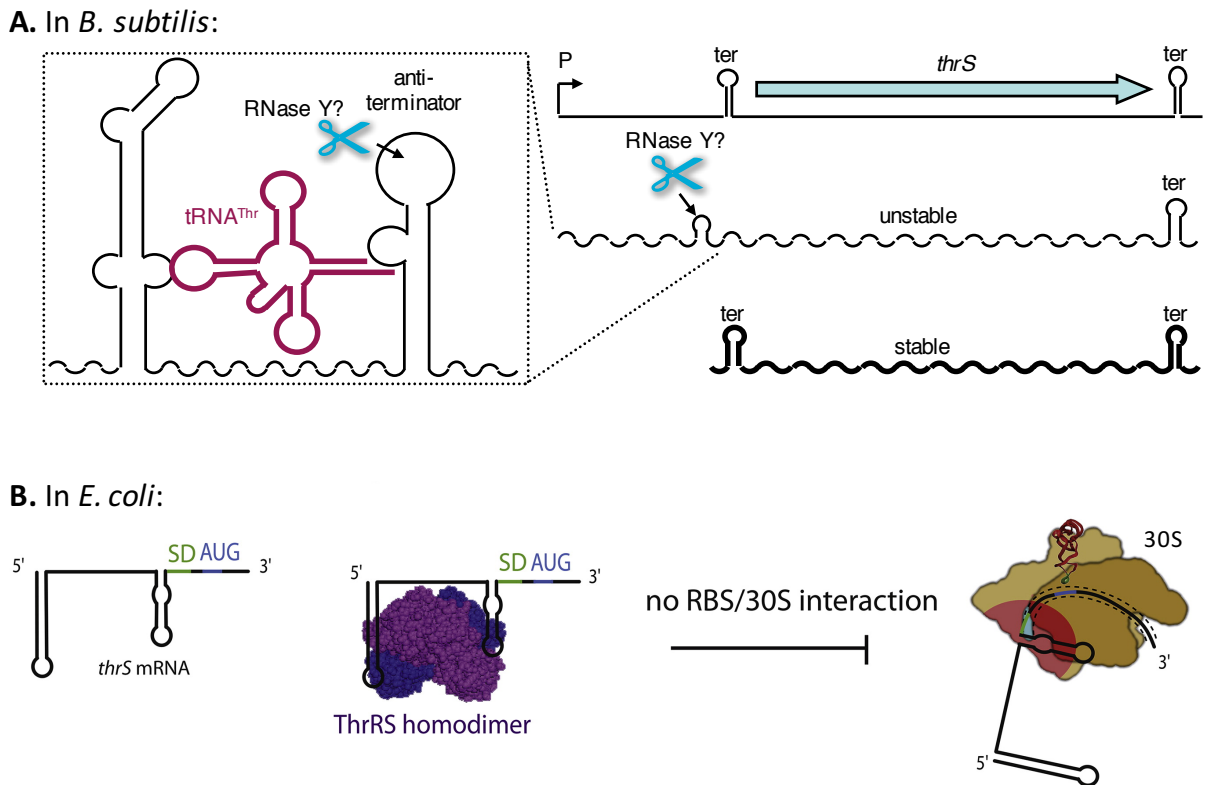

Figure 9: Strategies for regulation of *thrS* expression in *B. subtilis* and in *E. coli*

A) In *B. subtilis, thrS* expression is regulated at the transcriptional level *via* T-box mediated antitermination and processing of the *thrS* transcript. The left panel shows binding of the uncharged $tRNA^{Thr}$ (purple cloverleaf structure) to the *thrS* leader mRNA, stabilizing the antiterminator hairpin. The position of suspected RNase Y cleavage in the loop of the antiterminator structure is indicated by a blue scissors. The right panel shows the transcriptional organization of the *thrS* gene, with promoter (P) and terminators (ter). Transcripts are indicated by wavy lines, with the thickness of the line roughly proportional to the transcript abundance *in vivo*.

B) In *E. coli,* the *thrS* gene is auto-regulated at the translational level. The ThrS homodimer (in purple) binds stem-loop structures in the mRNA operator region that mimic tRNA ligands. Because the binding site is close to the RBS (ribosome binding site), ThrS binding inhibits interaction with the ribosome.

Figure adapted from (Condon, 2009; Duval et al., 2015)

acid to all corresponding tRNAs, although some organisms have more than one AaRS for a particular amino acid (e.g. ThrS and ThrZ in *B. subtilis*) (Putzer et al., 1990). In these cases, paralogous AaRSs are often expressed under different growth conditions. AaRSs mostly interact specifically with one or more of the following elements: the discriminator base (N73), the acceptor stem or the anticodon (Delarue, 1995). Additional interactions have also been shown to occur and a variety of modified nucleotides can act as strong determinants for cognate aminoacylation (Koh and Sarin, 2018).

During amino acid starvation, AaRSs run out of amino acid substrates and uncharged tRNAs accumulate in the cell. On the one hand, this leads to a general activation of the bacterial stringent response (see part III). On the other hand, amino acid starvation provokes an increase in cognate AaRS expression in an attempt to scavenge ever-diminishing pools of amino acids more efficiently. AaRS expression regulation mechanisms are diverse. In *E. coli*, for example, the *thrS* gene encoding the threonyl-tRNA synthetase is auto-regulated at the translational level (Springer et al., 1985). To do so, ThrS interacts with two stem-loop structures in mRNA operator region located upstream of the ribosome binding site in an analogous way to its interaction with its tRNA ligands (Figure 9) (Romby et al., 1990, 1996). In *B. subtilis, thrS* gene expression is regulated by a totally different mechanism known as T-box mediated transcription antitermination (Figure 9). Indeed, *thrS* is one of 20 so-called T-box genes in *B. subtilis* that are regulated by the ratio of uncharged to charged cognate tRNAs (Grundy and Henkin, 1993). During threonine starvation, uncharged $tRNA^{Thr}$ binds to the *thrS* leader sequence and stabilizes an antiterminator structure in the mRNA, prohibiting formation of a terminator sequence upstream of the *thrS* coding sequence and therefore promoting transcriptional read-through and expression of threonyl-tRNA synthetase (Putzer et al., 1995, 2002).

iv. Transfer RNA synthesis, quality control and turnover

Only 14 tRNA genes out of the 86 found in the *E. coli* K12 genome are part of ribosomal RNA (rRNA) transcription units. In contrast, in *B. subtilis,* 60 of the 85 tRNA genes are associated with rRNA operons, 54 of which are located immediately downstream of the 5S rRNA genes. Because of the strong association of tRNA genes with rRNA operons in *B. subtilis,* regulation of tRNA gene expression generally follows that of the rRNA gene

expression. The remaining tRNAs are expressed under the control of promoters with the same regulatory features as those for rRNAs, as occurs in *E. coli* (See section on regulation of rRNA synthesis).

The factors and mechanisms that govern tRNA stability in bacteria are not well understood. It has been observed in *E. coli,* that a thermodynamically unstable precursor tRNA mutant is poly-adenylated and subsequently degraded by PNPase (Li et al., 2002). Transfer RNA precursors are much more sensitive to polyadenylation than their mature counterparts due to their exposed 3' hydroxyl residues (Li et al., 2002; Mohanty et al., 2012). These studies suggest the existence of tRNA quality control mechanisms that resemble the generic turnover of unstable RNA (mRNA) in many ways. Because of their abundance in the cell and their relative stability in comparison to mRNA, tRNAs are often considered as "house-keeping" RNAs that are only degraded when compromised in quality. This vision has been challenged recently with the observation that tRNAs are highly unstable during early amino acid starvation, with the majority of cellular tRNAs being degraded within 20 minutes after the onset of starvation (Svenningsen et al., 2017). In this study, it was shown that tRNA degradation occurs in a ppGpp-independent manner and that both non-cognate and cognate tRNAs for the depleted amino acid are degraded, regardless whether they are charged or not. They further observed tRNA degradation in response to inhibition of transcription by rifampicin, which lead them to propose a model in which the tRNA pool is a highly regulated dynamic entity, with surplus tRNA being degraded whenever the demand for protein synthesis is reduced. Moreover, a recent study in *Vibrio cholerae* revealed the existence of a bacterial tRNA quality control system in which hypomodification sensitizes albeit mature tRNAs to decay mediated by the RNA degradosome (Kimura and Waldor, 2019). Thus, in a strain deleted for the ThiI enzyme – responsible for synthesis of 4-thiouridine ($_s^4$U) which is present (at position 8) on a subset of tRNA species – levels of different tRNAs typically containing $_s^4$U are reduced by rapid tRNA decay.

Overall, the tRNA pool could be more regulated and quality controlled than previously thought, with regulation occurring both at the level of transcription and degradation.

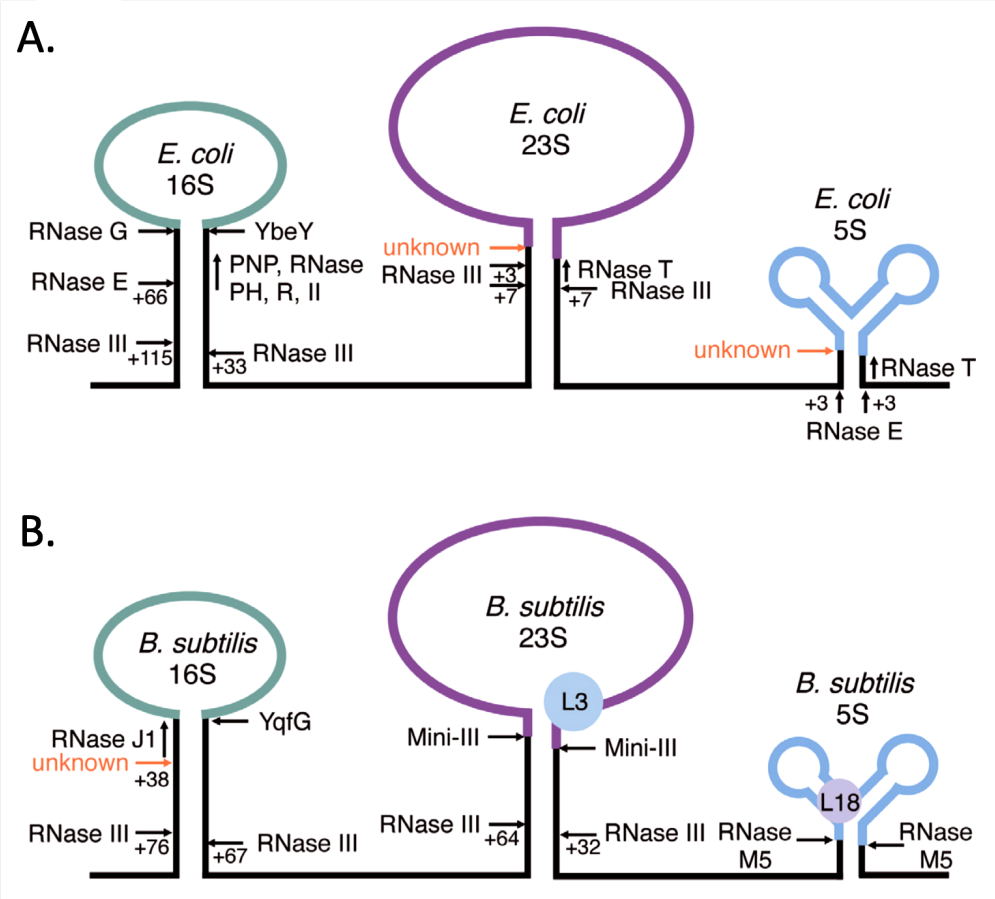

Figure 10: Ribosomal RNA processing reactions in *Escherichia co*li (A) and *Bacillus subtilis* (B)

Thick green, purple and blue lines represent mature 16S, 23S and 5S rRNAs, respectively. Arrows and their distances from the mature 5' and 3' ends indicate the cleavage sites of the major processing enzymes. Unknown enzymes are indicated in red. Ribosomal proteins that serve as cofactors in the *B. subtilis* processing reactions are shown as colored spheres.

Figure adapted from (Baumgardt et al., 2018)

b. Ribosomal RNA maturation

Ribosomes are large ribonucleoprotein complexes containing ribosomal proteins and three ribosomal RNAs: the 16S rRNA in the small ribosomal subunit and the 23S and 5S rRNAs in the large ribosomal subunit (for more details about ribosome biogenesis see section II). Bacterial rRNA genes are usually encoded in large operons, *E. coli* and *B. subtilis* possess 7 and 10 *rrn* operons, respectively, containing the 16S, 23S, and 5S genes, in this order, sometimes interspersed with tRNA genes (Figure 10) (Srivastava and Schlessinger, 1990). Thus, transcription from these operons generates a single polycistronic precursor (30S rRNA precursor). This precursor is converted into functional mature rRNAs *via* a series of nucleolytic processing events and base/sugar modifications that take place in the context of the assembling ribosome (Deutscher et al. 2009). In *B. subtilis*, in *E. coli* and in most other bacteria studied, ribosome assembly occurs co-transcriptionally and the initial separation of the individual rRNAs and final rRNA trimming is intimately associated with r-protein binding. Note that some bacteria do not possess this canonical organization of *rrn* genes: *Rickettsia prowazekii, Mycoplasma gallisepticum, Mycoplasma hyopneumoniae* and *Borrelia burgdorfei*, all having small genome sizes (around 1 Mb). The gram-negative pathogen *Helicobacter pylori* was also found to have an unusual arrangement of its *rrn* genes: the 16S rRNA gene is separated from the ribosomal cluster encoding 23S and 5S rRNA on the chromosome (Tomb et al., 1997).

As exemplified in the beginning of this chapter, *E. coli* and *B. subtilis* have evolved with different sets of RNases and remarkably, of at least ten known intermediary and final processing steps only two processing reactions are shared (Figure 10) (see (Condon, 2009) for review). The first shared step is an endoribonucleolytic cleavage by RNase III that takes place in long double-stranded processing stalks formed by hybridization of complementary precursor sequences at the 5' and 3' ends of both 16S and 23S rRNA. RNase III is the founding member of a family of double-stranded ribonucleases that also includes Dicer and Drosha, well-known for their roles in the generation of siRNAs and miRNAs in eukaryotes. Cleavage by RNase III occurs as soon as this structure is formed, and before transcription of the operon is completed explaining why the 30S rRNA precursor is not detected in a wild type cell (Gegenheimer and Apirion, 1975). The three separated rRNA molecules subsequently undergo further processing reactions to yield the mature functional rRNAs

(Dunn and Studier, 1973; Herskovitz and Bechhofer, 2000). Remarkably, In *H. pylori*, where the 16S and 23S rRNA genes are transcribed separately, initial processing of the three rRNAs is also carried out by RNase III that cleaves in conventional stem-loop structures flanking the 23S and 16S rRNA mature sequences but also in an atypical stem-loop upstream of 5S rRNA (Iost et al., 2019).

i. 16S rRNA maturation

In *E. coli,* cleavage of the 30S rRNA precursor by RNase III generates a 17S molecule containing 115-nt and 33-nt precursor sequences on the 5’ and 3’ sides of the 16S mature sequence, respectively (Figure 10) (Li et al., 1999a). A similar 16S rRNA precursor is generated in *B. subtilis* containing either 76 nts or 140 nts at the 5’ end, depending on the *rrn* operon, and 67 nts precursor sequences at the 3’ end (Britton et al., 2007). These leader and trailer sequences are removed in a further step that occurs once ribosome assembly is complete. Removal of the 5’ and 3’ extensions constitutes an important quality control step in ribosome biogenesis, because they can serve as on-ramps for exoribonucleases (e.g. RNase R) to degrade poorly assembled particles. The 3’ processing reaction is particularly important for making available the anti-Shine-Dalgarno sequence at the 3’ end of 16S rRNA for efficient translation initiation (Baumgardt et al., 2018). Maturation of the 16S rRNA 5’ end is achieved by the cooperative action of RNase E and RNase G in *E. coli* (Li et al., 1999a). In *B. subtilis,* 16S rRNA 5’ maturation is catalyzed by the 5’-3’ exoribonuclease activity of RNase J1, presumably in complex with RNase J2 (Britton et al., 2007; Mathy et al., 2007). Two pathways have been proposed for 16S rRNA 3’ maturation in *E. coli:* endoribonucleolytic cleavage by YbeY (Davies et al., 2010; Jacob et al., 2013) or exoribonycleolytic action of four redundant RNases: PNPase, RNase PH, RNase R and RNase II (Sulthana and Deutscher, 2013).

Recently, 16S rRNA 3’ maturation in *B. subtilis* was shown to involve YqfG, an ortholog of *E. coli* YbeY making it the only shared enzyme of the six major rRNA final processing reactions (Baumgardt et al., 2018). The *ybeY* gene is ubiquitous in bacteria and is one of 206 genes that comprise the predicted bacterial minimal gene set (Gil et al., 2004). *E. coli ybeY* mutants have striking defects in ribosome function including decreased ribosome activity, reduced translation fidelity and altered translation initiation factor binding

(Davies et al., 2010). Moreover, deletion of *ybeY* causes broad defects in 16S, 23S and 5S rRNA processing in this organism. In *B. subtilis,* its ortholog YqfG is essential and cells depleted for this enzyme have a specific defect for 16S 3' rRNA processing and fail to accumulate 70S ribosomes. However, its essential nature is partially suppressed and 70S particles re-accumulate in cells also lacking RNase R. This suggests that, in *B. subtilis,* maturation of 16S rRNA by YqfG is an important ribosome quality control step, because 70S ribosomes harboring 3' immature 16S rRNAs are degraded by RNase R (Baumgardt et al., 2018).

ii. 23S rRNA maturation

Although maturation of the 16S rRNA stills occurs in an RNase III mutant (*Δrnc*) in *E. coli*, maturation of the 23S rRNA is completely defective. Indeed, RNase III processing is mandatory for the final accurate processing of the 23S rRNA in this organism, indicating that the 23S rRNA precursor containing 3 to 7 extra nucleotides on each end that accumulates in an RNase III mutant can be assembled into functional ribosomes. The enzyme that further processes the 23S rRNA 5' end is still unknown in *E. coli*, while the 3' end is matured by the distributive 3'-exoribonuclease RNase T (Li et al., 1999b). RNase T is not conserved in *B. subtilis,* where 23S rRNA is matured by a completely different pathway. Indeed, another enzyme from the RNase III family called Mini-III, was shown to cleave on both sides of the processing stalk to directly produce 5' and 3' mature ends (Redko et al., 2008). Mini-III is an endoribonuclease homologous to the catalytic domain of RNase III that also forms dimers. However, Mini-III lacks the classical double-stranded RNA (dsRNA) binding domain located at the C-terminus of all other members of this family and has its own RNA binding motif integrated into the catalytic domain(Redko et al., 2008). Mini-III has weak activity on *in vitro*-transcribed 23S rRNA and requires L3 protein as a cofactor for efficient cleavage of the pre-23S rRNA (Redko and Condon, 2009). This likely provides a quality control checkpoint for proper 50S assembly before triggering final rRNA processing. Remarkably, Mini-III homologs are present in *A. thaliana* chloroplasts; RNC3 and RNC4 are thought to act on multiple classes of RNA: they participate both in rRNA maturation and intron recycling suggesting a broad role of these enzymes in the resolution of RNA-RNA duplexes.

An alternative pathway for 23S rRNA maturation exists in Mini-III deletion mutants

(*ΔmrnC*) that is catalyzed by exoribonucleases: RNase J1 for the 5' end and RNase PH and YhaM for the 3' end (Redko and Condon, 2010). This alternative pathway results in slightly different, but functional 23S rRNA ends (since the *ΔmrnC* mutant does not have a major growth phenotype) and may be the vestige of an older pathway that can also be found in some Proteobacteria such as *Sinorhizobium meliloti* (Madhugiri and Evguenieva-Hackenberg, 2009).

iii. 5S rRNA maturation

The 5' end of the 5S rRNA precursor (9S rRNA) is generated by the RNase III cleavage that occurs in the 23S rRNA processing stalk in both *E. coli* and *B. subtilis,* while the 3' end of pre-5S rRNA is quite variable as it depends on the structure of each *rrn* operon, i.e. whether the 5S rRNA gene is followed by a transcription terminator or downstream tRNAs (Figure 10). In *E. coli,* RNase E cleaves in a single stranded region on each site of the 9S rRNA and generates a precursor with 3-nt extensions on both ends. Final maturation of the 3' extremity is carried out by the 3' exoribonuclease RNase T, while the 5' end is processed by an unknown RNase.

B. subtilis has found a completely different strategy for 5S rRNA maturation: a dedicated ribonuclease called RNase M5 cleaves 9S rRNA on both sides of a double-stranded stem, to yield mature 5S rRNA simultaneously. RNase M5 is related to the ancient Toprim domain family of enzymes involved in DNA replication and repair. Although RNA cleavage by RNase M5 is predicted to resemble that of DNA cleavage by the topoisomerases, the key catalytic tyrosine residue of the topoisomerases is lacking in RNase M5 (Allemand et al., 2005). Similar to 16S and 23S rRNA maturation, the final processing of the 5S rRNA occurs following ribosome assembly and probably acts as a quality control step. Indeed, RNase M5 cleavage is dependent on the prior binding of the L18 protein to the pre-5S rRNA. Whether L18 acts as an RNA chaperone by allowing pre-5S rRNA to adopt the correct conformation for cleavage, or whether it is directly involved in the recruitment of RNase M5 is not clear (the precise role of L3 in 23S rRNA maturation also remains unclear) (Pace et al., 1984; Redko and Condon, 2009). Moreover, like 23S rRNA maturation, 5S rRNA maturation is not essential for efficient ribosome function in *B. subtilis;* cells deleted for the *rnmV* gene (encoding RNase M5) have no major defect in growth rate and 5S rRNA precursor species are both found in ribosomes and polysomes isolated from this strain (Condon et al., 2001).

A.

Modified nucleoside in the 16S rRNA	Modification enzyme
Ψ516	RsuA
m^7G527	RsmG
m^2G966	RsmD
m^5C967	RsmB
m^2G1207	RsmC
m^4Cm1402	RsmH, RsmI
m^5C1407	RsmF
m^3U1498	RsmE
m^2G1516	RsmJ
m_2^6A1518	RsmA (KsgA)
m_2^6A1519	RsmA (KsgA)

B.

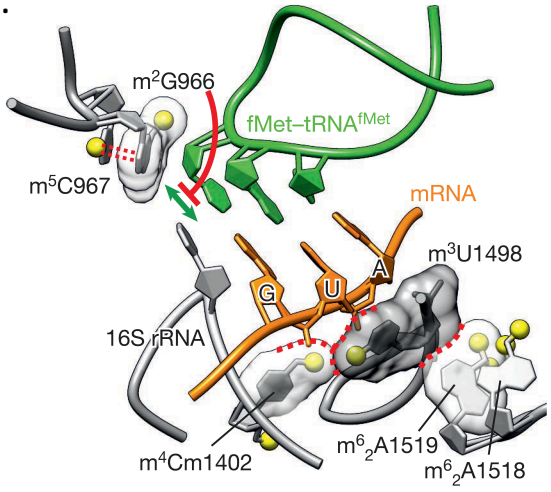

Figure 11: Modifications of the 16S rRNA

A) Table of the 11 modified nucleosides of the *E. coli* 16S rRNA and their associated enzymes.

B) Close-up of the ribosome decoding center showing that rRNA modifications cluster at the functional centers of the ribosome. The methyl group of m^5C967 stacks onto the m^2G966 base. The methyl group of m^2G966 (yellow) restricts the mobility of the initiator tRNA (green). An interaction network of four modified nucleotides stabilizes mRNA (orange) binding to the P site.

Figure adapted from (Fischer et al., 2015)

In summary, most of the enzymes responsible for the final maturation steps in *E. coli*, RNase E, RNase G and RNase T, are not found in *B. subtilis* and *vice versa*, where the enzymes RNase J1, Mini-III and RNase M5 play the key roles (Condon, 2009). The only exception is YbeY/YqfG involved in the maturation of the 3' end 16S rRNA (Baumgardt et al., 2018; Davies et al., 2010; Jacob et al., 2013). Thus, nature has invented rRNA processing pathways at least twice in bacteria and up to four times when one considers that these pathways are different again in the Archaea and in eukaryotes.

iv. rRNA modifications

In addition to the maturation steps described above, rRNAs (except for 5S rRNA) are subjected to post-transcriptional chemical modifications, mainly methylation and pseudo-uridinylation (for review, see (Sergiev et al., 2011)). The *E. coli* ribosome contains 24 methylated nucleosides, ten in 16S (Figure 11) and fourteen in 23S rRNA as well as ten pseudo-uridines, one in 16S and nine in 23S rRNA. Most modifications concern widely conserved residues and are clustered in functionally important regions of the ribosome such as the tRNA-mRNA interaction region of the 30S ribosomal subunit or the peptidyl transferase center and the intersubunit bridge in the 50S subunit (Decatur and Fournier, 2002). The exact role of the modifications is still unknown, as no single rRNA modification has been found to be essential for ribosome function. However, it has been suggested that the modifications could provide structural support to flexible regions to optimize ribosomal function: for example, the methyl group from m^2G966 on the 16S rRNA has been shown to restrict the mobility of the initiator tRNA fMet-tRNA^{fMet} in the P-site (Figure 11) (Fischer et al., 2015).

Modifications of rRNA are suggested to take place in specific "windows" throughout ribosome assembly, as modification enzymes function on different substrates of early or late ribosomal assembly (Sergiev et al., 2011). An illustration of this is the mechanism of action of the methyltransferases RsmB and RsmD that modify the consecutive bases G966 and G967 of the 16S rRNA. These two methyltransferases act sequentially in ribosome assembly, as RsmB modifies 16S rRNA prior to the binding of r-proteins S7 and S19, whereas RsmD only functions after the binding of those two r-proteins (Weitzmann et al., 1991). Modification enzymes often compete with the binding of r-proteins during ribosome assembly, leading to

the hypothesis that the primary role of some of these enzymes could be the prevention of conformational changes or assistance in assembly due to their binding/dissociation rather than the modification itself (Connolly et al., 2008; Liu, 2004; Mangat and Brown, 2008).

An interesting rRNA modification enzyme is KsgA that dimethylates residues A1518 and A1519 of the 16S rRNA and that is suggested to function as a checkpoint during 30S assembly (Connolly et al., 2008). These consecutive dimethylations are conserved in almost all ribosomes from the three domains of life and are catalyzed by the universally conserved KsgA/Dim1p enzyme family and their study revealed their evolutionarily and functional significance (O'Farrell, 2006). The *E. coli ΔksgA* mutant exhibits a cold-sensitive phenotype and accumulates free subunits, which are two hallmarks of mutation in ribosome assembly cofactors (see next section) (Connolly et al., 2008). In agreement, KsgA was found to be involved in 30S assembly and its deletion results in a 16S rRNA processing defect. In their study, Culver and colleagues observed that the presence of a KsgA mutant with no methylation activity is more detrimental to ribosome assembly that the total absence of KsgA, as the mutant form stays stably bound to the 30S. These data suggest a checkpoint role for KsgA in late ribosomal assembly, where methylation triggers its detachment from assembling 30S (Connolly et al., 2008).

II. Ribosome biogenesis and degradation

Ribosome biogenesis is the process leading to the formation of the small 30S subunit and large 50S subunit in bacteria that will further assemble in a 70S particle for translation. During translation initiation, the 30S subunit associates with mRNA through base-pairing between the anti-Shine-Dalgarno (anti-SD) sequence at the 3' end of 16S rRNA and the SD sequence in the mRNA (for review, see (Simonetti et al., 2008). The translation initiation complex formation starts with the 30S subunit that is kept dissociated from the 50S subunit by the binding of IF3 (initiation factor 3). The consecutive binding of two other initiation factors (IF2 and IF1) promotes association with the aminoacylated and formylated initiator tRNA (fMet-tRNA^{fMet}) and the mRNA. This step is followed by accommodation of the mRNA resulting in the formation of an active 30S initiation complex that can next engage the 50S subunit to form the 70S initiation complex. The 50S subunit is responsible for peptide bond formation and the catalytic center is located within the RNA component, thus the ribosome is indeed a ribozyme (Nissen et al., 2000).

The cryo-electron microscopy (cryo-EM) structure of the *B. subtilis* ribosome was obtained quite recently (Sohmen et al., 2015) and the majority of rRNA arrangements structurally resembles the *E. coli* ribosome (Schuwirth et al., 2005). The *B. subtilis* small subunit contains 20 ribosomal proteins (designated S2–S21) and the 16S rRNA, which is 1,553-nt in length, whereas the large subunit is made up of 32 proteins (designated L1–L36) and two rRNAs: the 23S rRNA, which is 2,928-nt in length, and the 5S rRNA, which is 116-nt in length. There is no L8 protein in *B. subtilis,* nor a canonical L25*.* However, the *ctc* gene encodes a general stress response protein that possesses an N-terminal domain similar to L25*.* The Ctc protein, expressed under control of the alternative sigma factor σ^B, was shown to be a ribosomal protein homolog that could be required for accurate translation under stress conditions (Schmalisch et al., 2002). Other alternative r-proteins homologs exist in *B. subtilis*: for example, RpmEB (L31*), RpmGC (L33*), RpsNB (S14*) that belong to the Zur regulon. They are expressed in response to zinc deprivation to functionally replace ribosomal proteins requiring zinc for function (Nanamiya and Kawamura, 2010; Shin and Helmann, 2016).

1. Bacterial ribosome biogenesis

Ribosome biogenesis, requires the coordinated synthesis, folding, cleavage, post-transcriptional modification of rRNA, and the translation, folding, post-translational modification and binding of >50 r-proteins. The process of ribosome biogenesis is highly complex and, as we have seen, needs to be performed accurately and efficiently to avoid triggering quality control mechanisms. Indeed, ribosome assembly consists of an alternating series of rRNA conformational changes and protein-binding events, whereby protein binding drives and stabilizes local rRNA structure, while inducing conformational changes to create new binding sites for later r-proteins (Davis and Williamson, 2017). This incrementally drives the rRNA structure to the final native state (Holmes and Culver, 2005). Although highly complex, this multistep process is strikingly efficient, as the production of a complete ribosome takes less than 2 minutes in exponentially growing *E. coli* (Chen et al., 2012; Lindahl, 1975). *In vivo*, the assembly process is co-transcriptional and can be directly observed by electron microscopy of rDNA operons in "Miller spreads" (Miller et al., 1970).

a. *In vitro* ribosomal reconstitution experiments

Assembly of the *E. coli* ribosome has been studied for some time *in vitro* by a series of reconstitution experiments. Indeed, in the 1960s, Traub and Nomura demonstrated that the active 30S subunit could be assembled *in vitro* from purified r-proteins and rRNA (Traub and Nomura, 1968). This represented a major breakthrough and allowed a dissection of ribosome assembly pathways by directly testing r-protein binding interdependences, for example. By varying the order of addition of the different r-proteins to the 16S rRNA, 30S subunit assembly was shown to be hierarchical, with primary binding proteins that can stably bind to the naked 16S rRNA, and secondary and tertiary binding proteins whose binding relies on the prior binding of primary and secondary binders, respectively. In the 1970s, a similar approach allowed Nierhaus and Dohme to successfully assemble functional 50S subunits, although this reconstitution was done in non-physiological conditions (Nierhaus and Dohme, 1974). Studies on both 30S and 50S subunit assembly *in vitro* identified reconstitution intermediates that needed to be heated and/or exposed to high magnesium concentrations to continue the assembly process. In this type of *in vitro*

reconstitution experiments, ribosome assembly involves the synchronous binding of r-proteins to mature full-length rRNAs, whereas inside cells, the ribosome biogenesis process is asynchronous, with co-transcriptional binding of r-proteins to nascent rRNA precursors. Therefore, the question still remained until recently whether the assembly maps and intermediates characterized *in vitro* recapitulate the assembly process existing inside cells.

b. *In vivo* assembly intermediates

Ribosome assembly is extremely rapid *in vivo* compared to *in vitro* reconstitution experiments. For example, 50S subunit assembly takes less than a couple of minutes *in vivo* at 37°C whereas *in vitro* 50S assembly requires one hour and a half at 50°C (Nierhaus, 1991). *In vivo* assembly is more complex because of its co-transcriptional nature and the involvement of dozens of assembly cofactors (Cf sub-section d). A significant challenge for the study of ribosome assembly *in vivo* is that intermediates are not abundant under normal growth conditions. Thus, much of our understanding of ribosome assembly *in vivo* has resulted from analysis of genetically or chemically perturbed cells that accumulate assembly intermediates. This includes the use of conditional mutants, temperature-sensitive strains, deletion of genes encoding specific assembly factors or cells treated with ribosome-targeting antibiotics (see (Shajani et al., 2011) for review). The biochemical and structural characterization of these incomplete particles provides some insights into the nature of the intermediates in the assembly pathway upstream of the block. However, data obtained with these approaches can be difficult to interpret, as the accumulating intermediates may have progressed significantly beyond the point of initial perturbation to become thermodynamically stable off-pathway intermediates (Razi et al., 2017a).

Several recent studies demonstrated that ribosomal assembly is a mixture of sequential and parallel elements (Chen et al., 2012; Davis et al., 2016). This provides a rich landscape of alternative assembly pathways in which different precursors are not assembled in the exact same way. This property is probably essential for the robustness and the efficiency of ribogenesis, as it can buffer the system against transient changes in r-protein availability, for example. Recent approaches such as high-throughput quantitative mass-spectrometry (qMS), have permitted an examination of *in vivo* ribosome assembly intermediates in regular growth conditions (Chen and Williamson, 2013). In this method, r-protein levels across a

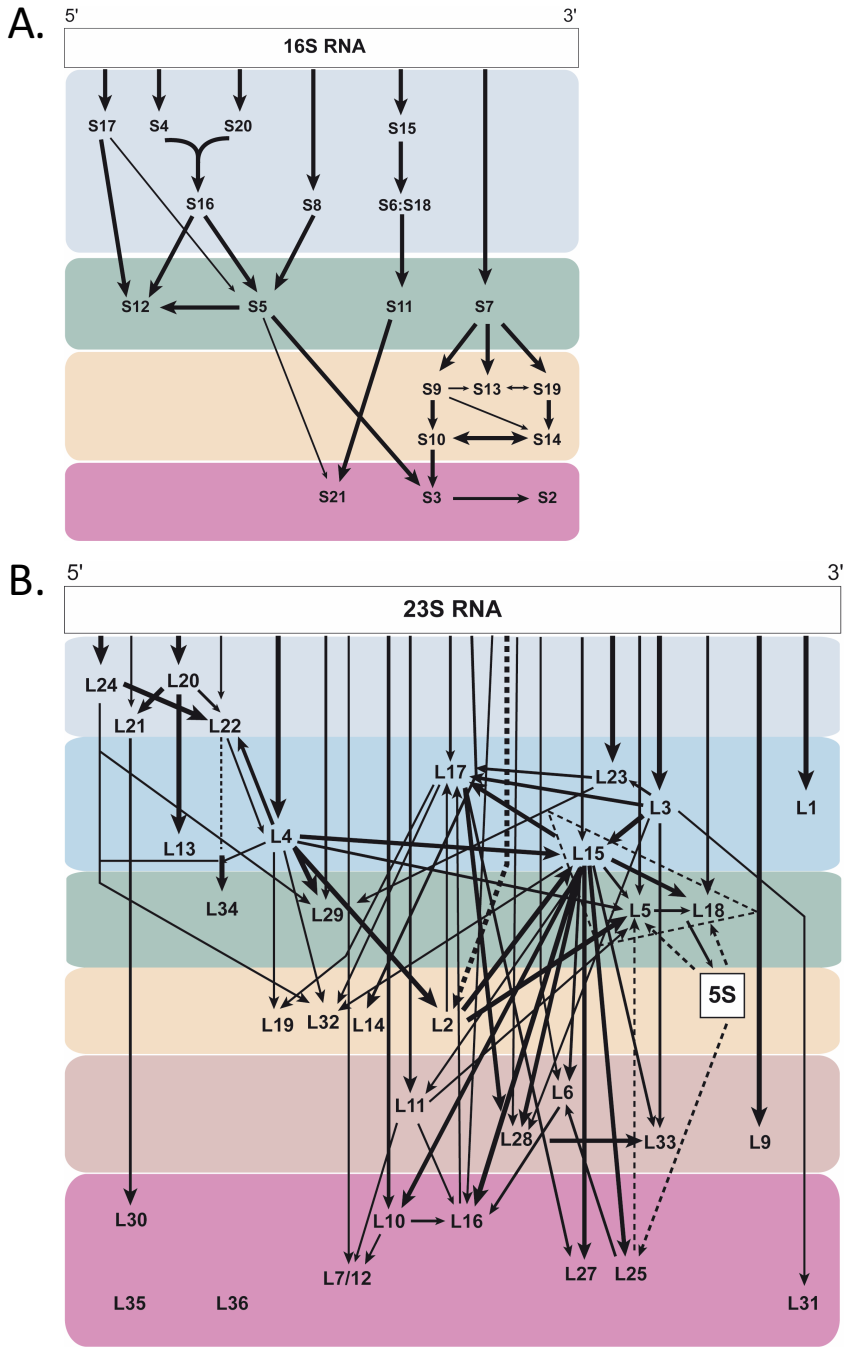

Figure 12: *In vivo* 30S subunit (A) and 50S subunit (B) assembly maps.

Normalized r-proteins levels were determined in successive sucrose gradient fractions of wild-type cell extracts by quantitative mass-spectrometry and assembly maps were obtained by clustering assembly intermediates according to progressively later fractions. The colors correspond to groups of r-proteins found across successive fractions of the sucrose gradient and represents from blue to pink, proteins found in smaller early-stage intermediates to larger late-stage intermediates for each subunit. Four and six distinct groups of r-protein assembly were found for the 30S and 50S subunit, respectively.

Figure adapted from (Chen and Williamson, 2013)

sucrose gradient are quantified by mass-spectrometry using an isotope-labeled ribosome spike as an external standard for normalization. Pulse-labeling experiments further permit confirmation that the native pre-30S and pre-50S species identified are real *in vivo* on-pathway assembly intermediates and not dead-end particles or degradation products. *In vivo* assembly maps were obtained by clustering those *bona fide* assembly intermediates in sucrose gradient fractions of increasing density (Figure 12). For 30S subunit assembly, four distinct assembly groups emerged (Chen and Williamson, 2013) (represented by different colors on Figure 12). The most abundant r-proteins in all the fractions correspond to the first assembly group. This group contains 5' and central domain primary and secondary binding r-proteins. The second group comprises 3' domain primary binders and tertiary binders of the 5' domain. Third group of assembly is constituted by secondary and tertiary binders of the 3' domain. And finally, the fourth group contains r-proteins that are depleted in most pre-30S and 30S fractions and complete in 70S fractions, *i.e.* the tertiary binding proteins S2, S3 and S21. Overall, this assembly map illustrates the directionality of subunit assembly related to the co-transcriptional nature of this process. Both 30S and 50S r-protein assembly maps obtained with the qMS technique are coherent with binding dependencies determined by early *in vitro* studies and are in general agreement with those obtained previously.

c. Role of r-proteins in rRNA folding and ribosome assembly

Structural studies, combined with a variety of biochemical and biophysical experiments led to the hypothesis that ribosome assembly is in fact an RNA folding problem (see (Davis and Williamson, 2017) for review). Indeed, the major functions of r-proteins in the assembly processes are proposed to be the guiding of the rRNAs into proper conformations, the stabilization of native rRNA tertiary structures, and the protection of the naked rRNAs from degradation by the cellular RNases. Indeed, RNA structure probing experiments provided evidence that most native rRNA secondary structures are formed in an r-protein independent manner, whereas tertiary rRNA contacts were often dependent on r-protein binding events (Adilakshmi et al., 2008). Some of the r-proteins have important functions in promoting rRNA maturation (L3 for Mini-III cleavage or L18 for M5 cleavage, for example), constituting ribosome assembly checkpoints (Pace et al., 1984; Redko and Condon, 2009).

Ribosomal proteins have been shown, especially in *E. coli*, to be extensively modified

with post-translational modifications. Six r-proteins are methylated (S11, L3, L11, L7/L12, L16 and L33), three are acetylated (S5, S18 and L7) and the protein S12 is methylthiolated (Nesterchuk et al., 2011). Studies of *B. subtilis* ribosomal proteome suggest that some of those modifications are not conserved in *Firmicutes*: S12 and L12 modifications are entirely absent, while L11 is methylated on different residues than in *E. coli* (Lauber et al., 2009). However, the significance and function of r-protein modifications remains poorly understood. It is worth noting that the acetyl-transferase RimJ, responsible for S5 acetylation, has been suggested to have evolved with dual activities in *E. coli*, as it was shown to play a role in ribosome assembly independently of its acetyltransferase activity. RimJ overexpression was found to suppress small subunit assembly defects of a S5 r-protein mutant (carrying a G28D substitution) independently of its acetyl-transferase activity (Roy-Chaudhuri et al., 2010).

Systematic inactivation of ribosomal proteins genes in *B. subtilis* have revealed that of the 57 genes encoding r-proteins, 22 are non-essential and can be deleted individually (Akanuma et al., 2012). This result is similar to what was found in *E. coli* where 22 of the 54 r-proteins (about 60% overlap) genes were individually non-essential (Shoji et al., 2011). Interestingly, in *B. subtilis,* eight of the r-proteins deletion mutants (S6, S21, L1, L23, L29, L32, L34 and L36) displayed abnormal ribosome sedimentation profiles (Akanuma et al., 2012). The importance of r-proteins for ribosome assembly and function can be exemplified in humans where various severe genetic diseases, collectively referred to as “ribosomopathies”, are associated with mutations in r-protein genes (McCann and Baserga, 2013; Narla and Ebert, 2010). For example, Diamond-Blackfan anemia, a rare congenital syndrome of bone marrow failure is associated with mutations in several genes encoding r-proteins from both the small and the large ribosomal subunits (most frequent mutations affect RPS19, RPL5 and RPL11) (for review, see (Narla and Ebert, 2010)). Most of these mutations cause a dramatic decrease in expression of the corresponding r-protein suggesting that the resulting haplo-insufficiency is the basis for the pathology (Campagnoli et al., 2008).

d. Accessory ribogenesis factors

Unlike the r-proteins, dozens of accessory factors (also known as cofactors) are involved in ribogenesis without being part of the mature ribosome in the end (Figure 13)

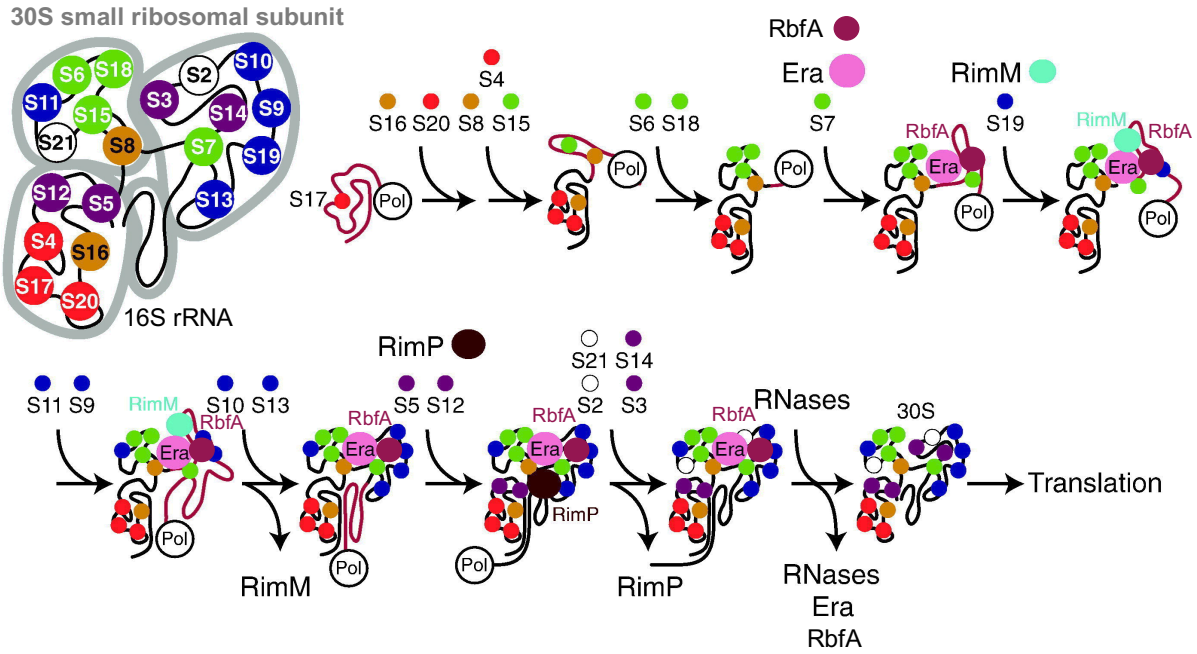

Figure 13: 30S ribosomal subunit assembly and involvement of assembly cofactors

Proposed co-transcriptional model of small ribosomal subunit assembly *in vivo* and the points at which factors Era, RimM, RimP and RbfA are required. The 30S subunit consists of three major domains: the 5' domain (lower left), the central domain (upper left), and the 3' major domain (upper right), with the 3' minor domain in the center. The r-proteins bind to the nascent unfolded rRNA (represented in red) as soon as their binding site become available. Era is involved throughout different steps of assembly, while RimM facilitates 3' domain assembly. RimP acts during the later stages of r-protein binding, and RNases mature the rRNA termini. Note that RbfA was added to the scheme according experimental evidence obtained by (Datta et al., 2007) that shows that this cold shock response protein interacts with helix 28 on the opposite side to the Era binding site.

Figure adapted from (Bunner et al., 2010)

(Shajani et al., 2011; Wilson and Nierhaus, 2007). These protein factors facilitate the assembly process, explaining why ribosome assembly is much more rapid *in vivo* than *in vitro*. The putative roles of these cofactors include the avoidance of kinetic assembly traps caused by local rRNA misfolding, the facilitation of r-protein binding and the sensing of quality control checkpoints during the assembly process (Woodson, 2008). Accessory factors include 1) the rRNA maturation RNases, 2) the r-protein and rRNA modification enzymes (discussed in section I.2.b) and 3) ribosome assembly cofactors *per se.* This last category includes helicases, GTPases and other maturation factors with chaperone functions. The role of ribosome assembly cofactors has been mainly studied in *E. coli*, either by investigating their function during *in vitro* reconstitution experiments (Bunner et al., 2010) or by analyzing the repercussions of their absence (or inactivation) on *in vivo* ribosome assembly (Leong et al., 2013). In contrast to yeast, where almost all ribosome assembly cofactors are essential, most bacterial assembly cofactors are non-essential (Hage and Tollervey, 2004). This may imply that they have redundant functions, that the reaction they catalyze can be bypassed by parallel pathways or that they are essential only in specific conditions such as at cold temperature. In the following sections, I will briefly describe each category of cofactor involved in assembly of 30S and 50S ribosomal subunits. In Table 1 (Supplementary), I have listed specific cofactors known to be directly or indirectly involved in small ribosomal subunit assembly, which is more directly related to this thesis. Because their precise roles are sometimes unclear, I chose known defects in either 30S subunit assembly or 16S rRNA processing (an indirect indicator of an assembly defect) as criteria for inclusion in this table.

i. DEAD-box RNA helicases

DEAD-box helicases are a large family of RNA helicases found in all the three domains of life. They possess RNA-dependent ATPase activity and ATP-dependent RNA remodeling activity, and are characterized by the presence of an Asp-Glu-Ala-Asp (DEAD) motif among the twelve conserved motifs of their conserved helicase core (see (Linder and Jankowsky, 2011) for review). Aside from their conserved core, DEAD-box proteins often possess additional variable N- or C-terminal domains that confer their specificity for substrates and interaction partners, and are thus involved in their individual function and regulation. DEAD-box RNA helicases play important roles in remodeling RNA molecules and in facilitating a

variety of RNA-protein interactions that are key in many cellular processes. In eukaryotic cells, RNA helicases are implicated in all processes that involve RNA, including transcription, splicing, mRNA export, ribosome biogenesis, translation, and mRNA decay.

In bacteria, the role of DEAD-box RNA helicases is narrower and they are mainly involved in ribosome assembly and mRNA decay. *E. coli* encodes five different RNA helicases: SrmB, CsdA, DbpA, RhlE, and RhlB (Iost and Dreyfus, 2006; Kalman et al., 1991). RhlB is solely involved in mRNA decay, and is an integral part of the RNA degradosome with RNase E, PNPase and enolase (Py et al., 1996). The four other *E. coli* helicases are linked to ribosome biogenesis although their precise molecular function in this process often remains poorly understood (Charollais et al., 2004; Gentry et al., 2016; Redder et al., 2015). The SrmB protein was the first ATP-dependent RNA helicase to be clearly characterized as a cofactor for large subunit assembly in *E. coli:* analysis of a *ΔsrmB* strain revealed an aberrant ribosome profile with reduced amounts of the 50S subunits and an accumulation of a 40S particle lacking r-proteins L13, L28, L34, L35 and L36 (Charollais et al., 2003). This helicase has been suggested to be involved in recruitment of L13, a protein that binds the 5' region of 23S rRNA at early stages (Charollais et al., 2003). It was proposed that SrmB is tethered to the assembling large ribosomal subunit through interactions with L4 and L24, and that it plays a role in rRNA folding preventing formation of alternative structures (Proux et al., 2011; Trubetskoy et al., 2009). Moreover, SrmB likely plays multiple roles in ribosome assembly as it was recently shown to control r-protein synthesis (of L13 and S9), therefore regulating ribosome assembly indirectly (Iost and Jain, 2019).

The Gram-positive bacteria *B. subtilis* contains four DEAD-box enzymes, CshA, CshB, DeaD, and YfmL that are all dispensable for growth at 37°C. Deletion of the *cshA, cshB* or *yfmL* genes led to cold-sensitive phenotypes and to distinct ribogenesis defects whereas the *ΔdeaD* strain did not show any detectable defect (Lehnik-Habrink et al., 2013). Indeed, *ΔcshA, ΔcshB* and *ΔyfmL* mutants all have altered ribosome profiles in sucrose gradients, with distinct relative amounts of individual subunits and mature 70S particles, suggesting that the three DEAD-box RNA helicases have distinct functions in the formation of properly assembled ribosomes. CshA is suggested to be a functional homolog of RhlB as it is part of the RNA degradosome-like network in *B. subtilis* (Lehnik-Habrink et al., 2010). To date, although precise roles remain elusive, ribosome assembly DEAD-box helicases in *B. subtilis*

are thought to be mostly involved in 50S assembly, as is the case in *E. coli* (Iost and Dreyfus, 2006; Lehnik-Habrink et al., 2013). It is noteworthy that these enzymes all share similar levels of sequence homology and it is therefore difficult to determine their orthology relationships.

ii. GTPases

GTPases are molecular switches that shift between an inactive GDP-bound state and an active effector-binding GTP-bound state. They are involved in a wide range of cellular processes and several have been implicated in the biogenesis of bacterial, mitochondrial, chloroplast and eukaryotic ribosomes (for review see (Britton, 2009)). In contrast to the other assembly factors identified in bacteria, the majority of ribosome assembly GTPases (RA-GTPases) are essential for growth. All conditional mutants of RA-GTPases display a reduced level of 70S ribosomes in the cell, likely due to improper assembly of individual subunits. In *B. subtilis,* RA-GTPases include RbgA, YsxC and YphC implicated in 50S subunit assembly, and Era, CpgA and YqeH that play roles in 30S assembly. In the coming paragraphs, I will focus on the roles of the three RA-GTPases involved in small subunit assembly, the main subject of this thesis.

Era is highly conserved in bacteria and was shown to have multiple functions, among them an involvement in the cell cycle, cell division and ribosome assembly (Britton, 2009). The first hint that Era was involved in ribosome assembly came from the identification of 16S rRNA dimethylase KsgA as a multicopy suppressor of a cold sensitive *era* mutation (Lu and Inouye, 1998). Era binds to the 16S rRNA of the 30S subunit and Era-depleted cells show decreased quantities of 70S ribosomes, an accumulation of 50S particles and have 30S subunits with immature 16S rRNA (Inoue et al., 2003). Era is thought to be a checkpoint protein that prevents incompletely assembled 30S subunits from forming premature translation initiation complexes. Era binding locks the 30S subunit in a conformation that is not favorable for association with the 50S subunit (Sharma et al., 2005). Moreover, cryo-EM and crystal structures of Era bound to the 30S subunit show that Era binding, albeit close to the 3’ end of unprocessed 16S rRNA, leaves the 16S rRNA 3’ cleavage site and 33-nt extension exposed to RNA maturation enzymes (Sharma et al., 2005; Tu et al., 2009). More recently, the *E. coli* 16S rRNA 3’ end maturase YbeY, was found to interact directly with

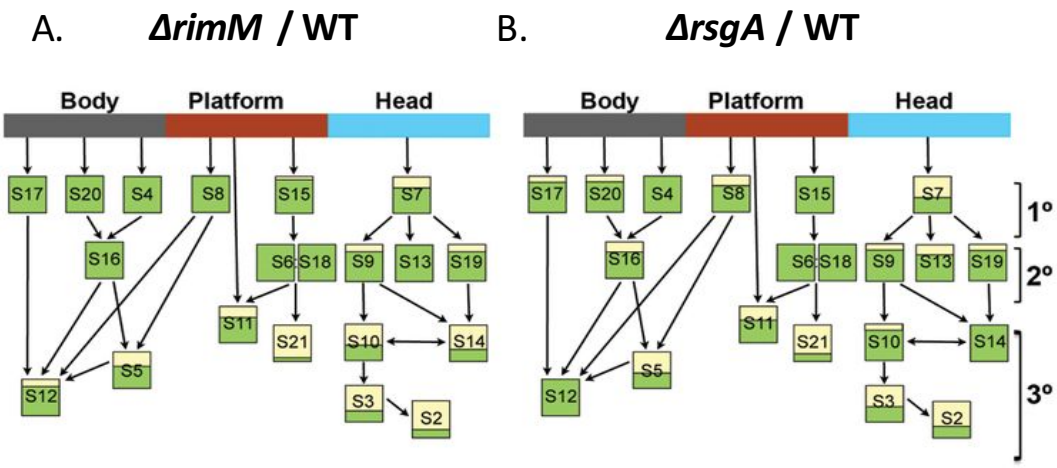

Figure 14: Protein complement of immature 30S subunits accumulated in the *ΔrimM* and *ΔrsgA* strains.

The relative level for each r-protein with respect to wild-type parental cells is expressed as the ratio *ΔrimM*/WT and *ΔrsgA*/WT for the *ΔrimM* and *ΔrsgA* mutants, respectively. The average *ΔrimM*/WT ratios were plotted in the Nomura assembly maps (lower panels) and shown along with a similar analysis performed for the free 30S subunits purified from the *ΔrsgA* strain under identical conditions (data taken from (Jomaa et al., 2011)). The proportion of the box colored in yellow is proportional to the degree of underrepresentation of each r-protein in the 30S subunits purified from *ΔrimM* and *ΔrsgA* cells. The groups of primary (1°), secondary (2°), and tertiary (3°) proteins are indicated.

Adapted from (Leong et al., 2013).

Era and S11, leading to the proposal that Era may play a direct role in 16S rRNA maturation, guiding YbeY to its site of action on the ribosome (Vercruysse et al., 2016). Consistent with this idea, *era* and *ybeY* are encoded in the same operon in many Gram-positive bacteria and Era actually is fused with YbeY as a single polypeptide in some *Clostridia* species (Jacob et al., 2013). Era was also identified as a genetic suppressor of an *rsgA* mutant in *E. coli,* suggesting a role for this other GTPase in 30S subunit assembly (Campbell and Brown, 2008). Interestingly, in *E. coli* Era is co-expressed with a distinct rRNA maturation enzyme, RNase III.

CpgA (referred as RsgA and YjeQ in *E. coli*) represents a subfamily of GTPases characterized by a circular permutation of the 5 canonical G motifs composing their GTPase domain (Leipe et al., 2002). *E. coli* RsgA was shown to interact both with late assembly immature 30S and mature 30S particles. Actually, RsgA binding affinity is higher for the mature 30S subunit which is quite unexpected for an assembly cofactor (Thurlow et al., 2016). A cryo-EM structure revealed that RsgA binds in the decoding center region. Its binding prevents association with initiation factors IF2 and IF3, suggesting a similar role to Era in impeding premature formation of translation initiation complexes (Jomaa et al., 2011). RsgA is thought to bind pre-30S subunits when the chaperone RbfA (see below) is still bound, as it was shown to promote its release (Goto et al., 2011). In addition to promoting the detachment of RbfA, RsgA causes conformational changes in helix 44 of the 16S rRNA and is suspected to test translation proofreading ability of the small subunit by flipping out the base moiety of A1492 from the helix (Razi et al., 2017a). A1492 and the adjacent A1493 play an important role in stabilizing the codon-anticodon interaction in the A-site and are flipped out in the proofreading conformation of the ribosome. RsgA is therefore thought to be the last checkpoint of 30S subunit assembly before releasing the proofreading competent particle into the pool of actively translating ribosomes (Razi et al., 2017a). A *ΔrsgA* mutant was shown to accumulate immature 30S particules having a late assembly defect (Figure 14). The tertiary r-proteins S2, S3, S5 and S21 are the most reduced along with the primary r-protein S7 binding the head domain; other proteins are also slightly under-represented (S8, S9, S10, S11, S13, S16, S17, S19) (Jomaa et al., 2011; Leong et al., 2013). Interestingly, RsgA and its *S. aureus* ortholog CpgA (but not *B. subtilis* CpgA) were shown to bind the stringent response effector (p)ppGpp (see section III) (Corrigan et al., 2016; Zhang et al., 2018). Era has similarly been shown to bind (p)ppGpp in all three organisms, suggesting a strong

connection between the amino acid availability and ribosome assembly. Lately, in addition to its role in ribosome assembly, *B. subtilis* CpgA was shown to moonlight as a metabolite proofreading enzyme, functioning as a phosphatase to eliminate toxic accumulation of 4-phosphoerythronate (4PE) in the pentose phosphate pathway of glucose metabolism (Sachla and Helmann, 2019).

Like RsgA, YqeH is a circularly permutated GTPase, found in diverse groups of bacteria and plants, but not in *E. coli* (Leipe et al., 2002). In *B. subtilis*, YqeH depletion leads to specific depletion of the 30S subunit and 16S rRNA degradation (Loh et al., 2007; Uicker et al., 2007). However, unlike other RA-GTPases discussed above, no interaction with the ribosome or ribosome subunits has yet been observed (Loh et al., 2007). The plant *Arabidopsis thaliana* possess a YqeH ortholog, called AtNOS, that is likely to be involved in mitochondrial ribosome assembly (Moreau et al., 2008). However, in *A. thaliana,* as in *B. subtilis*, the precise role of this GTPase in ribosome assembly still remains elusive.

iii. Energy independent RNA chaperones

Several additional proteins that do not exhibit a measurable NTPase activity like the RA-GTPases and ATP-dependent DEAD-box helicases have been shown to play important roles in ribosome assembly (for review, see (Shajani et al., 2011)). Ribosome maturation factor P (RimP) is important for maturation of the 30S subunit. This protein associates with 30S particles and immature 16S rRNA accumulates in a *ΔrimP* mutant concomitantly with a defective ribosome assembly profile (Nord et al., 2009). Immature 30S particles accumulating in a *ΔrimP* mutant are depleted for r-proteins S2, S3, S5, S12 and S21 suggesting a role for RimP in formation of the central pseudoknot region (Sashital et al., 2014).

The *rimP* gene is part of an operon containing the *rbfA* gene that encodes the Ribosome binding factor A, another key ribosome assembly chaperone. RbfA is a cold shock protein that interacts with the 5'-terminal helix region of the 16S rRNA (Dammel and Noller, 1995). The RbfA binding site lies close to the decoding center of the 30S subunit, near the binding site of the chaperone RimM (Ribosome maturation factor M) and those of the RA-GTPases Era and RsgA/CpgA (Datta et al., 2007; Thurlow et al., 2016). This suggests that these factors contribute to the formation of the functional 30S core in a cooperative manner

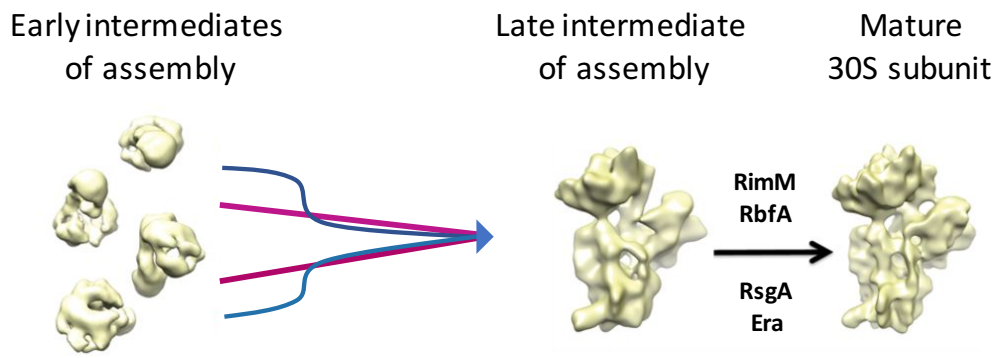

Figure 15: Early convergence model for the assembly of the 30S subunit.

This model suggests that multiple parallel assembly pathways converge into a late assembly intermediate. A group of functionally related assembly factors (RimM, RbfA, RsgA and Era) will target this intermediate and catalyze the last step of maturation.

Figure adapted from (Leong et al., 2013).

(Razi et al., 2017b). The chaperones RbfA and RimM may proofread the folding of the rRNA and pre-30S assembly at different stages of the process (Culver, 2005). Experiments from the Woodson and Williamson laboratories have shown the existence of multiple parallel pathways of 30S subunit assembly, suggesting that cofactors are involved in guiding the folding landscape of rRNA and specific protein-RNA interactions to facilitate productive conformations (Adilakshmi et al., 2008; Talkington et al., 2005). The Ortega lab has proposed a model of "early convergence" where the multiple parallel early assembly pathways converge into a late assembly intermediate and suggested that the latter is the substrate for the cooperative action of the functionally related cofactors RbfA, RimM, Era and RsgA (Figure 15) (Leong et al., 2013). Consistent with this model, *ΔrimM* and *ΔrsgA* strains accumulate comparable immature 30S subunits: in both cases the tertiary r-proteins S2, S3 and S21 have the highest degree of reduction, while S7, S9 and S19 were more moderately depleted (Figure 14). In contrast to the *ΔrsgA* mutant, the primary and secondary binding r-proteins of the head domain S8, S17, S20 and S16 are present at normal levels in the *ΔrimM* mutant that rather exhibits reduced levels of late r-proteins S12 and S14 (Figure 14) (Leong et al., 2013).

2. Ribosome quality control

Although ribosomes and rRNAs are stable in growing cells, they can be degraded as part of ribosome assembly quality control or during physiological responses to specific stress conditions (for review see (Deutscher, 2009)). Despite their central role in ribosome metabolism, ribosome quality control and degradation mechanisms have received little attention in bacteria. Most of the results presented here were obtained in *E. coli,* unless otherwise stated.

- *Ribosome assembly quality control*

As illustrated earlier, ribosome biogenesis is a highly complex process requiring the co-transcriptional and sequential binding of r-proteins onto the nascent rRNA as well as the correct folding, maturation and post-transcriptional modification of rRNA (Shajani et al., 2011). Thus, although cells have evolved mechanisms to improve the accuracy of ribosome assembly, it is likely that a basal number of defective particles is continuously produced in

growing cells due to errors in r-protein binding or rRNA folding. Understandably, quality control mechanisms exist to monitor ribosome biogenesis and rapidly degrade defective particles that could interfere with protein synthesis. Although ribosome biogenesis quality control has been studied more broadly in eukaryotes than in prokaryotes, such mechanisms are likely to be key in all types of cells, as they ensure the production of functional machineries that faithfully decode genetic information from mRNA to protein (Karbstein, 2013).

Intriguingly, functional checks of assembling ribosomes were shown in yeast to involve action of translation itself. Indeed, newly-made precursor subunits are thought to undergo a translation "test-drive" with their mature partners to ensure that they are functional before the final maturation events occur (Karbstein, 2013). A similar mechanism may occur in bacteria, as it was shown in *E. coli* that initiator tRNA plays a role in triggering final 16S rRNA trimming in *E. coli* (Shetty and Varshney, 2016). Final rRNA trimming is believed to rubber-stamp ribosome assembly, protecting correctly assembled particles from degradation by limiting the access of exoribonucleases to the ends of rRNA (Baumgardt et al., 2018). In both *B. subtilis* and in *E. coli,* RNase R is believed to be involved in quality control of rRNA (Baumgardt et al., 2018; Jacob et al., 2013). Early experiments in *E. coli* using RNase R mutants in combination with a thermosensitive mutation of PNPase, demonstrated that stable rRNA does turn over, as exemplified by a large accumulation of rRNA fragments in the double mutant (Cheng and Deutscher, 2003). These fragments were shown to arise from initial RNase E cleavages, and to accumulate in the absence of the two exonucleases because they are not further degraded (Sulthana et al., 2016). Accumulation of these fragments is deleterious for the cells as it interferes with ribosomal assembly, probably by competing with nascent rRNA transcripts for the pool of available r-proteins. Besides, rRNA processing is also a quality control mechanism that discriminates mature particles from poorly assembled ones: for example, the 16S 3' rRNA processing by YqfG that prevents mature 30S from degradation by RNase R (Baumgardt et al., 2018). It is worth noting that RNase R degrades 70S particles containing a 16S rRNA precursor but not pre-30S, suggesting that RNase R requires subunits to be associated for its function in quality control.

Direct evidence of rRNA quality control for defective ribosomes came from the observation that rRNA mutants defective for ribosome assembly led to rRNA degradation.

Indeed, study of a series of 23S rRNA deletion mutants revealed that some were integrated into ribosomal particles whereas others were not and were ultimately degraded (Liiv et al., 1996). It was also shown that mutations in the 5' leader sequence of 16S rRNA affect both the synthesis of 16S rRNA and its assembly into the 30S subunit, leading to decreased 16S rRNA stability (Schäferkordt and Wagner, 2001). As mentioned earlier, rRNA maturation in *B. subtilis* has an integrated ribosome assembly quality control checkpoint, as proteins L3 and L18 are required for 23S rRNA cleavage by Mini-III and 5S rRNA cleavage by M5, respectively (Pace et al., 1984; Redko and Condon, 2009).

– *Ribosome degradation under stress conditions*

In addition to rRNA degradation *via* ribosome quality control that probably occurs at basal levels throughout growth, ribosomes can also be extensively degraded during starvation or following damage to the cell membrane (Deutscher, 2009). As part of a "growth rate control" mechanism (described below), bacterial cells adjust their ribosome concentration mainly at the level of synthesis. However, in case of rapid nutritional deprivation, excess ribosomes are degraded and the ability to recycle macromolecular components is likely to play an important role in survival (Kaplan and Apirion, 1975). During amino acid starvation, translation activity slows down, leading to an increase in free ribosomal subunits that were shown to be susceptible to RNases because of their exposed RNA intersubunit interfaces (Zundel et al., 2009). Degradation of rRNA during starvation was shown to rely on initial cleavages by RNase E, similar to ribosome degradation during quality control. However, in contrast to quality control, rRNA degradation during starvation targets ribosomes that were previously stable. Moreover, during starvation, RNase E cleavages in the 16S rRNA are prompted by an initial trimming of nucleotides from its 3' end by RNase PH, as opposed to the RNase PH-independent degradation of rRNA occuring during quality control (Basturea et al., 2011; Sulthana et al., 2016). It is noteworthy that RNase II and RNase R are involved in the degradation of RNase E-generated fragments to mononucleotides during starvation, whereas during quality control RNase E-generated fragments are further degraded by PNPase and RNase R (Basturea et al., 2011).

Damage to the cellular membrane also triggers ribosome degradation in *E. coli*, in this case, through the release of the endoribonuclease RNase I from the periplasm of Gram-negative species into the cytoplasm. This nonspecific RNase degrades ribosomes extensively,

including intact mature 70S ribosomes that are generally resistant to the action of RNases (Deutscher, 2009). Whether RNase I could also be involved in ribosome degradation during physiological responses to starvation, for example, is still unclear. It is also not clear whether a similar mechanism of rRNA degradation occurs in Gram-positive cells with a compromised cell envelope. However, *B. subtilis* has both an extracellular RNase (RNase Bsn) (Nakamura et al., 1992) and a cell-wall associated RNase (YhcR) (Oussenko et al., 2004) that could potentially fulfill this role.

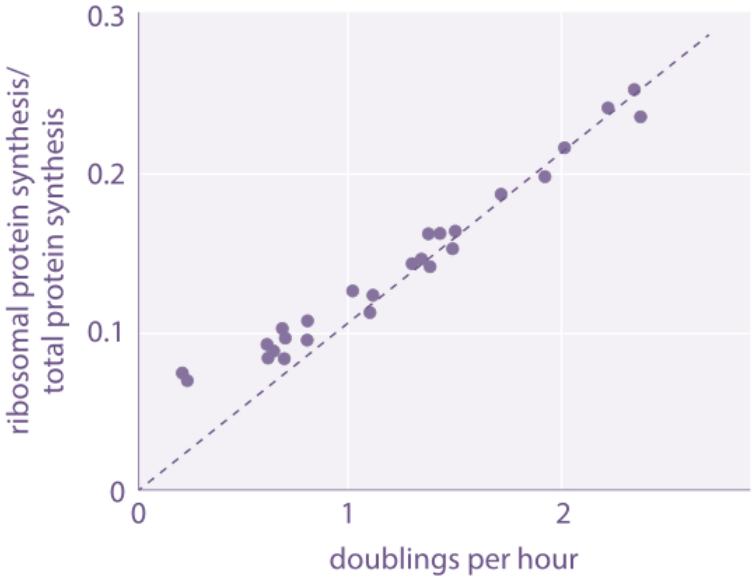

Figure 16: Ribosome synthesis as a function of growth rate

Measurements were performed on cultures in balanced growth. The ratio of the ribosome fraction to growth rate is relatively constant for the faster growth rates in the range of 24-40 minutes.

Adapted from (Neidhardt et al., 1994).

III. Regulation of ribosome synthesis and the role of the alarmone (p)ppGpp

Intuitively, cells need to adjust their number of ribosomes to fit their requirements for translation. This regulation is believed to occur mainly at the level of ribosome synthesis, and more precisely by regulation of rRNA transcription initiation. Early studies of rRNA transcription regulation uncovered the crucial role that the alarmone (p)ppGpp played in this process. Further research characterized the molecular determinants of control by (p)ppGpp and uncovered the effects of this molecule on both the regulation of rRNA synthesis and transcription globally. In this section, from an historical point of view, I will give an overview of the regulation of ribosome synthesis and the contribution of (p)ppGpp from an historical point of view. I will then provide a non-exhaustive review on the expansive role that this molecule is now recognized to play in bacterial physiology.

1. Regulation of ribosome synthesis

Maaløe, Kjeldgaard and others from the “Copenhagen school” documented in early studies that the macromolecular composition of the bacterial cell was related to its metabolic activity. Indeed, these studies of bacterial physiology revealed that the amounts of these macromolecules are exponential functions of growth rate at a given temperature and that their relative proportions vary with the growth rate (Schaechter et al., 1958). Since protein is the major constituent of any cell, ribosome synthesis is also tightly coupled to growth rate. The regulation of ribosome synthesis ensures the ability of the cell to adapt to changing translational requirements, while preventing the over-investment of cellular resources in the energy-costly process of ribogenesis. Thus, bacterial cells adjust their ribosome concentration such that fast growing cells can have up to 10-fold more ribosomes than slow growing ones (Dennis and Bremer, 2008). This regulation of ribosome biosynthesis is known as “growth rate control” and describes a linear relationship between cellular ribosome content and a wide range of growth rates (Figure 16). However, at very slow growth rates, cells appear to maintain an excess of non-translating ribosomes maybe to allow a rapid response upon relief of the nutritional limitation (Koch and Deppe, 1971).

Stress conditions such as the nutrient shortage occurring at the onset of stationary phase results in the conversion of 70S ribosomes into hibernating 100S ribosomes (Beckert et al., 2017). This phenomenon involves dimerization of excess of 70S ribosomes into an inactive stored 100S form through the binding of ribosome modulation factor (RMF) or hibernation promoting factor (HPF) (for review see (Yoshida and Wada, 2014)). When conditions become favorable for growth again, hibernating ribosomes quickly dissociate into active 70S ribosomes as part of an important survival strategy for bacteria.

a. Ribosomal RNA regulation and the discovery of the stringent response

The synthesis of ribosomes is primarily controlled at the level of initiation of rRNA synthesis, with r-protein synthesis tightly tuned to rRNA levels through mechanisms that will be described below. Historically, the first identified mechanism of control of rRNA transcription was the stringent response in *E. coli*, characterized through the isolation of "relaxed" (*rel*) mutants that had lost the ability to shut-down stable RNA synthesis in conditions where protein synthesis was inhibited due to amino acid starvation. The effectors of the stringent response are guanosine tetra-phosphate (ppGpp) and guanosine penta-phosphate (pppGpp), collectively referred to as (p)ppGpp. These "alarmones" were first characterized by their sudden appearance in thin layer chromatographs of total nucleotides extracted from amino acid-starved *E. coli* cells and are therefore historically known as "magic spots I and II" (Cashel and Gallant, 1969). Accumulation of (p)ppGpp during amino acid starvation was shown to be concomitant with the shut-down of rRNA and tRNA synthesis (Cashel and Rudd, 1987). Relaxed mutants, on the other hand, failed to synthesize (p)ppGpp or cease rRNA synthesis under the same conditions. (p)ppGpp was later shown to bind RNA polymerase in *E. coli* and inhibit initiation of transcription at rRNA and tRNA promoters specifically (Ross et al., 2013).

Later work expanded the role of (p)ppGpp far beyond the stringent response and showed that it plays a broader role in bacterial physiology, participating in resource allocation both in stressed and unstressed conditions. Optimization of growth rate according to nutrient availability is important for bacterial survival. Therefore, bacteria have evolved various signaling pathways to monitor their environmental conditions and to adapt to

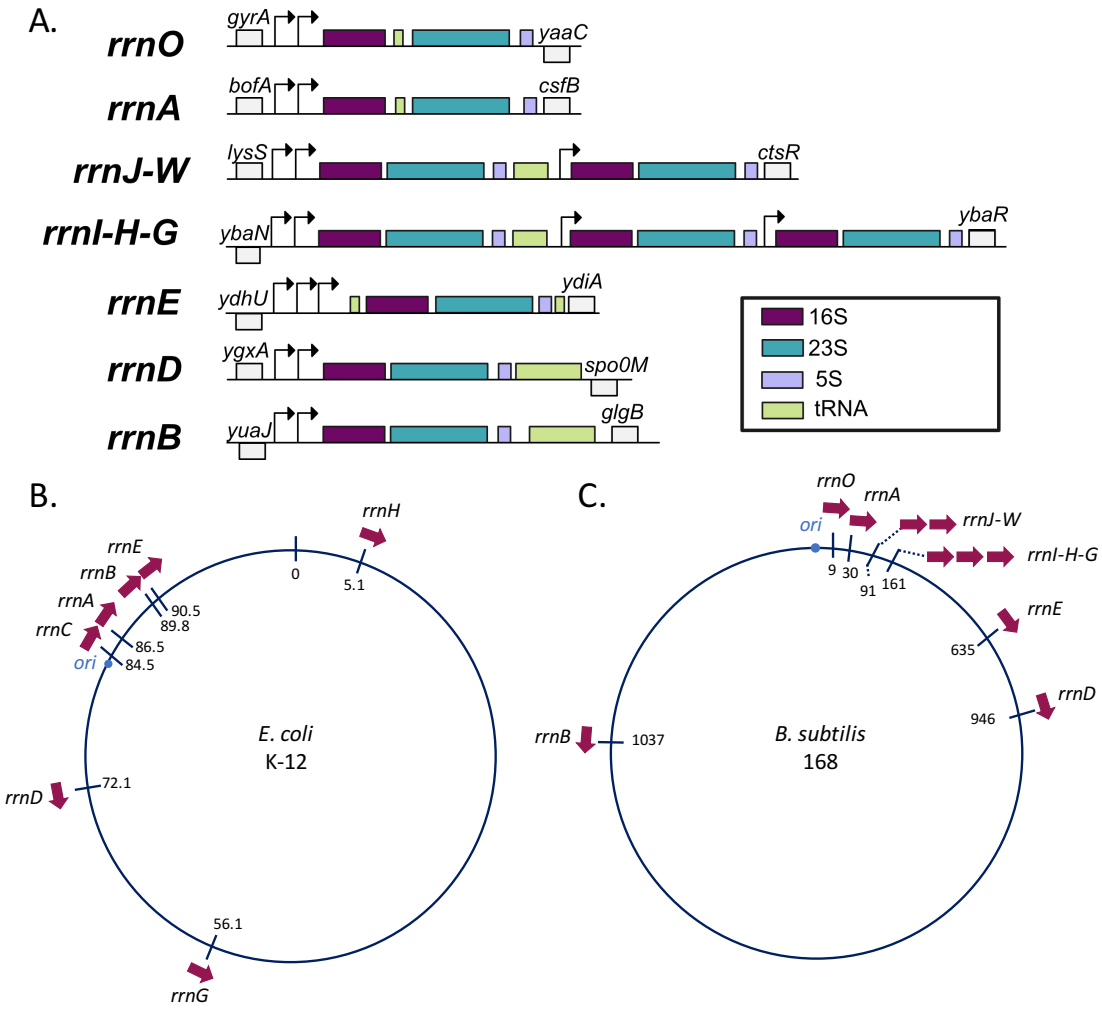

Figure 17: Organization of the ten *B. subtilis rrn* operons and location of *rrn* operons in *E. coli* and *B. subtilis*

A) *B. subtilis* contains 10 *rrn* operons, their structure is represented with a color code for 16S, 23S, 5S and tRNA genes indicated in the bottom right box.

B) *E. coli* contains 7 *rrn* operons; their position on the chromosome is indicated in minutes and their orientation is represented by the arrow.

C) *B. subtilis* contains 10 *rrn* operons, the numbers indicate their distance (in kbp) from the origin of replication (ori). Arrows indicate orientation of *rrn* genes.

Figure adapted from (Condon et al., 1993; Nanamiya et al., 2010; Natori et al., 2009)

changes. In response to external stimuli, most of these systems provoke concentration changes in secondary messenger molecules, including (p)ppGpp, cyclic adenosine monophosphate (c-AMP) and cyclic di-guanosine monophosphate (c-di-GMP), that are pleiotropic regulators of key molecular targets leading to rapid induction of an appropriate cellular response (Pesavento and Hengge, 2009).

The impact of (p)ppGpp on transcription was further demonstrated in transcriptome analyses of several bacterial species (Traxler et al., 2008). When nutrients become limiting for growth, (p)ppGpp alters transcription globally, shifting nutritional resources to other priorities, including amino acid biosynthesis. The various signals triggering the production of (p)ppGpp and its different regulatory roles during stress responses will be discussed below (see (Hauryliuk et al., 2015) for review). The stringent response constitutes an extreme case of regulation by (p)ppGpp as this molecule is produced in maximal amounts (millimolar range) under these conditions. In fact, the regulatory effects of (p)ppGpp also take place at much lower concentrations and play a fundamental role in the maintenance of cellular homeostasis in regular growth conditions. Notably, (p)ppGpp is involved in adjustment of rRNA synthesis to the bacterial growth rate through complex transcriptional regulatory networks (see section on Growth rate control).

i. Ribosomal RNA transcription regulation

As mentioned earlier, rRNA synthesis is the rate-limiting step in ribosome synthesis in both *E. coli* and *B. subtilis* (Henkin, 2002) and its regulation occurs primarily at the level of *rrn* transcription initiation. Although most of the genes that encode ribosomal proteins are present as a single copy per genome, the copy number of rRNA operons differs greatly between bacteria (Klappenbach et al., 2001). For example, *Mycoplasma* and *Mycobacterium* species have a single rRNA operon whereas the genomes of *E. coli* and *B. subtilis* contain seven and ten *rrn* operons, respectively (Figure 17). The majority of *rrn* operons is located near the origin of chromosomal replication and under rapid growth conditions, the *rrn* copy number is significantly amplified (>30 copies) by the fact that replication is initiated multiple times before each cell divides, with daughter cells inheriting already partially replicated chromosomes (Henkin, 2002). In this way, transcription of *rrn* operons accounts for more than a half of the cell's total RNA synthesis in rapidly growing cells

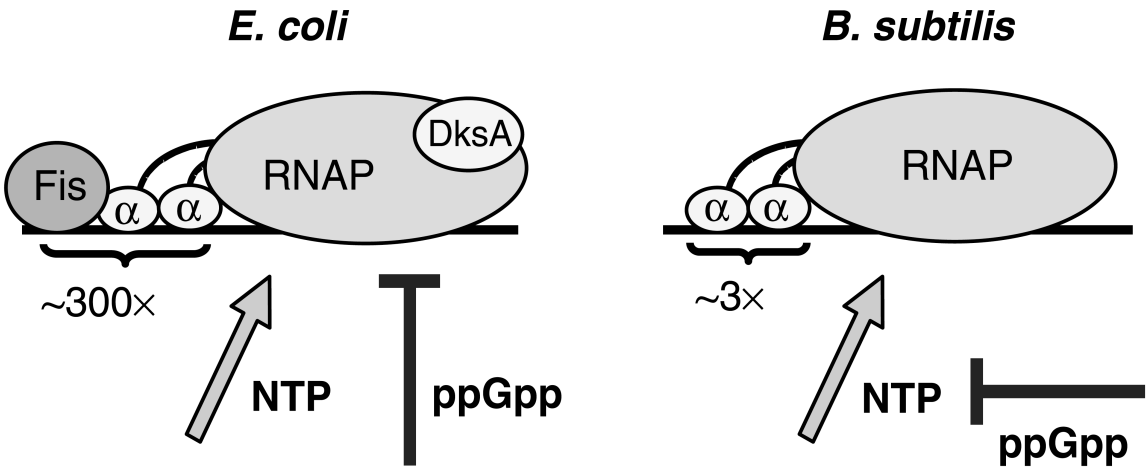

Figure 18: Schematic of mechanisms contributing to *rrn* promoter activity in *E. coli versus B. subtilis*

The open complexes of *rrn* promoters are intrinsically short-lived in both organisms. In E. coli, iNTP acts as a positive effector whereas (p)ppGpp acts as a negative effector directly affecting open complex stability. Although changing iNTP and (p)ppGpp concentrations regulate rRNA promoter activities in both bacteria, in *B. subtilis* rRNA transcription inhibition by (p)ppGpp is thought to be indirect *via* the reduction of GTP levels (which is the iNTP of the ten *B. subtilis rrn* operons). Fis (factor for inversion stimulation) is a transcriptional regulator involved in activation of *rrn* operon transcription in *E. coli*. Fis is absent in *B. subtilis* and it is currently not known how *B. subtilis rrn* promoters achieve their strength.

Figure adapted from (Krásný and Gourse, 2004)

(Dennis and Bremer, 2008).

In *E. coli, rrn* transcription originates at two tandem promoters P1 and P2. Transcription from these promoters increases or decreases in response to growth rate (growth rate control) and ceases in response to amino acid starvation (stringent response). In the tandem configuration, the P1 promoter is the major target for regulation, especially by growth rate control, while the downstream promoter (P2) is less active, being largely occluded by RNA polymerase (RNAP) molecules initiating transcription at P1 (see (Condon et al., 1995) for review). In *E. coli*, the high basal level of *rrn* transcription relies mainly on regulatory sequences immediately upstream of the P1 promoter that bind the two α-subunits of RNAP (the UP-element) and sequences further upstream that bind the transcription activator Fis, leading to 20- to 50-fold and 3- to 8-fold increase in promoter activity, respectively (Figure 18) (Krásný and Gourse, 2004). In *E. coli,* the transcription factor DksA binds both the secondary channel of RNAP and (p)ppGpp, thus potentiating the effects of the alarmone on transcriptional regulation (Paul et al., 2004). Because *rrn* promoters form open complexes with very short half-lives compared to most other promoters, they are highly sensitive to changing concentrations of their initiating nucleotide (iNTP) concentration (Gaal et al., 1997). Moreover, (p)ppGpp binding to the *E. coli* RNAP and DksA is known to increase the rate of open complex collapse, which likely explains the inhibition of rRNA transcription during stringent response (Gourse et al., 2018). Usually, the discriminator region, i.e. the DNA sequence between the -10 box and the +1 transcriptional start site, governs whether (p)ppGpp has a repressing (GC-rich region) or activating effect (AT-rich region) on transcription (Wagner, 2002). tRNA genes located outside of *rrn* operons possess promoters ressembling *rrn P1* promoters (see below) and are thus also regulated in the same way (Jinks-Robertson et al., 1983).

B. subtilis uses a different strategy to *E. coli* to control rRNA synthesis during the stringent response (Krásný and Gourse, 2004). Six *rrn* operons have tandem P1-P2 promoters (*rrnA, rrnB, rrnD, rrnI, rrnJ, rrnO*) and four have only a single promoter (*rrnE, rrnG, rrnH, rrnW*) (Figure 17). As in *E. coli,* the *rrn* P1 promoters display more pronounced changes with growth rate and stress than their respective *rrn* P2 promoters. In *Firmicutes*, (p)ppGpp does not physically interact with RNAP and no DksA homolog has been found. All *B. subtilis rrn* promoters initiate with GTP as iNTP and can be controlled directly by the cellular

concentration of GTP. The effect of (p)ppGpp on *rrn* promoter activity is indirect and results from modulation of GTP pools (Figure 18), by binding to and inhibiting the GmK and HprT enzymes involved in the *de novo* and salvage pathways of GTP synthesis, respectively (Kriel et al., 2012) (see III.3.a. and Figure 24).

Therefore, (p)ppGpp can regulate transcription both directly and indirectly and the underlying mechanisms can vary between species.

– *Growth rate control*

As described above, the number of ribosomes and therefore the synthesis of rRNA, has been shown to be regulated to match the growth rate afforded by the medium (Dennis and Bremer, 2008; Koch and Deppe, 1971). Early studies reported an inverse linear correlation between rRNA synthesis and the levels of (p)ppGpp (Ryals et al., 1982; Sarubbi et al., 1988). Although there were some initial disagreements between the main groups studying this phenomenon, it is now generally accepted that (p)ppGpp is indeed the effector of growth rate control of ribosome synthesis (Potrykus et al., 2011). (p)ppGpp is present at concentrations in the millimolar range upon induction of stringent response as opposed to the micromolar range of concentrations found during steady state growth (Cashel and Rudd, 1987; Wagner, 2002). The model of growth-rate dependent regulation of ribosome synthesis has been established in *E. coli,* where (p)ppGpp was proposed to directly modulate *rrn* expression by restricting the numbers of RNAP initiating at rRNA and tRNA promoters. This implies that stringent response is an extreme case of growth rate dependent regulation and that (p)ppGpp also acts at lower concentrations than those produced during stringent response. As a result, in addition to its role during the amino acid stress response, this alarmone plays an important role in the maintenance of cell homeostasis. In *E. coli,* SpoT has been proposed to maintain the basal level of (p)ppGpp found during exponential growth, whereas RelA is responsible for the production of large amounts of (p)ppGpp during the stringent response (Murray and Bremer, 1996). However, it is still unclear by which mechanism SpoT senses growth rate to adjust (p)ppGpp production.

– *Feedback control*

rRNA synthesis is also regulated by the number of copies of functional *rrn* operons

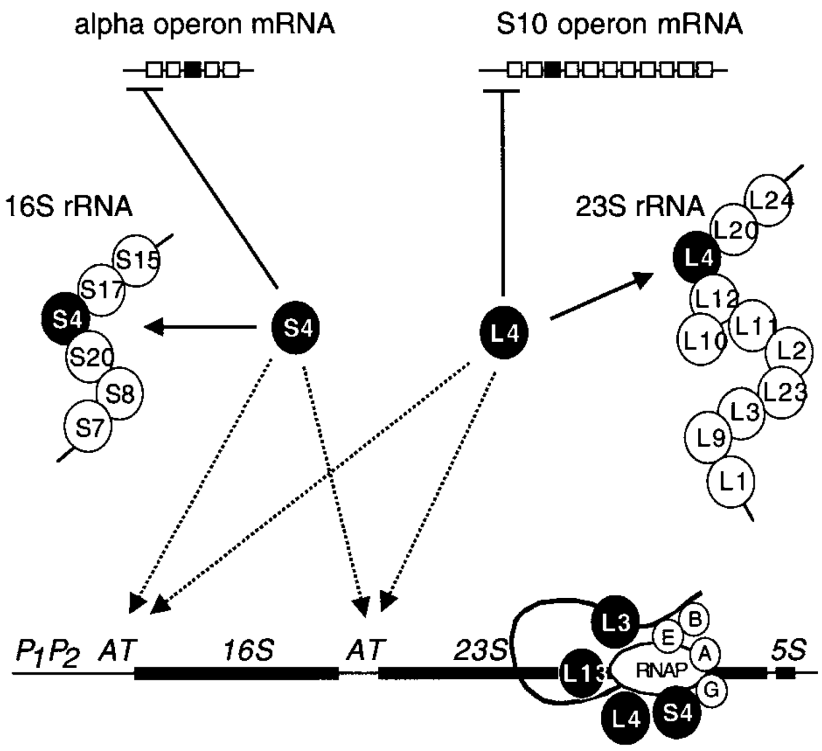

Figure 19: Model of the *rrn* antitermination complex.

This model shows putative tethering of the RNA AT (antitermination) sequence to the transcription complex. The Nus factors NusA, NusB, NusE and NusG are represented by single-letter abbreviations. The r-proteins proposed to participate in the antitermination complex are represented in black. Regulatory r-proteins S4 and L4, that are in excess over rRNA will simultaneously decrease expression of their own operons (represented at the top) by translational feedback control (solid lines), and by increased synthesis of rRNA caused by stimulated assembly of antitermination complexes at the leader and spacer AT motifs. 16S and 23S rRNA are shown associated with known primary binding proteins.

Figure adapted from (Torres, 2001).

through a mechanism known as feedback control. This control mechanism also acts primarily at the level of transcription initiation at the *rrn* P1 promoters. This model proposes that the cell's translational capacity is monitored to adjust ribosome production according to needs. The feedback model resulted from gene dosage experiments with strains carrying an intact or a defective copy of an *rrn* operon on a multicopy plasmid (Jinks-Robertson et al., 1983). Additional ectopic functional copies did not result in increased production of rRNA, but rather lead to a reduction in the expression of chromosomal *rrn* operons to keep the overall rRNA synthesis levels unchanged. In contrast, strains expressing a defective copy of the *rrn* operon (inactivated by an internal deletion in the rRNA coding region), failed to repress transcription of the chromosomal copies, showing that this control is related to the number of functional ribosomes. Reciprocally, inactivation of chromosomal *rrn* operons causes an increase in expression of the remaining copies, consistent with the model of feedback regulation by the amount of functional ribosomes (Condon et al., 1993). The mechanism of feedback control is still unclear. One might have expected that derepression of the expression of the remaining intact *rrn* operons would be accompanied by a decrease in (p)ppGpp levels, if the effector of feedback control was the same as growth rate control, but this was apparently not the case (Condon et al., 1993).

– *Antitermination*

To ensure stoichiometric production of each ribosomal subunit, rRNA transcripts must somehow escape polar effects on transcription. The phenomenon of polarity was first observed when mutations causing premature translation termination were found to reduce transcription of the downstream genes in the same operon due to an increase in premature transcription termination (Adhya and Gottesman, 1978). Indeed, translation is usually coupled to the transcription of mRNA in bacteria, with the presence of ribosomes on the transcript restricting the access of the transcription termination factor Rho to these transcripts. Transcription of untranslated rRNAs escapes polarity *via* a mechanism known as antitermination. Briefly, specific RNA sequences (known as AT for antitermination) located in the leader region upstream of the mature 16S rRNA sequence and in the spacer region between the 16S and 23S rRNA are bound by Nus factors (NusA, NusB, NusE/S10 and NusG) forming a termination-resistant RNAP elongation complex capable of transcribing many kilobases of untranslated RNA without stopping (Figure 19) (for review, see

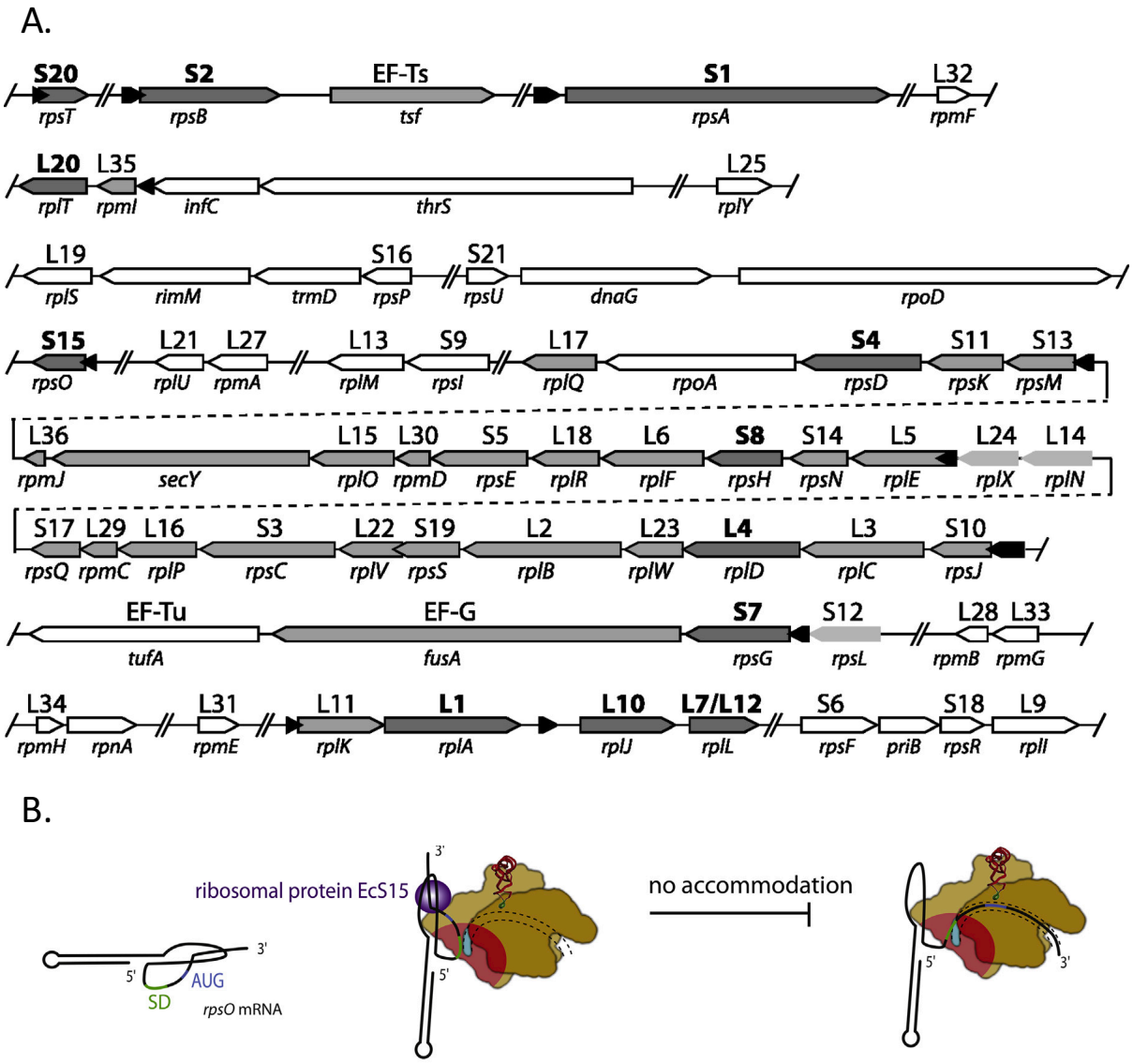

Figure 20: Ribosomal protein gene organization in *E. coli* and the example of S15 autogenous control.

A) Gene and protein names are given below and above each arrow, respectively. Black arrows represent autoregulatory RNA structures and grey arrows represent genes that are autogenously regulated. Dark grey indicates proteins responsible for regulation and light grey corresponds to genes with reported retro-regulation.

B) Ribosomal protein S15 from *E. coli* (in purple) prevents accommodation of its own mRNA into the ribosome decoding channel using an entrapment mechanism.

Figure adapted from (Duval et al., 2015; Fu et al., 2013).

(Condon et al., 1995)). The antitermination complex potentially contributes to correct ribosome assembly at multiple levels. First, it ensures that all RNAPs get to the end of the long *rrn* operon without falling off, which would generate truncated rRNAs that could potentially titrate r-proteins and inhibit assembly (Schäferkordt and Wagner, 2001). Second, the transcription antitermination complex was found to contain several early assembled r-proteins (S4, L3, L4 and L13). It has been proposed that this may contribute to assembly by "delivering" r-proteins to their sites of binding on the nascent rRNAs (Torres, 2001). Lastly, the *rrn* antitermination system increases the transcription elongation rate (over 80 nts per second versus 40 nts per second for mRNA), which may benefit ribosome assembly by avoiding rRNA folding kinetic traps (Vogel and Jensen, 1995).

b. Regulation of r-protein synthesis

Regulation of r-protein expression occurs mainly at the level of translation. This is critical to be able to achieve the correct stoichiometry between rRNA and r-proteins in the ribosome. Two mechanisms control r-protein expression to achieve these stoichiometric relationships: translational coupling and autogenous control.

– *Translational coupling*

Most r-protein genes are encoded in densely packed operons with other r-protein genes, other components of the translation machinery and/or genes encoding ribosome assembly cofactors or, in some cases, components of the transcription apparatus (Figure 20). In this context, translation of a particular r-protein gene usually depends on translation of the preceding gene through a process called translational coupling. For example, translation of the upstream gene may melt an RNA secondary structure that sequesters the ribosome binding site of the downstream gene and thereby expose it for initiation. Or the ribosome itself might be transferred directly from the termination codon of the upstream gene to the initiation codon of the downstream gene. Such mechanisms can coordinate expression of as many as 11 gene products from a single r-protein mRNA (as shown for the S10 operon in *E. coli*) (Nomura et al., 1984).

– *Autogenous control*

Ribosomal protein synthesis in *E. coli* is also subjected to "autogenous control" or

"feedback regulation". Indeed, specific r-proteins are able to bind their own mRNA and regulate expression of their own operons. Most regulatory r-proteins are "primary" binding proteins i.e. that they can bind directly to naked rRNA *in vitro* (Fu et al., 2013). During balanced growth, r-proteins are rapidly incorporated into assembling ribosomes. However, in conditions where more of a regulatory r-protein accumulates than can be incorporated into ribosomes, this r-protein can bind its own mRNA at a structure that mimics its primary binding site on the ribosome (operator sequence) to exert repression (Figure 19) (Guillier et al., 2005; Mathy et al., 2004). Since the regulatory r-proteins are often encoded by the first cistron of r-proteins operons, blocking the translation of the first gene of the operon, thereby represses all translationally coupled downstream genes. The so-called repressor r-proteins include S1, S2, S4, S7, S8, S15, S20, L1, L4, L10, L7/L12 and L20 (Figure 20) (Nomura et al., 1984; Portier et al., 1990). Autogenous regulation by S15 (*rpsO*), for example, has been investigated both in *E. coli* and in *Thermophilus thermophilus* and was shown to rely on different regulatory mechanisms. In *T. thermophilus* S15 binding to the *rpsO* mRNA masks the RBS (ribosome binding site) preventing its interaction with the 30S subunit. In contrast, *E. coli* S15 binding to a pseudoknot structure in *rpsO* mRNA does not abolish interaction with the 30S subunit, but rather prevents *rpsO* accommodation into the ribosome decoding channel, thus, inhibiting translation by a "trapping" mechanism (Figure 20) (Duval et al., 2015; Marzi et al., 2007).

2. Diversity of (p)ppGpp metabolism enzymes

As we have seen in the previous section, (p)ppGpp was initially identified for its crucial role in ribosome synthesis regulation both during steady state growth and during stress. Interestingly, a plethora of enzymes capable of (p)ppGpp synthesis and/or degradation have been identified through the bacterial kingdom and these nucleotides are now recognized to be pleiotropic regulators of several bacterial functions. In the following two sections I will give an overview of the different (p)ppGpp metabolizing enzymes and the recent insights into their function, before presenting a non-exhaustive list of some of the regulatory roles of these nucleotides.

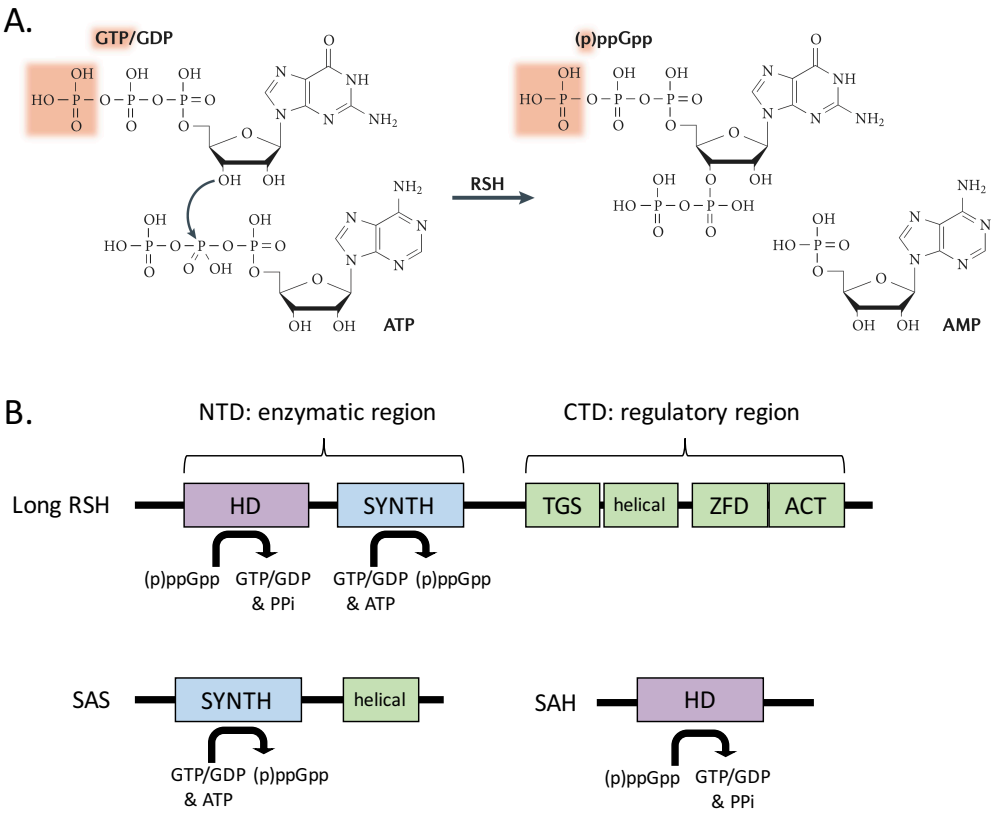

Figure 21: (p)ppGpp synthesis and a schematic of the enzymes involved in its metabolism

A) Guanosine tetraphosphate and guanosine pentaphosphate (referred as (p)ppGpp) synthesis by RelA-SpoT homologs enzymes (RSH) consumes ATP and either GDP or GTP, respectively. The γ-phosphate moiety of GTP and pppGpp is highlighted in orange; these moieties are not present in GDP and ppGpp. The alarmones (p)ppGpp and nucleotides GTP/GDP are highly similar, differing only by the presence of the pyrophosphate moiety attached to the 3'-OH of the ribose.

B) Long RSH proteins consist of an enzymatic N-terminal domain (NTD) and a regulatory C-terminal domain (CTD). The NTD comprises a HD domain (hydrolase domain, in purple) that degrades (p)ppGpp into PPi and GTP or GDP, and a SYNTH domain (synthetase domain, in blue) that converts GTP/GDP and ATP to (p)ppGpp. The CTD regulatory region contains (in green) a TGS domain (ThrRS, GTPase and SpoT domain), a conserved alpha helical domain (helical), a ZFD domain (zinc-finger domain) and an ACT domain (aspartate kinase, chorsimate and TyrA domain). Small alarmone synthetase (SAS) and small alarmone hydrolase (SAH) contains a single SYNTH or HD domain, respectively.

Figure adapted from (Hauryliuk et al., 2015; Irving and Corrigan, 2018).

Nucleotide-based signaling systems typically have distinct enzymatic activities that synthesize and degrade second messenger molecules that can act as allosteric regulators (Pesavento and Hengge, 2009). ppGpp and pppGpp are formed by the addition of the pyrophosphate moiety of ATP to the 3' position of GDP and GTP, respectively (Figure 21). Several enzymes with hydrolyze and/or synthetase activities are involved in (p)ppGpp metabolism (Steinchen and Bange, 2016). These enzymes can be divided into three major groups: "long" RSH enzymes (RelA/SpoT homologs) bearing both hydrolase and synthetase domains and "short" enzymes containing either the synthetase or hydrolase domain only, known as SAS (Small Alarmone Synthetase) and SAH (Small Alarmone Hydrolase), respectively (Figure 21). These enzymes are widely distributed in bacteria and can coexist in various combinations (Atkinson et al., 2011) (Figure 23). For example, *E. coli* has two RSHs: RelA and SpoT, whereas *B. subtilis* has one RSH (named RelA or Rel_{Bs}) and two SASs (YwaC or RelP, and YjbM or RelQ).

a. Long RSHs (RelA-SpoT Homologs)

Historically, (p)ppGpp synthesis was identified as a ribosome-associated activity triggered by amino-acid starvation in *E. coli* as part of the so-called "stringent response". The gene encoding the (p)ppGpp synthetase was named *relA* for the relaxed phenotype of the mutant characterized by the alleviation of stringent control of rRNA transcription (Cashel and Rudd, 1987). The *relA* gene encodes a synthetase domain (SYNTH) that can synthetize both ppGpp and pppGpp (Haseltine and Block, 1973). (p)ppGpp hydrolase activity was subsequently identified and shown to be encoded by the *spoT* gene (Stamminger and Lazzarini, 1974). The SpoT protein is a bifunctional enzyme carrying a SYNTH domain with weak synthetase activity and a hydrolysis domain (HD) with strong (p)ppGpp degradation activity (Sarubbi et al., 1989). Note that the HD domain is also present in RelA, but is inactive due to the lack of key catalytic residues. The RelA and SpoT proteins are exclusively found in the β- and γ-subdivisions of the Proteobacteria and are thought to arise from the duplication and of an ancestral *rel* gene (Figure 23) (Mittenhuber, 2001). *B. subtilis* possess an ancestral bi- functional RSH protein encoded by the *relA* gene that is widespread in Gram-positives (Wendrich and Marahiel, 1997). Long RSHs also usually contain other characteristic domains

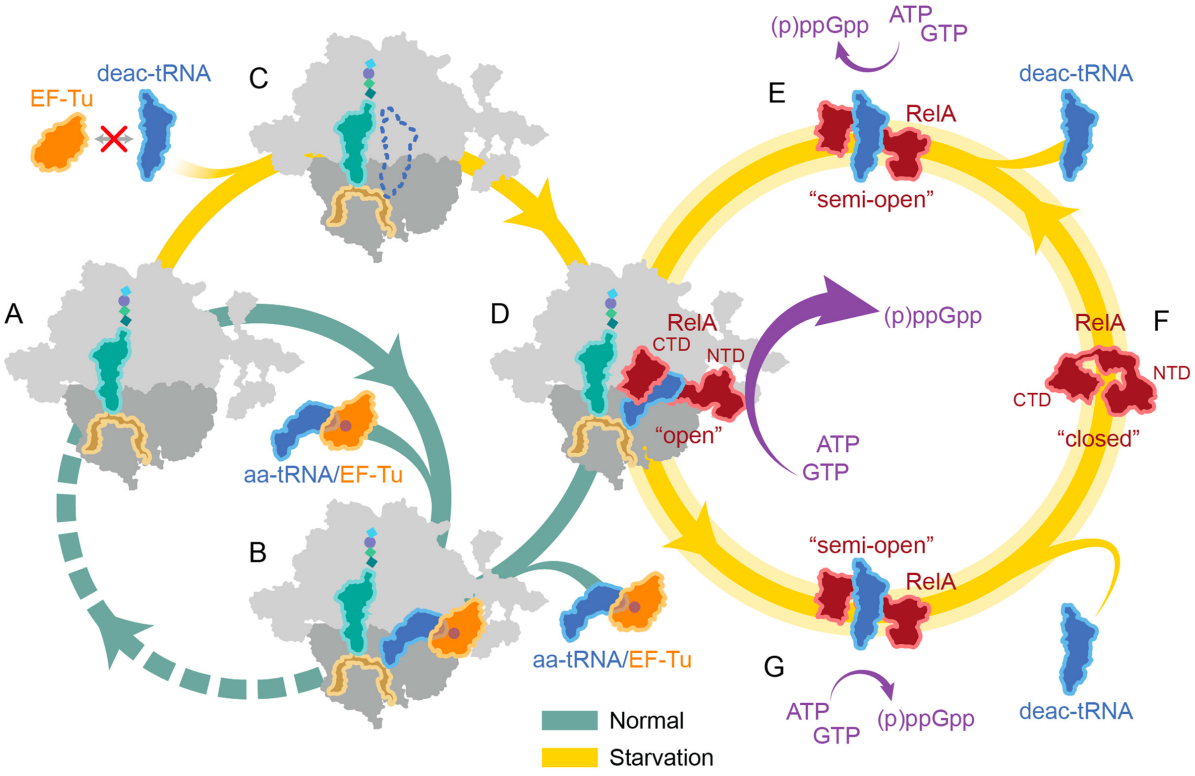

Figure 22: Model for RelA action during the stringent response

(A and B) Under optimal conditions, aminoacyl-tRNAs (aa-tRNAs) are delivered by EF-Tu (in orange) to the A-site of the ribosome (along the green pathway).

(C to G) Under starvation conditions (yellow pathway), the interaction of RelA (in red) with the deacetylated tRNA in the A-site of the ribosome leads to the conversion of RelA from a "closed" to an "open" conformation and thereby stimulates high levels of (p)ppGpp synthesis (see text). The deacetylated tRNA adopts a distorted conformation (named A/R-tRNA) which is stabilized by RelA, i.e. the anticodon stem loop interacts with the mRNA while the acceptor 3' end contacts RelA. Note that the RelA interaction with the CCA-end, suggests its involvement in discriminating deacetylated from aminoacylated tRNAs.

Figure adapted from (Arenz et al., 2016).

in their carboxy-terminal domain (CTD) region (Hauryliuk et al., 2015; Irving and Corrigan, 2018). Cryo-EM studies revealed that the Rel/RelA CTD contains the regulatory and ribosome-binding regions responsible for uncharged tRNA sensing during the stringent response (Agirrezabala et al., 2013; Brown et al., 2016).

Early experiments showed that presence of uncharged tRNA in the ribosome acceptor site (A-site) acts as a marker of amino acid deficiency and triggers the stringent response (Haseltine and Block, 1973). Different models exist either where RelA associates with the uncharged tRNA independently of the ribosome and loads it into the empty A-site or RelA "hops" from one ribosome to another and senses when an uncharged tRNA is bound in the A-site (Brown et al., 2016; Winther et al., 2018). The "hopping model" was proposed to explain how such a low amounts of RelA (one RelA for every 200 ribosomes (Pedersen and Kjeldgaard, 1977)) are sufficient to sample the whole translating ribosome population (Wendrich et al., 2002). Regardless, to ensure proper activation of (p)ppGpp synthesis, RelA has to discriminate between charged and uncharged tRNAs present in the ribosomal A-site. Cryo-EM studies revealed that, contrary to amino-acylated tRNA that has its 3' end buried deep in the peptidyl-transferase center, uncharged tRNA in the A-site adopts a distorted conformation (named A/R-tRNA) making contacts with both the A-site codon and the CTD of RelA, leading to its activation (Figure 22–D) (Agirrezabala et al., 2013; Brown et al., 2016). As mentioned earlier, RelA has a multi-domain architecture with an N-terminal domain (NTD) region containing the (p)ppGpp HD and SYNTH domains, whereas the CTD is responsible for ribosome binding and regulation (Agirrezabala et al., 2013). Free RelA is thought to adopt an auto-inhibitory conformation ("closed" conformation), where the CTD is involved in oligomerization or in an intramolecular interaction with the SYNTH domain that inhibits (p)ppGpp synthesis (Figure 22–F) (Gropp et al., 2001; Yang and Ishiguro, 2001). The interaction of RelA with uncharged tRNA and the ribosome has been proposed to promote an open conformation, suppressing auto-inhibition and triggering (p)ppGpp synthesis (Figure 22–D) (Arenz et al., 2016; Brown et al., 2016). RelA activation causes it to detach from the ribosome. However, it is not clear whether (p)ppGpp synthesis occurs on the ribosome or as RelA is detached (English et al., 2011; Li et al., 2016; Wendrich et al., 2002). RelA is subjected to positive allosteric regulation by (p)ppGpp which, above a certain threshold, induces a positive feedback leading to several rounds of (p)ppGpp synthesis by RelA in the dissociated

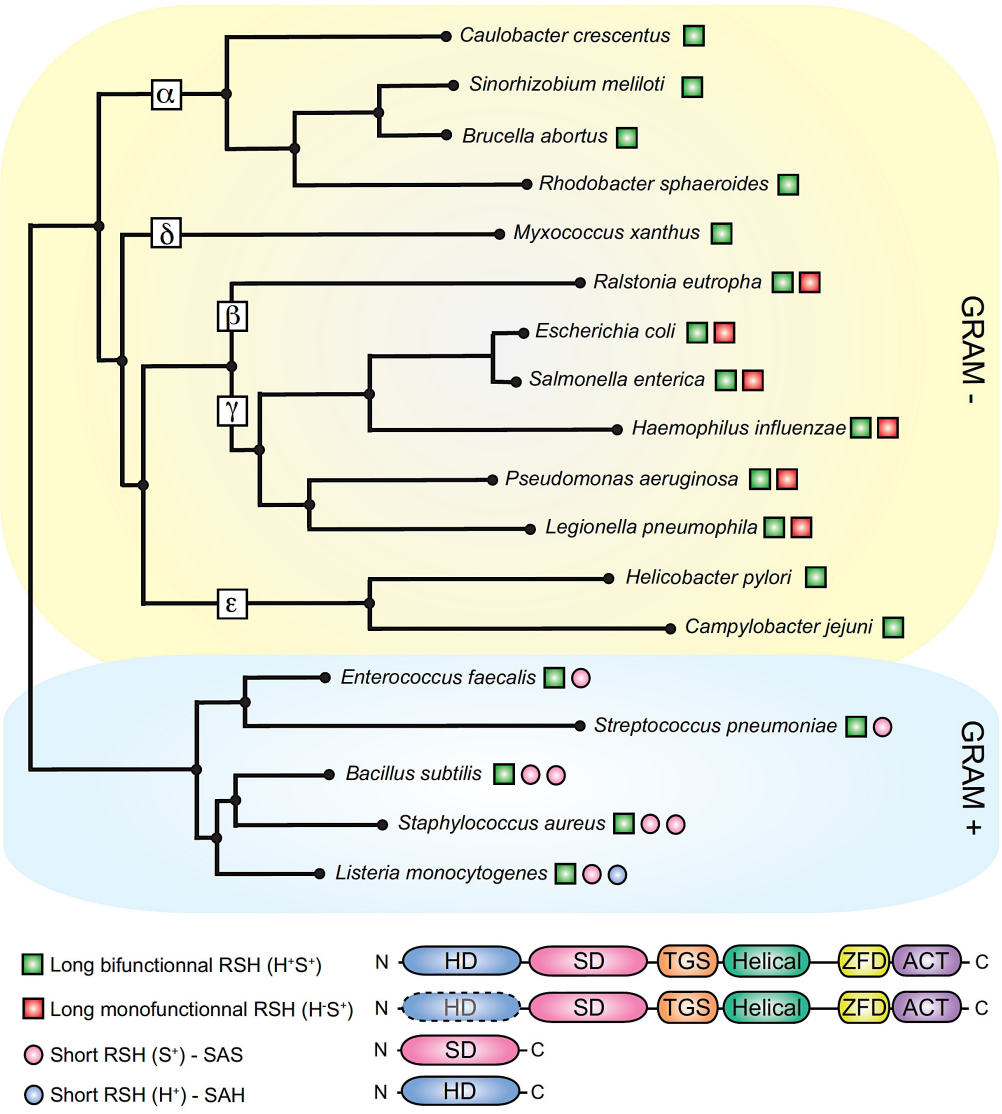

Figure 23: Overview of the architecture and distribution of RSH enzymes in a selection of Gram + and Gram – bacteria

Conservation of long bifunctional RSHs (Rel or SpoT; green squares), long monofunctional RSHs (RelA; red squares), short synthetases (SAS; pink circles) and short hydrolases (SAH; blue circles) in representative species in Gram + and Gram − bacteria. The different classes of Proteobacteria (α, β, δ, ε and γ) are indicated. HD: hydrolase domain; SD: synthetase domain; TGS: Threonyl-tRNA synthetase, GTPase and SpoT; ZFD: zinc-finger domain; ACT: Aspartokinase, Chorismate mutase and TyrR. Note that RSHs represented in this tree arise from computational predictions (see (Atkinson et al., 2011)), some of them have not been functionally characterized, yet.

Figure adapted from (Ronneau and Hallez, 2019).

state, driving the induction of the stringent response (Shyp et al., 2012).

Besides bacteria, where they are widespread (Atkinson et al., 2011), long RSHs orthologs have also been found in eukaryotes bearing chloroplasts that derived from the endosymbiotic acquisition of a cyanobacterium by a eukaryotic organism (Tozawa and Nomura, 2011). The land plant *Arabidopsis thaliana* possess four nuclear-encoded RSH proteins: AtRSH1, AtRSH2, AtRSH3 and AtCRSH, all localizing to chloroplasts (van der Biezen et al., 2000; Mizusawa et al., 2008). Accumulation of (p)ppGpp in plant chloroplasts was found to be triggered by stress conditions such as wounding, heat shock, high salinity or acidity. As in *E. coli,* (p)ppGpp inhibits chloroplast RNA polymerase *in vitro,* establishing the existence of a bacterial-like stringent response in plants (Takahashi et al., 2004). Moreover, AtCRSH is a Ca^{2+} dependent RSH, suggesting a link between (p)ppGpp-mediated regulation and the Ca^{2+} signaling pathway of land plants (Tozawa et al., 2007).

b. Small Alarmone Synthetases and Hydrolases (SAS and SAH)

In addition to Rel, the ancient bi-functional long form RSH, *B. subtilis* also possess two smaller mono-functional (p)ppGpp synthetases encoded by the *ywaC* and *yjbM* genes (Nanamiya et al., 2008). YwaC and YjbM proteins (also known as SAS_1 and SAS_2, or RelP and RelQ) are ~25kDa and only consist of a (p)ppGpp synthetase domain homologous to that of RelA/SpoT family members (Figure 21). YwaC and YjbM homologs are found in the Firmicutes (e.g. *B. subtilis, Staphylococcus aureus, Streptococcus mutans* and *Listeria monocytogenes*). A third class of SAS proteins called RelV was identified in the γ-Proteobacterium *Vibrio cholerae* (Figure 23). Despite their high sequence similarity, SAS proteins seem to play different functional roles by responding to different stress signals (Steinchen and Bange, 2016). Indeed, structural studies of *B. subtilis* RelP/YwaC and RelQ/YjbM revealed that although these SAS proteins have highly similar (p)ppGpp synthetase domains and form comparable homotetrameric complexes, they have different properties in their guanosine binding regions presumably explaining their distinct functions (Steinchen et al., 2018). RelP/YwaC possesses a rigid G-loop that facilitates binding of GDP/GTP substrates, whereas the more flexible G-loop of RelQ/YjbM is less effective in substrate binding but is subjected to allosteric regulation by (p)ppGpp. Moreover, *relQ/yjbM* is transcribed in logarithmic growth and its expression decreases before entry in stationary

phase, whereupon *relP/ywaC* transcription is sharply induced (Nanamiya et al., 2008). It has been suggested that RelQ/YjbM acts as an amplifier of the stress signal triggered by Rel/RelA (Steinchen et al., 2018). In contrast, RelP/YwaC is a highly active (p)ppGpp synthetase suggested to function independently of Rel/RelA. It was notably shown to trigger 100S ribosome formation (Tagami et al., 2012). Furthermore, *relP/ywaC* belongs to the σ^M and σ^W regulons, known to be involved in the response to cell wall stress, suggesting a role for this SAS under these conditions (Irving and Corrigan, 2018).

It is noteworthy that, small alarmone hydrolases (SAH) bearing only the HD domain have been predicted computationally in different bacterial species, such as a MESH1-like protein in *Listeria monocytogenes*, although none have been functionally characterized yet (Atkinson et al., 2011). Surprisingly, SAH proteins have been identified in metazoans: Mesh1 has been characterized in humans and in *Drosophilia melanogaster.* However, their functional importance is so far unknown, as no (p)ppGpp synthetase activity has yet been identified in non-photosynthetic eukaryotes (Sun et al., 2010).

3. Impact of (p)ppGpp on other cellular processes

The term “stringent response” initially designated the specific cellular stress response to amino acid starvation but it is now used to include all responses leading to (p)ppGpp accumulation (for review, see (Irving and Corrigan, 2018)). As emphasized in the previous section, multiple (p)ppGpp metabolizing enzymes exist and are present in different combinations in different species (Atkinson et al., 2011). Differential regulation of the expression and activity of these enzymes allows bacteria to sense a variety of cues existing in the diverse environments they inhabit. In addition to reprogramming global transcription, (p)ppGpp also directly regulates several core bacterial processes such as central metabolism, fatty acid biosynthesis, DNA replication or ribosome assembly (for review, see (Dalebroux and Swanson, 2012)). A non-exhaustive description of some of the major effects of (p)ppGpp follows.

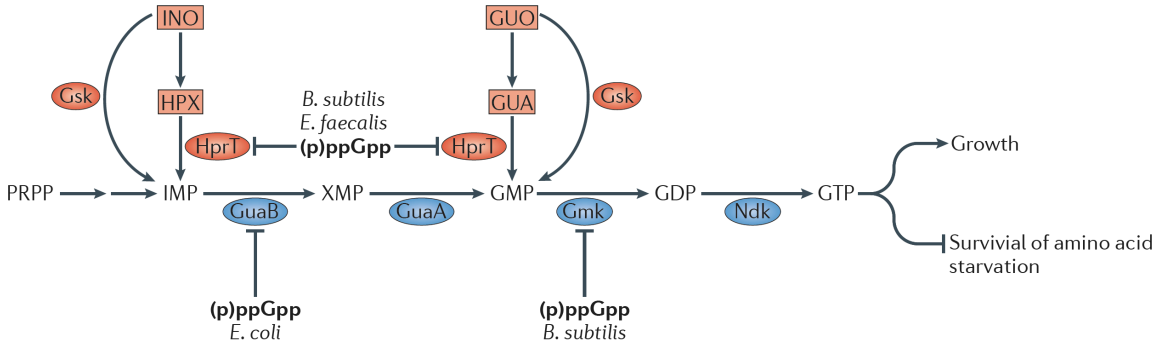

Figure 24: Role of (p)ppGpp in GTP homeostasis

In many bacteria, there are two pathways for GTP synthesis. The salvage pathway (in red) utilizes purine intermediates as substrates, for example, the nucleosides guanosine (GUO) and inosine (INO) or the nucleotides guanine (GUA) and hypoxanthine (HPX). This pathway involves the guanosine kinase (Gsk) and the hypoxanthine phosphoribosyltransferase (HprT) that convert nucleosides and nucleotides, respectively, into GMP or inosine 5'-phosphate (IMP). The *de novo* pathway uses phosphoribosyl pyrophosphate (PRPP) as a starting compound for the multistep synthesis of IMP, which is further converted to GTP. The IMP dehydrogenase (GuaB) turns IMP into xanthosine 5'-phosphate (XMP) that is further converted into GMP by the GMP synthase (GuaA). GMP undergoes sequential rounds of phosphorylation: GMP kinase (Gmk) forms GDP that is further converted to the final product GTP by the nucleoside diphosphate kinase (Ndk). Cellular GTP levels have a dual effect on bacterial physiology: above a certain threshold it increases growth rate; however, at high concentrations GTP inhibits growth and survival. The specific targets of (p)ppGpp-mediated control in GTP metabolism differ between species. For example, in *E. coli*, (p)ppGpp inhibits GuaB whereas in *B. subtilis* it rather targets HprT and Gmk.

Figure adapted from (Hauryliuk et al., 2015).

a. GTP metabolism

The synthesis of (p)ppGpp consumes GDP/GTP and ATP, thus, the induction of the stringent response was observed to coincide with a decrease in GTP pools both in *B. subtilis* and in *E. coli* (Gallant et al., 1971; Lopez et al., 1981). Within a certain range, GTP promotes growth and reduction of GTP pools below a certain threshold, such as during stringent response, inhibits growth. However, at high levels, GTP has cytotoxic effects and leads to inhibition of growth and reduction of survival after amino acid starvation.

Most bacteria possess two pathways for GTP biosynthesis: the *de novo* pathway sequentially converts phosphoribosyl pyrophosphate (PRPP) into inosine 5'-phosphate (IMP), whereas the salvage pathway uses purine intermediates coming from cellular degradation pathways or imported from the culture medium as starting compounds (Figure 24). The salvage pathway produces IMP or GMP from the purine intermediates hypoxanthine/inosine or guanine/guanosine, respectively. IMP is converted to GMP *via* the sequential action of GuaB and GuaA. Finally, the kinase Gmk converts GMP into GDP that is transformed into GTP by the kinase Ndk.

(p)ppGpp was suggested early on to directly inhibit GuaB, the IMP deshydrogenase, in *E. coli* (Figure 24) (Gallant et al., 1971). In *B. subtilis,* (p)ppGpp inhibition of GuaB activity is very moderate. The reduction in GTP pools rather originates from the inhibition of Gmk and HprT, involved in the *de novo* and salvage pathways, respectively (Figure 24) (Kriel et al., 2012; Liu et al., 2015). As mentioned above, in *B. subtilis,* (p)ppGpp does not target the RNAP directly but rather decreases GTP levels causing, among other effects, a reduction of transcription initiation at *rrn* promoters (Krásný and Gourse, 2004; Krásný et al., 2008). Cellular GTP levels also influence the DNA binding properties of the global transcriptional regulator CodY found in most Firmicutes (Sonenshein, 2005). Both GTP and branched-chain amino acids (BCAA) acts as co-repressors of CodY, increasing its affinity for its operator sequence (Handke et al., 2008). CodY represses the expression of a large regulon, containing genes involved in BCAA synthesis, catalytic pathways, competence, motility and sporulation (Molle et al., 2003; Sonenshein, 2005). This regulon is thus turned on during the stringent response due to the reduction in GTP levels.

In addition to its roles in the regulation of initiation of rRNA transcription as the iNTP and as a co-repressor of CodY, GTP is also involved in a variety of anabolic processes in the cell

that can explain its impact on bacterial cell growth (Pall, 1985). In a *B. subtilis* (p)ppGpp^0 strain, i.e. lacking the *relA, relP/ywaC* and *relQ/yjbM* genes and thus unable to synthesize (p)ppGpp, GTP is overproduced and the strain is starvation-sensitive due to the shut-down of BCAA synthesis (Kriel et al., 2014). (p)ppGpp exerts a negative feedback control on GTP synthesis even at the basal concentrations found during normal growth and GTP dysregulation cause cell death independently of amino acid starvation (Kriel et al., 2012). Therefore, (p)ppGpp plays a role in the regulation of GTP biosynthesis enzymes during both normal growth and starvation that is critical for *B. subtilis* viability.

b. Amino acid biosynthesis

Since stringent response is induced by amino acid starvation, the discovery that it can trigger the biosynthesis of certain amino acids make physiological sense. Indeed, both *E. coli* and *B. subtilis* (p)ppGpp^0 cells are auxotrophic for several amino acids. In *E. coli*, (p)ppGpp positively regulates various amino acid biosynthesis genes by directly binding to RNAP or *via* the passive redistribution of RNAPs after (p)ppGpp-mediated inhibition of stable RNA transcription (Potrykus and Cashel, 2008). The poly-auxotrophy of the (p)ppGpp^0 strain is rescued by different mutations in the RNAP in *E. coli*, whereas, in *B. subtilis*, the phenotype is suppressed by mutations mapping to genes involved in GTP biosynthesis (*guaA, guaB* and *gmk*) or in *codY*, consistent with the targets of (p)ppGpp in these bacteria (Kriel et al., 2012). The reduction of GTP levels by (p)ppGpp plays a key role in derepressing the expression of several amino acid biosynthesis genes both in a CodY-dependent and -independent manner (Kriel et al., 2014). The same effect on amino acid biosynthesis can be achieved by using the fungal GMP synthetase inhibitor decoyinine to reduce GTP pools.

c. Fatty acid biosynthesis

The production of (p)ppGpp was also found to increase after fatty acid starvation in *E. coli* (Seyfzadeh et al., 1993). Fatty acid scarcity is sensed in *E. coli* by the interaction of SpoT with deacylated ACP (acyl carrier protein) (Battesti and Bouveret, 2006). ACP is a central cofactor in lipid metabolism required for all biosynthetic reactions in the cell involving acyl chains. Under conditions of fatty acid starvation, interaction with ACP switches SpoT enzyme activity from (p)ppGpp hydrolysis to (p)ppGpp synthesis, resulting in an induction of the

stringent response (Battesti and Bouveret, 2006). In *B. subtilis*, (p)ppGpp is also likely to be involved in the fatty acid starvation response as (p)ppGpp^0 mutants display a much reduced survival during fatty acid shortage in comparison to wild type strains (Pulschen et al., 2017). The bi-functional Rel/RelA is suspected to be involved in this response, and survival of fatty acid shortage was correlated with a decrease in GTP levels, although no (p)ppGpp production was detected under these conditions (Pulschen et al., 2017).

(p)ppGpp has also been reported to control fatty acid synthesis at the level of transcription in *E. coli*: it represses both the *fabHDG* operon encoding fatty acid biosynthesis enzymes and the *accACBD* operon involved in lipid biosynthesis (Li and Cronan, 1993; Podkovyrov and Larson, 1996). (p)ppGpp further inhibits the promoter of the *fadR* gene encoding a global regulator of lipid metabolism, which activates multiple operons involved in fatty acid synthesis genes in *E. coli* (My et al., 2013). The synthesis of (p)ppGpp also affects the activity of enzymes involved in lipid metabolism. It directly inhibits the activity of PlsB, for example, a membrane-bound glycerol-3-phosphate acyltransferase responsible for the first step of lipid biosynthesis (Heath et al., 1994).

d. Replication

In *E. coli,* the initiation of DNA replication is inhibited both at slow growth rates and during starvation. (p)ppGpp is thought to be involved in this regulation by inhibiting transcription of the *dnaA* gene encoding the replication initiator protein (Zyskind and Smith, 1992). (p)ppGpp was also found to directly impede replication elongation by inhibiting DnaG primase in both *B. subtilis* and in *E. coli* (Maciąg et al., 2010; Wang et al., 2007). The primase is a specialized DNA-dependent RNA polymerase that synthesizes the short RNA primers necessary for the initiation of DNA synthesis by DNA polymerase during replication. Binding of (p)ppGpp to *B. subtilis* DnaG arrests replication forks throughout the chromosome without disrupting them, suggesting that (p)ppGpp may link replication with nutrient availability to preserve genomic integrity (Wang et al., 2007).

e. Ribosome assembly

Different screens aiming to identify additional (p)ppGpp binding proteins both in Gram-negatives and in Gram-positives found GTPases involved in translation and ribosome

assembly (Corrigan et al., 2016; Kanjee et al., 2012; Zhang et al., 2018). Given the structural similarity between pppGpp/ppGpp and GTP/GDP, respectively, (p)ppGpp binding to GTPases is not surprising. The alarmone binds the essential GTPase Obg, which has been implicated in several cellular functions such as DNA replication, stress adaptation and ribosome biogenesis (for review, see (Kint et al., 2014)). Obg is thought to be an anti-association factor that binds the 50S ribosome subunit in a (p)ppGpp and GTP dependent manner, as it was observed that ppGpp-Obg remains bound to 50S particles (Feng et al., 2014). The two GTPases Era and CpgA, involved in 30S subunit biogenesis, and belonging to the same subfamily as Obg, were also characterized as (p)ppGpp target proteins (Corrigan et al., 2016). These studies demonstrated that the GTPase activity of these proteins is inhibited by binding the alarmone, leading to a reduction in 70S ribosomes and reduced growth rates in *S. aureus.* The inhibition of bacterial GTPases by (p)ppGpp has been suggested to be a conserved process in Gram-positive bacteria, as some ribosome assembly GTPases from *Enterococcus faecalis* and *B. subtilis* are also bound by the alarmone (Corrigan et al., 2016).

f. Persistence and virulence

The stringent response results in a dramatic slow down of growth that has been implicated in various bacterial survival processes, among them: adaptation to different environments, virulence, persistence, motility and biofilm production. Bacterial persisters are dormant variants of regular cells that appear stochastically in microbial populations and are highly tolerant to antibiotics. A link between persistence and (p)ppGpp came from the observation that *E. coli hipA* mutants display a “high persistence” phenotype that is dependent on (p)ppGpp (Korch et al., 2003). HipA is a serine-threonine kinase that is the toxin component of the toxin-antitoxin module HipAB. HipA phosphorylates the active center of glutamyl-tRNA synthetase (GltX), inhibiting aminoacylation, and thereby generating “hungry” codons in the ribosomal A-site that trigger RelA-dependent (p)ppGpp synthesis to mediate persistence (Germain et al., 2013). The role of (p)ppGpp in the establishment of the persister cell state is likely the reduction of growth rate since a reduction of growth rate promotes persistence even in the absence of (p)ppGpp (Chowdhury et al., 2016).

Bacterial pathogens also require (p)ppGpp to control the expression or activity of key virulence regulators (for review, see (Dalebroux et al., 2010)).For example, the expression of

virulence genes encoded by pathogenicity island 1 was found to be (p)ppGpp-dependent in the intracellular pathogen *Salmonella typhimurium*. Thus, a *S. typhimurium* mutant deficient in (p)ppGpp synthesis (*ΔrelA ΔspoT*) has highly attenuated virulence and is non-invasive (Pizarro-Cerdá and Tedin, 2004).

All together, these results illustrate that (p)ppGpp plays a variety of roles in bacterial adaptation to the environment.

Goal of study

Preliminary results from our team suggested that depletion of RNase P, the essential 5' tRNA maturation enzyme, led to a specific 16S rRNA 3' maturation defect in *B. subtilis*. We later observed that this rRNA maturation defect was more broadly caused by accumulation of immature tRNAs, since depletion for RNase Z, the endonuclease involved in 3' tRNA maturation caused a similar defect. The aim of my thesis was to better understand the link between tRNA processing and the maturation of the 16S rRNA, two major components of the translation machinery. The 3' maturation of the 16S rRNA by YqfG/YbeY is an important step in preparing 30S subunit to interact optimally with the Shine-Dalgarno sequence during initiation of translation and has been proposed by our group and others to constitute a quality control step in 30S biogenesis in bacteria. As has been largely reported in the literature, ribosome biogenesis consumes a major portion of the cell's energy and is therefore extensively regulated.

Our working hypothesis was that the lack of 16S rRNA 3' maturation was in fact the consequence of a defect in 30S small ribosomal subunit assembly, i.e. that depletion of tRNA maturases somehow perturbed ribosome assembly, rather than having a direct effect on YbeY/YqfG expression. Because both RNase P and RNase Z are essential, we worked with depletion strains where the *rnpA* or *rnpB* genes (encoding RNase P protein and RNA subunit, respectively) or the *rnz* gene (encoding RNase Z) were placed under the control of inducible promoters. Removing the inducer permitted us to analyze the effects of tRNA maturase depletion on rRNA maturation and ribosome assembly *in vivo*. First, we showed that 30S subunit assembly was indeed defective in RNase P and RNase Z depletion strains. We proposed that this occurred either at the level of expression or activity of specific ribosome assembly cofactors involved in 30S subunit assembly in *B. subtilis*. Although the expression of some cofactors was indeed perturbed in cells depleted for tRNA maturases, we showed that this did not play a major role in the assembly phenotype. However, because these strains are characterized by an accumulation of tRNA precursors, we hypothesized that they could induce the stringent response in a manner similar to uncharged tRNAs. Since accumulation of (p)ppGpp is known to inhibit the activity of certain GTPases involved in ribosome assembly, we evaluated this possibility and its potential impact on 16S rRNA processing.

Results

Chapter 1: tRNA maturation defects lead to inhibition of rRNA processing *via* synthesis of pppGpp

By studying the effect of tRNA maturase depletion on rRNA processing we have uncovered a coupling mechanism between tRNA processing and 16S rRNA 3' maturation. The characterization of this mechanism is the main contribution of this thesis, namely, the triggering of (p)ppGpp production by immature tRNAs and the ability of the stringent response to inhibit 16S rRNA 3' processing. These experimental results have been published and the research article is included here as formatted in the *Molecular Cell* journal (with attached methods section and supplementary material). Other results obtained during this PhD that have not been included in the publication will be presented in Chapter 2.

Article

Molecular Cell

tRNA Maturation Defects Lead to Inhibition of rRNA Processing via Synthesis of pppGpp

Graphical Abstract

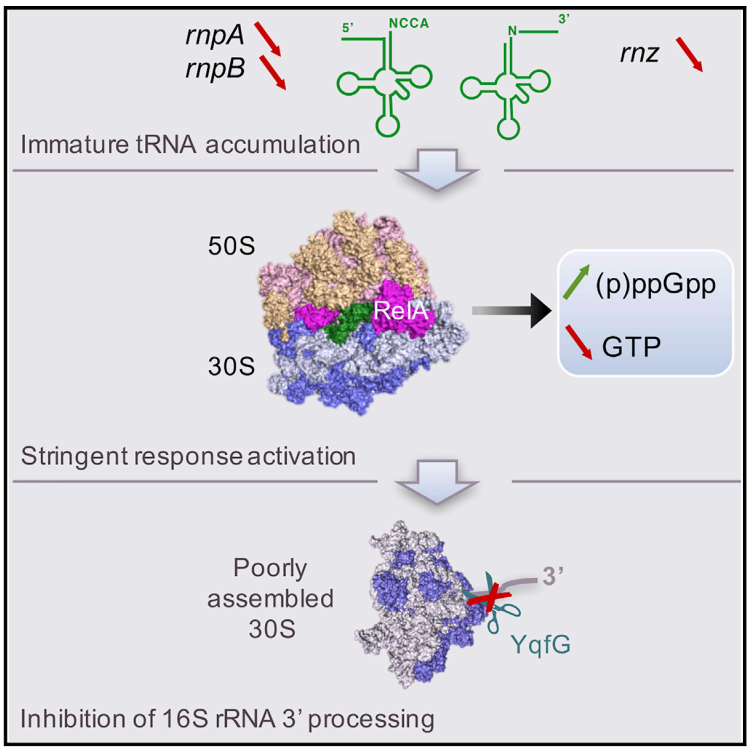

Authors

Aude Trinquier, Jonathan E. Ulmer, Laetitia Gilet, ..., Lauriane Kuhn, Frédérique Braun, Ciarán Condon

Correspondence

frederique.braun@ibpc.fr (F.B.), condon@ibpc.fr (C.C.)

In Brief

In this paper, Trinquier et al. show that an accumulation of immature tRNAs in the Gram-positive model organism *Bacillus subtilis* leads to activation of the RelA-dependent stringent response, a defect in late 30S ribosome subunit assembly, and specific inhibition of 16S rRNA 3′ processing.

Highlights

- tRNA processing defects lead to specific inhibition of 16S rRNA 3′ processing
- Accumulation of immature tRNAs cause late 30S ribosome assembly defects
- Unprocessed tRNAs lead to RelA-dependent production of (p)ppGpp
- Stringent response blocks 16S rRNA processing more rapidly than its transcription

Trinquier et al., 2019, Molecular Cell *74*, 1227–1238
June 20, 2019
https://doi.org/10.1016/j.molcel.2019.03.030

CellPress

Molecular Cell
Article

tRNA Maturation Defects Lead to Inhibition of rRNA Processing via Synthesis of pppGpp

Aude Trinquier,[1] Jonathan E. Ulmer,[1,4] Laetitia Gilet,[1] Sabine Figaro,[1] Philippe Hammann,[2] Lauriane Kuhn,[2] Frédérique Braun,[1,3,*] and Ciarán Condon[1,3,5,*]
[1]UMR8261 (CNRS-Université Paris Diderot), Institut de Biologie Physico-Chimique, 13 rue Pierre et Marie Curie, 75005 Paris, France
[2]Plateforme Proteomique Strasbourg – Esplanade, Institut de Biologie Moléculaire et Cellulaire, CNRS FR1589, 15 rue Descartes, 67084 Strasbourg Cedex, France
[3]These authors contributed equally
[4]Present address: UMR3664, Institut Curie-PSL-CNRS, 26 rue d'Ulm, 75248 Paris Cedex 05, France
[5]Lead Contact
*Correspondence: frederique.braun@ibpc.fr (F.B.), condon@ibpc.fr (C.C.)
https://doi.org/10.1016/j.molcel.2019.03.030

SUMMARY

rRNAs and tRNAs universally require processing from longer primary transcripts to become functional for translation. Here, we describe an unsuspected link between tRNA maturation and the 3′ processing of 16S rRNA, a key step in preparing the small ribosomal subunit for interaction with the Shine-Dalgarno sequence in prokaryotic translation initiation. We show that an accumulation of either 5′ or 3′ immature tRNAs triggers RelA-dependent production of the stringent response alarmone (p)ppGpp in the Gram-positive model organism *Bacillus subtilis*. The accumulation of (p)ppGpp and accompanying decrease in GTP levels specifically inhibit 16S rRNA 3′ maturation. We suggest that cells can exploit this mechanism to sense potential slowdowns in tRNA maturation and adjust rRNA processing accordingly to maintain the appropriate functional balance between these two major components of the translation apparatus.

INTRODUCTION

Ribosomes are the platform for protein synthesis in all cells. Remarkably, the peptidyl transfer activity of this large ribonucleoprotein complex is provided by its RNA component, and the discovery of this property of ribosomes and those of other catalytic RNAs (ribozymes) has fueled the notion of an ancient RNA world in which the major cellular functions were once RNA based. Bacterial ribosomes contain three rRNAs (16S, 23S, and 5S rRNA) that are generally transcribed as part of a large 30S precursor molecule and that assemble with >50 ribosomal proteins to form this translation center (Noller and Nomura, 1987). In *E. coli* and in most other bacteria studied, transcription, initial separation of the individual rRNAs, and r-protein assembly all occur concomitantly and require additional cofactors and quality-control checkpoints along the way to ensure the correct order of events and a stable functional ribosome at the end of this intricate process (Shajani et al., 2011).

By far the greatest proportion of a bacterial cell's biosynthetic capacity and energy consumption is devoted to ribosome biogenesis (Bremer and Dennis, 1996). Because of this energy cost, rRNA transcription is tightly regulated to match the growth rate afforded by the culture medium, a phenomenon known as metabolic control (Pao and Gallant, 1978; Stent and Brenner, 1961). One of the key effectors of this process is guanosine penta- or tetra-phosphate, collectively referred to as (p)ppGpp and historically known as magic spot (Cashel and Rudd, 1987). In *E. coli*, (p)ppGpp binds to RNA polymerase with the help of the DksA protein to downregulate initiation at rRNA promoters at slower growth rates or during amino acid starvation (the stringent response) when rRNA transcription is essentially halted (Ross et al., 2016). The stringent response permits a global readjustment of the cell's metabolism, including inhibition of fatty acid biosynthesis, DNA replication, induction of amino acid biosynthesis, and the establishment of the persister cell state upon exposure to antibiotics or other severe stress conditions (Amato et al., 2013; Chowdhury et al., 2016; My et al., 2015; Polakis et al., 1973; Traxler et al., 2008; Wang et al., 2007). (p)ppGpp has also been implicated in the inhibition of translation by blocking the activity of translation factors EF-Tu, EF-G, and IF2 and the association of ribosomal subunits through its interaction with ObgE (Feng et al., 2014; Miller et al., 1973; Milon et al., 2006; Mitkevich et al., 2010). In *Bacillus subtilis*, (p)ppGpp is similarly an effector of the stringent response, but rather than binding to RNA polymerase, it inhibits the synthesis of GTP by binding to two enzymes of the *de novo* and salvage pathways of GTP synthesis, Gmk and HprT, respectively (Kriel et al., 2012; Liu et al., 2015). Since rRNA promoters in both *E. coli* and *B. subtilis* are exquisitely sensitive to the concentration of the initiating nucleotide (iNTP), the decrease in GTP pools (the iNTP of all 10 rRNA operons in *B. subtilis*) leads to strong inhibition of rRNA transcription (Gaal et al., 1997; Krásný and Gourse, 2004).

The maturation of rRNA is also remarkably different between *E. coli* and *B. subtilis*, with only two processing reactions being shared out of at least ten known intermediary and final

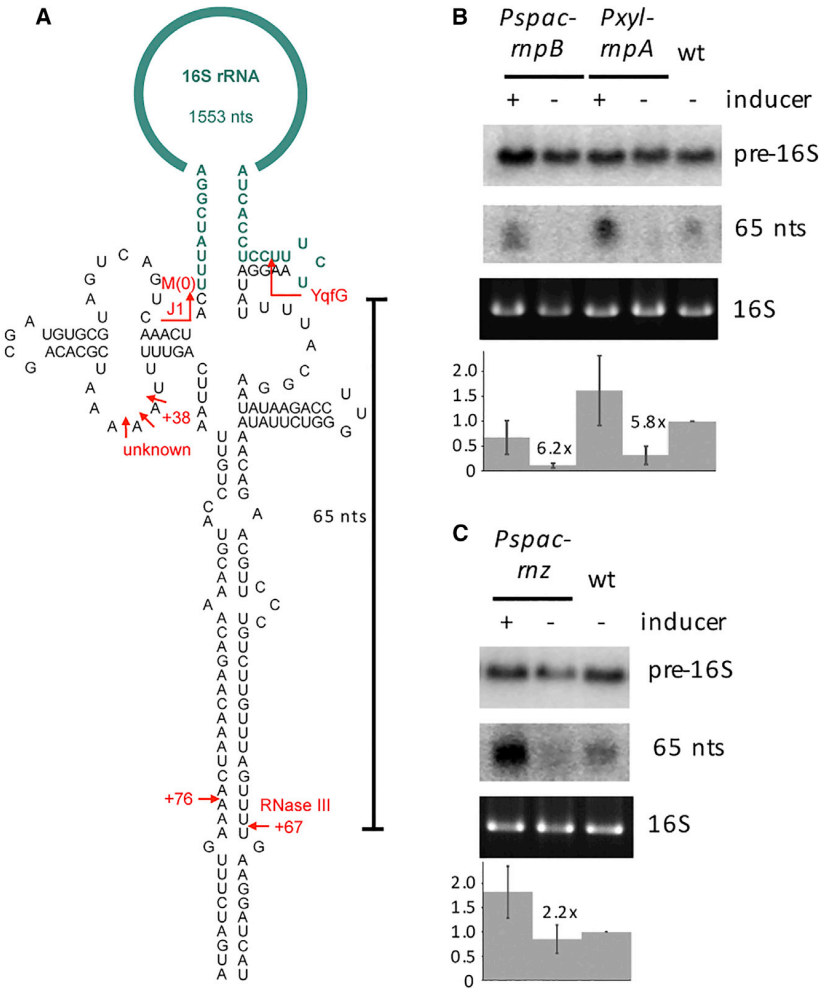

Figure 1. Depletion of tRNA Processing Enzymes Results in a Defect in 3′ Processing of 16S rRNA

(A) Schematic of 16S rRNA (*rrnW*) precursor showing mature sequence in green, precursor sequences in black, and key processing reactions in red.

(B and C) Northern blots showing the effect of depleting RNase P (*rnpB* or *rnpA*) (B) and RNase Z (*rnz*) (C) on accumulation of the 65 nt 3′ processing product. 5 μg of total RNA was probed with oligo CC172 (Table S1), specific for the 16S rRNA 3′ precursor, on agarose gels (top) and polyacrylamide gels (bottom) for optimal transfer of the ~1,620-nt and 65-nt species, respectively. The histograms show the calculation of processing efficiency (65-nt/pre-16S) for each strain, normalized to WT, with SDs as shown (n = 4 *rnpB* and *rnpA*; n = 3 *rnz*; n = 7 WT). The fold differences in processing efficiencies between depleted and nondepleted strains are indicated on each histogram.

processing steps. The first is the co-transcriptional cleavage of the primary transcript by RNase III that occurs in the long double-stranded processing stalks formed by hybridization of complementary precursor sequences at the 5′ and 3′ ends of both 16S (Figure 1A) and 23S rRNA. Cleavage by RNase III separates the three rRNA molecules, which subsequently undergo further processing reactions to yield the mature functional rRNAs (Dunn and Studier, 1973; Herskovitz and Bechhofer, 2000). The enzymes responsible for most of the final maturation steps in *E. coli*, RNase E, RNase G, and RNase T, are not found in *B. subtilis* and vice versa, where the enzymes RNase J1, Mini-III, and RNase M5 play the key roles (Condon, 2014). The only exception is the enzyme involved in the maturation of the 3′ end 16S rRNA, called YbeY in *E. coli* (Jacob et al., 2013) and YqfG in *B. subtilis* (Baumgardt et al., 2018).

The final rRNA trimming steps serve to protect rRNAs from degradation by limiting access to exoribonucleases and are thought to occur at the end of the assembly of each subunit to rubber stamp the assembly process (Baumgardt et al., 2018; Li et al., 1998). Thus, mutations that perturb 30S or 50S subunit assembly generally block the final processing of 16S and 23S rRNA (Bylund et al., 1998; Charollais et al., 2003; Hase et al., 2009; Hwang and Inouye, 2006; Nord et al., 2009; Sayed et al., 1999). In *E. coli*, a number of maturation factors, including GTPases (RsgA and Era), RNA chaperones (RimM, RimP, and RbfA) and modification enzymes (e.g., RimJ and KsgA) are known to be involved in 30S ribosomal subunit assembly (Shajani et al., 2011). In addition to having homologs for each of these factors, *B. subtilis* has at least one additional GTPase, called YqeH, involved in the 30S assembly process (Loh et al., 2007; Uicker et al., 2007).

In this paper, we describe the discovery of a link between tRNA maturation by RNase P and RNase Z in *B. subtilis* and processing of the 3′ end of 16S rRNA by YqfG. RNase P is historically one of the first enzymes whose catalytic moiety was shown to be an RNA, encoded by the *rnpB* gene (Guerrier-Takada et al., 1983). Its primary function is the maturation of the 5′ end of tRNAs. The enzyme also contains a small basic protein subunit, encoded by the *rnpA* gene, that plays a role in substrate recognition and binding (Crary et al., 1998; Reich et al., 1988). Although the RNA component of RNase P is sufficient for catalysis *in vitro*, both the RNA and protein moieties are essential for cell viability *in vivo* (Waugh and Pace, 1990; Wegscheid et al., 2006). There are two major pathways for the maturation of the 3′ end of tRNAs in *B. subtilis*. Approximately two-thirds of *B. subtilis* tRNAs (59 tRNAs whose CCA motif is encoded by their genes) are matured by a 3′–5′ exoribonucleolytic pathway involving the redundant activities of RNase PH, PNPase, RNase R, and YhaM (Wen et al., 2005). RNase Z is required for the 3′ maturation of 17 *B. subtilis* tRNAs lacking a CCA motif encoded in their genes (Pellegrini et al., 2003, 2012), while 10 non-CCA-encoding

tRNAs can be matured by either pathway (Wen et al., 2005). Here, we propose a model that couples tRNA maturation by RNases P and Z to 16S 3′ maturation via the production of (p)ppGpp, a decrease in GTP levels and a defect in 30S ribosomal subunit assembly by GTPases.

RESULTS

RNase P Depletion Inhibits Maturation of the 3′ End of 16S rRNA

In an experiment originally designed to identify enzymes involved in the maturation of 16S rRNA in *B. subtilis*, we screened a number of mutant strains lacking known ribonucleases for defects in 16S rRNA 3′ processing by northern blotting of total RNA. In wild type (WT) cells, a probe specific for 16S rRNA 3′ precursors detects both full-length precursors (~1,620 nt) and a 65-nt species extending from the proposed YqfG cleavage site to the downstream RNase III site (Figure 1A) (Baumgardt et al., 2018; Di-Chiara et al., 2016). To our surprise, depletion of either the protein (*rnpA*) or RNA (*rnpB*) subunit of the tRNA 5′ processing enzyme RNase P resulted in a strong reduction in 16S rRNA 3′ processing as indicated by the absence of the 65-nt species (Figure 1B). Depletion was achieved using integrative vectors that placed the native copy of the *rnpA* and *rnpB* genes under control of the xylose-inducible *Pxyl* promoter or the isopropyl β-D-1-thiogalactopyranoside (IPTG)-inducible *Pspac* promoter, respectively, and growing cells in the presence of glucose to shut off expression of the *Pxyl-rnpA* construct or in the absence of IPTG to shut off expression of *Pspac-rnpB*. Processing efficiency, quantified as the ratio of the 65-nt species to that of the full-length 16S rRNA precursor (65-nt/pre-16S), was reduced by 6.2- and 5.8-fold under conditions of *rnpB* and *rnpA* depletion, respectively, compared to those in the presence of inducer. Since we had already identified a candidate for the 16S rRNA 3′ cleavage reaction, the essential enzyme YqfG (Baumgardt et al., 2018), we suspected the effect of RNase P depletion on 16S rRNA processing was indirect and was the consequence of a defect in tRNA maturation. Depletion of the RNA subunit of RNase P had a stronger effect on tRNA maturation than depletion of the protein subunit (Figure S1), presumably reflecting the relative stabilities of the two components of the enzyme, and this more than likely accounts for the stronger effect of *rnpB* depletion on 3′ processing of 16S rRNA.

The Effect of RNase P Depletion Is Specific for the 3′ End of 16S rRNA

We asked whether the effect of RNase P depletion was specific to the 3′ end of 16S rRNA or whether other rRNA processing reactions were affected. The 5′ end of 16S rRNA is matured by the 5′-exoribonuclease RNase J1 in *B. subtilis* (Britton et al., 2007; Mathy et al., 2007), while the 5′ and 3′ ends of 23S rRNA are simultaneously processed by the double-strand-specific enzyme Mini-RNase III (Figures S2A and S2B) (Redko et al., 2008). We examined the 5′ processing of 16S and 23S rRNA by primer extension using an oligonucleotide complementary to the early mature sequences to detect 5′ precursors extending as far as the upstream RNase III cleavage sites. By proxy, assay of 23S rRNA 5′ processing also determines the efficiency of 3′ processing, since both strands of the processing stalk are cleaved together (Redko et al., 2008). Depletion of *rnpA* did not have a major effect on 5′ maturation of either 16S or 23S rRNA (Figures S2C and S2D), indicating that the coupling with tRNA maturation is specific to the 16S rRNA 3′ processing reaction.

Depletion of RNase Z Has a Similar Effect on 16S 3′ Processing to Depletion of RNase P

We next asked whether the inhibition of 16S 3′ processing was restricted to RNase P or whether it would similarly occur in cells depleted for the tRNA 3′ processing enzyme RNase Z, involved in the maturation of approximately one-third of *B. subtilis* tRNAs (Wen et al., 2005). In cells depleted for RNase Z, under the control of the *Pspac* promoter, the levels of the 65-nt species were strongly reduced, but not completely absent. This corresponded to a 2.2-fold decrease in processing efficiency (Figure 1C). Thus, while the effect of RNase Z depletion on 16S 3′ processing is less severe than depletion of RNase P, presumably because it has fewer tRNA substrates than RNase P, it is nonetheless evident. This result suggests that the 16S rRNA 3′ processing defect is the result of a general deficiency in tRNA maturation.

3′ Processing of 16S rRNA Is Affected in Mutants of the 30S Subunit Assembly Pathway

The effect of the tRNA maturation defects on 16S rRNA processing could occur through an effect on the expression or activity of the 3′ processing enzyme itself, YqfG, or on any of the major 30S ribosomal subunit assembly factors, since final processing is considered to occur post-assembly. We first screened a number of mutants lacking or depleted for specific 30S ribosomal proteins and assembly factors to determine which, if any, were affected in 16S rRNA 3′ processing in *B. subtilis*. No major defects were observed in cells lacking the r-protein S5 acetylase RimJ orthologs YdaF or YjcK, the 16S rRNA methylase KsgA, the RNA chaperones RimP (YlxS in *B. subtilis*) or RbfA, or the r-protein S21 (*ΔrpsU*) (Figures 2A and 2B). However, strains lacking the RNA chaperone RimM, the GTPases CpgA (equivalent to *E. coli* RsgA), or the *B. subtilis*-specific YqeH all showed greater degrees of 16S rRNA 3′ processing deficiency, as did cells depleted for the essential GTPase Era or the 3′ processing enzyme YqfG, as seen previously (Baumgardt et al., 2018). Thus, as in *E. coli*, a number of different proteins involved in *B. subtilis* 30S subunit biogenesis have an impact on 16S rRNA processing and are potential intermediates in the mechanism coupling 16S rRNA 3′ processing to tRNA maturation.

Depletion of RNase P or RNase Z Results in Altered mRNA Levels of Several Key 30S Assembly Factors

We performed northern blots to determine whether the expression of any of the genes encoding different 30S assembly factors with a major impact on 16S rRNA 3′ processing was altered in cells depleted for RNase P or RNase Z. Remarkably, mRNA levels coding for two 30S assembly proteins, the GTPases Era and YqeH, increased under depletion conditions for either tRNA maturase (Figure 2C), while the expression of two mRNAs, encoding the RNA chaperone RimM and the GTPase CpgA, decreased (Figure 2D). Some mRNAs were relatively unchanged

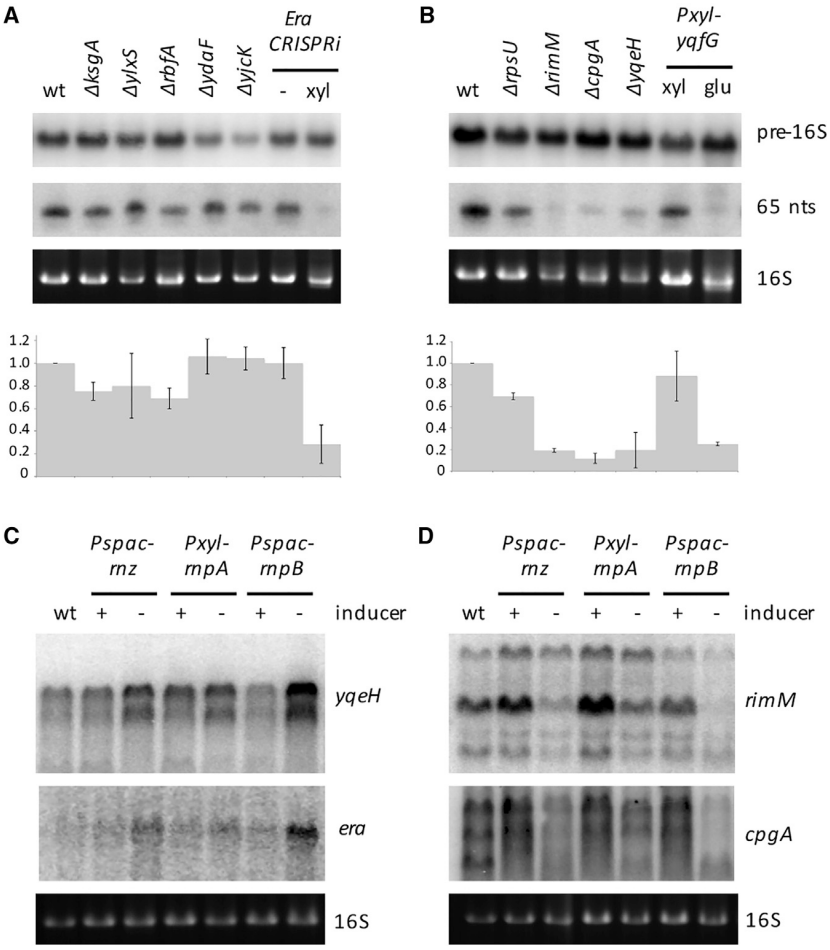

Figure 2. Depletion of tRNA Processing Enzymes Results in Perturbed Expression of Genes Involved in 30S Ribosome Biogenesis

(A) Northern blots showing the effects of *ΔksgA*, *ΔylxS (rimP)*, *ΔrbfA*, *ΔydaF (rimJ1)*, *and ΔyjcK (rimJ2)* deletions and Era depletion (in 168 *trpC2* background) on 16S rRNA 3′ processing efficiency.

(B) Northern blot showing the effects of YqfG depletion and *ΔrpsU* (S21), *ΔrimM*, *ΔcpgA*, and *ΔyqeH* deletions (in W168 background) on 16S rRNA 3′ processing efficiency. The histograms show the calculation of processing efficiency (65-nt/pre-16S) for each strain, normalized to WT, with SDs as shown (n = 2).

(C) Northern blots showing upregulation of *era* (probe CC1846) and *yqeH* (probe CC1847) expression in strains depleted for RNase P (*Pxyl-rnpA* and *Pspac-rnpB*) and RNase Z (*Pspac-rnz*).

(D) Northern blots showing downregulation of *rimM* (probe CC1845) and *cpgA* (riboprobe) expression in the same depletion strains.

(e.g., *rimP*/*ylxS* and *rbfA*), while others (e.g., *yqfG*) were too low to be detected by northern blot (data not shown). Thus, under conditions of RNase P or Z depletion, the transcript levels of a number of key assembly factors are perturbed and could account for the 16S 3′ processing defect because their levels are insufficient for 30S assembly or because they poison the assembly process when overexpressed.

Depletion of RNase P or RNase Z Results in a Defect in 30S Subunit Assembly

To determine whether a decrease in tRNA maturation levels leads to a defect in 30S subunit assembly in *B. subtilis*, we subjected ribosomes isolated from cells depleted for RNase P (*rnpA*) or RNase Z to sucrose gradient analysis under low-magnesium (Mg) conditions (3 mM) to dissociate ribosomal subunits. Under RNase P and RNase Z depletion conditions, the 30S peak was slightly broader than that seen in WT cells, with a small shoulder corresponding to the early 30S fractions (Figure 3A). The 16S rRNA present in these early fractions (fraction 10) is aberrant and shows two additional species, one slightly larger and one slightly smaller than mature 16S rRNA, corresponding to precursor and partially degraded 16S rRNA species (Figure 3B). We have seen this pattern previously with the depletion of the 16S 3′ processing enzyme YqfG (Baumgardt et al., 2018). We measured the levels of individual ribosomal proteins present in fraction 10 by liquid chromatography-tandem mass spectrometry (LC-MS/MS) and compared them to the content of the mature 30S peak (fraction 12) of WT cells. In cells depleted for RNase P (*rnpA*), a number of late assembly ribosomal proteins were significantly reduced, including S2, S3, S14, and S21, which were present at ≤10% of WT, and S5, S9, and S13, which were ≤50% of WT (Figure 3C). A milder but overlapping defect was observed with the RNase Z depletion strain, with the late proteins S2, S3, and S14 showing defective levels at ≤50% of WT (Figure 3D). Thus, depletion of RNase P and RNase Z indeed results in a late 30S subunit assembly defect that could account for the defect in 16S rRNA 3′ processing. The observation that only specific (late) r-proteins were affected in this experiment confirms that at this point in the depletion curve, we have not yet reached the point of a global shutdown in r-protein synthesis.

The late assembly defect is very reminiscent of that seen in *E. coli* cells lacking RimM (Bunner et al., 2010; Guo et al., 2013; Leong et al., 2013), which along with *cpgA* was one of the two assembly factor mRNAs downregulated by depletion of the tRNA maturation enzymes in *B. subtilis* (Figure 2D). We therefore asked whether RimM performed a similar function in *B. subtilis* by performing sucrose gradient and mass spectrometry analysis similar to those described for the depletion of RNase P and RNase Z. In the *ΔrimM* strain, the 30S peak was shifted significantly toward a precursor form (Figure S3A), confirmed by the analysis of 16S rRNA, which showed primarily the precursor and degraded 16S rRNA species and very little

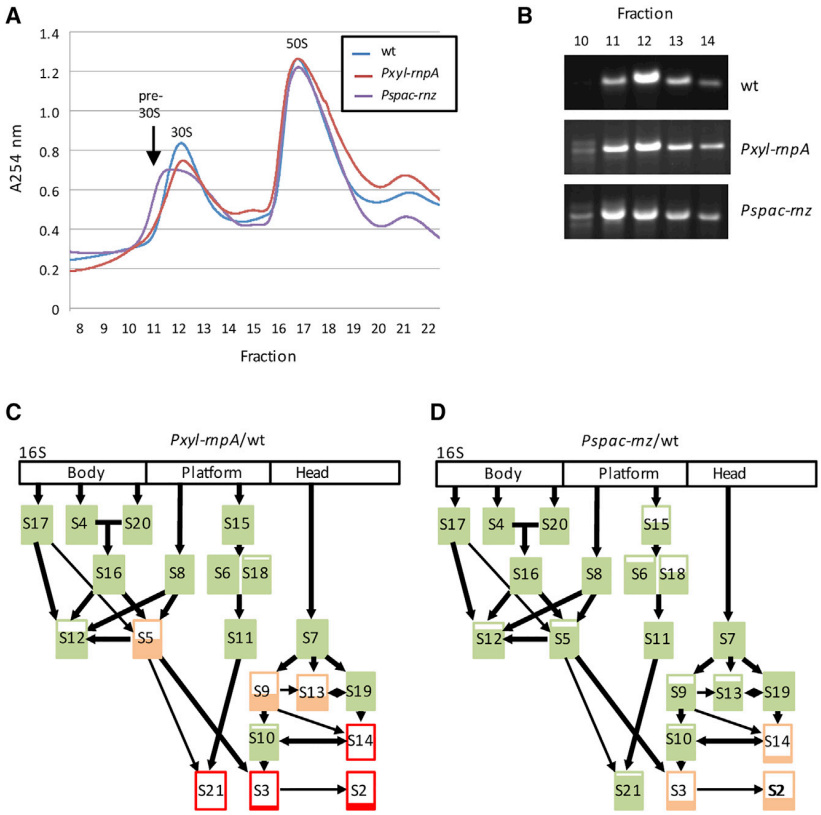

Figure 3. Effect of RNase P and Z Depletions on Ribosome Assembly

(A) Sucrose gradients in 3 mM Mg of WT, *Pxyl-rnpA*, and *Pspac-rnz* depletion strains grown in the absence of inducer.

(B) 16S rRNA profile in sucrose gradients from (A).

(C) LC-MS/MS analysis (n = 3) of pre-30S fractions in WT versus *Pxyl-rnpA* and *Pspac-rnz* depletion strains grown in the absence of inducer. The number of spectra for each protein was first normalized to the total spectra observed in each fraction and then normalized to the equivalent number in WT. The percent fill of each box represents the amount of each ribosomal protein compared to WT. Proteins shown in red are represented at ≤10%; orange indicates >10% but ≤50% of WT and green >50% of WT. Assembly map is from Chen and Williamson (2013).

mature 16S rRNA (Figure S3B). We analyzed the r-protein content of fractions 10 and 11 from this gradient by mass spectrometry and saw very similar defects to those observed with the RNase P and the milder RNase Z depletion strains, respectively. Fraction 10 showed reduced levels of the late assembly proteins S2, S3, S9, S10, S14, S19, and S21 (≤50% of WT; Figure S3C), whereas fraction 11 showed a milder defect with lower levels of S2, S3, and S14 (Figure S3D). Thus, reduced levels of *rimM* expression in RNase P or RNase Z depletion strains could potentially account for the defect observed in 30S subunit assembly. In *E. coli*, RbgA (CpgA in *B. subtilis*) has been shown to have a similar role to RimM in late 30S assembly (Leong et al., 2013). Therefore, we also considered the possibility that the reduced *cpgA* mRNA levels in tRNA maturase depletion strains might equally contribute to the 30S assembly defect.

Perturbation of Assembly Factor mRNA Levels upon RNase P Depletion Is Not Sufficient to Account for the 16S rRNA Processing Defect

To directly test the hypothesis that the decreased *rimM* and *cpgA* mRNA levels could account for the defect in 16S rRNA 3′ maturation in strains depleted for tRNA processing enzymes, we asked whether we could complement the processing deficiency by ectopic expression of these two mRNAs. We constructed a single integrative vector expressing both *rimM* under control of the arabinose-dependent *Pxsa* promoter (Franco et al., 2007) and *cpgA* under control of the bacitracin-dependent *Plia* promoter (Toymentseva et al., 2012). Even leaky expression of *rimM* or *cpgA* from this construct was sufficient to complement the respective 16S 3′ processing defects in *rimM* and *cpgA* mutants, showing that the construct is functional (Figure S4A; compare lanes 3 and 4 and lanes 6 and 8). However, ectopic expression of *rimM* alone, or *rimM* with *cpgA*, failed to rescue the 16S rRNA 3′ processing defect in cells depleted for *rnpB* (Figure S4B, compare lane 6 and 4). Similarly, ectopic expression of the 3′ processing enzyme YqfG (Baumgardt et al., 2018), whose native mRNA we had failed to detect by northern blot (above), did not restore 16S rRNA 3′ processing under RNase P depletion conditions (Figure S4C). Lastly, overexpression of the GTPase genes *era* or *yqeH* from a plasmid in a WT background had no impact on 16S rRNA 3′ maturation (Figures S4D and S4E), ruling out the possibility that the increase in expression of these mRNAs observed in RNase P and RNase Z depletion strains could poison 30S subunit assembly. Although we have not formally ruled out the possibility that multiple cumulative effects are responsible, these experiments suggest that the impact of tRNA processing defects on 16S rRNA 3′ maturation is unlikely to be due to the perturbation of the expression of 30S assembly factors or processing enzymes alone.

Defects in tRNA Processing Lead to the Induction of the Stringent Response via RelA

Having discounted the possibility that altered expression levels of 30S assembly factors were solely responsible for the 16S rRNA processing defect, we speculated that the activity of these proteins might be impacted by perturbations in tRNA processing. It was recently shown that the alarmone (p)ppGpp was a competitive inhibitor of GTPases involved in 30S ribosome biogenesis in *S. aureus*, notably Era and RbgA (CpgA in *B. subtilis*) (Corrigan et al., 2016). We therefore considered the possibility that the synthesis of (p)ppGpp might be induced by immature tRNA in a

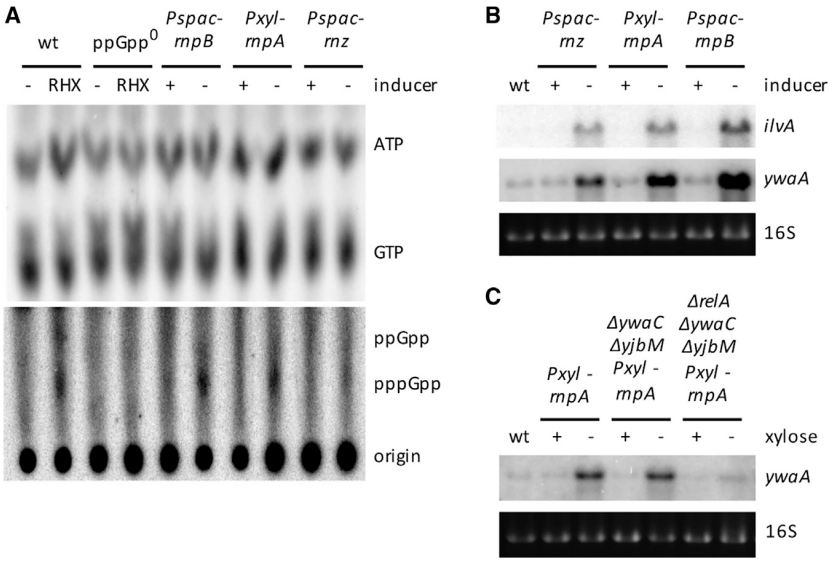

Figure 4. Depletion of tRNA Processing Enzymes Leads to Induction of the Stringent Response

(A) Depletion of tRNA processing enzymes leads to the production of (p)ppGpp. Thin-layer chromatography (TLC) analysis of ^{32}P-labeled nucleotides extracted from *Pspac-rnpB*, *Pxyl-rnpA*, and *Pspac-rnz* depletion strains grown in the absence of inducer. Arginine hydroxamate (RHX; 250 μg/mL) was added to WT cultures and strains unable to make (p)ppGpp (ppGpp^0) as positive and negative controls. Note that the top and bottom halves of the chromatogram are exposed for different times.

(B) Defects in tRNA processing cause derepression of the CodY regulon. Northern blot showing derepression of *ilvA* and *ywaA* gene expression in *Pspac-rnpB*, *Pxyl-rnpA*, and *Pspac-rnz* depletion strains growing in the presence and absence of inducer.

(C) Derepression of the CodY-regulated *ywaA* mRNA in *rnpA*-depleted strains is RelA dependent. Northern blot showing *ywaA* gene expression in the *Pxyl-rnpA* depletion strains growing in the presence and absence of xylose in WT, *yjbM ywaC* double-mutant, and *yjbM ywaC relA* triple-mutant (ppGpp^0) genetic backgrounds.

manner similar to the mechanism involving RelA and uncharged tRNA (i.e., via the stringent response). We first asked whether depletion of RNase P or RNase Z led to an accumulation of (p)ppGpp in *B. subtilis* by adding ^{32}P-labeled inorganic phosphate to cultures, extracting total nucleotides with formic acid and analyzing them by thin-layer chromatography (TLC). The migration position of (p)ppGpp was determined by adding the stringent response inducer arginine hydroxamate (RHX) to WT cells and to a ppGpp^0 strain unable to synthesize (p)ppGpp because it lacks the three known synthetases RelA, YwaC, and YjbM (Kriel et al., 2012). Strains depleted for RNase P (*rnpA* or *rnpB*) showed strongly increased synthesis of pppGpp, while depletion of RNase Z showed a much weaker effect (Figure 4A), coherent with their relative impacts on 16S 3′ processing and 30S ribosome assembly. That the main form of the alarmone synthesized was the penta-phosphate derivative (pppGpp) was previously observed for *B. subtilis* (Wendrich and Marahiel, 1997).

Given the high background signal in the TLC assay, we wished to confirm that the levels of (p)ppGpp observed upon depletion of RNase P or RNase Z were physiologically relevant. To do this, we assayed the expression of the *ywaA* and *ilvA* genes, two members of the *B. subtilis* CodY regulon, whose expression is known to increase during the stringent response due to resulting decrease in GTP pools (Kriel et al., 2012). The expression of both *ywaA* and *ilvA* was strongly derepressed in strains depleted for either the RNA or protein subunits of RNase P and more weakly derepressed in response to depletion for RNase Z (Figure 4B), consistent with the direct assay of (p)ppGpp levels in these strains (Figure 4A). We will use derepression of *ywaA* as an indirect measure of *in vivo* guanosine nucleotide pools for the rest of this paper.

To ask whether the synthesis of (p)ppGpp was dependent on the two synthetases YwaC and YjbM or on the synthetase-hydrolase RelA, we examined the expression of *ywaA* in cells depleted for RNase P (*rnpA*) in a *ywaC yjbM* background or a strain lacking all three (p)ppGpp synthesizing enzymes. The experiment was done in this way because *relA* single mutants rapidly accumulate suppressor mutations in the two synthetase genes (Natori et al., 2009). Expression of *ywaA* was still strongly derepressed in the double *ywaC yjbM* mutant but no longer occurred in the triple *ywaC yjbM relA* mutant (ppGpp^0 strain; Figure 4C), showing that the primary sensor of the tRNA maturation defect is the stringent response effector RelA.

16S 3′ Processing Is Partially Restored in ppGpp^0 Strains Depleted for RNase P and RNase Z

If (p)ppGpp is an effector in the tRNA-16S rRNA maturation coupling mechanism, we would predict that 16S 3′ processing should be impacted to a lesser degree by depletion of RNase P and RNase Z in ppGpp^0 strains. This was indeed the case. In RNase P depletion strains, 16S processing efficiency was partially restored in the ppGpp^0 background (Figure 5). The processing efficiency improved from a 5.8-fold deficiency to only a 2.6-fold defect upon depletion of *rnpA* in a ppGpp$^+$ versus ppGpp^0 background and from 6.2-fold to 2.4-fold deficiency upon depletion of *rnpB*. In RNase Z depletion strains, which still show some 16S 3′ processing in ppGpp$^+$ strains, there was no improvement in maturation efficiency in the ppGpp^0 background (2.2-fold defect compared to 2.6-fold in ppGpp$^+$ versus ppGpp^0 backgrounds; data not shown), consistent with the lower level of (p)ppGpp synthesis upon depletion of RNase Z and the generally milder effect of RNase Z depletion on 16S rRNA 3′ processing. Since 16S rRNA maturation efficiency is not completely restored in a ppGpp^0 background, this suggests that (p)ppGpp is not the only effector of the coupling mechanism between tRNA and 16S rRNA 3′ processing.

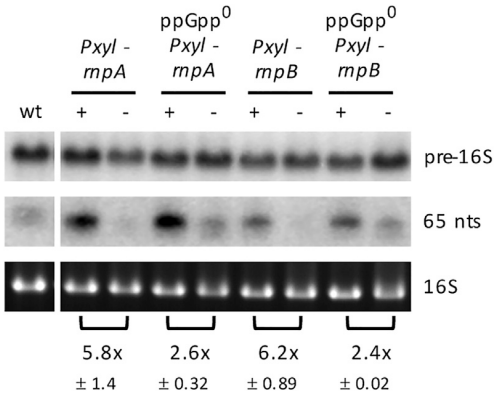

Figure 5. 16S rRNA 3′ Processing Is Partially Restored in RNase P-Depleted Cells in a ppGpp^0 Background

Northern blot comparing the effect of depleting RNase P (*rnpA* or *rnpB*) in a ppGpp+ and ppGpp^0 background on the accumulation of the 65 nt 3′ processing product. The fold differences in processing efficiencies, normalized to WT, between depleted and nondepleted strains are indicated underneath the northern blots, with SDs as shown (n = 4 *rnpB* and *rnpA*; n = 2 *rnpB* ppGpp^0 and *rnpA* ppGpp^0, n = 7 WT).

Increased (p)ppGpp Levels and Decreased GTP Pools Inhibit 16S 3′ Processing in the Absence of tRNA Processing Defects

We next asked whether the synthesis of (p)ppGpp or a decrease in intracellular GTP levels would inhibit 16S rRNA 3′ processing in the absence of a defect in tRNA maturation. We did this in three ways, each time using the CodY-regulated *ywaA* gene as a sensitive gauge of the changes in nucleotide pools. We first asked whether classical induction of the stringent response by amino acid starvation would also lead to a defect in 16S 3′ rRNA processing. Addition of RHX to WT cells led to a decrease in the production of the 65-nt species over time that significantly outpaced the rate of inhibition of 16S rRNA transcription, as measured by levels of remaining full-length precursor (Figure 6A). Thus, induction of the stringent response not only inhibits rRNA transcription, as previously observed, but also impedes 16S rRNA 3′ processing. Second, we constructed a strain that allowed us to induce (p)ppGpp synthesis in the absence of either defects in tRNA processing or amino acid starvation. In this strain, the three (p)ppGpp synthetase genes (*ywaC*, *yjbM*, and *relA*) were inactivated in their native loci and an ectopic copy of the *ywaC* synthetase gene was placed under control of the *Pxyl* promoter in the *amyE* locus. Addition of xylose to this strain led to a strong induction of ppGpp synthesis as measured by TLC (Figure 6B), and this was confirmed by showing derepression of *ywaA* gene expression by northern blot at different times after addition of xylose to the growth medium (Figure 6C). Reduced levels of the 65-nt 16S 3′ rRNA processed species were observed only 2 min after addition to xylose to the culture, well before synthesis of the full-length 16S rRNA precursor began to decrease, 15 min after xylose addition. In agreement, calculation of the processing efficiency (65-nt/full-length), showed a steady decrease over the full time course of the experiment, even after the point where inhibition of 16S rRNA transcription became evident (Figure 6C). Thus, induction of (p)ppGpp synthesis in the absence of amino acid starvation also results in a deficiency in 16S 3′ processing. Lastly, we investigated whether a decrease in GTP synthesis would have an impact on 16S 3′ rRNA processing independently of (p)ppGpp production by adding the fungal GMP synthetase inhibitor decoyinine to cultures. Addition of decoyinine to WT cells led to a rapid decrease in 16S rRNA 3′ processing efficiency, suggesting that a decrease in GTP levels is sufficient to inhibit the different GTPases that play a role in 30S ribosomal subunit assembly and ultimately cause the 16S rRNA 3′ maturation defect (Figure 6D). However, it does not rule out an additional contribution from direct inhibition of the ribosome biogenesis GTPases by (p)ppGpp, as proposed in *S. aureus* (Corrigan et al., 2016).

DISCUSSION

This paper describes an intriguing observation that tRNA processing mutants completely abolish 16S 3′ processing. We worked backward from an original hypothesis that the expression or activity of certain 30S ribosome assembly factors was affected to show that there was indeed a specific late 30S biogenesis defect. Finally, we discovered the missing link: that unprocessed tRNAs can induce the stringent response and the synthesis of (p)ppGpp. We propose a model in which unprocessed tRNAs enter the ribosome A-site, similar to uncharged tRNA, and trigger RelA-dependent (p)ppGpp synthesis (Figure 7). The synthesis of (p)ppGpp can have two effects: directly, through competitive inhibition of assembly factor GTPase activity, as proposed by Grundling and coworkers in *S. aureus* (Corrigan et al., 2016), or indirectly, through the decrease in GTP pools necessary for their activity. Our data suggest that in *B. subtilis* at least, the decrease in GTP pools is sufficient to lead to problems in late 30S ribosome assembly and, consequently, to the deficiency in the maturation of 16S rRNA.

With only minor accommodations, the structure of RelA on the ribosome (PDB: 5iqr) could accept both 5′ and 3′ tRNA precursors (Figure S5). RelA recognizes C74 and C75 of the CCA motif of uncharged tRNA through a stacking interaction with His432 and hydrogen bond interactions with Arg438 (Arenz et al., 2016; Brown et al., 2016; Loveland et al., 2016). It is possible that similar interactions could occur with non-cytosine bases in the equivalent positions of non-CCA containing tRNA 3′ precursors that accumulate in RNase-Z-depleted cells. Since a free 3′-hydroxyl group of the terminal A-residue was proposed to be necessary for (p)ppGpp synthesis by RelA *in vitro* (Sprinzl and Richter, 1976), a different accommodation process would be necessary to account for the ability of 3′ extended tRNA precursors to stimulate (p)ppGpp synthesis in RNase Z-depleted cells. It will be interesting to determine the molecular details of this recognition mechanism. Shetty and Varshney recently showed that three consecutive GC base pairs in acceptor stem of the initiator tRNA played an important role in licensing the final rRNA processing reactions during the first round of initiation complex formation in *E. coli* (Shetty and Varshney, 2016). Although these experiments did not directly implicate the

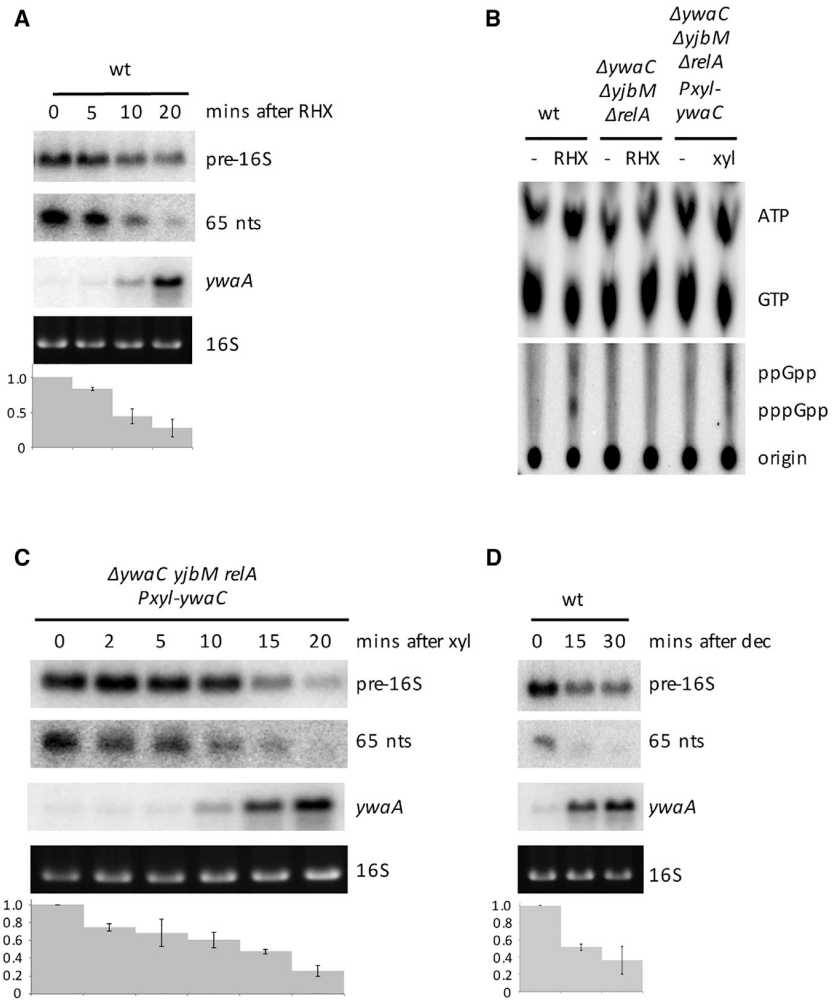

Figure 6. Increased (p)ppGpp Synthesis and Decreased GTP Levels Inhibit 16S rRNA 3′ Processing in the Absence of tRNA Processing Defects

(A) Induction of the stringent response by amino acid starvation results in defects in 16S rRNA 3′ processing. Northern blots performed on total RNA after addition of arginine hydroxamate (RHX; 250 μg/mL) to WT cultures at times indicated. Quantification of processing efficiency (65-nt/pre-16S) is calculated underneath the northern blots, normalized to the untreated sample, with SDs as shown (n = 2). The blot in the top panel was reprobed with oligo CC2213 specific for the CodY-regulated *ywaA* gene.

(B and C) Induction of (p)ppGpp synthesis is sufficient to cause defects in 16S rRNA 3′ processing.

(B) TLC showing production of (p)ppGpp in *ywaC yjbM relA* strains expressing *ywaC* under control of the xylose promoter in the *amyE* locus 30 min after addition of RHX (250 μg/mL) or xylose (2%) to cell cultures.

(C) Northern blot performed on total RNA after addition of xylose (2%) to *ywaC yjbM relA* strains expressing *ywaC* under control of the xylose promoter at the times indicated, with SDs as shown (n = 2).

(D) Inhibition of GTP synthesis results in defects in 16S rRNA 3′ processing. Northern blot performed on total RNA after addition of decoyinine (dec; 500 μg/mL) to WT cultures at the times indicated, with SDs as shown (n = 2).

stringent response, they showed that correct tRNA structure in the A-site is important for 16S rRNA processing. From a physiological standpoint, both these observations and ours indicate that other tRNA forms besides uncharged tRNA in the A-site may be able to activate RelA.

We have previously shown that the 16S 3′ processing step is a quality control event that rubber stamps the correct completion of the 30S assembly process and that small subunits that are not processed correctly are rapidly degraded by RNase R (Baumgardt et al., 2018). Here, we show that inhibition of 16S 3′ processing during the stringent response is much more rapid than the inhibition of rRNA transcription. Hence, upon encountering translational stress, bacterial cells possess a mechanism that not only shuts down transcription of rRNAs but also blocks the assembly of existing precursors into functional ribosomal subunits and rapidly degrades the partially assembled pre-rRNAs. This suggests that the effect of (p)ppGpp production on *de novo* ribosome production is more rapid and extensive than previously understood. Our experiments show that cells can exploit this mechanism to sense potential slowdowns in tRNA maturation and adjust ribosome production accordingly. This would maintain the appropriate functional balance between these two major components of the translation apparatus. Indeed, it makes physiological sense to slow down ribosome assembly and processing under conditions where the levels of mature tRNAs available for translation are even transiently diminished. Expression levels of the *rnpA*, *rnpB*, and *rnz* RNAs are relatively constant over ~100 growth conditions tested (Nicolas et al., 2012), suggesting that the synthesis levels of these enzymes does not vary much in cells. We suspect therefore that the coupling mechanism may play a role in fine-tuning ribosome biogenesis and rRNA processing to minor perturbations in tRNA maturation that occur when the tRNA processing enzymes are transiently out-titrated by tRNA synthesis levels during the cell cycle.

Processing of the 3′ end of 16S rRNA is restored to approximately half of its normal levels when tRNA maturation enzymes are depleted in a ppGpp^0 background, suggesting that (p)ppGpp is not the only effector of this coupling phenomenon. One possibility is that the perturbation in mRNA levels of the 30S assembly factors, in particular the decrease in levels of the mRNA encoding the GTPase CpgA, contributes to this phenomenon. Although ectopic expression of *cpgA* failed to complement the 16S rRNA processing defect in cells depleted for RNase P, the ectopically produced enzyme would also be

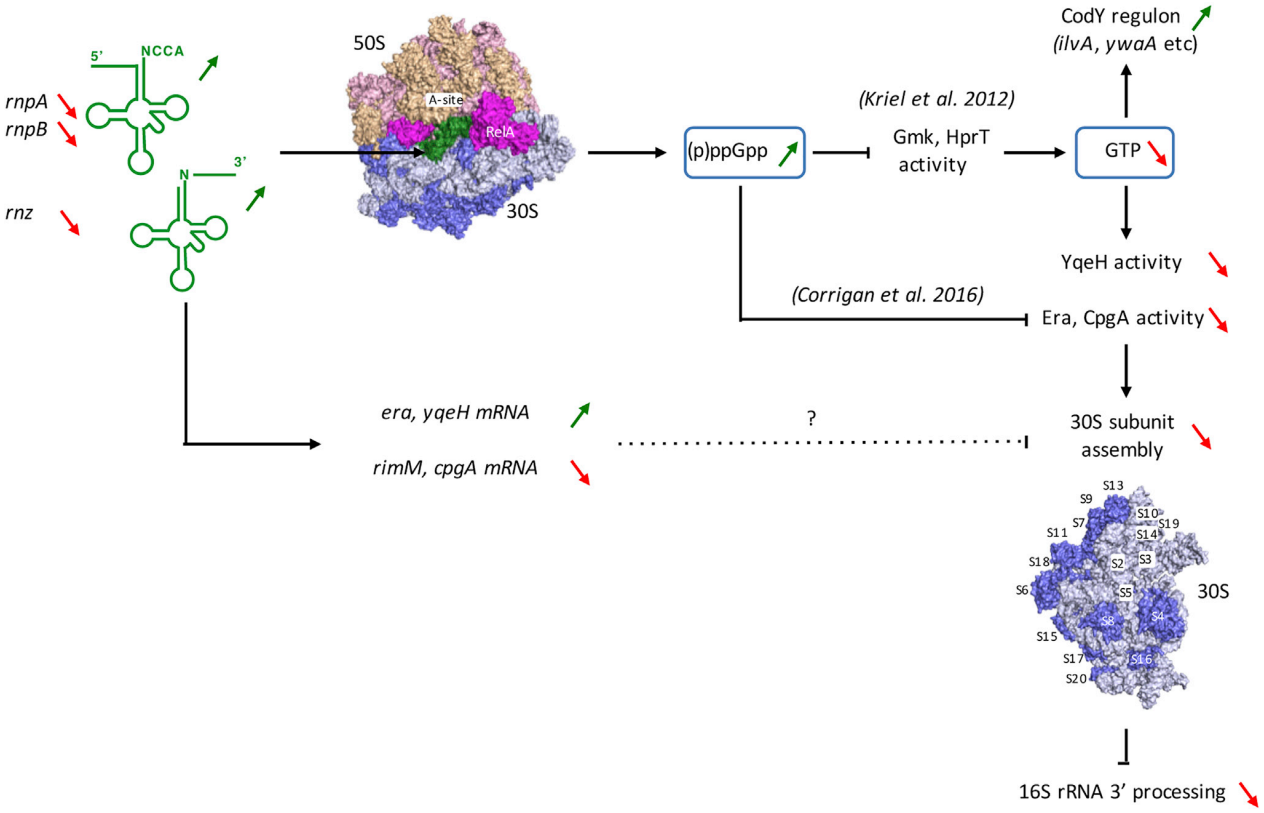

Figure 7. Model for Coupling of tRNA and 16S rRNA 3′ Processing

Precursor tRNAs (green) and RelA occupy the A-site of the ribosome and provoke synthesis of (p)ppGpp. Upward pointing green arrows show increased synthesis or activity, and downward pointing red arrows show decreases. Increased (p)ppGpp levels inhibit the synthesis of GTP by binding to Gmk and HprT (Kriel et al., 2012), leading to derepression of the CodY regulon and potentially inhibit the GTPase activity of Era and CpgA (Corrigan et al., 2016). The decreased GTP pools may also affect the GTPase activity of Era, CpgA, and YqeH, resulting in late 30S assembly defects, represented by the absence of the ribosomal proteins S2, S3, S5, S14, S19, and S21. The assembly defect in turn leads to a defect in 16S rRNA 3′ processing. It is also possible that perturbation of expression of 30S assembly factors contributes to the assembly defect upon accumulation of tRNA precursors.

predicted to be inhibited by the ambient levels of (p)ppGpp and GTP in cells accumulating tRNA precursors. Second, although ectopic expression of the RNA chaperone RimM or the 16S 3′ processing enzyme YqfG also failed to complement 16S rRNA processing in cells depleted for RNase P, we have not formally eliminated the possibility that the activity of these proteins is somehow impacted by (p)ppGpp or GTP levels. The mechanism through which tRNA depletion results in increased or decreased mRNA levels of several 30S mRNA assembly factors is currently unknown. Our preliminary data suggest that this is a mixture between transcriptional and post-transcriptional effects (data not shown), and this will be developed in detail in a later study.

The effect of RNase P and RNase Z depletion on rRNA processing is specific for the 3′ end of 16S rRNA. Given the current models that all final processing steps occur post-assembly in *E. coli*, it is surprising that 5′ maturation was not also affected. This may suggest some differences in the order of events between Gram-positive and negative bacteria. An earlier study showed that tRNA functional defects in *E. coli* could lead to nonspecific problems with both 16S and 23S rRNA maturation, but the mechanism involved was not addressed (Slagter-Jäger et al., 2007). In another study that may be related to the coupling mechanism described here, the Deutscher group showed in the 1970s that the strong growth defects of *E. coli* strains lacking nucleotidyl-transferase activity, required to repair the terminal CCA motif of tRNAs, could be suppressed by inactivation of the *relA* gene (Deutscher et al., 1977). This observation is coherent with our data that tRNA maturation defects promote the synthesis of (p)ppGpp and potentially extends this phenomenon to Gram-negative bacteria. Coordination between tRNA processing and ribosome biogenesis has also been proposed in yeast, based on the observation that the transport factor Sxm1p ferries both the tRNA processing cofactor Lhp1p and the ribosomal proteins Rpl16p, Rpl21p, and Rpl34p from the cytoplasm to the nucleoplasm (Rosenblum et al., 1997). The link between tRNA maturation and ribosome biogenesis may therefore be universally conserved, but with distinct mechanisms from one group of organisms to the next.

STAR★METHODS

Detailed methods are provided in the online version of this paper and include the following:

- KEY RESOURCES TABLE
- CONTACT FOR REAGENT AND RESOURCE SHARING
- EXPERIMENTAL MODEL AND SUBJECT DETAILS
- METHOD DETAILS
  - Bacterial cultures
  - RNA isolation and Northern blots
  - Primer extension
  - Sucrose gradients
  - Mass spectrometry analysis and data processing
  - (p)ppGpp measurement
- QUANTIFICATION AND STATISTICAL ANALYSIS
- DATA AND SOFTWARE AVAILABILITY

SUPPLEMENTAL INFORMATION

Supplemental Information can be found online at https://doi.org/10.1016/j.molcel.2019.03.030.

ACKNOWLEDGMENTS

We thank J.D. Wang for strains lacking *ywaC*, *yjbM*, and *relA* and advice on how to build a (p)ppGpp-overproducing strain. We thank both J.D. Wang and R. Gourse for advice on how to measure (p)ppGpp levels by TLC. We thank lab members and M. Springer, C. Tisné, M. Catala, R. Britton, E. Maisonneuve, V. Hauryliuk, and M. Cashel for helpful comments. This work was supported by funds from the CNRS (UMR8261), Université Paris VII-Denis Diderot, the Agence Nationale de la Recherche (ARNr-QC) and the Labex (Dynamo) program. The mass spectrometry instrumentation was funded by the University of Strasbourg, IdEx "Equipement mi-lourd" 2015.

AUTHOR CONTRIBUTIONS

A.T., J.E.U., L.G., and S.F. performed the experiments; P.H. and L.K. performed mass spectrometry analysis. All authors participated in analyzing data. C.C., F.B., and A.T. wrote the paper. F.B. and C.C. are co-supervisors of PhD student A.T.

DECLARATION OF INTERESTS

The authors declare no competing interests.

Received: January 11, 2019
Revised: March 7, 2019
Accepted: March 24, 2019
Published: April 16, 2019

SUPPORTING CITATIONS

The following references appear in the Supplemental Information: Ben-Yehuda et al. (2003); Figaro et al. (2013); Gössringer et al. (2006); Guérout-Fleury et al. (1995); Guérout-Fleury et al. (1996); Kim et al. (1996); Koo et al. (2017); Peters et al. (2016); Steinmetz and Richter (1994).

REFERENCES

Amato, S.M., Orman, M.A., and Brynildsen, M.P. (2013). Metabolic control of persister formation in *Escherichia coli*. Mol. Cell *50*, 475–487.

Arenz, S., Abdelshahid, M., Sohmen, D., Payoe, R., Starosta, A.L., Berninghausen, O., Hauryliuk, V., Beckmann, R., and Wilson, D.N. (2016). The stringent factor RelA adopts an open conformation on the ribosome to stimulate ppGpp synthesis. Nucleic Acids Res. *44*, 6471–6481.

Baumgardt, K., Gilet, L., Figaro, S., and Condon, C. (2018). The essential nature of YqfG, a YbeY homologue required for 3′ maturation of *Bacillus subtilis* 16S ribosomal RNA is suppressed by deletion of RNase R. Nucleic Acids Res. *46*, 8605–8615.

Bechhofer, D.H., Oussenko, I.A., Deikus, G., Yao, S., Mathy, N., and Condon, C. (2008). Analysis of mRNA decay in Bacillus subtilis. Methods Enzymol *447*, 259–276.

Ben-Yehuda, S., Rudner, D.Z., and Losick, R. (2003). RacA, a bacterial protein that anchors chromosomes to the cell poles. Science *299*, 532–536.

Bremer, H., and Dennis, P.P. (1996). Modulation of chemical composition and other parameters of the cell by growth rate. In *Escherichia coli* and *Salmonella*: Cellular and Molecular Biology, F.C. Neidhardt, R. Curtiss, J.L. Ingraham, E.C. Lin, K.B. Low, B. Magasanik, W.S. Reznikoff, M. Riley, M. Schaechter, and H.E. Umbarger, eds. (American Society for Microbiology), pp. 1553–1569.

Britton, R.A., Wen, T., Schaefer, L., Pellegrini, O., Uicker, W.C., Mathy, N., Tobin, C., Daou, R., Szyk, J., and Condon, C. (2007). Maturation of the 5′ end of *Bacillus subtilis* 16S rRNA by the essential ribonuclease YkqC/RNase J1. Mol. Microbiol. *63*, 127–138.

Brown, A., Fernández, I.S., Gordiyenko, Y., and Ramakrishnan, V. (2016). Ribosome-dependent activation of stringent control. Nature *534*, 277–280.

Bunner, A.E., Nord, S., Wikström, P.M., and Williamson, J.R. (2010). The effect of ribosome assembly cofactors on *in vitro* 30S subunit reconstitution. J. Mol. Biol. *398*, 1–7.

Bylund, G.O., Wipemo, L.C., Lundberg, L.A., and Wikström, P.M. (1998). RimM and RbfA are essential for efficient processing of 16S rRNA in *Escherichia coli*. J. Bacteriol. *180*, 73–82.

Cashel, M., and Rudd, K.E. (1987). The stringent response. In *Escherichia coli* and *Salmonella* typhimurium: Cellular and Molecular Biology, F.C. Neidhardt, ed. (American Society for Microbiology), pp. 1410–1438.

Charollais, J., Pflieger, D., Vinh, J., Dreyfus, M., and Iost, I. (2003). The DEAD-box RNA helicase SrmB is involved in the assembly of 50S ribosomal subunits in *Escherichia coli*. Mol. Microbiol. *48*, 1253–1265.

Chen, S.S., and Williamson, J.R. (2013). Characterization of the ribosome biogenesis landscape in *E. coli* using quantitative mass spectrometry. J. Mol. Biol. *425*, 767–779.

Chicher, J., Simonetti, A., Kuhn, L., Schaeffer, L., Hammann, P., Eriani, G., and Martin, F. (2015). Purification of mRNA-programmed translation initiation complexes suitable for mass spectrometry analysis. Proteomics *15*, 2417–2425.

Chowdhury, N., Kwan, B.W., and Wood, T.K. (2016). Persistence increases in the absence of the alarmone guanosine tetraphosphate by reducing cell growth. Sci. Rep. *6*, 20519.

Condon, C. (2014). RNA processing. In Reference Module in Biomedical Sciences, M. Capan, ed. (Elsevier).

Corrigan, R.M., Bellows, L.E., Wood, A., and Gründling, A. (2016). ppGpp negatively impacts ribosome assembly affecting growth and antimicrobial tolerance in Gram-positive bacteria. Proc. Natl. Acad. Sci. USA *113*, E1710–E1719.

Crary, S.M., Niranjanakumari, S., and Fierke, C.A. (1998). The protein component of *Bacillus subtilis* ribonuclease P increases catalytic efficiency by enhancing interactions with the 5′ leader sequence of pre-tRNAAsp. Biochemistry *37*, 9409–9416.

Deutscher, M.P., Setlow, P., and Foulds, J. (1977). *relA* overcomes the slow growth of *cca* mutants. J. Mol. Biol. *117*, 1095–1100.

DiChiara, J.M., Liu, B., Figaro, S., Condon, C., and Bechhofer, D.H. (2016). Mapping of internal monophosphate 5′ ends of *Bacillus subtilis* messenger RNAs and ribosomal RNAs in wild-type and ribonuclease-mutant strains. Nucleic Acids Res. *44*, 3373–3389.

Dunn, J.J., and Studier, F.W. (1973). T7 early RNAs and Escherichia coli ribosomal RNAs are cut from large precursor RNAs in vivo by ribonuclease 3. Proc. Natl. Acad. Sci. USA *70*, 3296–3300.

Durand, S., Gilet, L., and Condon, C. (2012). The essential function of *B. subtilis* RNase III is to silence foreign toxin genes. PLoS Genet. *8*, e1003181.

Feng, B., Mandava, C.S., Guo, Q., Wang, J., Cao, W., Li, N., Zhang, Y., Zhang, Y., Wang, Z., Wu, J., et al. (2014). Structural and functional insights into the mode of action of a universally conserved Obg GTPase. PLoS Biol. *12*, e1001866.

Figaro, S., Durand, S., Gilet, L., Cayet, N., Sachse, M., and Condon, C. (2013). *Bacillus subtilis* mutants with knockouts of the genes encoding ribonucleases RNase Y and RNase J1 are viable, with major defects in cell morphology, sporulation, and competence. J. Bacteriol. *195*, 2340–2348.

Franco, I.S., Mota, L.J., Soares, C.M., and de Sá-Nogueira, I. (2007). Probing key DNA contacts in AraR-mediated transcriptional repression of the *Bacillus subtilis* arabinose regulon. Nucleic Acids Res. *35*, 4755–4766.

Gaal, T., Bartlett, M.S., Ross, W., Turnbough, C.L., Jr., and Gourse, R.L. (1997). Transcription regulation by initiating NTP concentration: rRNA synthesis in bacteria. Science *278*, 2092–2097.

Gössringer, M., Kretschmer-Kazemi Far, R., and Hartmann, R.K. (2006). Analysis of RNase P protein (rnpA) expression in *Bacillus subtilis* utilizing strains with suppressible rnpA expression. J. Bacteriol. *188*, 6816–6823.

Guérout-Fleury, A.M., Shazand, K., Frandsen, N., and Stragier, P. (1995). Antibiotic-resistance cassettes for *Bacillus subtilis*. Gene *167*, 335–336.

Guérout-Fleury, A.M., Frandsen, N., and Stragier, P. (1996). Plasmids for ectopic integration in *Bacillus subtilis*. Gene *180*, 57–61.

Guerrier-Takada, C., Gardiner, K., Marsh, T., Pace, N., and Altman, S. (1983). The RNA moiety of ribonuclease P is the catalytic subunit of the enzyme. Cell *35*, 849–857.

Guo, Q., Goto, S., Chen, Y., Feng, B., Xu, Y., Muto, A., Himeno, H., Deng, H., Lei, J., and Gao, N. (2013). Dissecting the in vivo assembly of the 30S ribosomal subunit reveals the role of RimM and general features of the assembly process. Nucleic Acids Res. *41*, 2609–2620.

Hase, Y., Yokoyama, S., Muto, A., and Himeno, H. (2009). Removal of a ribosome small subunit-dependent GTPase confers salt resistance on *Escherichia coli* cells. RNA *15*, 1766–1774.

Herskovitz, M.A., and Bechhofer, D.H. (2000). Endoribonuclease RNase III is essential in *Bacillus subtilis*. Mol. Microbiol. *38*, 1027–1033.

Hwang, J., and Inouye, M. (2006). The tandem GTPase, Der, is essential for the biogenesis of 50S ribosomal subunits in *Escherichia coli*. Mol. Microbiol. *61*, 1660–1672.

Jacob, A.I., Köhrer, C., Davies, B.W., RajBhandary, U.L., and Walker, G.C. (2013). Conserved bacterial RNase YbeY plays key roles in 70S ribosome quality control and 16S rRNA maturation. Mol. Cell *49*, 427–438.

Kim, L., Mogk, A., and Schumann, W. (1996). A xylose-inducible *Bacillus subtilis* integration vector and its application. Gene *181*, 71–76.

Koo, B.M., Kritikos, G., Farelli, J.D., Todor, H., Tong, K., Kimsey, H., Wapinski, I., Galardini, M., Cabal, A., Peters, J.M., et al. (2017). Construction and analysis of two genome-scale deletion libraries for Bacillus subtilis. Cell Syst. *4*, 291–305.e297.

Krásný, L., and Gourse, R.L. (2004). An alternative strategy for bacterial ribosome synthesis: *Bacillus subtilis* rRNA transcription regulation. EMBO J. *23*, 4473–4483.

Kriel, A., Bittner, A.N., Kim, S.H., Liu, K., Tehranchi, A.K., Zou, W.Y., Rendon, S., Chen, R., Tu, B.P., and Wang, J.D. (2012). Direct regulation of GTP homeostasis by (p)ppGpp: a critical component of viability and stress resistance. Mol. Cell *48*, 231–241.

Leong, V., Kent, M., Jomaa, A., and Ortega, J. (2013). *Escherichia coli rimM* and *yjeQ* null strains accumulate immature 30S subunits of similar structure and protein complement. RNA *19*, 789–802.

Li, Z., Pandit, S., and Deutscher, M.P. (1998). Polyadenylation of stable RNA precursors *in vivo*. Proc. Natl. Acad. Sci. USA *95*, 12158–12162.

Liu, K., Myers, A.R., Pisithkul, T., Claas, K.R., Satyshur, K.A., Amador-Noguez, D., Keck, J.L., and Wang, J.D. (2015). Molecular mechanism and evolution of guanylate kinase regulation by (p)ppGpp. Mol. Cell *57*, 735–749.

Loh, P.C., Morimoto, T., Matsuo, Y., Oshima, T., and Ogasawara, N. (2007). The GTP-binding protein YqeH participates in biogenesis of the 30S ribosome subunit in *Bacillus subtilis*. Genes Genet. Syst. *82*, 281–289.

Loveland, A.B., Bah, E., Madireddy, R., Zhang, Y., Brilot, A.F., Grigorieff, N., and Korostelev, A.A. (2016). Ribosome●RelA structures reveal the mechanism of stringent response activation. eLife *5*, e17029.

Mathy, N., Bénard, L., Pellegrini, O., Daou, R., Wen, T., and Condon, C. (2007). 5′-to-3′ exoribonuclease activity in bacteria: role of RNase J1 in rRNA maturation and 5′ stability of mRNA. Cell *129*, 681–692.

Miller, D.L., Cashel, M., and Weissbach, H. (1973). The interaction of guanosine 5′-diphosphate, 2′ (3′)-diphosphate with the bacterial elongation factor Tu. Arch. Biochem. Biophys. *154*, 675–682.

Milon, P., Tischenko, E., Tomsic, J., Caserta, E., Folkers, G., La Teana, A., Rodnina, M.V., Pon, C.L., Boelens, R., and Gualerzi, C.O. (2006). The nucleotide-binding site of bacterial translation initiation factor 2 (IF2) as a metabolic sensor. Proc. Natl. Acad. Sci. USA *103*, 13962–13967.

Mitkevich, V.A., Ermakov, A., Kulikova, A.A., Tankov, S., Shyp, V., Soosaar, A., Tenson, T., Makarov, A.A., Ehrenberg, M., and Hauryliuk, V. (2010). Thermodynamic characterization of ppGpp binding to EF-G or IF2 and of initiator tRNA binding to free IF2 in the presence of GDP, GTP, or ppGpp. J. Mol. Biol. *402*, 838–846.

My, L., Ghandour Achkar, N., Viala, J.P., and Bouveret, E. (2015). Reassessment of the genetic regulation of fatty acid synthesis in *Escherichia coli*: global positive control by the dual functional regulator FadR. J. Bacteriol. *197*, 1862–1872.

Natori, Y., Tagami, K., Murakami, K., Yoshida, S., Tanigawa, O., Moh, Y., Masuda, K., Wada, T., Suzuki, S., Nanamiya, H., et al. (2009). Transcription activity of individual *rrn* operons in *Bacillus subtilis* mutants deficient in (p)ppGpp synthetase genes, *relA, yjbM,* and *ywaC*. J. Bacteriol. *191*, 4555–4561.

Nicolas, P., Mäder, U., Dervyn, E., Rochat, T., Leduc, A., Pigeonneau, N., Bidnenko, E., Marchadier, E., Hoebeke, M., Aymerich, S., et al. (2012). Condition-dependent transcriptome reveals high-level regulatory architecture in *Bacillus subtilis*. Science *335*, 1103–1106.

Noller, H.F., and Nomura, M. (1987). Ribosomes. In *Escherichia coli* and *Salmonella typhimurium*: Cellular and Molecular Biology, F.C. Neidhardt, J.L. Ingraham, K.B. Low, B. Magasanik, M. Schaechter, and H.E. Umbarger, eds. (ASM Press), pp. 104–126.

Nord, S., Bylund, G.O., Lövgren, J.M., and Wikström, P.M. (2009). The RimP protein is important for maturation of the 30S ribosomal subunit. J. Mol. Biol. *386*, 742–753.

Pao, C.C., and Gallant, J. (1978). A gene involved in the metabolic control of ppGpp synthesis. Mol. Gen. Genet. *158*, 271–277.

Pellegrini, O., Nezzar, J., Marchfelder, A., Putzer, H., and Condon, C. (2003). Endonucleolytic processing of CCA-less tRNA precursors by RNase Z in *Bacillus subtilis*. EMBO J. *22*, 4534–4543.

Pellegrini, O., Li de la Sierra-Gallay, I., Piton, J., Gilet, L., and Condon, C. (2012). Activation of tRNA maturation by downstream uracil residues in *B. subtilis*. Structure *20*, 1769–1777.

Peters, J.M., Colavin, A., Shi, H., Czarny, T.L., Larson, M.H., Wong, S., Hawkins, J.S., Lu, C.H.S., Koo, B.M., Marta, E., et al. (2016). A comprehensive, CRISPR-based functional analysis of essential genes in bacteria. Cell *165*, 1493–1506.

Polakis, S.E., Guchhait, R.B., and Lane, M.D. (1973). Stringent control of fatty acid synthesis in *Escherichia coli*. Possible regulation of acetyl coenzyme A carboxylase by ppGpp. J. Biol. Chem. *248*, 7957–7966.

Redko, Y., Bechhofer, D.H., and Condon, C. (2008). Mini-III, an unusual member of the RNase III family of enzymes, catalyses 23S ribosomal RNA maturation in *B. subtilis*. Mol. Microbiol. *68*, 1096–1106.

Reich, C., Olsen, G.J., Pace, B., and Pace, N.R. (1988). Role of the protein moiety of ribonuclease P, a ribonucleoprotein enzyme. Science *239*, 178–181.

Rosenblum, J.S., Pemberton, L.F., and Blobel, G. (1997). A nuclear import pathway for a protein involved in tRNA maturation. J. Cell Biol. *139*, 1655–1661.

Ross, W., Sanchez-Vazquez, P., Chen, A.Y., Lee, J.H., Burgos, H.L., and Gourse, R.L. (2016). ppGpp binding to a site at the RNAP-DksA interface accounts for its dramatic effects on transcription initiation during the stringent response. Mol. Cell *62*, 811–823.

Sayed, A., Matsuyama, Si., and Inouye, M. (1999). Era, an essential *Escherichia coli* small G-protein, binds to the 30S ribosomal subunit. Biochem. Biophys. Res. Commun. *264*, 51–54.

Schneider, D.A., Murray, H.D., and Gourse, R.L. (2003). Measuring control of transcription initiation by changing concentrations of nucleotides and their derivatives. Methods Enzymol *370*, 606–617.

Shajani, Z., Sykes, M.T., and Williamson, J.R. (2011). Assembly of bacterial ribosomes. Annu. Rev. Biochem. *80*, 501–526.

Shetty, S., and Varshney, U. (2016). An evolutionarily conserved element in initiator tRNAs prompts ultimate steps in ribosome maturation. Proc. Natl. Acad. Sci. USA *113*, E6126–E6134.

Slagter-Jäger, J.G., Puzis, L., Gutgsell, N.S., Belfort, M., and Jain, C. (2007). Functional defects in transfer RNAs lead to the accumulation of ribosomal RNA precursors. RNA *13*, 597–605.

Sprinzl, M., and Richter, D. (1976). Free 3′-OH group of the terminal adenosine of the tRNA molecule is essential for the synthesis in vitro of guanosine tetraphosphate and pentaphosphate in a ribosomal system from *Escherichia coli*. Eur. J. Biochem. *71*, 171–176.

Steinmetz, M., and Richter, R. (1994). Plasmids designed to alter the antibiotic resistance expressed by insertion mutations in *Bacillus subtilis*, through in vivo recombination. Gene *142*, 79–83.

Stent, G.S., and Brenner, S. (1961). A genetic locus for the regulation of ribonucleic acid synthesis. Proc. Natl. Acad. Sci. USA *47*, 2005–2014.

Toymentseva, A.A., Schrecke, K., Sharipova, M.R., and Mascher, T. (2012). The LIKE system, a novel protein expression toolbox for *Bacillus subtilis* based on the lial promoter. Microb. Cell Fact. *11*, 143.

Traxler, M.F., Summers, S.M., Nguyen, H.T., Zacharia, V.M., Hightower, G.A., Smith, J.T., and Conway, T. (2008). The global, ppGpp-mediated stringent response to amino acid starvation in *Escherichia coli*. Mol. Microbiol. *68*, 1128–1148.

Uicker, W.C., Schaefer, L., Koenigsknecht, M., and Britton, R.A. (2007). The essential GTPase YqeH is required for proper ribosome assembly in *Bacillus subtilis*. J. Bacteriol. *189*, 2926–2929.

Wang, J.D., Sanders, G.M., and Grossman, A.D. (2007). Nutritional control of elongation of DNA replication by (p)ppGpp. Cell *128*, 865–875.

Waugh, D.S., and Pace, N.R. (1990). Complementation of an RNase P RNA (*rnpB*) gene deletion in *Escherichia coli* by homologous genes from distantly related eubacteria. J. Bacteriol. *172*, 6316–6322.

Wegscheid, B., Condon, C., and Hartmann, R.K. (2006). Type A and B RNase P RNAs are interchangeable in vivo despite substantial biophysical differences. EMBO Rep. *7*, 411–417.

Wen, T., Oussenko, I.A., Pellegrini, O., Bechhofer, D.H., and Condon, C. (2005). Ribonuclease PH plays a major role in the exonucleolytic maturation of CCA-containing tRNA precursors in *Bacillus subtilis*. Nucleic Acids Res. *33*, 3636–3643.

Wendrich, T.M., and Marahiel, M.A. (1997). Cloning and characterization of a *relA/spoT* homologue from *Bacillus subtilis*. Mol. Microbiol. *26*, 65–79.

STAR★METHODS

KEY RESOURCES TABLE

REAGENT or RESOURCE	SOURCE	IDENTIFIER
Bacterial and Virus Strains		
See Table S1 for *Bacillus subtilis* strains used in this study and Table S2 for details on new constructs.	N/A	N/A
Chemicals, Peptides, and Recombinant Proteins		
[P32] $KH_2{}^{32}PO_4$ (1mCi/ml)	Perkin-Elmer	Cat#NEX063001MC
ATP, [γ-32P]- 3000Ci/mmol 10mCi/ml EasyTide	Perkin-Elmer	Cat#BLU502A500UC
UTP, [α-32P]- 3000Ci/mmol 10mCi/ml EasyTide	Perkin-Elmer	Cat#BLU507H500UC
Decoyinine (Augustmycin A)	Abcam	Cat#ab144238
L-Arginine hydroxamate hydrochloride	Sigma-Aldrich	Cat#A7380
Bacitracin from Bacillus licheniformis, ≥ 60000 U/g (Potency)	Sigma-Aldrich	Cat#11702
Formic acid (≥97%)	MP biomedicals	Cat#0215116290
Sequencing grade modified trypsin	Promega	Cat#V5111
DNase I	Sigma-Aldrich	Cat#DN25
RNase A	Sigma-Aldrich	Cat#R6513
Set of dATP, dCTP, dGTP and dTTP	Promega	Cat#U1240
rATP, rCTP, rGTP and rUTP	Promega	Cat#E6011, E6041, E6031, E6021
Roti Hybri Quick	Roth	Cat#A981.1
Ultrahyb	Life technologies	Cat#AM8669
Aquaphenol water-saturated	MP biomedicals	Cat#AQUAPH01
AMV Reverse Transriptase	New England Biolabs	Cat#M0277
Deposited Data		
Mendeley raw imaging data (e.g., uncropped and unannotated agarose gels, Northern blots and thin layer chromatography autoradiograms).	This work	10.17632/d4wrkvdtjp.1
Oligonucleotides		
See Table S3 for list of primers used in this study	N/A	N/A
Recombinant DNA		
See Table S4 for list of plasmids used in this study.	N/A	N/A
Software and Algorithms		
Pymol 2.3.0	Schrödinger	RRID: SCR_000305
Fiji	https://fiji.sc/	RRID: SCR_002285
Proline v1.4	http://www.proline.profiproteomics.fr/	N/A
Mascot v2.5	Matrix Science, London, UK	N/A
Other		
QExactive+ mass spectrometer	Thermo-Fisher Scientific, USA	N/A
EASY-nanoLC-1000	Thermo-Fisher Scientific, USA	N/A
French Press	Glen Mills, USA	N/A
PhosphorImager screens	GE HealthCare Life Sciences	N/A
Typhoon scanner	GE HealthCare Life Sciences	N/A
Glass beads acid-washed	Sigma-Aldrich	Cat#G1145
Piston Gradient Fractionator	Biocomp	N/A
Gradient Master	Biocomp	N/A
Membrane Amersham Hybond-N+	GE HealthCare Life Sciences	Cat#RPN203B
PEI Cellulose TLC plate, Baker-flex	J.T.Baker	Cat#2002564
Disruptor Genie Digital Cell Disruptor	Thermo-Fisher Scientific, USA	Cat#15577345

CONTACT FOR REAGENT AND RESOURCE SHARING

Further information and requests for resources and reagents should be directed to and will be fulfilled by the Lead Contact Ciarán Condon (condon@ibpc.fr).

EXPERIMENTAL MODEL AND SUBJECT DETAILS

B. subtilis strain W168 and *B. subtilis 168 trpC*. All mutant strains used were derived from these two parental strains, by transformation with PCR products, plasmids or chromosomal DNA from both previously published strains or new constructs. A list of all strains used is provided in Table S1. Details of new strains and plasmid constructs are provided in Tables S2 and S4, respectively.

METHOD DETAILS

Bacterial cultures

All cultures were grown in 2xYT medium. Overnight cultures were grown in the presence of appropriate antibiotics. Experimental cultures did not contain antibiotics, except when necessary for maintaining plasmids. For depletion studies, overnight cultures grown in the presence of inducer (1 mM IPTG or 2% xylose) were washed three times in an equal volume of pre-warmed medium and inoculated into fresh medium with or without inducer at OD_{600} = 0.05 (*rnpA* and *rnz*) or 0.2 (*rnpB*), the empirically determined optimal depletion conditions for the respective strains. For the depletion of RnpA, cells were inoculated into fresh medium containing glucose (2%) to tighten repression of the *Pxyl* promoter. Cultures were followed until they reached a plateau, typically around OD_{600} = 0.6 for *rnpA* and *rnz*, and 0.3 for *rnpB*, and harvested for RNA preparation.

For amino acid starvation, arginine hydroxamate (RHX) was added at 250 μg/mL at $0D_{600}$ = 0.3. For inhibition of GTP synthesis, decoyinine was dissolved at 1 mg/mL in 2xYT pre-warmed to 37°C and an equal volume added to 1 mL cultures at OD_{600} = 0.6 (final concentration 500 μg/mL). For the CRISPRi strain targeting *era* expression, cells were grown overnight in 2xYT and diluted in the presence or absence of 1% xylose. Cells were grown to OD_{600} = 0.5 before harvesting.

RNA isolation and Northern blots

RNA was typically isolated from 1 mL mid-log phase *B. subtilis* cells growing in 2xYT medium by the glass beads/phenol, a modification of the method described in (Bechhofer et al., 2008). For strains that plateau at very low OD_{600}, e.g., the *rnpB* depletion strain, greater volumes of cell culture (up to 8 mL) were harvested. Frozen cell pellets were resuspended in 200 μL ice-cold TE-Buffer (10 mM Tris, pH 7.5, 1 mM EDTA) and transferred to a tube containing 25 μL chloroform, 6.25 μL 20% SDS and 100 μL glass beads for lysis by three 1 min vortexing steps at max speed on a Disruptor Genie (Scientific Industries) separated with 1 min intervals on ice. After centrifugation, the supernatant was transferred to 200 μL water-saturated phenol on ice and vortexed again (with the same vortexing protocol as above) before being centrifuged for 10 min at 16,000 x g at 4°C. The supernatant was then mixed with 200 μL water-saturated phenol and 100 μL chloroform, vortexed for 1 min at full speed and centrifuged again for 10 min at 16,000 x g at 4°C. RNA was precipitated at −20°C by adding 3 volumes of 95% ethanol stored at −20°C and 0.1 volumes of 10M LiCl before being washed, dried, and resuspended in 50 μL water. For Northern blots, 5 μg total RNA was run on 1% agarose or 5% acrylamide gels and transferred to hybond-N membranes (GE-Healthcare), by capillary transfer or electrotransfer, respectively. Hybridization was performed using 5′-labeled oligonucleotides using Ultra-Hyb (Life Technologies) or Roti-Hybri-Quick (Roth) hybridization buffers at 42°C for a minimum of 4 hours. Membranes were washed twice in 2 × SSC 0.1% SDS (once rapidly at room temperature (RT), once for 5 min at 42°C) and then twice for 5 mins in 0.2 × SSC 0.1% SDS at 42°C, as described in Durand et al. (2012).

Primer extension

Primer extension assays were done using a modified version of the protocol described in Britton et al. (2007) on total *B. subtilis* RNA extracted as described above, but with an additional treatment with DNase I to remove chromosomal DNA. 0.5 pmol of 5′-labeled (^{32}P) oligonucleotides was added to 5 μg of RNA in 5 μL final volume RT buffer (50 mM Tris-HCl, pH 8.3, 10 mM $MgCl_2$, 80 mM KCl) and denatured at 75°C for 4 min. The denatured mixture was frozen on dry ice for 2 mins and then transferred to ice to thaw. Oligonucleotides CC058 and CC257 were used to assay 5′ processing of 16S and 23S rRNAs, respectively. A 5.2 μL mix containing 2 mM each dNTP, 8 mM dithiothreitol (DTT), 4 units AMV reverse transcriptase (NEB) in RT buffer was then added. Reaction mixtures were incubated for 30 min at 45°C, stopped with 5 μL of 95% formamide, 20 mM EDTA, 0.05% bromophenol blue, 0.05% xylene cyanol and loaded on 5% sequencing gels.

Sucrose gradients

B. subtilis 30S and 50S ribosomal particles were separated from 50 mL of log phase *B. subtilis* cells (OD_{600} = 0.5). Cells were centrifuged and resuspended in 1 mL ice cold Buffer A (20 mM Tris-HCl pH 7.5, 200 mM NH_4Cl, 6 mM β-Mercaptoethanol) containing 3 mM $MgCl_2$ and 4 μg/mL DNase I and lysed by two passages in an ice-cold French Press (Glen Mills) at 20,000 psi. The lysate was cleared at 13,200 rpm for 30 mins at 4°C in a bench top centrifuge. A maximum of 500 μL of lysate was loaded on a 10%–30% sucrose gradient in Buffer A containing 3 mM $MgCl_2$ and centrifuged at 23,000 rpm for 16h at 4°C in an SW41 rotor (Beckmann).

500 μL fractions were collected using a Piston Gradient Fractionator (Biocomp) for analysis on agarose gels or mass spectrometry. 70S ribosomes were prepared similarly but with Buffer A containing 10 mM $MgCl_2$ and centrifugation at 18,600 rpm for 16h.

Mass spectrometry analysis and data processing

Mass-spectrometry analysis was performed in triplicate. Proteins in sucrose gradient fractions were digested with sequencing-grade trypsin (Promega, Fitchburg, MA, USA). Each fraction (500 ng of digested peptides) was further analyzed by nanoLC-MS/MS on a QExactive+ mass spectrometer coupled to an EASY-nanoLC-1000 (Thermo-Fisher Scientific, USA) as described previously (Chicher et al., 2015). Data were searched against the *Bacillus subtilis* SwissProt sub-database with a decoy strategy (SwissProt release 2017_09, taxon 224308, 4294 forward protein sequences). Peptides and proteins were identified with Mascot algorithm (version 2.5, Matrix Science, London, UK) and data were further imported into Proline v1.4 software (http://www.proline.profiproteomics.fr/). Proteins were validated on Mascot pretty rank equal to 1, Mascot score above 25, and 1% FDR on both peptide spectrum matches (PSM score) and protein sets (Protein Set score). Proline package was further used to align proteins across all samples and to compute the Spectrum Counting values. The total number of MS/MS fragmentation spectra was used to relatively quantify each protein across all samples. The number of spectra for each 30S ribosomal protein was first normalized to the total number of spectra identified in each mutant sample and then normalized to the equivalent value obtained for the wt. Raw and processed data are given in Table S5. The % occurrence of each ribosomal protein compared to wt is reported as a % fill of the relevant box on the assembly maps shown in Figures 3 and S3.

(p)ppGpp measurement

Synthesis of (p)ppGpp was measured with a protocol adapted from Wang et al. (2007). $KH_2{}^{32}PO_4$ (1mCi/ml; Perkin Elmer) was added to depletion cultures growing in 2xYT a final concentration of 100 μCi/ml at $OD_{600} \approx 0.1$ (or from the beginning in the case of *rnpB*). At $OD_{600} = 0.5$ (or ≈ 0.3 for the *rnpB* depletion strain) 250 μL of culture was mixed with 55 μL 2M ice-cold formic acid and frozen on dry ice. Samples were left on ice for 20 mins and centrifuged at 4°C for 15 mins to collect the supernatant. PEI-cellulose TLC plates (J.T.Baker) were prepared by sequential immersion in distilled H_2O, air drying, immersion in methanol and a second air-drying step. Then, 20 μL of extracts were spotted progressively (2 uL at a time, dried by hairdryer on cold setting) on the plate and plates were developed in 1.5 M KH_2PO_4 (pH = 3.4) as described in Schneider et al. (2003). The region of the plate containing the unincorporated label was cut off before overnight exposure to PhosphorImager screens and scanning using a GE Typhoon scanner.

QUANTIFICATION AND STATISTICAL ANALYSIS

Northern blots were scanned using a GE Typhoon scanner. The resulting (.gel) image was quantified by drawing rectangles around individual bands using Fiji software. Processing efficiency was calculated from the ratio of the 65-nt species to the pre-16S species and normalized to the ratios calculated for the wt samples present on each gel. Experiments were performed at least in duplicate (the actual number of repetitions is given in the legend to each figure). Standard errors were calculated in Microsoft Excel.

DATA AND SOFTWARE AVAILABILITY

Raw and processed data for the mass-spectrometry experiment are given in Table S5. Raw imaging data (e.g., uncropped, unannotated agarose gels, Northern blots and thin layer chromatography autoradiograms) corresponding to individual figure panels have been deposited in Mendeley Data: https://doi.org/10.17632/d4wrkvdtjp.1

Molecular Cell, Volume *74*

Supplemental Information

tRNA Maturation Defects Lead to Inhibition of rRNA Processing via Synthesis of pppGpp

Aude Trinquier, Jonathan E. Ulmer, Laetitia Gilet, Sabine Figaro, Philippe Hammann, Lauriane Kuhn, Frédérique Braun, and Ciarán Condon

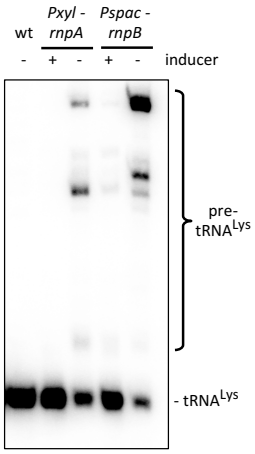

Figure S1, related to Figure 1: Effects of *rnpA* and *rnpB* depletion on processing of $tRNA^{Lys}$. The Northern blot was probed with oligo CC1915, complementary to the mature portion of the *trnJ-lys* tRNA.

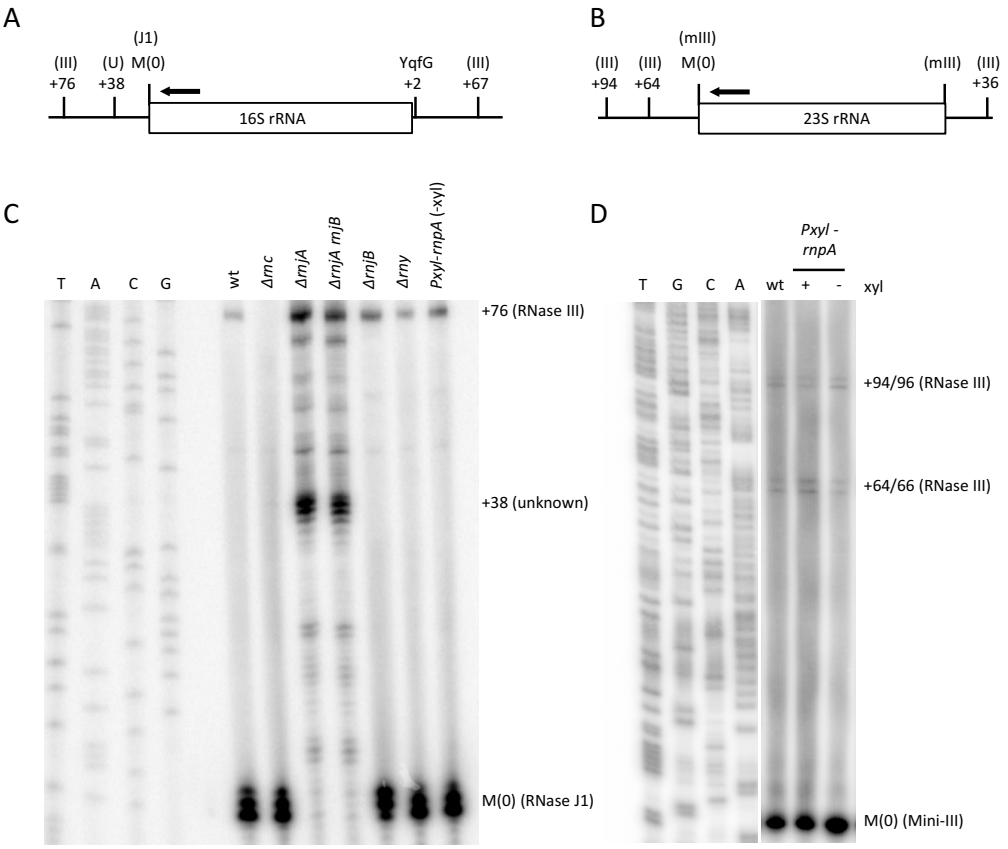

Figure S2, related to Figure 1: RNase P depletion is specific to the 3' processing of 16S rRNA. (A) Schematic of primer extension assay of 16S rRNA 5' processing, showing cleavage sites for RNase III (III), the unknown RNase (U), RNase J1 (J1) and YqfG. The primer used (CC058) is schematized by a black arrow. (B) Schematic of primer extension assay of 23S rRNA 5' processing, showing cleavage sites for RNase III (III) and Mini-III (mIII). The primer used (CC257) is schematized by a black arrow. (C) Primer extension assay of 16S rRNA 5' processing using oligo CC058 performed on total RNA isolated from wild-type (WT) or strains lacking RNase III (Δ*rnc*), RNase J1 (Δ*rnjA*), RNase J2 (Δ*rnjB*), RNase Y (Δ*rny*), or depleted for the protein subunit of RNase P (*rnpA*). (D) Primer extension assay of 23S rRNA 5' processing using oligo CC257, performed on total RNA isolated from WT and the *rnpA*-depletion strain in the absence of xylose (xyl).

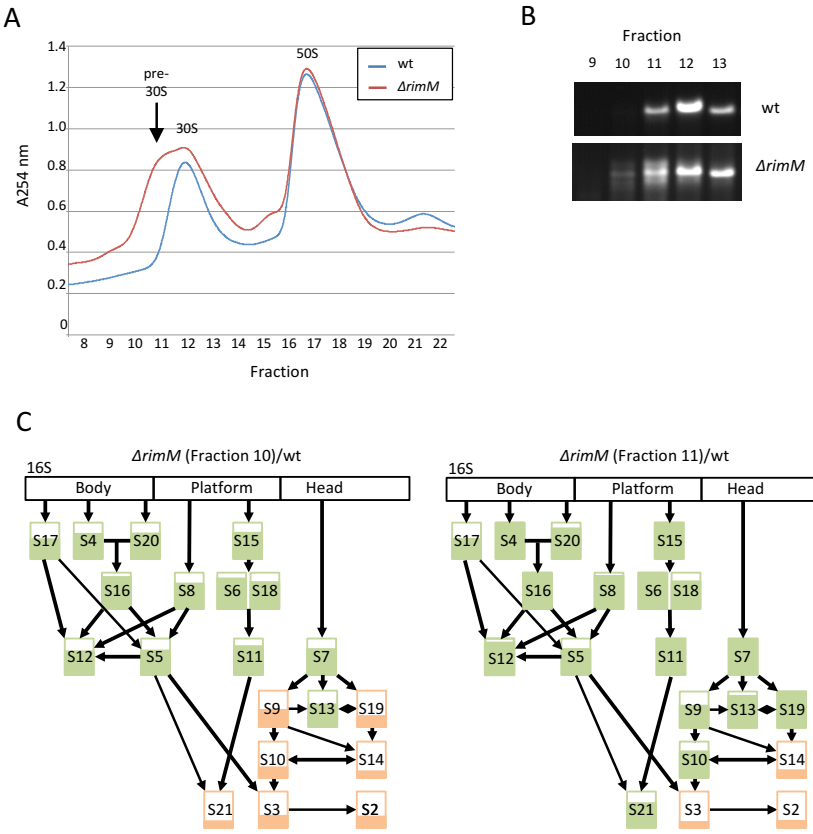

Figure S3, related to Figure 3: The effect of RNase P and Z depletions on ribosome assembly is similar to that of cells lacking the late assembly factor RimM. (A) Sucrose gradients of wt vs *ΔrimM* mutants (B) 16S rRNA profile in sucrose gradients (C) LC-MS/MS analysis (n=2) of pre-30S fractions in wt vs *ΔrimM* mutants. The number of peptides for each protein were first normalized to the total peptides observed in each fraction and then normalized to the equivalent number in wt. Early fraction 10 in the *ΔrimM* mutant was compared to early fraction 11 in wt; late fraction 11 in the *ΔrimM* mutant was compared to mature fraction 12 in wt. The percent fill of each box represents the amount of each ribosomal protein compared to wt. Proteins shown in orange are represented at >10% but ≤ 50% of wt; green > 50% of wt.

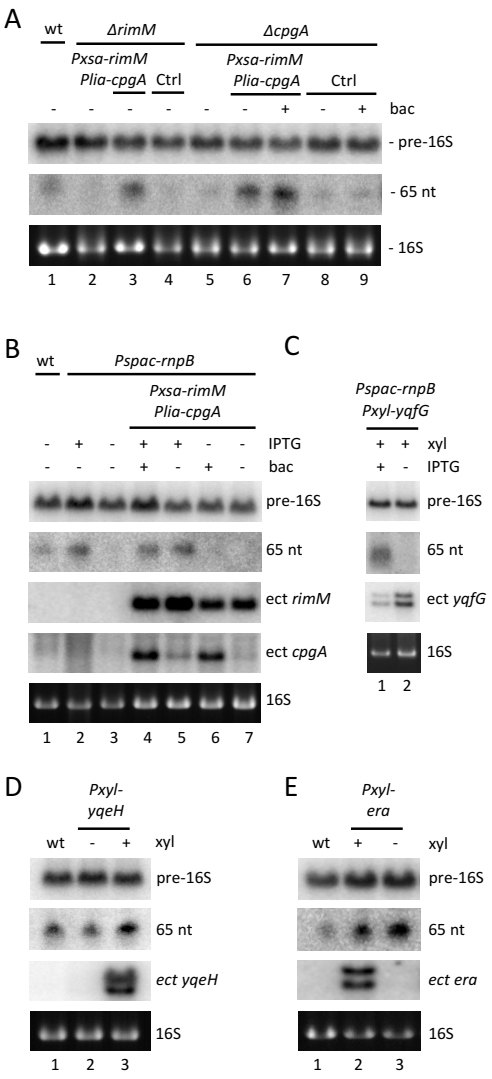

Figure S4, related to Figure 2: Perturbation of individual assembly factor mRNA levels is unlikely to explain defects in 16S 3' processing. (A) The *Pxsa-rimM + Plia-cpgA* vector is functional. Control experiment showing complementation of 16S rRNA 3' processing defects of *ΔrimM* and *ΔcpgA* strains by ectopic expression of *rimM* and *cpgA,* respectively. Note that expression of *Pxsa-rimM* is leaky and yields about 2-fold excess of *rimM* mRNA in the absence of arabinose, compared to expression from the native locus (not shown). Expression of *Plia-cpgA* is also leaky; addition of bacitracin (bac) yields similar levels of *cpgA* mRNA to expression from the native locus (not shown). Ctrl is the empty vector control. (B) 16S 3' processing is not restored in *rnpA*-depleted cells ectopically expressing *rimM* alone or together with *cpgA*. (C) 16S 3' processing is not restored in *rnpA*-depleted cells ectopically expressing *yqfG.* (D)+(E) 16S 3' processing is not inhibited upon over-expression of either *era* or *yqeH* in a wt background. 5 μg of total RNA was probed with oligo CC172, specific for the 16S rRNA 3' precursor, on agarose gels (upper panel) and polyacrylamide gels (lower panel) in each case for optimal transfer of the ~ 1620 nt and 65 nt species.

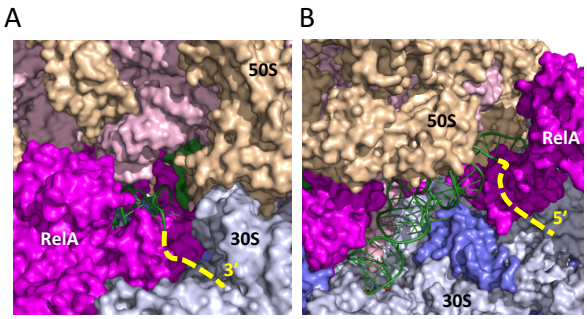

Figure S5, related to Figure 7: RelA bound to the A-site of the ribosome can accomodate tRNA precursors. (A) Possible pathway for tRNA 3' extensions (yellow dotted line). RelA is shown in space filling mode in pink, the 30S subunit in light blue (16S rRNA) and dark blue (30S proteins), the 50S subunit in pink (23S rRNA) and wheat (50S proteins), the A-site tRNA in cartoon mode and the P-site tRNA in space filling mode are shown in green (B) Possible pathway for tRNA 5' extensions. Color scheme as in panel (A).

Table S1. *B. subtilis* strains used in this study, related to Star Methods.

Strains	Genotype	Source/Ref.
SSB318	W168 *Pspac-rnpB:pMUTIN ery*	(Wegscheid et al., 2006)
SSB1002	W168 *trp+*	Lab strain
SSB1003	168 *trpC2*	BGSC*
CCB321	W168 *Pspac-rnz:pMUTIN ery* pMAP65 *kan*	This study; (Pellegrini et al., 2003)
CCB418	W168 *txpA -10Δ yonT::ery rnc::spc*	(Durand et al., 2012)
CCB434	W168 *rnjA::spc*	(Figaro et al., 2013)
CCB441	W168 *rny::spc*	(Figaro et al., 2013)
CCB078	W168 *rnjB::spc*	(Britton et al., 2007)
CCB501	W168 *rnjB::spc rnjA::kan*	(Figaro et al., 2013)
CCB504	W168 *Pxyl-rnpA Cm*	This study; (Gossringer et al., 2006)
CCB622	W168 *rpsU::ery*	This study
CCB654	BKE00420 168 *trpC2 ksgA::ery*	(Koo et al., 2017)
CCB656	BKE16590 168 *trpC2 ylxS::ery*	(Koo et al., 2017)
CCB657	BKE16650 168 *trpC2 rbfA::ery*	(Koo et al., 2017)
CCB664	W168 *rimM::ery*	This study; (Koo et al., 2017)
CCB751	W168 *Pspac-yqfG:pMUTIN ery amyE::pX-yqfG Cm* pMAP65 *kan*	(Baumgardt et al., 2018)
CCB1026	W168 *Pspac-rnpB:pMUTIN ery amyE::pX-yqfG Cm*	This study; (Baumgardt et al., 2018)
CCB1050	W168 *yjbM::spc ywaC::kan relA::ery*	This study; (Kriel et al., 2012)
CCB1055	W168 *yjbM::spc ywaC::kan Pxyl-rnpA Cm*	This study; (Gossringer et al., 2006; Kriel et al., 2012)
CCB1057	W168 *yjbM::spc ywaC::kan Pxyl-rnpA Cm relA::ery*	This study; (Gossringer et al., 2006; Kriel et al., 2012)
CCB1076	W168 *relA::ery::tet*	This study; (Gossringer et al., 2006; Kriel et al., 2012)
CCB1098	W168 *amyE::pX-yqeH*	This study
CCB1125	W168 *yjbM::spc ywaC::kan amyE::pX-ywaC Cm relA::ery*	This study; (Gossringer et al., 2006)
CCB1136	W168 *yjbM::spc ywaC::kan Pspac-rnz:pMUTIN relA::ery::tet* pMAP65 *kan*	This study; (Kriel et al., 2012; Pellegrini et al., 2003)
CCB1137	W168 *yjbM::spc ywaC::kan Pspac-rnpB:pMUTIN relA::ery::tet*	This study; (Kriel et al., 2012; Wegscheid et al., 2006)
CCB1156	W168 *cpgA::kan*	This study; (Koo et al., 2017)
CCB1158	W168 *yqeH::kan*	This study; (Koo et al., 2017)
CCB1159	W168 *amyE::pX-era*	This study
CCB1194	W168 *amyE::pDR111-Plia-cpgA-Pxsa-rimM spc Pspac-rnpB:pMUTIN ery*	This study; (Wegscheid et al., 2006)
CCB1198	W168 *amyE::pDR111-Plia-cpgA-Pxsa-rimM spc cpgA::kan*	This study; (Koo et al., 2017)
CCB1199	W168 *amyE::pDR111spc cpgA::kan*	This study; (Koo et al., 2017)
CCB1200	W168 *amyE::pDR111-Plia-cpgA-Pxsa-rimM spc rimM::ery*	This study; (Koo et al., 2017)
CCB1201	W168 *amyE::pDR111 spc rimM::ery*	This study; (Koo et al., 2017)
CCB1207	BKK04210 168 *trpC ydaF::kan*	(Koo et al., 2017)
CCB1208	BKK11890 168 *trpC yjcK::kan*	(Koo et al., 2017)
CCB1209	BEC25290 168 *trpC lacA::Pxyl-dcas9 ery amyE::Pveg-sgRNA(era) Cm*	(Peters et al., 2016)

**Bacillus* genetic stock center

Table S2 Construction of new strains, related to Star Methods

Strain number	Plasmid	PCR fragment	Oligos for insert amplification	Description	Source/Ref.
CCB622	-	Overlapping PCR	CC1506/1508 *rpsU* up CC1510/1511 rpsU down CC1507/1509 ery cassette	*rpsU* up and down were amplified from gDNA. *ery* was amplified from pDG641. Overlapping PCR was performed with underlined oligos. Deletion construct was re-amplified from genome and sequenced.	This study; pDG641 (Guerout-Fleury et al., 1995)
CCB1026	674			pX-yqfG linearized with KpnI and integrated into *amyE*	(Baumgardt et al., 2018)
CCB1076	pET	-		Contains tet cassette recombined into *relA::ery* construct to change antibiotic resistance	(Steinmetz and Richter, 1994)
CCB1098	790	-		pX-yqeH linearized with KpnI and integrated into *amyE*	This study
CCB1125	792	-		pX-ywaC linearized with KpnI and integrated into *amyE*	This study
CCB1159	821	-		pX-era linearized with KpnI and integrated into *amyE*	This study
CCB1194	822	-		pDR111-PliaI-cpgA Pxsa-rimM linearized with NcoI and integrated into *amyE*	This study

Table S3. Oligonucleotides used in this study, related to Star Methods
Non-hybridising sequences are shown in lower case letters. Restriction sites are underlined

Oligo	Gene	Sequence
CC172	16S 3' precursor	AAAACTAAACAAGACAGGGAACG
CC058	*rrnW* 16S rRNA	CAGCGTTCGTCCTGAGCCAG
CC257	*rrnW* 23S rRNA	ATATGAGCTCCATCGGCTCCTAGTGCCAAGGCATC
CC1501	*yqfG fwd*	atatactagtGGATTGAATATCCGGAGGCTACTAAG
CC1502	*yqfG + ter rvs*	taacggatccaaaaaggccatccgtcaggatggccGCATGCACGAAGCTTTTGAAGAATCG
CC1506	*rpsU up fwd*	GCTGAATCCGCTGATGCAAAAGAAGATG
CC1507	*rpsU up-ery fwd*	GGTGTATTCGGAGGGAGGGAAAGAGAGAATGAGACATGCTACACCTCCG
CC1508	*rpsU up-ery rvs*	CGGAGGTGTAGCATGTCTCATTCTCTCTTTCCCTCCCTCCGAATACACC
CC1509	*ery-rpsU down rvs*	CAAGAAGACTCATAAATCCACCCTCTTCGCACCAGCGAAAACTGGTTTAAGCC
CC1510	*ery-rpsU down fwd*	GGCTTAAACCAGTTTTCGCTGGTGCGAAGAGGGTGGATTTATGAGTCTTCTTG
CC1511	*rpsU down rvs*	GCAGCACGGAATCCTTTGATTTGAAGC
CC1560	*rpsU*	CTAGCAGCTTCAGACTTTTTCTTGCGC
CC1845	*rimM*	GAAATCACCCGCACTTCGCCTTTGATTCCGTG
CC1846	*era*	CCTTGTTTCTCGTCGTTTGGGGCTTATCGC
CC1847	*yqeH*	CGACCAGAGAGTCCGTTTCTCCAATACCGTG
CC1848	*yqfG*	CTGACAGAAACTTCAGCCTGATCCTGAACGC
CC1915	*trnJ-lys* mature	GACTCGAACCTTCGACCCTCTGATTAAAAG
CC2185	*era fwd*	taaactagtGGAGGATTTACATGACGAACGAAAGC
CC2186	*era + ter rvs*	taaggatccaaaaaggccatccgtcaggatggccCACACACGGGAAGAGATTAATATTCGTCCTC
CC2187	*yqeH fwd*	taaactagtGGGAGGAGTAAGAAATGGAAAAGGTTG
CC2188	*yqeH + ter rvs*	taaggatccaaaaaggccatccgtcaggatggccCACCTCTCCCCTTTTCTTAAATTAATGAACGCCG
CC2200	*cpgA fwd*	CAACGAGCTTATCAGGCCGCCAATTTGCAAC
CC2201	*cpgA + PT7 rvs*	gctctaatacgactcactatagggACGTGTGAATCAGCTCCACGTGGCGGG
CC2213	*ywaA*	GATGCAGAGGCGGTCGTTTGATTGATTCAG
CC2215	*ilvA*	CACATCCGGATCATCGAACGGATGGATAAACGTC
CC2235	*ywaC fwd*	atatactagtTAAAGGAGATGACGAACATGGATTTATCTG
CC2236	*ywaC + ter rvs*	atatggatccaaaaaggccatccgtcaggatggccGCACTTGGGTGCCGTCTTTTTTAATCCACTTC
CC2250	*Pxsa fwd*	gacgaaggatccCATATTTATAAATACATACGTAC
CC2251	*Pxsa rvs*	gacgaaaagcttGTAAGCGCTTTTACTAGTATTATATTATATATGTTC
CC2349	*PliaI fwd*	tatatgaattcCGGATCTTTAAAACGCCATGCCTC
CC2350	*PliaI-cpgA fwd*	gccttaataattttgccctcaggcatCGATGATCCTCCTTACGTTTTCC
CC2351	*PliaI-cpgA rvs*	GGAAAACGTAAGGAGGATCATCGatgcctgagggcaaaattattaaggc
CC2352	*cpgA rvs*	tatatgaattcGATGGTGCAACCTTTACATTATGC
CC2353	*Pxsa fwd*	atatctcgagGGATCCCATATTTATAAATACATACG
CC2354	*Pxsa-rimM fwd*	gctttgtcatatgatcacctcCttccaAAGCTTGTAAGCGCTTTTACTAG
CC2355	*Pxsa-rimM rvs*	CTAGTAAAAGCGCTTACAAGCTTtggaaGgaggtgatcatatgacaaagc
CC2356	*rimM rvs*	atatgcatgcCTCGACAAAAAGGCCATCCGTCAG

Table S4 Plasmid construction, related to Star Methods

Plasmid number	Initial vector	Insert	Oligos for insert amplification	Description	Source/Ref.
790	pX	*yqeH*	CC2187 + CC2188	Insert amplified from gDNA and cloned in SpeI/BamHI under *Pxyl* control.	This study; (Kim et al., 1996)
792	pX	*ywaC*	CC2235 + CC2236	Insert amplified from gDNA and cloned in SpeI/BamHI under *Pxyl* control.	This study; (Kim et al., 1996)
801	pDG1662	*Pxsa*	CC2250 + CC2251	Insert amplified from gDNA and cloned in BamHI/HindIII site	This study; (Guerout-Fleury et al., 1996)
812	pDR111	*cpgA*	CC2349 + CC2350 CC2351 + CC2352	*PliaI* was amplified from pLIKE(int), *cpgA* was amplified from gDNA. *PliaI-cpgA* was obtained by overlapping PCR with underlined oligos and inserted in pDR111 (EcoRI), and a clone in same orientation as the *rrnB* terminator was selected.	This study; pDR111 (Ben-Yehuda et al., 2003) pLIKE(int) (Toymentseva et al., 2012)is from the BGSC*
821	pX	*era*	CC2185 + CC2186	Insert amplified from gDNA and cloned in SpeI/BamHI under *Pxyl* control.	This study; (Kim et al., 1996)
822	pDR111-*cpgA*	*Pxsa-rimM*	CC2353 + CC2354 CC2355 + CC2356	*Pxsa* was amplified from pDG1662-Pxsa (plasmid 801), *rimM* was amplified from gDNA. *Pxsa-rimM* was obtained by overlapping PCR with underlined oligos and cloned in pDR111-PliaI-cpgA (XhoI/SphI) (plasmid 812) with double selection for ampicillin and spectinomycin resistance.	This study; Pxsa (Franco et al., 2007)

**Bacillus* genetic stock center

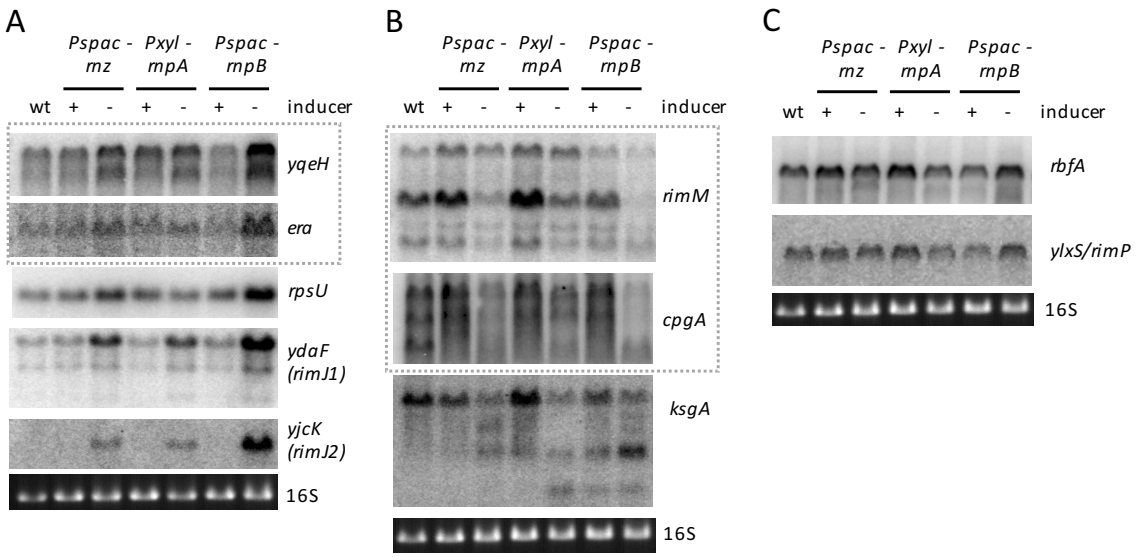

Figure 25: Depletion of tRNA processing enzymes results in perturbed expression of some proteins involved in 30S subunit assembly.

(A) Up-regulated genes, (B) Down-regulated genes. Others 30S subunit assembly cofactors mRNAs are not affected (C). The grey dotted line shows previously published portions of the figure (Chapter 1, Figure 2) shown again here to allow comparison.

Chapter 2: Effect of tRNA maturase depletion on ribosome assembly cofactor gene expression.

In results presented in the article in Chapter 1, we showed that depletion of tRNA maturase activity affects ribosome assembly leading to a specific 30S subunit late assembly defect. We also observed that several mRNAs encoding ribosome assembly cofactors were affected: transcripts encoding GTPases Era and YqeH were up-regulated during tRNA maturase depletion, whereas mRNAs encoding the GTPase CpgA and the RNA chaperone RimM were down-regulated. Because RNase P has very few direct mRNA targets (see Introduction), and because RNase Z depletion has comparable effects on the expression of these mRNAs, we considered it unlikely that the effects we observed were directly due to RNase P or RNase Z cleavages. We therefore wished to better understand by which mechanism(s) tRNA maturase depletion affected the levels of the cofactor encoding mRNAs. Because *rimM* is a known key player of small ribosomal subunit assembly (Cf. Introduction) and, since the late 30S ribosome assembly defect we observed was very similar to that observed in *E. coli* and *B. subtilis* Δ*rimM* mutants (Introduction, Figure 14 and Chapter 1, Figure S3), we put a particular focus on exploring the determinants responsible for the decrease in *rimM* expression in response to tRNA maturase depletion.

1. tRNA maturase depletion alters cofactor mRNA stability

In Chapter 1, we showed that depletion of RNase P or RNase Z results in altered mRNA levels (by up- or down-regulation) of four key 30S assembly cofactors (Era, YqeH, RimM and CpgA). The expression of several other cofactors was also affected during tRNA maturase depletion: the *ydaF* and *yjcK* transcripts (encoding potential homologs of the *E. coli* RimJ acetylase), and the *rpsU* transcript encoding r-protein S21 were up-regulated, whereas the transcript encoding the methyltransferase KsgA was down-regulated, with a visible accumulation of degradation intermediates (Figure 25). Expression of the *rbfA* and *ylxS/rimP* mRNAs were relatively unchanged, showing that tRNA maturase depletion does not cause non-specific perturbation of every cofactor gene expression in *B. subtilis.*

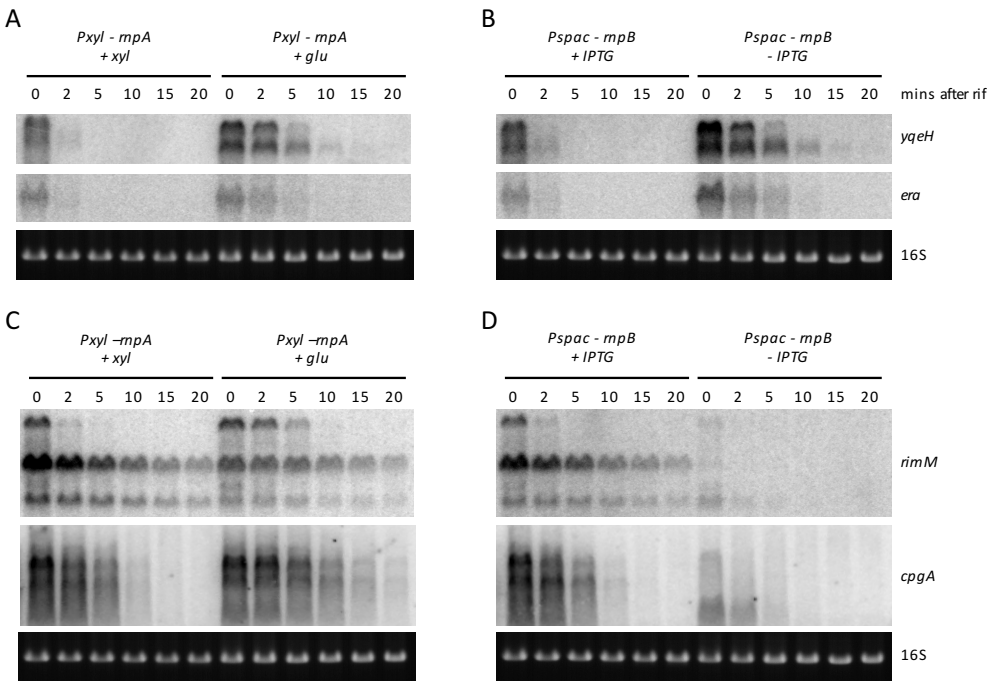

Figure 26: Effect of depleting RNase P on the stability of mRNAs encoding proteins involved in 30S subunit assembly.

(A) Upregulated genes are stabilized under conditions of *rnpA* (A) or *rnpB* (B) depletion. Downregulated genes are subjected to a mixture of transcriptional and post-transcriptional effects under conditions of *rnpA* (C) or *rnpB* (D) depletion.

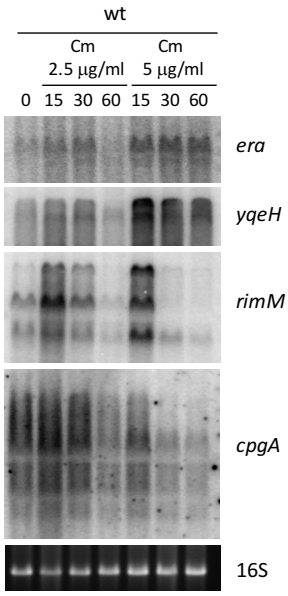

Figure 27: Effect of chloramphenicol treatment at sub-inhibitory (2.5 µg/mL) and minimal inhibitory concentration (5 µg/mL) on expression of cofactors mRNA (*era*, *yqeH* and *rimM*) in a wt strain.

To determine whether tRNA maturase impacted mRNA expression of the key cofactors at the transcriptional or post-transcriptional level, we measured mRNA stability after rifampicin treatment in RNase P (*rnpA* or *rnpB*) induced or depleted cultures. The up-regulated transcripts (*yqeH* and *era*) were both stabilized during *rnpA* and *rnpB* depletion (Figure 26, A and B) suggesting that they are affected by RNase P depletion mainly at the post-transcriptional level. We can imagine that the lack of functional tRNAs during tRNA maturase depletion increases ribosome stalling on translated mRNAs (Ishimura et al., 2014). Thus, the increased stability of *yqeH* and *era* might be due to ribosome stalling on these mRNAs, e.g. by blocking the access of ribonucleases to cleavage sites. To test this hypothesis, we sought to recapitulate the effect by pausing translation in a different manner, using the translation elongation inhibitor chloramphenicol (Cm). Indeed, the addition of sub-inhibitory (2.5 µg/mL) and minimal inhibitory (MIC; 5 µg/mL) concentrations of Cm to WT cells also increased the levels of the *yqeH* and *era* mRNAs (Figure 27), suggesting that the stabilization of these transcripts in tRNA maturase depletion strains is most likely due to the lack of mature tRNA and ribosome stalling.

The two down-regulated transcripts (*rimM* and *cpgA*) were strongly destabilized in *rnpB* depleted cells (Figure 26, D), suggesting that the decrease in expression also primarily occurs at a post-transcriptional level in this strain. A similar decrease in expression was seen after 30 minutes at high (MIC) Cm concentration in WT cells, suggesting that this phenomenon is also linked to ribosome stalling. Thus, presumably, for these mRNAs, when non-functional tRNA precursors accumulate in *rnpB*-depletion strain, ribosomes eventually stall at sites that preferentially allow RNase access (in contrast to *yqeH* and *era).*

The results obtained with the *rnpA* depletion strain (Figure 26,C) painted a more complex picture for the regulation of the *rimM* and *cpgA* mRNAs. Despite the down-regulation of mRNA levels seen in Figure 25, depletion of *rnpA* appeared to stabilize the full-length *rimM* transcript and the two major *cpgA* mRNAs. The difference between effects observed for *rnpA* and *rnpB* depleted strains is possibly due to the fact that the *rnpB* depletion is considerably more severe than that of *rnpA* (Cf. Chapter 1). These results suggest that down-regulation of *rimM* and *cpgA* may arise from a mixture of transcriptional (down) and post-transcriptional (up initially, then down) effects and that one or the other effect predominates depending on the severity of RNase P depletion. Indeed, upon close

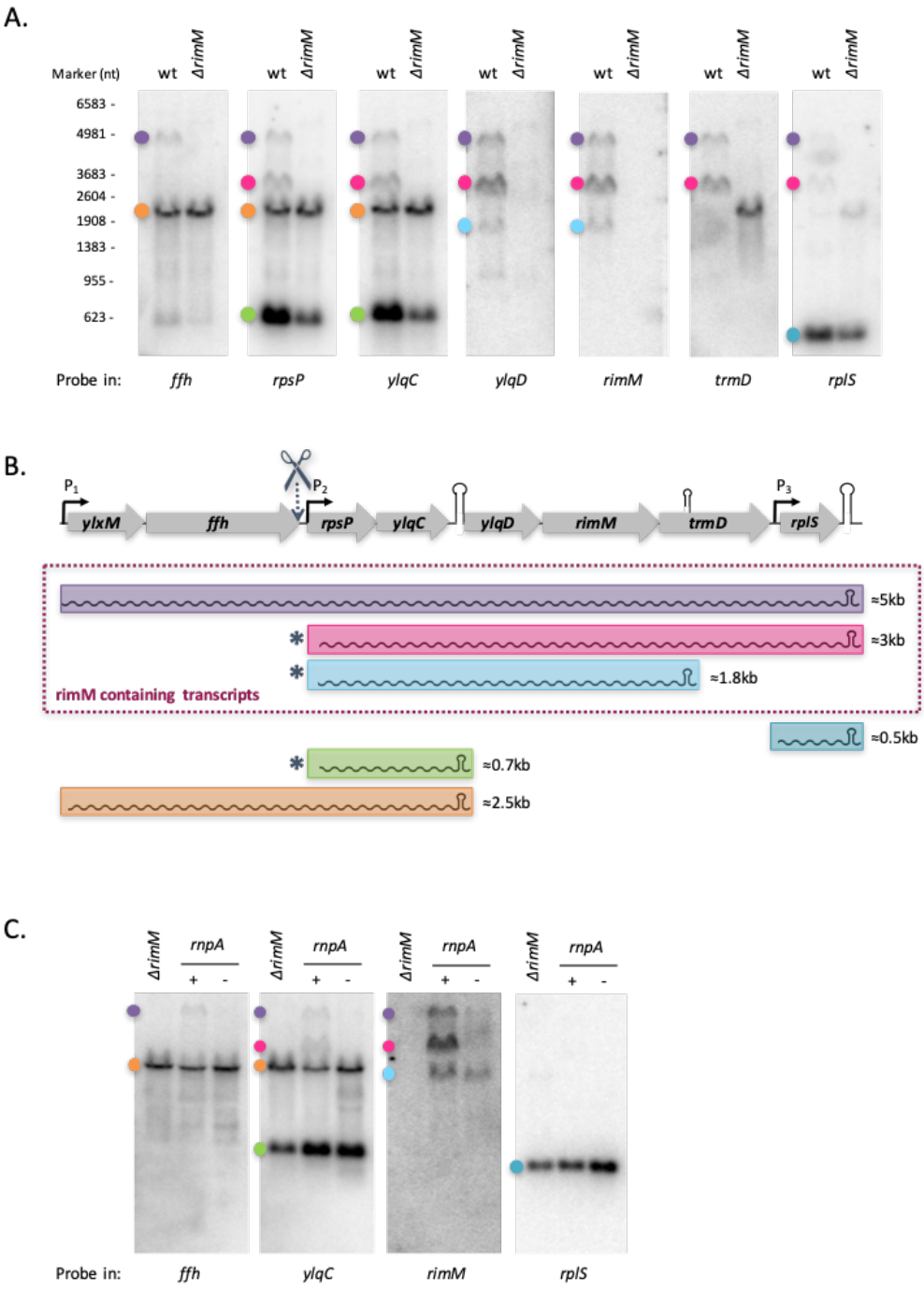

Figure 28: Northern blot analysis of the *rimM* operon.

(A) Total RNA from wt or *ΔrimM* strain was probed with oligonucleotide probes targeting different genes of the operon (indicated below panel). Color points correspond to the species represented in (B). Note that the *rimM* genomic region and transcripts are not drawn to scale, approximate transcripts sizes are indicated at the right in kilobases (kb). The (*) indicates transcripts that could be processed by the Y-complex resulting in two different 5' ends. The distance between the processing site and the *rpsP* TSS (P_2) is only 18 nts; therefore, we cannot distinguish processed species from primary transcripts on this Northern blot. (C) Northern blot assessing the sensitivity of the different mRNA species to RNase P depletion (*rnpA*). The color code is the same as in (A) and (B).

inspection, *rimM* mRNA levels initially increase at 15 mins and then decrease after further exposition to Cm at both sub-inhibitory and MIC doses, consistent with the notion of opposing responses to severe *vs* less severe levels of translation inhibition.

2. Analysis of *rimM*-containing transcripts

Because *rimM* expression results in the production of three distinct transcripts, all of them down-regulated during tRNA maturase depletion, and because the *ΔrimM* phenotype closely fitted the 30S late assembly defect observed in strains depleted for RNase P or RNase Z, we attempted to narrow down the molecular determinants of this regulation. The *rimM* gene is encoded in a large operon containing several genes related to the translation machinery: ribosomal proteins genes (*rpsP* encoding S16 and *rplS* encoding L19), signal recognition particle components (encoded by *ffh* and *ylxM*) and *trmD* that encodes a tRNA methyltransferase. To characterize the gene composition of the three *rimM*-containing transcripts, we performed northern blots with probes located in ORFs of the neighboring genes. We identified six different transcripts originating from this operon (Figure 28). Promoters upstream of *ylxM* (P_1 or U1312.M17) and *rplS* (P_3 or U1313.M17) were identified earlier by transcriptome analysis, as well as terminators downstream of *ylqC* and *rplS* (D888 and D889, respectively) (Nicolas et al., 2012). We identified two transcripts originating from P_1, the full-length mRNA (5 kb-long, in purple) that terminates downstream of *rplS,* and a shorter transcript (2.5 kb-long, in orange) that terminates after *ylqC* and does not contain the *rimM* ORF. The smallest species identified (500 bp, in dark blue) corresponds to the mono-cistronic *rplS* transcript. Because no transcription start site had been identified at that time in the *ffH-rpsP* intergenic region, we hypothesized that the three other RNAs (3 kb-long in pink; 1.8 kb-long in light blue and 0.7 kb-long in green) result from processing of the P_1 originating transcripts. End-enrichment RNA sequencing (Rend-seq) data obtained in the meantime by Gene Wei Li's lab revealed that this intergenic region indeed contain an RNase Y cleavage site dependent on interaction with the Y-complex (DeLoughery et al., 2018).

Additionally, they identified a third transcription start site (TSS; P_2) located in front of *rpsP* and only 18 nts downstream of the RNase Y cleavage site. Therefore, the three above-mentioned transcripts (marked with a star in Figure 28,B) could either be P_2-primary transcripts or processed transcripts arising from RNase Y cleavage of P_1-primary transcripts

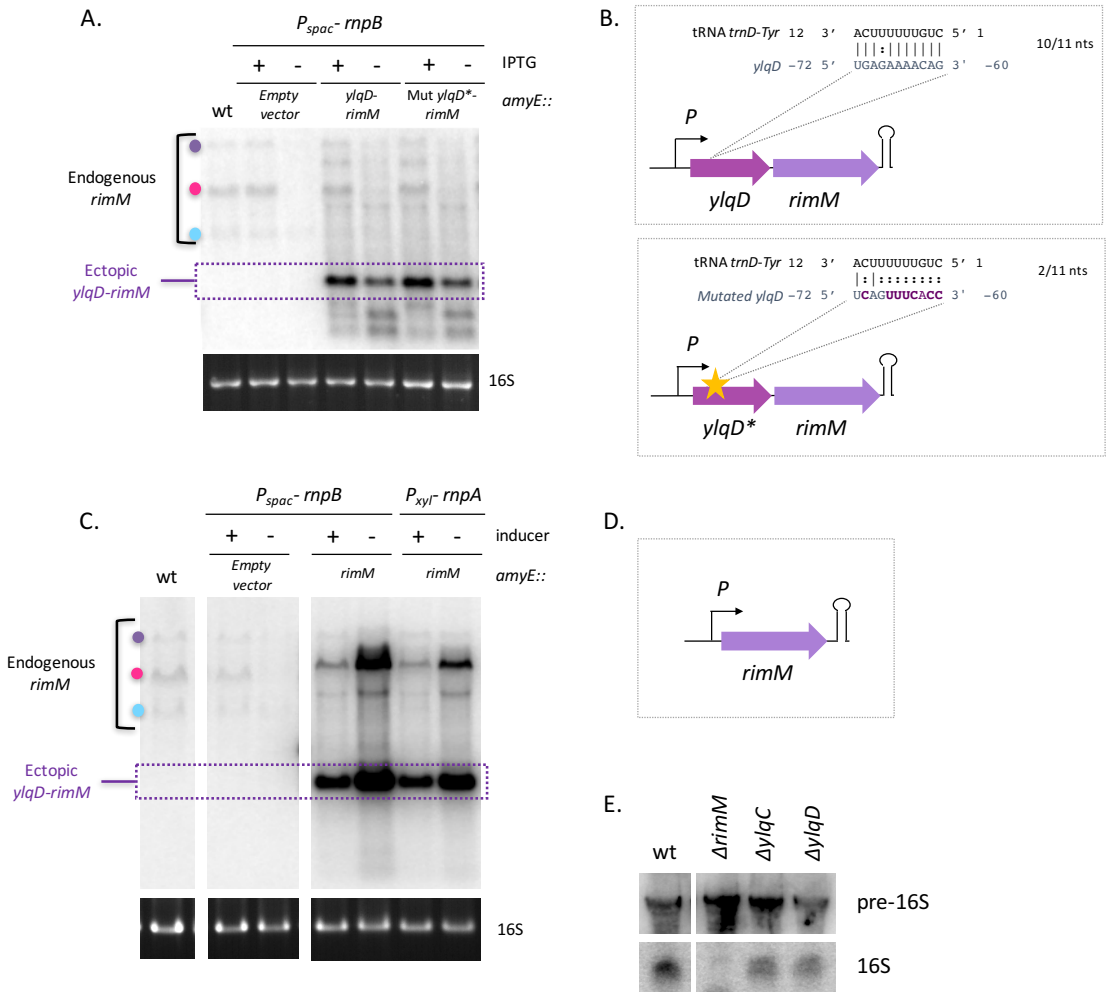

Figure 29: Effect of RNase P depletion on ectopic constructs encoding the RimM ribosome assembly cofactor.

(A) Northern blot showing the effect of RNase P depletion (*rnpB*) on expression of an ectopic *ylqD-rimM* short operon containing a wt or mutated (*) potential target sequence for *trnD-Tyr* pre-tRNA binding. Color points identifying *rimM* endogenous transcripts follow the same code as in Figure 26, B) Schematic of ectopic *ylqD-rimM* contructs placed under control of the constitutive promoter (P) used in A. The zoom in shows the putative binding with *trnD-Tyr* pre-tRNA and its disruption in the mutated *ylqD*-rimM* construct. C) Northern blot showing the effect of RNase P depletion (*rnpA* or *rnpB*) on expression of an ectopic *rimM* short operon. B) Schematic of ectopic *rimM* contruct placed under control of the constitutive promoter (P) used in panel C. E) Northern blot showing the effects of *ΔylqC* or *ΔylqD* deletions on accumulation of the 65 nt 3' processing product.

(or a mixture of both). Note that we cannot discriminate between these primary and processed transcripts as they co-migrate on agarose gels since their difference in length is only 18 nts.

Overall, our analysis of the *rimM* operon by Northern blot corroborates the results published by DeLoughery and colleagues (DeLoughery et al., 2018). A small increase in Rend-seq read counts was also visible within the *trmD* ORF that could correspond to a weak terminator. Termination at this site would account for the third *rimM* containing transcript (1.8 kb-long, in light blue), which is less expressed than the other two. Accordingly, this transcript is not detected with the *trmD* probe located further downstream in the ORF. Interestingly, of the six transcripts we identified in this operon, only the three containing *rimM* were sensitive to RNase P depletion (Figure 28, panel C). Furthermore, since transcription from P_1 led to the production of both RNase P-sensitive and -insensitive transcripts (in purple and orange, respectively), we concluded that the RNase P-dependent down-regulation of *rimM* expression was, at least partially, post-transcriptional, consistent with the above observations.

3. Expression of *rimM* is regulated at the post-transcriptional level *via* a determinant located within the *ylqD* ORF

By comparison of RNase P depletion sensitive and non-sensitive transcripts arising from the *rimM* operon (Figure 28, panel C), we narrowed the potential region of regulation to the sequence spanning the *ylqD* and *rimM* ORFs. To further identify the sequence elements responsible for down-regulation of *rimM*, we sub-cloned different regions of the operon under control of a constitutive promoter. Constructions were integrated into the chromosome at the *amyE* locus and levels of the ectopic transcript were analyzed by Northern blot in RNase P-depleted cells using a probe specific for the *rimM* ORF. The short synthetic *ylqD-rimM* operon was still sensitive to RNase P depletion, confirming a post-transcriptional effect and indicating that the region responsible for the regulation is still included in this shorter construct (Figure 29, panels A and B). On the contrary, a construct restricted to the *rimM* ORF was up-regulated in response to RNase P depletion (Figure 29, panels C and D). This result suggests that the region responsible for post-transcriptional down-regulation of *rimM*-containing transcripts is located within the *ylqD* ORF.

Since 5'-unprocessed tRNAs accumulate in RNase P depleted cells, we wondered whether they could act as post-transcriptional regulators of target mRNAs by base pairing to their targets *via* their 5' single-stranded extensions. Using Target RNA 2, a prediction program used for identifying targets of small RNAs (sRNAs) in bacteria, we identified an 11-nt region within the *ylqD* ORF that could potentially base-pair with the 5' immature extension of unprocessed *trnD-Tyr* tRNA (Figure 29, panel B). To test whether this sequence was involved in down-regulation of the *ylqD-rimM* construct in cells depleted for RNase P, we weakened the putative base pairing interaction by introducing mutations in the *ylqD* mRNA sequence (while maintaining the YlqD amino acid sequence as much as possible) (Figure 29, panel B). The mutated *ylqD-rimM** construct was still down-regulated under conditions of RNase P depletion, however, more or less excluding the possibility that 5' extended *trnD-Tyr* acts as a post-transcriptional regulator of this operon. Thus, the sequence element within *ylqD* responsible for down-regulation of this operon under conditions of tRNA maturase depletion remains unknown.

The *rimM* gene is known to encode a ribosome assembly cofactor involved in late 30S subunit assembly in *E. coli* (Cf. Introduction). Furthermore, we observed in the *B. subtilis ΔrimM* strain that 16S rRNA 3' processing is inhibited, a hallmark of ribosome assembly defect. Because we narrowed the region of RNase P-dependent regulation of the *rimM* operon to the *ylqD* ORF, and because the *rimM* operon displays a high degree of synteny between *E. coli* and *B. subtilis,* except for the presence of the two genes of unknown function (*ylqC* and *ylqD*) between the *rpsP* and *rimM* genes in *B. subtilis,* we asked whether either of the genes of unknown function might also be involved in 30S subunit assembly. However, both *ΔylqC* and *ΔylqD* cells display efficient 16S rRNA 3' processing (Figure 29, E), suggesting that neither of these two proteins play a significant role in 30S assembly.

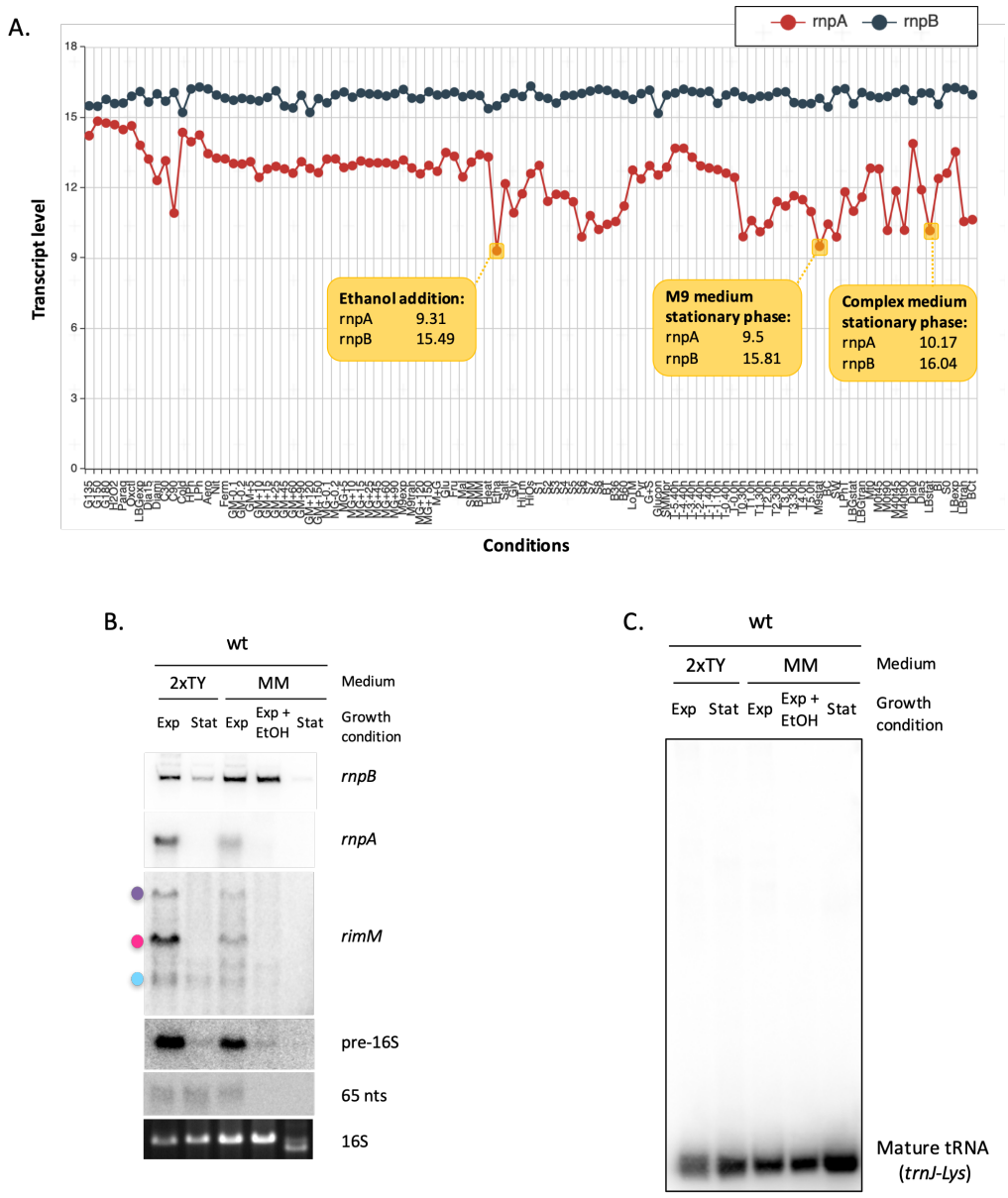

Figure 30: Ethanol stress and stationary phase affect levels of RNase P-encoding transcripts without causing tRNA processing defects.

(A) *rnpB* (blue) and *rnpA* (red) transcript levels over 100 different growth conditions (from (Nicolas et al., 2012)). The three conditions indicated in yellow (ethanol stress and stationary phase in complex and minimal medium) result in reduced *rnpA* RNA levels. For each condition, *rnpA* and *rnpB* RNA levels are indicated in the box. B) Northern blot comparing RNA levels of *rnpB* (first panel, acrylamide gel), *rnpA* and *rimM* (second and third panel, agarose gel) following ethanol addition (EtOH) or during exponential (Exp) or stationary (Stat) phase in minimum (MM) or complex (2xTY) medium. Color points identifying *rimM* transcripts follow the same code as in Figure 26. Last two panels are Northern blot showing the effect of ethanol treatment and growth phase (in minimum and complex medium) on 16S rRNA 3' processing. C) Northern blot probed for *trnJ-Lys* showing no pre-tRNA accumulation in the different conditions tested.

4. Down-regulation of *rimM* under physiological conditions of reduced RNase P expression is independent of immature tRNA accumulation

We next asked whether the down-regulation of *rimM* we observed during RNase P depletion, could occur in physiological conditions where RNase P expression is reduced. The level of expression of *rnpB* RNA is relatively constant in tilling array experiments in over a hundred conditions tested, whereas *rnpA* mRNA levels decrease upon ethanol addition and stationary phase in both complex and minimal media (Figure 30, A) (Nicolas et al., 2012). We confirmed that *rnpA* RNA expression was reduced to levels below detection in these three conditions in comparison with exponential growth in the respective medium, by Northern blot (Figure 30, B). Ethanol treatment did not affect *rnpB* RNA levels; however, they were reduced during stationary phase (both in minimal and complex medium), in contrast to the tilling array data. Interestingly, *rimM* expression varied similarly to *rnpA* in the conditions tested.

We could not adequately analyze whether 16S rRNA 3' processing was affected under these conditions because pre-16S levels were sharply reduced, presumably due to transcriptional shut-down (Figure 30,B). Furthermore, species shorter than mature 16S rRNA were visible on the agarose gel during stationary phase in minimal medium, suggesting rRNA degradation has begun under these particular conditions, as occurs in *E. coli* (Luidalepp et al., 2016). Instead, we asked whether tRNA maturation was affected in stationary phase or upon addition of ethanol using a probe for *trnJ-Lys* tRNA. Surprisingly, despite the decreased levels of *rnpA* expression in all three conditions, and *rnpB* in stationary phase, we did not observe an accumulation of pre-tRNAs (Figure 30, C). The remaining cellular RNase P activity therefore appears to be sufficient for the pool of tRNAs transcribed during stationary phase and ethanol stress. These experiments suggest that the down-regulation of *rimM* expression that accompanies the decrease in *rnpA* and *rnpB* expression under these physiological conditions is independent of immature tRNA accumulation. As many components of the translation apparatus are down-regulated under conditions of slower growth, the decreased expression of rimM under these conditions is thus likely to be a manifestation of a similar growth control process and distinct from the down-regulation that occurs under conditions of strong RNase P depletion.

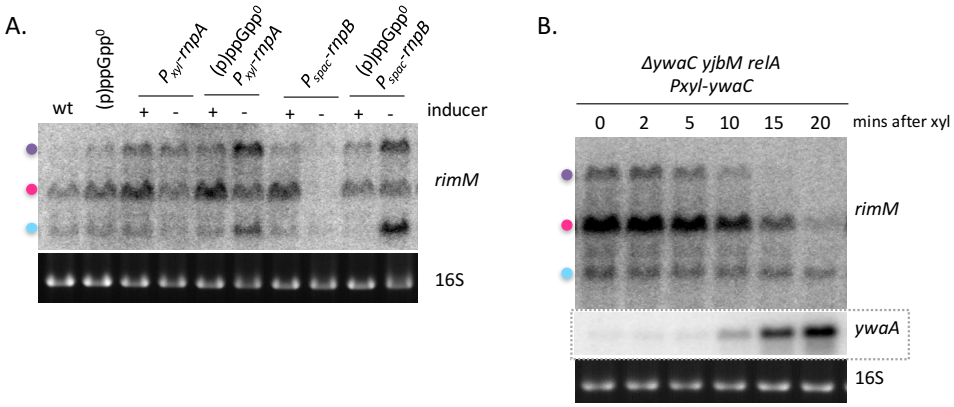

Figure 31: Influence of (p)ppGpp and growth on *rimM* expression.

(A) Northern blot comparing the effect of RNase P depletion (*rnpB* or *rnpA*) in a (p)ppGpp^{+} and (p)ppGpp^{0} background on *rimM* expression. (B) Northern blot of *rimM* expression after induction of (p)ppGpp production using a xylose inducible *ywaC* in *ΔywaC yjbM relA* background. Grey dotted line indicates previously published data. Color points identifying *rimM* transcripts follow the same code as in Figure 26.

5. Down-regulation of *rimM* in RNase P depletion strains depends partially on (p)ppGpp production.

Considering that tRNA maturase depleted cells trigger a RelA-dependent production of (p)ppGpp (Cf. Chapter 1), we asked whether *rimM* down-regulation in these cells was dependent on (p)ppGpp production by measuring *rimM* expression in (p)ppGpp^0 strains depleted for *rnpA* or *rnpB*. If (p)ppGpp is an effector, the effect of RNase P depletion on *rimM* expression should be reduced or abolished in the (p)ppGpp^0 background. The effects on the three *rimM* transcripts were not the same (Figure 31, panel A). The larger (purple) and the smaller (blue) *rimM* species were no longer down-regulated (but rather up-regulated) after RNase P depletion in the (p)ppGpp^0 background indicating a (p)ppGpp dependent effect on these two transcripts. The intermediate transcript (pink), however, was down-regulated by RNase P depletion both in (p)ppGpp$^+$ and (p)ppGpp^0 background, suggesting that it is affected by tRNA maturase depletion in a (p)ppGpp-independent manner. Note that, as explained in section 2, the two smaller *rimM* species we observe (pink and blue) are potentially four different transcripts. Each band can either correspond to a primary transcript (transcribed from P_2), or a processed transcript (resulting from cleavage of P_1-transcripts), or to a combination of both, which greatly complicates our analysis.

We next assessed whether (p)ppGpp could down-regulate *rimM* expression in the absence of tRNA processing defect using an engineered strain that allows us to produce (p)ppGpp in the absence of immature tRNA accumulation (or nutrient starvation) (Cf. Chapter 1). We observed that (p)ppGpp induction has no effect on the small (blue) *rimM* transcript, whereas the two other larger species (pink and purple) were down-regulated at different rates (Figure 31, panel B). Therefore, (p)ppGpp production alone does not recapitulate what is seen in tRNA maturase depleted cells, suggesting that additional regulatory events are involved. For example, it is possible that the growth slow-down in depleted cells also affects *rimM* expression at some level, independently of (p)ppGpp.

To test the importance of the slow-down in growth rate *per se* that occurs under tRNA maturase depletion conditions on the regulation of *rimM*-containing transcripts, we sought to reproduce the growth rate defect by depleting for an unrelated essential enzyme. We therefore performed Northern blot analysis on total RNA extracted from both RNase III (*rnc*) depletion and deletion strains. The double-strand specific endonuclease RNase III is essential

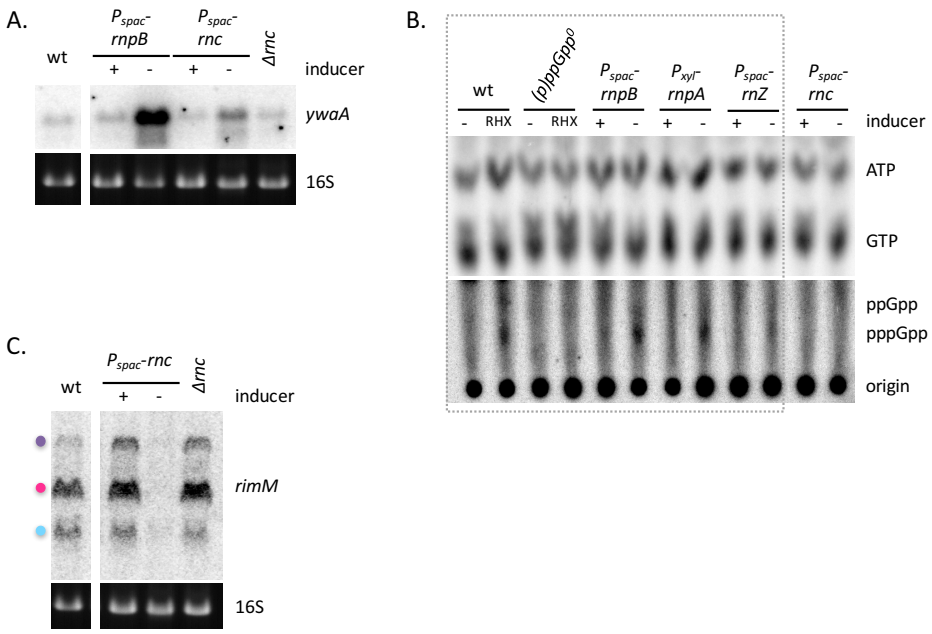

Figure 32: Study of growth-dependent regulation of *rimM* expression.

(A) Northern blot comparing the effect of RNase III deletion and RNase P or RNase III depletion on de-repression of the CodY-regulated gene *ywaA*. (B) RNase III depleted cells do not accumulate large amounts of (p)ppGpp as opposed to tRNA maturase depleted ones. Thin-layer chromatography (TLC) analysis of ^{32}P-labeled nucleotides extracted from tRNA maturase depleted cells (*rnpA-, rnpB-* or *rnZ-*) or RNase III depleted cells (*rnc-*). Arginine hydroxamate (RHX; 250mg/mL) was added to wt and (p)ppGpp^0 strains as positive and negative controls. Note that top and bottom halves are exposed for different times. The grey dotted line shows a previously published portion of the figure (Chapter 1, Figure 6) shown again here to allow comparison. (C) Northern blot comparing the effect of RNase III depletion or deletion on *rimM* expression. Color points identifying *rimM* transcripts follow the same code as in Figure 26.

in *B. subtilis* because it is required to silence expression of foreign toxin genes of two prophages (Skin and SPβ) (Durand et al., 2012b). Whereas depletion of RNase III in a WT background leads to growth arrest, RNase III can be deleted in a strain lacking the two prophages without marked effect on growth rate. It is worth noting that RNase III depleted cells show only a very limited de-repression of the CodY regulon in comparison with tRNA maturase depleted strains and do not accumulate visible amounts of (p)ppGpp on thin-layer chromatography (TLC) (Figure 32, panel A and B). This validates the use of RNase III depletion strains to examine the effect of growth rate on *rimM* expression and to distinguish this from the effect of accumulating high levels of (p)ppGpp. While RNase III deletion had no effect on *rimM* expression, all *rimM*-containing transcripts were completely down-regulated during RNase III depletion (Figure 32, panel C) confirming that growth rate plays a major role in the regulation of *rimM* expression.

All together, these data indicate that *rimM* down-regulation in tRNA maturase depleted cells is likely to be the result of the combined effects of growth rate and (p)ppGpp accumulation and perhaps other factors involved in transcriptional and post-transcriptional regulation (see Discussion).

Discussion and perspectives

In this section I will discuss the new results shown in Chapter 2 and re-discuss some of those in Chapter 1, adding some new perspectives. I will also show some new data that did not fit seamlessly into either Chapter 1 or 2, but that provide some answers to questions raised during this discussion.

1. 16S 3' rRNA processing as a post-transcriptional mechanism to regulate ribosome stability

This project started with the observation that cells with deficiencies in tRNA maturation also display a 16S rRNA 3' processing defect. We observed that overexpression of a functional YqfG could not restore 16S rRNA normal processing in the tRNA maturase depletion strain, suggesting that the problem is not insufficient levels of *yqfG* expression. We hypothesized that instead the accumulating immature 16S rRNA is not seen as a potential substrate by YqfG (Chapter 1, Figure S4,C). Given the current model that YqfG/YbeY processing occurs post-assembly (Baumgardt et al., 2018; Shetty and Varshney, 2016), we considered the possibility that 30S ribosomal subunit assembly could be affected in tRNA maturase depleted cells. Indeed, we showed that both RNase Z and RNase P depletion led to an accumulation of pre-30S subunits depleted for several late assembly r-proteins. This specific late 30S assembly defect is accompanied by a RelA-dependent production of (p)ppGpp, and we showed that this accumulation of (p)ppGpp is responsible for a significant portion of the 16S rRNA 3' processing defect observed in tRNA maturase-depleted cells. More broadly, we demonstrated that 16S rRNA 3' processing is also inhibited during the "classical" stringent response, *i.e.* even in the absence of immature tRNA accumulation.

Defects in the final trimming of 16S rRNA are a hallmark of perturbations in 30S ribosomal subunit assembly, with the retained 16S rRNA 3' extension serving as an on-ramp for initiation of degradation by RNase R (Baumgardt et al., 2018). Abolishing this specific rRNA processing event, catalyzed by YqfG in *B. subtilis*, thus provides a way to rapidly degrade defective ribosomes that could interfere with the function of their normal counterparts. Ribosome degradation also likely permits the recycling of ribosome

components. A major portion of cell biosynthetic capacity is devoted to making ribosomes and other components required for efficient translation: in fast growing *E. coli* cells, rRNA transcription accounts for more than 70% of total transcription, with expression of tRNAs and r-proteins accounting for about 15% of the remainder (Dennis and Bremer, 2008). Because of its associated cost, ribosome synthesis is tightly adjusted to cellular needs and a key molecular effector of this regulation is the alarmone (p)ppGpp (Cashel, 1969; Cashel and Kalbacher, 1970). When bacteria are starved for nutrients, (p)ppGpp production is triggered, leading to induction of the stringent response that is characterized by an inhibition of rRNA transcription and many other cellular readjustments. Remarkably, in our study, we observed that activating the stringent response affects 16S rRNA 3' processing even faster than the inhibition of rRNA transcription, as measured by a decrease in the ratio of the 65-nts 3' processed fragment to pre-16S rRNA and defined as processing efficiency in Chapter 1. This led us to propose that the stringent response not only blocks synthesis of new ribosomes *via* its effect on rRNA transcription initiation, but also shuts down the ongoing ribosome assembly by blocking the assembly of precursors into functional ribosomes by setting the RNase R-mediated quality control pathway in motion. In this way, the effect of stringent response on ribosome biogenesis is more rapid and extensive than previously thought, affecting ribosome biogenesis both at the transcriptional and post-transcriptional levels to stop synthesis of ribosomal components and to scavenge the partially assembled pre-rRNAs.

Although, we did not test this, based on *E. coli* models, the synthesis of (p)ppGpp could also be predicted to lead to an inhibition of the synthesis of tRNAs in *B. subtilis.* It would make physiological sense, not only to inhibit ribosome production, but to also shut down tRNA transcription under conditions where tRNA processing is perceived to be deficient in cells. This would be an interesting avenue to explore in the future.

2. Physiological relevance of the coupling of rRNA processing to tRNA maturation

We showed that an accumulation of immature tRNA led to a ribogenesis defect, at least partially *via* pppGpp production. We propose that coupling the 16S rRNA 3' maturation to the processing of tRNAs could allow the adjustment of ribosome biogenesis to the amount of mature tRNAs available for translation. To test the relevance of this coupling mechanism

in bacterial physiology, we looked for conditions where tRNA maturase amounts would be reduced. The *B. subtilis* condition-dependent transcriptome allowed us to identify three conditions where *rnpA* expression is decreased (Nicolas et al., 2012), but because we did not detect any immature tRNA accumulation in these conditions (Chapter 2, Figure 30), we assume that RNase P activity is still sufficient to mature the pool of pre-tRNA. However, during the cell cycle, stages may exist where tRNA transcription outpaces (at least transiently) the tRNA maturation capacity. For example, during *B. subtilis* spore germination RNA transcription (particularly of stable RNA) was shown to precede synthesis of protein and DNA (Armstrong and Sueoka, 1968). Thus, early germination could represent one physiological condition where unprocessed tRNA may transiently accumulate and where pppGpp synthesis could fine tune ribosome biogenesis appropriately.

Coupling between tRNA processing and rRNA maturation may be widespread in bacteria, since a prior study reported that defects in tRNA maturation increase the level of unprocessed 16S and 23S rRNAs in *E. coli*, although the mechanism was not addressed (Slagter-Jäger et al., 2007). Moreover, a functional initiator tRNA (having a correct structure) was shown to be required for licensing final 16S rRNA trimming during the first cycle of *E. coli* initiation complex formation (Shetty and Varshney, 2016). Although these observations do not necessarily imply that the stringent response is activated, it confirms the existence of close links between rRNA maturation and tRNA processing in bacteria other than *B. subtilis*. Interestingly, it also raises the possibility that the rRNA maturation defect we observed, could result from the deficiency in specific mature tRNAs (such as initiator tRNAs) rather than from global accumulation of pre-tRNAs. In yeast, a tRNA maturation factor (Lhp1p) and three ribosomal proteins (Rpl16p, Rpl21p and Rpl34p) are co-imported in the nucleus by the transport factor Sxm1p, suggesting that coordination of ribosome biogenesis with tRNA processing also exists in eukaryotes (Rosenblum et al., 1997). Further comforting the close link between tRNA processing and rRNA maturation in yeast, the low-abundance endoribonuclease Sen34p is both a component of the tRNA splicing holoenzyme (Trotta et al., 1997) and of the Tif6p complex involved in ribosome biogenesis (Volta et al., 2005). Accordingly, depletion of Sen34p was found to block tRNA splicing and impair 27S pre-rRNA maturation (Volta et al., 2005). Lastly, the yeast tRNA and rRNA processing machineries are suggested to be co-regulated by the ubiquitin ligase Rsp5p: *rps5* mutants were found to concomitantly accumulate pre-tRNAs and pre-rRNAs and to suffer extensive ribosome

degradation (Neumann et al., 2003; Shcherbik and Pestov, 2011).

The conservation of the coupling between tRNA and rRNA maturation, through different mechanisms in different organisms, suggests it plays an important role in cellular physiology.

3. The stringent response and the effect of GTP pools on 16S rRNA 3' maturation

We observed that (p)ppGpp production can affect ribogenesis and inhibit 16S rRNA 3' processing, even in absence of tRNA maturation defects. Accordingly, several GTPases involved in ribosome biogenesis (RA-GTPases) were recently identified as direct (p)ppGpp targets by genome-wide nucleotide-protein interaction screens both in Gram-negative (Zhang et al., 2018) and Gram-positive bacteria (Corrigan et al., 2016). As detailed in the introduction, (p)ppGpp also binds and inactivates enzymes involved in GTP biosynthesis leading to a drop in cellular GTP pools (Kriel et al., 2012). Interestingly, we observed that decreasing cellular GTP concentration by decoyinine treatment in the absence of (p)ppGpp accumulation, is sufficient to affect 16S rRNA 3' processing. Therefore, (p)ppGpp appears to affect RA-GTPases in two different ways: directly, by competitive binding to some RA-GTPases as proposed by the Gründling lab in *S. aureus* (Corrigan et al., 2016), or indirectly, through the decrease in GTP pools necessary for their activity. Both direct and indirect effects of (p)ppGpp on RA-GTPases could potentially co-exist *in vivo,* ensuring a rapid shut-down of RA-GTPase activity.

Moreover, (p)ppGpp could affect ribosome biogenesis *via* other indirect mechanisms. Because of its structural resemblance to GTP, (p)ppGpp can bind a variety of other nucleotide-binding proteins, as supported by results obtained in *E. coli* and *S. aureus* (Corrigan et al., 2016; Zhang et al., 2018). However, specific (p)ppGpp binding pockets also exist on certain proteins, as exemplified by *E. coli* RNA polymerase, which has two (Ross et al., 2016). In the Gram-positive bacterium *Streptomyces coelicolor,* (p)ppGpp has been shown to inhibit polynucleotide phosphorylase (PNPase), also by binding to a region distinct from the enzyme's active site (Gatewood and Jones, 2010). (p)ppGpp-mediated inhibition of PNPase in *S. coelicolor* results in an increase in bulk mRNA stability and thus, presumably, affects global gene expression. Interestingly, (p)ppGpp does not bind the *E. coli* PNPase,

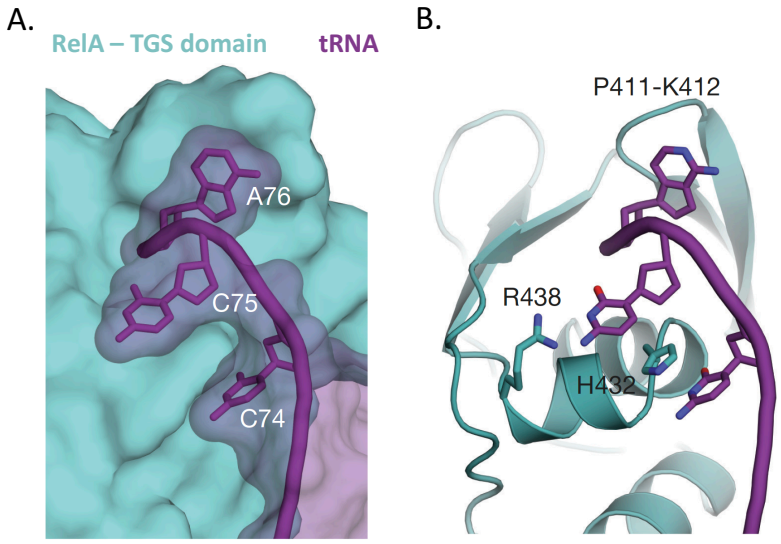

Figure 33: Molecular basis for recognition of uncharged A-site tRNA.

A. The 3' CCA (nucleotides 74-76) of the A-site tRNA (in purple) wraps around the surface of the RelA TGS domain (in blue).

B. The conformation of the CCA is maintained by interactions with residues of the TGS domain: C74 of the CCA motif stacks with His432, while C75 can form hydrogen bonds with Arg438.

Adapted from (Brown et al., 2016).

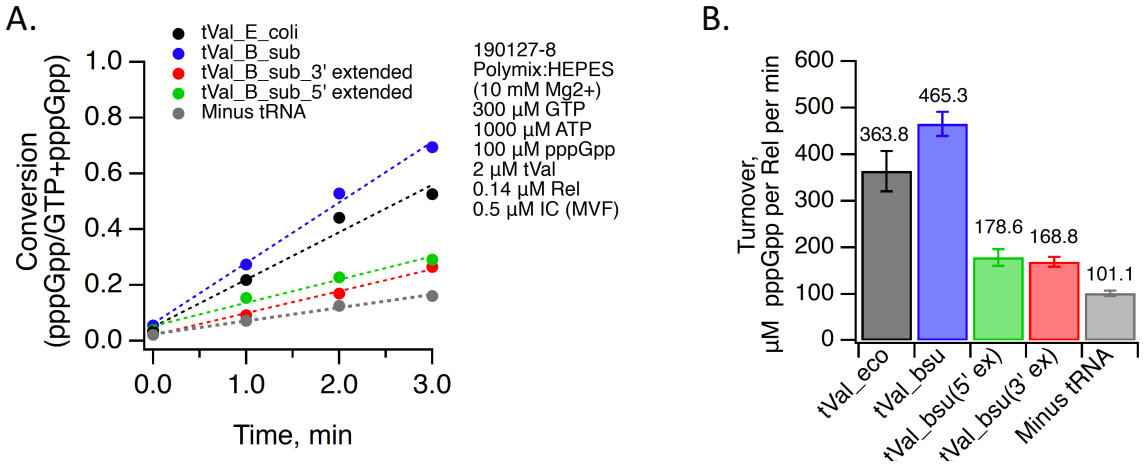

Figure 34: 5' and 3' pre-tRNAs are weaker activators of RelA than uncharged tRNAs *in vitro*.

(A) Kinetics of GTP conversion in pppGpp *in vitro* by Rel/RelA in presence of initiation complex (IC) and mature tRNA-Valine (blue and black for the *B. subtilis* (bsu) and *E. coli* (eco) Val-tRNAs, respectively), pre-tRNAs (5'-pre-tRNA (5' ex) or 3'-pre-tRNA (3' ex) in green and red, respectively) or no tRNA (negative control in grey). (B) Turnover rates measured in the *in vitro* assay. Same color code as in A. The number above bar indicates average turnover (µM pppGpp/Rel/min).

Experiments were done by Hiraku Takada and Vasili Hauryliuk (collaboration).

highlighting a species-specificity of (p)ppGpp binding to certain proteins (Gatewood and Jones, 2010). Although a systematic identification of (p)ppGpp-protein interactions has not yet been performed in *B. subtilis* for lack of a genome-wide over-expression library, PNPase and RNA helicases would be interesting candidates to test for as enzymes that might mediate (p)ppGpp-dependent changes in gene expression in this organism (see section 0, below).

4. Unprocessed tRNAs as a new determinant for (p)ppGpp synthesis

Our results suggest that unprocessed tRNAs trigger RelA-dependent (p)ppGpp production. Theoretically, both 3' and 5' unprocessed tRNAs could fit in the ribosomal A-site of a RelA-associated ribosome (PDB: 5iqr) with minor accommodations (Chapter 1, figure S5). Structural studies showed that RelA recognizes uncharged tRNAs in the A-site by interaction of its TGS domain residues H432 and R438 with nucleotides C74 and C75 of the uncharged tRNA CCA motif in *E. coli* (Figure 33) (Arenz et al., 2016; Brown et al., 2016; Loveland et al., 2016). The 3' hydroxyl group of the terminal A76 residue was also reported to be required for RelA activation in early studies (Sprinzl and Richter, 1976). Given our current knowledge, activation of RelA by 3'-unprocessed tRNAs would require other molecular determinants to rationalize their ability to promote (p)ppGpp synthesis in RNase Z depleted cells. To assess the RelA activation capacity of 5'- and 3'-unprocessed tRNAs, compared to uncharged tRNAs, our collaborators (Hiraku Takada and Vasili Hauryliuk) performed an *in vitro* assay of (p)ppGpp production in presence of purified initiation complex (IC) and RelA (Figure 34). As expected, mature uncharged tRNAs induced (p)ppGpp production at a rate of about 400 µM (p)ppGpp per RelA per minute. Basal levels of (p)ppGpp production were also detected in absence of tRNA at ~100 µM (p)ppGpp/RelA/min, due to the known passive RelA activation by interaction with the ribosome. Both 5'- and 3'-unprocessed tRNAs induced a weak (p)ppGpp production (~175 µM (p)ppGpp/RelA/min), which was above the basal levels of the negative control, but still low in comparison to canonical RelA activation by uncharged tRNAs. Thus, while productive, both 5'- and 3'-unprocessed tRNAs are significantly weaker activators of RelA than uncharged tRNAs, consistent with the important role of the 3' OH moiety of the CCA motif in RelA activation. Although we accumulated similar levels of (p)ppGpp in RNase P-depleted

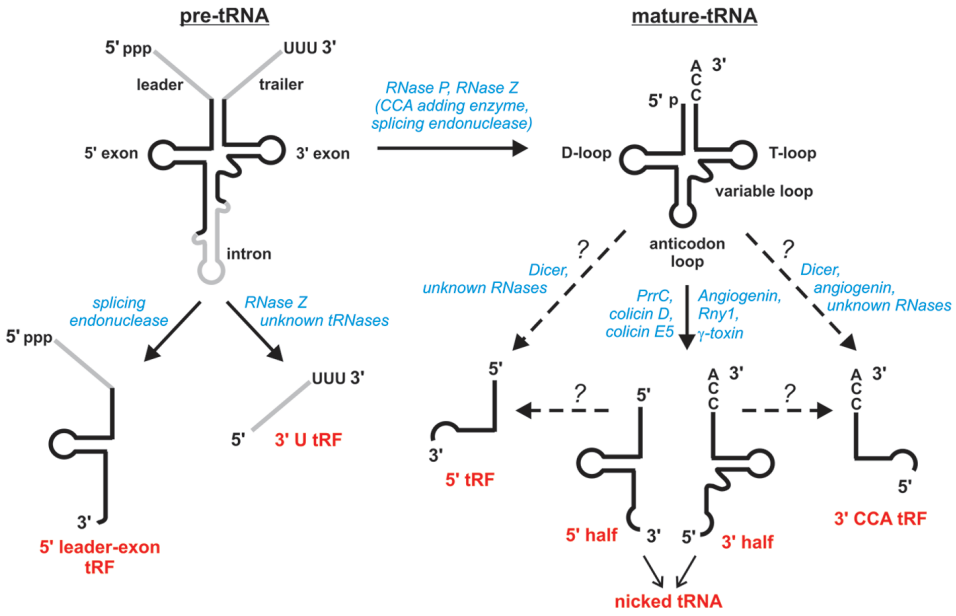

Figure 35: Processing of the tRFs identified so far in prokaryotes or eukaryotes.

Both pre-tRNA and mature tRNA can give rise to smaller tRNA pieces. Different nucleases suggested to be involved in tRNA maturation and/or fragmentation are listed in blue. Whereas endonucleases involved in tRNA halves production are well studied (PrrC, colicin D and colicin E5 in bacteria; Rny1 and γ-toxin in certain yeast strains; angiogenin in human), the processing enzymes involved in tRF generation are less clear.

Figure adapted from (Gebetsberger and Polacek, 2013).

cells to amino-acid starved cells *in vivo* (Chapter 1, figure 4), the time required for this accumulation was much shorter in the latter case (10 mins vs > 1 hour), consistent with the *in vitro* observations.

It is also possible that unprocessed tRNAs additionally activate RelA-dependent (p)ppGpp synthesis *in vivo* by an indirect mechanism. In tRNA maturase depleted cells, unprocessed tRNAs accumulate at the expense of mature tRNA; hence it is possible that pre-tRNAs outcompete their cognate mature tRNAs for binding to modification enzymes and/or aminoacyl-tRNA synthetases (AaRS) in the cell. AaRS enzymes recognize their cognate tRNAs by a series of identity determinants, mostly residues in the anticodon loop and the acceptor stem (Giegé and Springer, 2016) that would theoretically also be available in pre-tRNAs. A competition for AaRS binding could lead to a decrease in the aminoacylation levels of cognate mature tRNAs and trigger the stringent response in the classical way. The existence of this type of alternative mechanism has not yet been explored, but could be approached by asking whether immature tRNAs can inhibit AaRS charging of mature cognate tRNAs *in vitro*.

5. Unprocessed tRNAs and gene regulation

Beyond their canonical role during protein synthesis, tRNAs have been implicated in the regulation of several biological processes (for review, see (Katz et al., 2016; Raina and Ibba, 2014)). The fact that tRNAs have been hijacked during evolution for functions outside of translation *per se* is not surprising, given that they are ancient and extremely conserved molecules. A new class of small non-coding RNAs has emerged quite recently called tRNA-derived fragments (tRFs) or tRNA-derived small RNAs, whose biological roles are not yet well understood (Lee et al., 2009). For a long time, tRFs were considered to be non-functional by-products of tRNA processing and degradation reactions. Different types of tRFs exist, which differ in the cleavage position of the mature or precursor tRNA transcript (Figure 35) and that have progressively been recognized to play regulatory roles. tRFs have been particularly studied in humans, where they have been shown to be involved in regulation of a variety of cellular processes, among them: global translation, cellular proliferation, apoptosis and epigenetic inheritance (Kumar et al., 2016). Interestingly, a 3'-tRF was identified in human cells as essential for cellular viability: this tRF plays a role in fine-tuning ribosome biogenesis

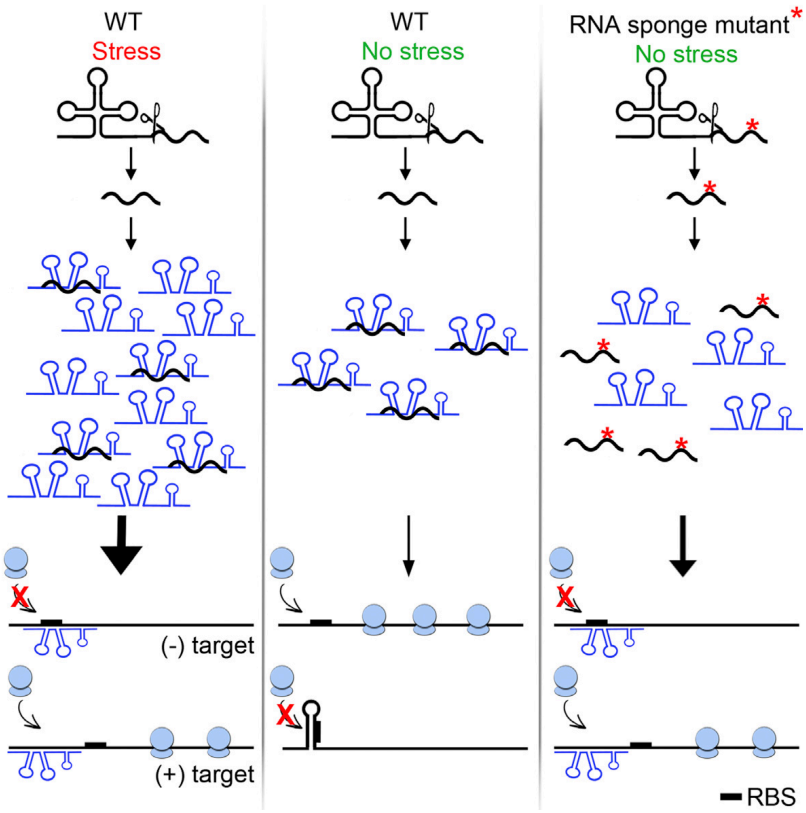

Figure 36: The 3' external transcribed spacer (3'ETS) from pre-tRNA^{LeuZ} represses transcriptional noise from repressed sRNAs.

During stress, the expression of RybB and RyhB sRNAs is induced and they efficiently regulate their targets as their levels highly exceed those of the sponge. In absence of stress, transcriptional noise results in the production of low levels of RybB and RyhB sRNAs that are sponged by the 3'ETS. The RNA sponge mutant has a reduced fitness in comparison with the WT in physiological conditions because basal levels of RybB and RyhB are no longer titrated and regulate target mRNAs.

under normal physiological conditions by post-transcriptionally regulating translation of at least two r-protein mRNAs. It was also found to be overexpressed in tumors, suggesting a further role in cancer development (Kim et al., 2017). The biogenesis and function of tRFs has received relatively little attention in prokaryotes. One of the only examples of tRFs with a regulatory function reported so far is a 3' external transcribed spacer (3'ETS) that is a stable intermediate of the processing of the polycistronic pre-tRNA^{LeuZ} by RNase E. This tRF was proposed to act as an RNA sponge by binding to the RybB and RyhB sRNAs in *E. coli* and is thought to contribute to cellular fitness by titrating the basal levels of these sRNAs that originate from transcriptional noise (Lalaouna et al., 2015).

Although tRFs have not yet been identified in *B. subtilis*, if they were to exist, RNase P or RNase Z depletion would potentially affect their biogenesis and some post-transcriptional effects observed in RNase P or RNase Z depleted cells could at least theoretically arise from altered tRF levels. We originally hypothesized that pre-tRNAs could bind target mRNAs *via* their 5' or 3' extensions and cause post-transcriptional effects in the tRNA maturase depletion strains. tRFs with 5' or 3' extensions (pre-tRFs) could similarly behave as a new pool of potential regulatory sRNAs. Although the potential base-pairing we identified between the 5' extension of *trnD-Tyr* and the *rimM* transcripts does not seem to play a role in the down-regulation of *rimM* expression (Chapter 2, Figure 29), this doesn't preclude the possibility that other pre-tRNAs or pre-tRFs could be involved in post-transcriptional regulatory events in *B. subtilis*.

6. The (p)ppGpp-independent effect on 16S rRNA 3' processing in tRNA maturase depleted cells

Our data indicates that (p)ppGpp is not the only effector of the coupling between tRNA processing and 16S rRNA 3' maturation. Indeed, 16S rRNA 3' processing is restored to only half of the WT level when tRNA maturase depletion is performed in a (p)ppGpp^0 background. Several ribosome assembly cofactors are required for efficient ribosome biogenesis and final rRNA maturation (Cf. Introduction), and perturbation of their expression could account for a portion of the defect in 16S 3' maturation seen in tRNA maturase depleted cells. Accordingly, we found that expression of several ribosome assembly cofactors is modulated following tRNA maturase depletion (Cf. Chapter 1, Figure 2). The down-regulated *rimM* and

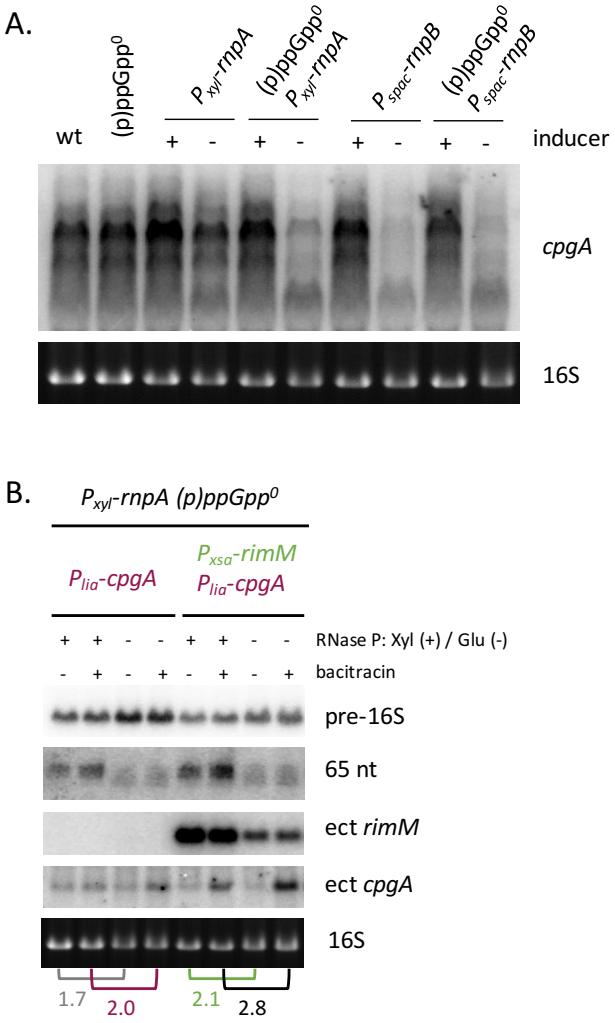

Figure 37: Perturbation of *cpgA* and *rimM* is unlikely to explain remaining 16S rRNA 3' processing in the RNase P depleted (p)ppGpp^0 strain.

(A) Northern blot comparing the effect of RNase P depletion (*rnpB* or *rnpA*) in a (p)ppGpp$^+$ and (p)ppGpp^0 background on *cpgA* expression. (B) 16S rRNA 3' processing is not restored in (p)ppGpp^0 *rnpA*-depleted cells ectopically expressing *rimM* alone or together with *cpgA*. The P_{xsa}-*rimM* and P_{lia}-*cpgA* constructs are the same as in Figure S4 of Chapter 1. Note that *rimM* expression is leaky and does not require inducer, whereas *cpgA* expression is induced by bacitracin (bac). The fold differences in processing efficiency between depleted and non-depleted strain are indicated with no overexpression (grey), with *rimM* overexpression alone (green), with *cpgA* overexpression alone (burgundy) or in combination with *rimM* (black).

cpgA transcripts were promising candidates as mediators of the ribogenesis problem because *ΔrimM* and *ΔcpgA* (*ΔyjeQ*) *E. coli* strains have 30S late assembly defects very similar to those we observed in RNase P-depleted cells (Leong et al., 2013). We investigated whether *rimM* and/or *cpgA* down-regulation was responsible for the 30S assembly defect and subsequent 16S 3' rRNA processing defect observed in tRNA maturase depleted cells by ectopically expressing RimM and CpgA in tRNA maturase depleted cells. Although this failed to restore 16S rRNA processing, one could imagine that the ectopically produced proteins could still be inhibited by the increased levels of (p)ppGpp caused by the accumulation of immature tRNAs. To test whether *rimM* and *cpgA* down-regulation was responsible for the remaining maturation defect seen in tRNA maturase depleted cells in absence of (p)ppGpp, we wished to repeat the ectopic expression experiment in a (p)ppGpp^0 background. Because the down-regulation of *rimM* expression was reversed upon RNase P depletion in a (p)ppGpp^0 background (Chapter 2, Figure 31), it seemed unlikely that a lack of RimM activity was responsible for the remaining maturation defect seen in absence of (p)ppGpp. In contrast, *cpgA* was still down-regulated in tRNA maturase depleted cells in absence of (p)ppGpp production (Figure 37,A); thus, a lack of this GTPase could potentially explain the (p)ppGpp-independent 16S rRNA 3' processing defect. Ectopic expression of *rimM* and *cpgA* alone or in combination failed to improve 16S rRNA processing in the (p)ppGpp^0 RNase P depleted strain (Figure 37,B). Thus, the down-regulation of *rimM* and *cpgA* is unlikely to be the sole cause of the remaining 16S rRNA 3' processing defect in these strains. We have not ruled out the possibility that some other combination of up- or down-regulation of cofactors upon depletion of tRNA maturase (or the combination of all effects) perturbs ribosome assembly independently of (p)ppGpp. It is also possible that the observed modulation of cofactor gene expression is a consequence rather than a cause of the ribogenesis defect. In any case, the factor(s) responsible for the (p)ppGpp-independent inhibition of the 16S rRNA 3' processing remain a mystery and a potential target for future studies.

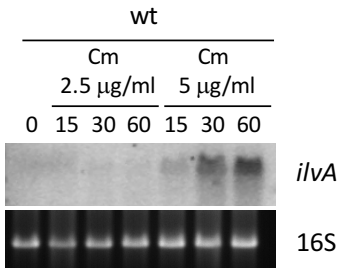

Figure 38: Effect of Cm treatment at sub-inhibitory (2.5 µg/mL) and minimal inhibitory concentration (5 µg/mL) on de-repression of a CodY-regulated gene (*ilvA*) in a wt strain.

7. Regulation of gene expression in tRNA maturase depletion strains

We wished to better understand how the expression of cofactors mRNAs was modulated during tRNA maturase depletion. In Chapter 2, I focused on the *rimM* mRNA as a case study for analysis of the regulation mechanisms occurring in tRNA maturase depleted cells. We showed that the regulation of cofactor gene expression in tRNA maturase-depleted cells arises from a mixture of transcriptional and post-transcriptional mechanisms, caused by a combination of pleiotropic effects including a reduction of growth rate and (p)ppGpp production. The possibility of direct regulation by unprocessed tRNAs or pre-tRFs acting as sRNAs has also been discussed above.

We further speculated that the accumulation of immature tRNAs during tRNA maturase depletion might increase ribosome stalling. Accordingly, a tRNA loss of function mutation leading to pre-tRNA processing defects was reported to induce ribosome stalling in mice (Ishimura et al., 2014). Because stalled ribosomes are known to affect mRNA decay in bacteria (Deana and Belasco, 2005), we hypothesized that some post-transcriptional effects might result from increased ribosome stalling in tRNA maturase depleted cells. In agreement, we observed that treatment with the translation elongation inhibitor chloramphenicol (Cm) recapitulates some of the effects of tRNA maturase depletion on cofactor mRNA. Interestingly, Cm treatment at sub-inhibitory concentration or at MIC did not impact cofactor mRNA levels identically. We further observed that Cm treatment at 5 µg/mL (but not at 2.5 µg/mL) de-repressed expression of the CodY regulon, suggestive of an activation of stringent response under these conditions (Figure 38). This may explain some of the differential effects of low *vs* high Cm concentration (Chapter 2, Figure 27) on cofactor gene expression. While Cm is a known inhibitor of stringent response induction in *E. coli* (Cashel, 1969; Kurland and Maaløe, 1962), the activation of stringent response in Cm-treated *B. subtilis* was previously observed (Rhaese et al., 1975), although the mechanism still remains elusive in both cases. This is an interesting case of divergence between these two organisms.

The production of (p)ppGpp upon depletion of tRNA maturases may have some additional post-transcriptional effects. As we discussed earlier, some proteins involved in RNA metabolism are direct targets of (p)ppGpp such as the PNPase in *S. coelicolor*

(Gatewood and Jones, 2010). (p)ppGpp could also regulate gene expression by binding RNA directly as suggested by the recent identification of riboswitches for ppGpp in a Gram-positive and a Gram-negative bacteria (Sherlock et al., 2018).

In conclusion, the main contribution of this thesis work is the characterization of a coupling mechanism between tRNA processing and rRNA maturation *via* RelA-dependent (p)ppGpp synthesis in *B. subtilis.* The alarmone (p)ppGpp was known to tightly adjust ribosome neo-synthesis to the cellular needs *via* the stringent response and the so-called "growth control" mechanism, exerted primarily at the level of rRNA transcription initiation. Here, we demonstrate that (p)ppGpp also post-transcriptionally affects ongoing ribosome assembly, providing an extra-layer of regulation to the process of ribosome biogenesis. We propose that this mechanism is involved in the fine tuning of ribosome production to the available amount of mature tRNAs, likely maintaining the functional balance between these two major components of the translation machinery. In the future, we could test whether other nucleotide-signaling molecules also contribute to this coupling mechanism. Indeed, a variety of nucleotide-based second messengers exists in bacteria (Pesavento and Hengge, 2009) and some have already been shown to cross-talk with (p)ppGpp signaling (Corrigan et al., 2015).

Bacterial strains

All *B. subtilis* strains used in this thesis were derived from W168 or 168 *trpC2* our WT laboratory strain is SSB1002, a W168 prototrophic strain.

This section concerns the strains constructed for the study presented in Chapter 2, other strains can be found in the "Experimental model and subject details" section of the paper. RNase III deletion and depletion strains were described before (Durand et al., 2012b). *ΔrimM*, *ΔylqC* and *ΔylqD* deletion mutants came from the *B. subtilis* knock-out collection (Koo et al., 2017) and were backcrossed in the SSB1002 genetic background. Other *B. subtilis* strains used in Chapter 2 are listed in Table 2. 1 and details of strains and plasmid constructs are provided in Table 2. 2 and Table 2. 3, respectively (See Supplementary section).

Table 2. 1 : Other *B. subtilis* strain used in this study

Strains	**Genotype**
CCB 994	W168 *Pspac-rnpB:pMUTIN ery amyE::pHM2-ylqD-rimM Cm*
CCB 1008	W168 *Pspac-rnpB:pMUTIN ery amyE::pHM2-ylqD*-rimM Cm*
CCB 1014	W168 *Pspac-rnpB:pMUTIN ery amyE::pHM2 Cm*
CCB 1017	W168 *Pspac-rnpB:pMUTIN ery amyE::pHM2-rimM Cm*
CCB 1031	W168 *Pxyl-rnpA Cm amyE::pHM2-rimM Spc*
CCB 1263	W168 *Pxyl-rnpA Cm yjbM::tet ywaC::kan relA::ery amyE::pDR111-Pxsa-rimM-Plia-cpgA Spc*
CCB 1264	W168 *Pxyl-rnpA Cm yjbM::tet ywaC::kan relA::ery amyE::pDR111- Plia-cpgA Spc*

Table 2. 2: Details of new strain constructs

Strain number	Plasmid	PCR fragment	Oligos for insert amplification	Description	Source/Ref.
CCB 994	pl752	-		pl752 linearized with XhoI and integrated into SSB318 *amyE* locus.	This study
CCB 1008	pl762	-		pl762 linearized with XhoI and integrated into SSB318 *amyE* locus.	This study
CCB 1014	pl606	-		pl606 linearized with XhoI and integrated into SSB318 *amyE* locus.	This study
CCB 1017	pl764	-		pl764 linearized with SpeI and integrated into SSB318 *amyE* locus.	This study
CCB 1031	pl764 and pCs (ECE74)	-		First, pl764 linearized with SpeI was integrated into *amyE* in WT. Than pl764 Cm cassette was switched to Spc using an antibiotic switching cassette vector (pCs / ECE74). The resulting strain was then transformed with CCB504 gDNA.	This study
CCB 1263	pl812			pl812 linearized with NcoI was integrated into *amyE* in the *yjbM ywaC* mutant. The resulting strain was then succesively transformed with CCB504 gDNA and *relA::ery* gDNA.	This study
CCB 1264	pl822			pl822 linearized with NcoI was integrated into *amyE* in the *yjbM ywaC* mutant. The resulting strain was then succesively transformed with CCB504 gDNA and *relA::ery* gDNA.	This study

Table 2. 3: Details of new plasmid constructs

Oligonucleotides sequences are reported in Table 2. 4.

Plasmid number	Initial vector	Insert	Oligos for insert amplification	Description	Source/Ref.
pl606	pHM2	Constitutive promoter		Promoter P_{spac} from pMUTIN-4M cloned without the operator sequence using EcoRI-HindIII restriction sites	This study; (Gendron et al., 1994)
pl752	pl606	*ylqD-rimM*	CC1985 + CC1986	Insert amplified from gDNA and cloned in BamHI/SalI under pl606 constitutive promoter.	This study
pl762	pl606	*ylqD*-rimM*	CC1985 + CC2012* CC2011* + CC1986	ylqD* and *rimM* were amplified from pl752. The CC2011*/CC2012 oligos introduce mutations in *ylqD* ORF. *ylqD*-rimM* overlap was obtained by overlap PCR with underlined oligos and cloned in BamHI/SalI.	This study
pl764	pl606	*rimM*	CC1986 + CC2034	Insert amplified from gDNA and cloned in BamHI/XhoI under pl606 constitutive promoter.	This study

Table 2. 4: Other oligonucleotides used for cloning

Non-hybridizing sequences are shown in lower case letters. Restriction sites are underlined.

Oligo	**Gene**	**Sequence**
CC1985	ylqD fw	TAAGGATCCGCTTAGGCAAAATAGAAAAGCCTGGACGAG
CC1986	rimM rvs	TAACTCGAGAAAAAGGCCATCCGTCAGGATGGCCGAGCACGCCTTCAAACATTTaGGGAAACAGCG
CC2011*	ylqD* fw	GGGGATGACTGGCATcAGtttcaccCAGCGAACACCATCGTC
CC2012*	ylqD* rvs	GACGATGGTGTTCGCTGggtgaaaCTgATGCCAGTCATCCCC
CC2034	rimM fw	ATATGGATCCTGGAAGAGGTGATCATATGACAAAGCGATGG

Experimental procedures

This section concerns mainly the experiments that have not been included in the article. Techniques used specifically for the article can be found in the "Method details" section of the paper.

I. General methods

i. Preparation and transformation of *B. subtilis* competent cells

To achieve natural competence, cells were grown in MD medium at 37°C with 200 rotations per minute (rpm) shaking (1X PC Buffer with addition of 2% glucose, 50 µg/mL L-Tryptophan, 11 µg/mL ammonium iron citrate, 2 mg/mL aspartic acid pH=7 and 3mM $MgSO_4$) supplemented with 2% casein hydrolysate. Typically, the curve inflection point is around OD_{600nm} = 1.2 and peak competence is achieved after 90 mins growth in stationary phase. Ten mL of cells were harvested by 10 mins centrifugation at 5000 rpm at room temperature and resuspended in 1 mL supernatant with addition of glycerol (10 % final concentration). Aliquots were conserved at -80°C until needed for transformation.

For transformation, an aliquot of competent cells (100 µL) was grown in 400 µL non-supplemented MD medium 20 mins at 37°C (with shaking) in presence of DNA: 0.25 µg of replicative plasmid, 2.5 µg of linearized integrative plasmid or 5 µg chromosomal DNA. Then, 200 µL 2xYT medium was added before continuing the growth for 90 mins at 37°C (with shaking). For selection of the transformants, cells were plated on LB agar in presence of the corresponding antibiotics (for concentrations, see section on bacterial cultures). Note that for preparation and transformation of depletion strains (where an essential gene is expressed under an inducible promoter), cells were always grown in presence of inducer.

ii. Preparation and transformation of *E. coli* competent cells

For cloning, *E. coli* cells from JM101 strain were used to amplify plasmids. JM101 chemo-competent cells were obtained by the rubidium method. Briefly, an exponential culture (grown in LB to OD_{600nm}= 0.6) was placed 10 mins on ice before centrifugation for 10 mins at

4°C at 5000 rpm to pellet the cells. The pellet was successively retrieved in 0.35 volumes (vol) ice cold buffer I (30 mM potassium acetate pH 5.8, 100 mM RbCl, 10 mM $CaCl_2$, 50 mM $MnCl_2$, 15% glycerol) and in 0.16 vol ice cold buffer II (10mM MOPS pH 6.5, 10mM RbCl, 75mM CaCl2, 15% glycerol) with a 10 mins waiting time on ice before the second centrifugation step. Aliquots were conserved at -80°C until needed for transformation. Buffer I and II are enriched in divalent cations that, together with rubidium ions, are thought to promote transformation by increasing membrane permeability and by promoting DNA uptake by neutralizing the negative charges of DNA and favoring its interaction with the cell membrane.

For transformation, an aliquot of chemically competent JM101 cells (100 µL) was incubated on ice for 30 mins in presence of 10-100 ng plasmid DNA, followed by a 45 secs heat shock at 42°C and a 2 mins chilling step on ice. Then, 800 µL 2xYT was added and cells were grown for 1 hour at 37°C with agitation. Finally, transformants were selected on LB agar plates supplemented with the corresponding antibiotic.

iii. Bacterial cultures

Unless stated otherwise, *B. subtilis* strains were grown in 2xYT liquid medium (1.6% peptone, 1% yeast extract, 1% NaCl) at 200 rpm at 37°C in $\leq$ 1/10 volume of the flask to ensure proper aeration. Overnight precultures were grown in presence of appropriate antibiotics and inducer (1mM IPTG or 2% xylose), in the case of depletion strains. Antibiotics were used at the following concentrations: 5 µg/mL for chloramphenicol, 1 µg/mL for erythromycin, 10 µg/mL for kanamycin, 5 µg/mL for phleomycin, 0.5 + 12.5 µg/mL erythromycin and lyncomycin, respectively for MLS and 20 µg/mL for tetracycline.

Experimental cultures were grown in the absence of antibiotics, except when it was required for plasmid maintenance. For depletion strains, overnight induced cultures were washed three times with pre-warmed 2xYT medium and inoculated at OD_{600} between 0.02 and 0.2, depending on the strain, in fresh medium with or without inducer. Generally, induced cells were harvested for RNA or protein preparation around OD_{600} = 0.6 and cells grown in the absence of the inducer were followed until they reach a plateau before being harvested. Inoculation and depletion conditions were determined empirically for each strain such that the depleted cells were harvested between OD_{600} = 0.3 and OD_{600} = 0.7. For RnpA depletion, for example, cultures were inoculated at OD_{600} = 0.05 in presence of 2% xylose

(inducer) or 2% glucose to tighten repression of the *Pxyl* promoter, which typically led to a growth arrest (plateau) around OD_{600} = 0.6. For *rnZ* and *rnpB* depletion strains, cultures were inoculated in presence or in absence of 1mM IPTG at OD_{600} = 0.05 and OD_{600} = 0.2, respectively. RNase Z and RnpB depleted cells typically plateau around OD_{600} = 0.6 and OD_{600}= 0.3, respectively.

To mimic amino acid starvation, we depleted charged arginine tRNAs by addition of arginine hydroxamate (RHX) at 250 mg/mL in cultures growing in 2xYT at OD_{600} = 0.3. For inhibition of GTP synthesis, decoyinine, an inhibitor of the GMP synthetase GuaA was dissolved at 1 mg/mL in 2xYT pre-warmed to 37°C and an equal volume added to 1 mL cultures at OD_{600} = 0.6 (final concentration 500 mg/mL). For the CRISPRi strain targeting *era* expression, cells were grown overnight in 2xYT and diluted in the presence or absence of 1% xylose. Cells were grown to OD_{600} = 0.5 before being harvested. The presence of xylose triggers expression of a nuclease-deactivated variant of *Streptococcus pyogenes* Cas9 (dCas9) that is targeted to the *era* gene by a single guide RNA (*sgRNA-era*) expressed under control of the constitutive P_{veg} promoter). The resulting complex base-paired to the *era* genomic locus sterically hinders transcription, leading to a knock-down in *era* expression.

To study the effect of translation pausing, we added the translation elongation inhibitor chloramphenicol (Cm) at sub-inhibitory (2.5 µg/ml) or minimal inhibitory concentration (5 µg/ml) to cells growing in 2xYT at OD_{600} = 0.6. Cells were harvested just before Cm addition (t_0) and 15, 30 and 60 mins after treatment.

We reproduced some growth conditions from the *B. subtilis* tilling array experiment known to lead to a decrease in *rnpA* expression, i.e. ethanol treatment and stationary phase in minimal and complex medium. Ethanol was added to cultures growing in minimal medium (M9 with 0.5 % glucose) at 4% (v/v) around OD_{600} = 0.4 and cells were harvested 10 mins after treatment. Cell pellets were washed with TE 0.1M NaCl before storage at -20 °C.

II. RNA techniques

i. RNA extraction

RNA extraction was typically performed using the glass beads / phenol protocol (adapted from (Bechhofer et al., 2008)) on 1 to 8 mL mid-log phase *B. subtilis* cells growing in 2xYT. Briefly, frozen cell pellets were resuspended in 200 µL ice-cold TE-buffer (10 mM Tris pH 7.5, 1 mM EDTA) and transferred to a tube containing 25 µL chloroform, 6.25 µL 20% SDS and 100 µL glass beads for lysis by three 1-min vortexing steps at max speed on a Disruptor Genie (Scientific Industries) separated with 1-min intervals on ice. After centrifugation for 10 mins at 16,000 x g at 4°C, the supernatant was transferred to 200 µL water-saturated phenol on ice and vortexed again (with the same 3 x 1 min protocol as above) before being centrifuged for 10 mins at 16,000 x g at 4°C. The supernatant was then mixed with 200 µL water-saturated phenol and 100 µL chloroform, vortexed for 1 min at full speed and centrifuged again for 10 mins at 16,000 x g at 4°C. RNA was precipitated at -20°C by adding 3 volumes of 95% ethanol stored at -20°C and 0.1 volume of 10M LiCl before being washed, dried, and resuspended in 30 to 100 µL water.

ii. Northern blots

To perform Northern blots, 5 µg total RNA were denatured for 5 mins at 95°C in RNA Gel loading dye (Thermo Scientific) before being separated on 1% agarose gels in 1X TBE (native) or on denaturing 5% acrylamide gels in 1X TBE + 7M urea. RNA was transferred from agarose gels to a hybond-N membrane (GE-Healthcare) by capillary transfer for 4 hours minimum in 1X transfer buffer (5X SSC, 0.01M NaOH). For Northerns of acrylamide gels, RNA was electro-transferred at 4°C in 0.5X TBE for 4 hours at 60V or overnight at 12V. RNA was cross-linked to the membrane by UV cross-linking at 120,000 microjoules/cm^2 using HL-200 Hybrilinker UV-crosslinker (UVP).

Probes for Northern blots were usually 25 to 30-nts DNA oligonucleotides radiolabeled on their 5' end by polynucleotide kinase (PNK). 10 pmol oligonucleotide was incubated 40 mins at 37°C with 50 µCi of ATP γ-^{32}P in presence of 1 µL PNK (Thermo Scientific) in a total volume of 20 µL. The reaction mixture was then eluted on a G50 column (GE-Healthcare) to remove unincorporated nucleotides. Some transcripts (such as *cpgA*) were detected using

riboprobes. RNA probes were synthesized by *in vitro* transcription with T7 RNAP (Promega) using ~250 ng PCR product (with an integrated T7 promoter on the non-coding strand) as DNA template, in presence of ATP, GTP, CTP and 20 µCi UTP α-^{32}P at 37°C for 90 mins. After 15 mins of DNase treatment at 37°C with 2 µL RQ1 DNase (Promega), riboprobes were purified by G50 column (GE-Healthcare). Membranes were pre-incubated in Ultra-Hyb (Life Technologies) for agarose blots or Roti-Hybri-Quick (Roth) for acrylamide blots for 1 hour and hybridized with radiolabeled probes for a minimum of 4 hours. Pre-incubation, hybridization and wash steps were performed at 42°C in the case of 5'-labeled oligonucleotides or at 68°C for riboprobes. Membranes were quickly rinsed once at room temperature in 2x SSC 0.1% SDS to remove non-hybridized probe before being washed once for 5 mins in the same buffer and then twice for 5 mins in 0.2x SSC 0.1% SDS. Northerns were exposed to PhosphorImager screens (GE Healthcare) and the signal was obtained by scanning with a Typhoon scanner (GE Healthcare). Fiji (ImageJ) software was used for quantifications.

Most oligonucleotides used for Northern blots are listed in the article supplemental material, other probes used for the study are listed in Table 2. 5.

Table 2. 5: Other oligonucleotides probes used in this thesis.

Oligo	Gene	Sequence
CC1005	*rnpA*	ACTGGCGGTTTGCAACTGATGTCCC
CC1006	*rnpB*	TGCGAGCATGGACTTTCCTCTACAG
CC2099	*ylqD*	CTCGGTTAAGACTTGCATAACGGCTACACGG
CC2100	*ylqC*	GTCATCTGGATGATCAACAAGCGGCGTCAC
CC2101	*trmD*	CTGCCTTTGATGTCAGGTCCTCGACCGCGTC
CC2103	*ffh*	GAAATCGTCTGCTGCAGTCGGTCGGCTAATC
CC2143	*rpsP*	GATGAAACGGCCGTCACGTGGTGAACGAGAATC
CC2144	*rplS*	CAGGACGGAACGCAGGAAGATCAGTACGAAG

iii. Rifampicin assay of RNA stability

B. subtilis strains were grown in 2xYT at 37°C with shaking as described above. At OD_{600nm} = 0.6 (or less for some depletion strains), rifampicin was added to a final concentration of 150 µg/mL in order to block new RNA synthesis. Samples were collected at different time points (e.g. 0, 2, 5, 10, 15 and 20 minutes) by mixing the cells with frozen 10mM sodium

azide (200 µL for 1.3 mL culture). Samples were vortexed until the sodium azide thawed, cells were pelleted by centrifugation at 4°C and the pellet was conserved at -20°C until RNA extraction. Total RNA was extracted with the phenol-chloroform method (see RNA isolation section) and Northern blots were performed as detailed above.

To determine mRNA half-lives, the signal for each time point was quantified using the Fiji software and normalized to the signal at time 0 (before addition of rifampicin) defined as 100%. The logs of the normalized values were then plotted against time to give linear RNA decay curves. mRNA half-lives were calculated from the linear regression coefficient (slope) of the experimental curves using the formula: $T\left(\frac{1}{2}\right) = -log2/slope.$

III. Ribosome gradients

B. subtilis cells were grown as described above to OD_{600nm} = 0.5 (or less for some mutants). 50 mL of culture were harvested by centrifugation for 5 mins at 5,000 rpm at 4°C before being washed in ice cold Buffer A (20 mM Tris-HCl pH 7.5, 200 mM NH_4Cl, 6 mM β-mercaptoethanol) containing 10 mM $MgCl_2$. Cell pellets were stored at -20°C until lysis. To prepare ribosomes, cells were resuspended in 1 mL Buffer A containing 10 mM $MgCl_2$ to maintain 70S ribosomes or 3 mM $MgCl_2$ to obtain dissociated subunits, with addition of DNase I (1 µg/mL) before mechanical lysis by two passages in an ice-cold French Press (Glen Mills) at 20,000 psi. The lysate was then cleared at 13,200 rpm for 30 mins at 4°C. A maximum of 500 µL cleared lysate was then loaded on a continuous 10%-30% sucrose gradient in buffer A (containing the same $MgCl_2$ concentration as during lysis). 30S and 50S subunits were separated in gradients containing 3 mM $MgCl_2$ by centrifugation at 23,000 rpm for 16 hours at 4°C in a SW41 rotor (Beckman), whereas gradients containing 10 mM $MgCl_2$ were centrifuged for the same time but at 18,600 rpm. 500 µL fractions were collected using a Piston Gradient Fractionator (Biocomp) with monitoring of absorbance at 254 nm, allowing visualization of the ribosome peaks. The rRNA content of the different fractions was analyzed on 1% agarose gels by mixing 10 µL fraction with an equal volume of 2X RNA Gel loading dye (Thermo Scientific) and loaded without a denaturing step.

Supplementary

Table 1: 30S ribosome assembly cofactors

In this table, I have listed cofactors known to be directly or indirectly involved in small subunit assembly, which is more directly related to this thesis. Because their precise roles are sometimes unclear, I chose known defects in either 30S assembly or 16S rRNA processing (an indirect indicator of an assembly defect) as criteria for inclusion in this Table. Multiple cofactor names can be found in the literature. An index indicates the organism (Ec for *E. coli* and Bs for *B. subtilis*). An asterisk (*) next to the cofactor's name indicates that the protein is found in *B. subtilis* but not in *E. coli.* Most of the results are from studies in *E. coli*; those obtained in *B. subtilis* are indicated in blue. The table is divided in four parts according each cofactor's activity: GTPase, RNA helicase, energy independent RNA chaperone or maturation enzyme.

Cofactor name(s)	Activity	Essential	Role in 30S or 50S assembly	Phenotype of the mutant (deletion or depletion strain)	Other experimental results
$CpgA_{Bs}$ **$RsgA_{Ec}$** **$YjeQ_{Ec}$** **$YloQ_{Bs}$**	GTPase	No	**30S** assembly and/or subunit joining.	• Reduced amount of 70S ribosomes[1,2]. • Accumulation of 30S precursor containing 17S rRNA precursor and lacking several late r-proteins: similar structural defect as a *ΔrimM* mutant[3]. • Distorted helix 44 and decoding center[4].	• Part of a 30S assembly checkpoint for the decoding center[5,6]. • (p)ppGpp binding protein[7,8].
Der_{Ec} **$YphC_{Bs}$** **EngA** **$YfgK_{Ec}$**	GTPase	Yes	**50S** late assembly	• Loss of 70S ribosomes and accumulation of individual subunits[9]. Same effect in *B. subtilis*[10]. • Accumulation of both 23S and 16S rRNAs precursors[9]. • Accumulation of 45S precursor (similar to RbgA-depleted cells) in *B. subtilis*[10].	• Contains two consecutive GTP binding domains. • EngA interacts with 50S peptidyl transferase center and induces significant structural changes[11]. • (p)ppGpp binding protein[7,8]. • Potential association with the ribosome under guanine control[12]. • YphC assists maturation of the functional core and central protuberance of *B. subtilis* 50S[13].

Era **Bex$_{Bs}$** **RbaA$_{Ec}$** **SdgE$_{Ec}$**	GTPase	Yes	**30S** assembly and maturation	• Loss of 70S ribosomes and accumulation of individual subunits[14]. • Accumulation of precursor 16S rRNA[14].	• (p)ppGpp binding protein[7,8]. • An *era ts* mutation can be suppressed by overexpression of *ksgA*[15]. • Era interacts with YbeY[16]. • Overexpression of Era suppresses the defects of *ΔrbfA* and *ΔrsgA* mutants[1,14] and partially suppresses the defects of a *ΔybeY* mutant[17].
Obg$_{Bs}$ **CgtA$_{Ec}$** **ObgE$_{Ec}$** **YhbZ$_{Ec}$**	GTPase	Yes	**50S** assembly and subunit joining (anti-association factor[18]).	• Decreased levels of 70S and polysomes [19,20]. • Increase in free 30S and 50S. • 16S rRNA and 23S rRNA processing defects.	• Conserved throughout evolution. • Multicopy suppressor of the rRNA methyltransferase *ΔrrmJ* mutant[21]. • Also involved in modulation of the general stress response, sporulation, persistence, chromosome segregation and replication[22,23,24]. • Interacts with SpoT[25]. • (p)ppGpp binding protein[8,23]. • Suggested to perform 50S assembly checkpoint[18].
YqeH$_{Bs}$*	GTPase	No	**30S** assembly / stability	• Loss of 30S subunits and reduction of 16S rRNA levels[29,30].	• Does not bind (p)ppGpp[8]. • *Arabidopsis thaliana* homolog of YqeH, AtNOS, may be involved in chloroplast and

				• Presence of pre-16S rRNA and 16S rRNA degradation products[30].	mitochondrial ribosome assembly[31].
SrmB$_{Ec}$ **RbaB**$_{Ec}$ **RhlA**$_{Ec}$	RNA Helicase (DEAD Box)	No	**50S** assembly	• Accumulation of 40S particles containing precursor 23S rRNA. • Accumulation of immature 30S containing 17S rRNA[36].	• SrmB is thought to be exclusively involved in 50S assembly, the effect on 30S assembly being an indirect consequence of the 50S biogenesis defect[36].
RbfA	Energy independent RNA Chaperone	No	**30S** assembly	• Accumulation of immature 16S rRNA[40].	• Same operon as *ylxS*$_{Bs}$*/rimP*$_{Ec}$. • Overexpression of RbfA partially suppresses the growth phenotype of a *ΔrimM* mutant[41]. • Part of a 30S assembly checkpoint for the decoding center[5,6]. • YjeQ promotes dissociation of RbfA during the final stages of maturation[42].
RimM **21K**$_{Ec}$ **YfjA**$_{Ec}$	Energy independent RNA Chaperone	No	**30S** assembly	• Slow growth [43]. • Accumulation of immature 16S rRNA[44]. • Accumulation of free 30S and 50S subunits[44].	• Part of a 30S late assembly checkpoint[45]. • Involved in the incorporation of late 30S r-proteins[46].
RimP$_{Ec}$ **YlxS**$_{Bs}$ **YhbC**$_{Ec}$	Energy independent	No	**30S** assembly	• Slow growth[50]. • Accumulation of immature 16S rRNA[50].	• Involved in the incorporation of late 30S r-proteins[46].

	RNA Chaperone			• Accumulation of free 30S and 50S subunits[50].	• Important for central pseudoknot formation[51].
KsgA **$RsmA_{Ec}$**	Modification enzyme	No	**16S rRNA** methyltransferase (methylates A1518 and A1519) and indirect effect on **30S** assembly	• Accumulation of immature 16S rRNA[37].	• *ksgA* is a multicopy suppressor of an *era* mutant[38]. • KsgA is universally conserved and orthologs from eukaryotes and archaea are able to complement KsgA function in bacteria[39]. • KsgA acts as a late regulator for 30S subunit maturation[37].
$RimJ_{Ec}$ **$YdaF_{Bs}$** **$YjcK_{Bs}$**	Modification enzyme	No	Acetylation of S5 r-protein and **30S** assembly	• No phenotype	• Alanine acetyltransferase specific for r-protein S5[47] • Associates with pre-30S subunits[48] • Role in maturation of the 30S subunit independently of its acetyltransferase activity [49]

References for Table1

1. Campbell, T. L. & Brown, E. D. Genetic interaction screens with ordered overexpression and deletion clone sets implicate the *Escherichia coli* GTPase YjeQ in late ribosome biogenesis. *J. Bacteriol.* **190**, 2537–2545 (2008).
2. Himeno, H. *et al.* A novel GTPase activated by the small subunit of ribosome. *Nucleic Acids Res.* **32**, 5303–5309 (2004).
3. Leong, V., Kent, M., Jomaa, A. & Ortega, J. *Escherichia coli rimM* and *yjeQ* null strains accumulate immature 30S subunits of similar structure and protein complement. *RNA* **19**, 789–802 (2013).
4. Jomaa, A. *et al.* Cryo-electron microscopy structure of the 30S subunit in complex with the YjeQ biogenesis factor. *RNA* **17**, 2026–2038 (2011).
5. Razi, A., Guarné, A. & Ortega, J. The cryo-EM structure of YjeQ bound to the 30S subunit suggests a fidelity checkpoint function for this protein in ribosome assembly. *Proc. Natl. Acad. Sci.* **114**, E3396–E3403 (2017).
6. López-Alonso, J. P. *et al.* RsgA couples the maturation state of the 30S ribosomal decoding center to activation of its GTPase pocket. *Nucleic Acids Res.* **45**, 6945–6959 (2017).
7. Zhang, Y., Zborníková, E., Rejman, D. & Gerdes, K. Novel (p)ppGpp Binding and Metabolizing Proteins ofEscherichia coli. *mBio* **9**, (2018).
8. Corrigan, R. M., Bellows, L. E., Wood, A. & Gründling, A. ppGpp negatively impacts ribosome assembly affecting growth and antimicrobial tolerance in Gram-positive bacteria. *Proc. Natl. Acad. Sci.* **113**, E1710–E1719 (2016).
9. Hwang, J. & Inouye, M. The tandem GTPase, Der, is essential for the biogenesis of 50S ribosomal subunits in Escherichia coli. *Mol. Microbiol.* **61**, 1660–1672 (2006).
10. Schaefer, L. *et al.* Multiple GTPases Participate in the Assembly of the Large Ribosomal Subunit in Bacillus subtilis. *J. Bacteriol.* **188**, 8252–8258 (2006).
11. Zhang, X. *et al.* Structural insights into the function of a unique tandem GTPase EngA in bacterial ribosome assembly. *Nucleic Acids Res.* **42**, 13430 (2014).
12. Muench, S. P., Xu, L., Sedelnikova, S. E. & Rice, D. W. The essential GTPase YphC displays a major domain rearrangement associated with nucleotide binding. *Proc. Natl. Acad. Sci.* **103**, 12359–12364 (2006).
13. Ni, X. *et al.* YphC and YsxC GTPases assist the maturation of the central protuberance, GTPase associated region and functional core of the 50S ribosomal subunit. *Nucleic Acids Res.* **44**, 8442–8455 (2016).
14. Inoue, K., Alsina, J., Chen, J. & Inouye, M. Suppression of defective ribosome assembly in a *rbfA* deletion mutant by overexpression of Era, an essential GTPase in *Escherichia coli*. *Mol. Microbiol.* **48**, 1005–1016 (2003).
15. Lu, Q. & Inouye, M. The gene for 16S rRNA methyltransferase (*ksgA*) functions as a multicopy suppressor for a cold-sensitive mutant of *era*, an essential RAS-like GTP-binding protein in Escherichia coli. *J. Bacteriol.* **180**, 5243–5246 (1998).
16. Vercruysse, M. *et al.* Identification of YbeY-Protein Interactions Involved in 16S rRNA Maturation and Stress Regulation in Escherichia coli. *mBio* **7**, e01785-16 (2016).
17. Ghosal, A., Babu, V. M. P. & Walker, G. C. Elevated Levels of Era GTPase Improve Growth, 16S rRNA Processing, and 70S Ribosome Assembly of Escherichia coli Lacking Highly Conserved Multifunctional YbeY Endoribonuclease. *J. Bacteriol.* **200**, e00278-18 (2018).
18. Feng, B. *et al.* Structural and Functional Insights into the Mode of Action of a Universally Conserved Obg GTPase. *PLOS Biol.* **12**, e1001866 (2014).
19. Matsuo, Y. *et al.* The GTP-binding Protein YlqF Participates in the Late Step of 50 S Ribosomal Subunit Assembly in *Bacillus subtilis*. *J. Biol. Chem.* **281**, 8110–8117 (2006).
20. Sato, A. *et al.* The GTP binding protein Obg homolog ObgE is involved in ribosome maturation. *Genes Cells* **10**, 393–408 (2005).
21. Tan, J., Jakob, U. & Bardwell, J. C. A. Overexpression of two different GTPases rescues a null mutation in a heat-induced rRNA methyltransferase. *J. Bacteriol.* **184**, 2692–2698 (2002).
22. Foti, J. J., Persky, N. S., Ferullo, D. J. & Lovett, S. T. Chromosome segregation control by *Escherichia coli* ObgE GTPase. *Mol. Microbiol.* **65**, 569–581 (2007).

23. Persky, N. S., Ferullo, D. J., Cooper, D. L., Moore, H. R. & Lovett, S. T. The ObgE/CgtA GTPase influences the stringent response to amino acid starvation in *Escherichia coli. Mol. Microbiol.* **73**, 253–266 (2009).
24. Verstraeten, N. *et al.* Obg and Membrane Depolarization Are Part of a Microbial Bet-Hedging Strategy that Leads to Antibiotic Tolerance. *Mol. Cell* **59**, 9–21 (2015).
25. Jiang, M., Sullivan, S. M., Wout, P. K. & Maddock, J. R. G-Protein Control of the Ribosome-Associated Stress Response Protein SpoT. *J. Bacteriol.* **189**, 6140–6147 (2007).
26. Uicker, W. C., Schaefer, L. & Britton, R. A. The essential GTPase RbgA (YlqF) is required for 50S ribosome assembly in *Bacillus subtilis*. *Mol. Microbiol.* **59**, 528–540 (2006).
27. Achila, D., Gulati, M., Jain, N. & Britton, R. A. Biochemical Characterization of Ribosome Assembly GTPase RbgA in Bacillus subtilis. *J. Biol. Chem.* **287**, 8417–8423 (2012).
28. Pausch, P. *et al.* Structural basis for (p)ppGpp-mediated inhibition of the GTPase RbgA. *J. Biol. Chem.* jbc.RA118.003070 (2018). doi:10.1074/jbc.RA118.003070
29. Loh, P. C., Morimoto, T., Matsuo, Y., Oshima, T. & Ogasawara, N. The GTP-binding protein YqeH participates in biogenesis of the 30S ribosome subunit in *Bacillus subtilis. Genes Genet. Syst.* **82**, 281–289 (2007).
30. Uicker, W. C., Schaefer, L., Koenigsknecht, M. & Britton, R. A. The Essential GTPase YqeH Is Required for Proper Ribosome Assembly in *Bacillus subtilis*. *J. Bacteriol.* **189**, 2926–2929 (2007).
31. Moreau, M., Lee, G. I., Wang, Y., Crane, B. R. & Klessig, D. F. AtNOS/AtNOA1 Is a Functional *Arabidopsis thaliana* cGTPase and Not a Nitric-oxide Synthase. *J. Biol. Chem.* **283**, 32957–32967 (2008).
32. Wicker-Planquart, C. & Jault, J.-M. Interaction between *Bacillus subtilis* YsxC and ribosomes (or rRNAs). *FEBS Lett.* **589**, 1026–1032 (2015).
33. Lehoux, I. E., Mazzulla, M. J., Baker, A. & Petit, C. M. Purification and characterization of YihA, an essential GTP-binding protein from *Escherichia coli*. *Protein Expr. Purif.* **30**, 203–209 (2003).
34. Hunger, K., Beckering, C. L., Wiegeshoff, F., Graumann, P. L. & Marahiel, M. A. Cold-Induced Putative DEAD Box RNA Helicases CshA and CshB Are Essential for Cold Adaptation and Interact with Cold Shock Protein B in Bacillus subtilis. *J. Bacteriol.* **188**, 240–248 (2006).
35. Lehnik-Habrink, M. *et al.* The RNA degradosome in *Bacillus subtilis*: identification of CshA as the major RNA helicase in the multiprotein complex. *Mol. Microbiol.* **77**, 958–971 (2010).
36. Lehnik-Habrink, M. *et al.* DEAD-Box RNA Helicases in *Bacillus subtilis* Have Multiple Functions and Act Independently from Each Other. *J. Bacteriol.* **195**, 534–544 (2013).
37. Connolly, K., Rife, J. P. & Culver, G. Mechanistic insight into the ribosome biogenesis functions of the ancient protein KsgA. *Mol. Microbiol.* **70**, 1062–1075 (2008).
38. Lu, Q. & Inouye, M. The gene for 16S rRNA methyltransferase (*ksgA*) functions as a multicopy suppressor for a cold-sensitive mutant of era, an essential RAS-like GTP-binding protein in *Escherichia coli. J. Bacteriol.* **180**, 5243–5246 (1998).
39. O'Farrell, H. C. Recognition of a complex substrate by the KsgA/Dim1 family of enzymes has been conserved throughout evolution. *RNA* **12**, 725–733 (2006).
40. Xia, B., Ke, H., Shinde, U. & Inouye, M. The Role of RbfA in 16S rRNA Processing and Cell Growth at Low Temperature in *Escherichia coli*. *J. Mol. Biol.* **332**, 575–584 (2003).
41. Bylund, G. O., Lövgren, J. M. & Wikström, P. M. Characterization of Mutations in the *metY-nusA-infB* Operon That Suppress the Slow Growth of a *ΔrimM* Mutant. *J. Bacteriol.* **183**, 6095–6106 (2001).
42. Jeganathan, A., Razi, A., Thurlow, B. & Ortega, J. The C-terminal helix in the YjeQ zinc-finger domain catalyzes the release of RbfA during 30S ribosome subunit assembly. *RNA* **21**, 1203–1216 (2015).
43. Bylund, G. O., Wipemo, L. C., Lundberg, L. A. C. & Wikström, P. M. RimM and RbfA Are Essential for Efficient Processing of 16S rRNA in *Escherichia coli*. *J. Bacteriol.* **180**, 73–82 (1998).
44. Lovgren, J. M. The PRC-barrel domain of the ribosome maturation protein RimM mediates

binding to ribosomal protein S19 in the 30S ribosomal subunits. *RNA* **10**, 1798–1812 (2004).
45. Culver, G. M. Assembly of the 30S ribosomal subunit. *Q. Rev. Biophys.* **38**, 397 (2005).
46. Bunner, A. E., Nord, S., Wikström, P. M. & Williamson, J. R. The Effect of Ribosome Assembly Cofactors on In Vitro 30S Subunit Reconstitution. *J. Mol. Biol.* **398**, 1–7 (2010).
47. Yoshikawa, A., Isono, S., Sheback, A. & Isono, K. Cloning and nucleotide sequencing of the genes *rimI* and *rimJ* which encode enzymes acetylating ribosomal proteins S18 and S5 of Escherichia coli K12. *Mol. Gen. Genet. MGG* **209**, 481–488 (1987).
48. Roy-Chaudhuri, B., Kirthi, N., Kelley, T. & Culver, G. M. Suppression of a cold-sensitive mutation in ribosomal protein S5 reveals a role for RimJ in ribosome biogenesis. *Mol. Microbiol.* **68**, 1547 (2008).
49. Roy-Chaudhuri, B., Kirthi, N. & Culver, G. M. Appropriate maturation and folding of 16S rRNA during 30S subunit biogenesis are critical for translational fidelity. *Proc. Natl. Acad. Sci.* **107**, 4567–4572 (2010).
50. Nord, S., Bylund, G. O., Lövgren, J. M. & Wikström, P. M. The RimP Protein Is Important for Maturation of the 30S Ribosomal Subunit. *J. Mol. Biol.* **386**, 742–753 (2009).
51. Sashital, D. G. *et al.* A combined quantitative mass spectrometry and electron microscopy analysis of ribosomal 30S subunit assembly in *E. coli*. *eLife* **3**, e04491 (2014).

References

Adhya, S., and Gottesman, M. (1978). Control of Transcription Termination. Annu. Rev. Biochem. *47*, 967–996.

Adilakshmi, T., Bellur, D.L., and Woodson, S.A. (2008). Concurrent nucleation of 16S folding and induced fit in 30S ribosome assembly. Nature *455*, 1268–1272.

Agaisse, H., and Lereclus, D. (1996). STAB-SD: a Shine–Dalgarno sequence in the 5′ untranslated region is a determinant of mRNA stability. Mol. Microbiol. *20*, 633–643.

Agirrezabala, X., Fernández, I.S., Kelley, A.C., Cartón, D.G., Ramakrishnan, V., and Valle, M. (2013). The ribosome triggers the stringent response by RelA via a highly distorted tRNA. EMBO Rep. *14*, 811–816.

Akanuma, G., Nanamiya, H., Natori, Y., Yano, K., Suzuki, S., Omata, S., Ishizuka, M., Sekine, Y., and Kawamura, F. (2012). Inactivation of ribosomal protein genes in Bacillus subtilis reveals importance of each ribosomal protein for cell proliferation and cell differentiation. J. Bacteriol. *194*, 6282–6291.

Allemand, F., Mathy, N., Brechemier-Baey, D., and Condon, C. (2005). The 5S rRNA maturase, ribonuclease M5, is a Toprim domain family member. Nucleic Acids Res. *33*, 4368–4376.

Arenz, S., Abdelshahid, M., Sohmen, D., Payoe, R., Starosta, A.L., Berninghausen, O., Hauryliuk, V., Beckmann, R., and Wilson, D.N. (2016). The stringent factor RelA adopts an open conformation on the ribosome to stimulate ppGpp synthesis. Nucleic Acids Res. *44*, 6471–6481.

Armstrong, R.L., and Sueoka, N. (1968). Phase transitions in ribonucleic acid synthesis during germination of Bacillus subtilis spores. Proc. Natl. Acad. Sci. U. S. A. *59*, 153–160.

Arraiano, C.M., Andrade, J.M., Domingues, S., Guinote, I.B., Malecki, M., Matos, R.G., Moreira, R.N., Pobre, V., Reis, F.P., Saramago, M., et al. (2010). The critical role of RNA processing and degradation in the control of gene expression. FEMS Microbiol. Rev. *34*, 883–923.

Asha, P.K., Blouin, R.T., Zaniewski, R., and Deutscher, M.P. (1983). Ribonuclease BN: identification and partial characterization of a new tRNA processing enzyme. Proc. Natl. Acad. Sci. U. S. A. *80*, 3301–3304.

Atkinson, G.C., Tenson, T., and Hauryliuk, V. (2011). The RelA/SpoT Homolog (RSH) Superfamily: Distribution and Functional Evolution of ppGpp Synthetases and Hydrolases across the Tree of Life. PLOS ONE *6*, e23479.

Basturea, G.N., Zundel, M.A., and Deutscher, M.P. (2011). Degradation of ribosomal RNA during starvation: Comparison to quality control during steady-state growth and a role for RNase PH. RNA *17*, 338–345.

Battesti, A., and Bouveret, E. (2006). Acyl carrier protein/SpoT interaction, the switch linking SpoT-dependent stress response to fatty acid metabolism. Mol. Microbiol. *62*, 1048–1063.

Baumgardt, K., Gilet, L., Figaro, S., and Condon, C. (2018). The essential nature of YqfG, a YbeY homologue required for 3′ maturation of Bacillus subtilis 16S ribosomal RNA is suppressed by deletion of RNase R. Nucleic Acids Res. *46*, 8605–8615.

Bechhofer, D.H., Oussenko, I.A., Deikus, G., Yao, S., Mathy, N., and Condon, C. (2008). Chapter 14 Analysis of mRNA Decay in Bacillus subtilis. In Methods in Enzymology, (Academic Press), pp. 259–276.

Beckert, B., Abdelshahid, M., Schäfer, H., Steinchen, W., Arenz, S., Berninghausen, O., Beckmann, R., Bange, G., Turgay, K., and Wilson, D.N. (2017). Structure of the Bacillus subtilis hibernating 100S ribosome reveals the basis for 70S dimerization. EMBO J. *36*, 2061–2072.

Belasco, J.G. (2010). All things must pass: contrasts and commonalities in eukaryotic and bacterial mRNA decay. Nat. Rev. Mol. Cell Biol. *11*, 467–478.

van der Biezen, E.A., Sun, J., Coleman, M.J., Bibb, M.J., and Jones, J.D. (2000). Arabidopsis RelA/SpoT homologs implicate (p)ppGpp in plant signaling. Proc. Natl. Acad. Sci. U. S. A. *97*, 3747–3752.

Blum, E., Carpousis, A.J., and Higgins, C.F. (1999). Polyadenylation Promotes Degradation of 3'-Structured RNA by the *Escherichia coli* mRNA Degradosome *in Vitro*. J. Biol. Chem. *274*, 4009–4016.

Braun, F. (1998). Ribosomes inhibit an RNase E cleavage which induces the decay of the rpsO mRNA of Escherichiacoli. EMBO J. *17*, 4790–4797.

Britton, R.A. (2009). Role of GTPases in Bacterial Ribosome Assembly. Annu. Rev. Microbiol. *63*, 155–176.

Britton, R.A., Wen, T., Schaefer, L., Pellegrini, O., Uicker, W.C., Mathy, N., Tobin, C., Daou, R., Szyk, J., and Condon, C. (2007). Maturation of the 5' end of Bacillus subtilis 16S rRNA by the essential ribonuclease YkqC/RNase J1. Mol. Microbiol. *63*, 127–138.

Brown, A., Fernández, I.S., Ramakrishnan, V., and Gordiyenko, Y. (2016). Ribosome-dependent activation of stringent control. Nature *534*, 277.

Bunner, A.E., Nord, S., Wikström, P.M., and Williamson, J.R. (2010). The Effect of Ribosome Assembly Cofactors on In Vitro 30S Subunit Reconstitution. J. Mol. Biol. *398*, 1–7.

Callaghan, A.J., Marcaida, M.J., Stead, J.A., McDowall, K.J., Scott, W.G., and Luisi, B.F. (2005). Structure of Escherichia coli RNase E catalytic domain and implications for RNA turnover. Nature *437*, 1187–1191.

Campagnoli, M.F., Ramenghi, U., Armiraglio, M., Quarello, P., Garelli, E., Carando, A., Avondo, F., Pavesi, E., Fribourg, S., Gleizes, P.-E., et al. (2008). RPS19 mutations in patients with Diamond-Blackfan anemia. Hum. Mutat. *29*, 911–920.

Campbell, T.L., and Brown, E.D. (2008). Genetic interaction screens with ordered overexpression and deletion clone sets implicate the Escherichia coli GTPase YjeQ in late ribosome biogenesis. J. Bacteriol. *190*, 2537–2545.

Campos-Guillen, J., Bralley, P., Jones, G.H., Bechhofer, D.H., and Olmedo-Alvarez, G. (2005). Addition of Poly(A) and Heteropolymeric 3' Ends in Bacillus subtilis Wild-Type and Polynucleotide Phosphorylase-Deficient Strains. J BACTERIOL *187*, 9.

Cao, G.J., and Sarkar, N. (1992). Identification of the gene for an Escherichia coli poly(A) polymerase. Proc. Natl. Acad. Sci. *89*, 10380–10384.

Carpousis, A.J. (2007). The RNA Degradosome of Escherichia coli: An mRNA-Degrading Machine Assembled on RNase E. Annu. Rev. Microbiol. *61*, 71–87.

Carpousis, A.J., Luisi, B.F., and McDowall, K.J. (2009). Chapter 3 Endonucleolytic Initiation of mRNA Decay in Escherichia coli. In Progress in Molecular Biology and Translational Science, (Academic Press), pp. 91–135.

Cashel, M. (1969). The Control of Ribonucleic Acid Synthesis in Escherichia coli IV. RELEVANCE OF UNUSUAL PHOSPHORYLATED COMPOUNDS FROM AMINO ACID-STARVED STRINGENT STRAINS. J. Biol. Chem. *244*,

3133–3141.

Cashel, M., and Kalbacher, B. (1970). The Control of Ribonucleic Acid Synthesis in Escherichia coli V. CHARACTERIZATION OF A NUCLEOTIDE ASSOCIATED WITH THE STRINGENT RESPONSE. J. Biol. Chem. *245*, 2309–2318.

Cashel, M., and Rudd, K.E. (1987). The stringent response. In Escherichia Coli and Salmonella Typhimurium, (Washington, DC: American Society for Microbiology), pp. 1410–1438.

Celesnik, H., Deana, A., and Belasco, J.G. (2007). Initiation of RNA Decay in Escherichia coli by 5′ Pyrophosphate Removal. Mol. Cell *27*, 79–90.

Chao, Y., Li, L., Girodat, D., Förstner, K.U., Said, N., Corcoran, C., Śmiga, M., Papenfort, K., Reinhardt, R., Wieden, H.-J., et al. (2017). In Vivo Cleavage Map Illuminates the Central Role of RNase E in Coding and Non-coding RNA Pathways. Mol. Cell *65*, 39–51.

Charollais, J., Pflieger, D., Vinh, J., Dreyfus, M., and Iost, I. (2003). The DEAD-box RNA helicase SrmB is involved in the assembly of 50S ribosomal subunits in Escherichia coli. Mol. Microbiol. *48*, 1253–1265.

Charollais, J., Dreyfus, M., and Iost, I. (2004). CsdA, a cold-shock RNA helicase from Escherichia coli, is involved in the biogenesis of 50S ribosomal subunit. Nucleic Acids Res. *32*, 2751–2759.

Chen, S.S., and Williamson, J.R. (2013). Characterization of the Ribosome Biogenesis Landscape in E. coli using Quantitative Mass Spectrometry. J. Mol. Biol. *425*, 767.

Chen, S.S., Sperling, E., Silverman, J.M., Davis, J.H., and Williamson, J.R. (2012). Measuring the dynamics of E. coli ribosome biogenesis using pulse-labeling and quantitative mass spectrometry. Mol. Biosyst. *8*, 3325–3334.

Cheng, Z.-F., and Deutscher, M.P. (2003). Quality control of ribosomal RNA mediated by polynucleotide phosphorylase and RNase R. Proc. Natl. Acad. Sci. *100*, 6388–6393.

Cheng, Z.-F., and Deutscher, M.P. (2005). An Important Role for RNase R in mRNA Decay. Mol. Cell *17*, 313–318.

Chowdhury, N., Kwan, B.W., and Wood, T.K. (2016). Persistence Increases in the Absence of the Alarmone Guanosine Tetraphosphate by Reducing Cell Growth. Sci. Rep. *6*, 20519.

Commichau, F.M., Rothe, F.M., Herzberg, C., Wagner, E., Hellwig, D., Lehnik-Habrink, M., Hammer, E., Völker, U., and Stülke, J. (2009). Novel Activities of Glycolytic Enzymes in Bacillus subtilis: Interactions with essential proteins involved in mRNA processing. Mol. Cell. Proteomics *8*, 1350–1360.

Condon, C. (2009). RNA Processing. In Encyclopedia of Microbiology (Third Edition), M. Schaechter, ed. (Oxford: Academic Press), pp. 395–408.

Condon, C., and Putzer, H. (2002). The phylogenetic distribution of bacterial ribonucleases. Nucleic Acids Res. *30*, 5339–5346.

Condon, C., French, S., Squires, C., and Squires, C. l. (1993). Depletion of functional ribosomal RNA operons in Escherichia coli causes increased expression of the remaining intact copies. EMBO J. *12*, 4305–4315.

Condon, C., Brechemier-Baey, D., Beltchev, B., Grunberg-Manago, M., and Putzer, H. (2001). Identification of the gene encoding the 5S ribosomal RNA maturase in Bacillus subtilis: mature 5S rRNA is dispensable for ribosome function. RNA *7*, 242–253.

Condon, C., Piton, J., and Braun, F. (2018). Distribution of the ribosome associated endonuclease Rae1 and the

potential role of conserved amino acids in codon recognition. RNA Biol. *15*, 683–688.

Condon, C.N., Squires, C., and Squires, C.L. (1995). Control of rRNA Transcription in Escherichia coli. MICROBIOL REV *59*, 23.

Connolly, K., Rife, J.P., and Culver, G. (2008). Mechanistic insight into the ribosome biogenesis functions of the ancient protein KsgA. Mol. Microbiol. *70*, 1062–1075.

Corrigan, R.M., Bowman, L., Willis, A.R., Kaever, V., and Gründling, A. (2015). Cross-talk between Two Nucleotide-signaling Pathways in Staphylococcus aureus. J. Biol. Chem. *290*, 5826–5839.

Corrigan, R.M., Bellows, L.E., Wood, A., and Gründling, A. (2016). ppGpp negatively impacts ribosome assembly affecting growth and antimicrobial tolerance in Gram-positive bacteria. Proc. Natl. Acad. Sci. *113*, E1710–E1719.

Culver, G.M. (2005). Assembly of the 30S ribosomal subunit. Q. Rev. Biophys. *38*, 397.

Dalebroux, Z.D., and Swanson, M.S. (2012). ppGpp: magic beyond RNA polymerase. Nat. Rev. Microbiol. *10*, 203–212.

Dalebroux, Z.D., Svensson, S.L., Gaynor, E.C., and Swanson, M.S. (2010). ppGpp Conjures Bacterial Virulence. Microbiol. Mol. Biol. Rev. *74*, 171–199.

Dammel, C.S., and Noller, H.F. (1995). Suppression of a cold-sensitive mutation in 16S rRNA by overexpression of a novel ribosome-binding factor, RbfA. Genes Dev. *9*, 626–637.

Daou-Chabo, R., Mathy, N., Bénard, L., and Condon, C. (2009). Ribosomes initiating translation of the hbs mRNA protect it from 5′-to-3′ exoribonucleolytic degradation by RNase J1. Mol. Microbiol. *71*, 1538–1550.

Datta, P.P., Wilson, D.N., Kawazoe, M., Swami, N.K., Kaminishi, T., Sharma, M.R., Booth, T.M., Takemoto, C., Fucini, P., Yokoyama, S., et al. (2007). Structural Aspects of RbfA Action during Small Ribosomal Subunit Assembly. Mol. Cell *28*, 434–445.

Davies, B.W., Köhrer, C., Jacob, A.I., Simmons, L.A., Zhu, J., Aleman, L.M., RajBhandary, U.L., and Walker, G.C. (2010). 2--Role of Escherichia coli YbeY, a highly conserved protein, in rRNA processing. Mol. Microbiol. *78*, 506–518.

Davis, J.H., and Williamson, J.R. (2017). Structure and dynamics of bacterial ribosome biogenesis. Phil Trans R Soc B *372*, 20160181.

Davis, J.H., Tan, Y.Z., Carragher, B., Potter, C.S., Lyumkis, D., and Williamson, J.R. (2016). Modular Assembly of the Bacterial Large Ribosomal Subunit. Cell *167*, 1610-1622.e15.

Deana, A., and Belasco, J.G. (2005). Lost in translation: the influence of ribosomes on bacterial mRNA decay. Genes Dev. *19*, 2526–2533.

Deana, A., Celesnik, H., and Belasco, J.G. (2008). The bacterial enzyme RppH triggers messenger RNA degradation by 5′ pyrophosphate removal. Nature *451*, 355–358.

Decatur, W.A., and Fournier, M.J. (2002). rRNA modifications and ribosome function. Trends Biochem. Sci. *27*, 344–351.

Deikus, G., Babitzke, P., and Bechhofer, D.H. (2004). Recycling of a regulatory protein by degradation of the RNA to which it binds. Proc. Natl. Acad. Sci. *101*, 2747–2751.

Delarue, M. (1995). Aminoacyl-tRNA synthetases. Curr. Opin. Struct. Biol. *5*, 48–55.

DeLoughery, A., Lalanne, J.-B., Losick, R., and Li, G.-W. (2018). Maturation of polycistronic mRNAs by the endoribonuclease RNase Y and its associated Y-complex in *Bacillus subtilis*. Proc. Natl. Acad. Sci. *115*, E5585–E5594.

Dennis, P.P., and Bremer, H. (2008). Modulation of Chemical Composition and Other Parameters of the Cell at Different Exponential Growth Rates. EcoSal Plus *3*.

Deutscher, M.P. (2006). Degradation of RNA in bacteria: comparison of mRNA and stable RNA. Nucleic Acids Res. *34*, 659–666.

Deutscher, M.P. (2009). Chapter 9 Maturation and Degradation of Ribosomal RNA in Bacteria. In Progress in Molecular Biology and Translational Science, (Academic Press), pp. 369–391.

Dreyfus, M., and Régnier, P. (2002). The Poly(A) Tail of mRNAs: Bodyguard in Eukaryotes, Scavenger in Bacteria. Cell *111*, 611–613.

Dunn, J.J., and Studier, F.W. (1973). T7 Early RNAs and Escherichia coli Ribosomal RNAs are Cut from Large Precursor RNAs In Vivo by Ribonuclease III. Proc. Natl. Acad. Sci. *70*, 3296–3300.

Durand, S., Gilet, L., Bessières, P., Nicolas, P., and Condon, C. (2012a). Three Essential Ribonucleases — RNase Y, J1, and III — Control the Abundance of a Majority of Bacillus subtilis mRNAs. PLOS Genet. *8*, e1002520.

Durand, S., Gilet, L., and Condon, C. (2012b). The Essential Function of B. subtilis RNase III Is to Silence Foreign Toxin Genes. PLOS Genet. *8*, e1003181.

Dutta, T., and Deutscher, M.P. (2009). Catalytic Properties of RNase BN/RNase Z from Escherichia coli: RNase BN is both an exo- and endoribonuclease. J. Biol. Chem. *284*, 15425–15431.

Dutta, T., and Deutscher, M.P. (2010). Mode of Action of RNase BN/RNase Z on tRNA Precursors: RNase BN DOES NOT REMOVE THE CCA SEQUENCE FROM tRNA. J. Biol. Chem. *285*, 22874–22881.

Duval, M., Simonetti, A., Caldelari, I., and Marzi, S. (2015). Multiple ways to regulate translation initiation in bacteria: Mechanisms, regulatory circuits, dynamics. Biochimie *114*, 18–29.

El Yacoubi, B., Bailly, M., and de Crécy-Lagard, V. (2012). Biosynthesis and Function of Posttranscriptional Modifications of Transfer RNAs. Annu. Rev. Genet. *46*, 69–95.

English, B.P., Hauryliuk, V., Sanamrad, A., Tankov, S., Dekker, N.H., and Elf, J. (2011). Single-molecule investigations of the stringent response machinery in living bacterial cells. Proc. Natl. Acad. Sci. *108*, E365–E373.

Eriani, G., Delarue, M., Poch, O., Gangloff, J., and Moras, D. (1990). Partition of tRNA synthetases into two classes based on mutually exclusive sets of sequence motifs. Nature *347*, 203.

Esquerré, T., Laguerre, S., Turlan, C., Carpousis, A.J., Girbal, L., and Cocaign-Bousquet, M. (2014). Dual role of transcription and transcript stability in the regulation of gene expression in Escherichia coli cells cultured on glucose at different growth rates. Nucleic Acids Res. *42*, 2460–2472.

Evans, D., Marquez, S.M., and Pace, N.R. (2006). RNase P: interface of the RNA and protein worlds. Trends Biochem. Sci. *31*, 333–341.

Feng, B., Mandava, C.S., Guo, Q., Wang, J., Cao, W., Li, N., Zhang, Y., Zhang, Y., Wang, Z., Wu, J., et al. (2014). Structural and Functional Insights into the Mode of Action of a Universally Conserved Obg GTPase. PLOS Biol. *12*, e1001866.

Figaro, S., Durand, S., Gilet, L., Cayet, N., Sachse, M., and Condon, C. (2013). Bacillus subtilis Mutants with Knockouts of the Genes Encoding Ribonucleases RNase Y and RNase J1 Are Viable, with Major Defects in Cell Morphology, Sporulation, and Competence. J. Bacteriol. *195*, 2340–2348.

Fischer, N., Neumann, P., Konevega, A.L., Bock, L.V., Ficner, R., Rodnina, M.V., and Stark, H. (2015). Structure of the E. coli ribosome–EF-Tu complex at <3 Å resolution by Cs-corrected cryo-EM. Nature *520*, 567–570.

Fu, Y., Deiorio-Haggar, K., Anthony, J., and Meyer, M.M. (2013). Most RNAs regulating ribosomal protein biosynthesis in Escherichia coli are narrowly distributed to Gammaproteobacteria. Nucleic Acids Res. *41*, 3491–3503.

Gaal, T., Bartlett, M.S., Ross, W., Jr, C.L.T., and Gourse, R.L. (1997). Transcription Regulation by Initiating NTP Concentration: rRNA Synthesis in Bacteria. *278*, 7.

Gallant, J., Irr, J., and Cashel, M. (1971). The Mechanism of Amino Acid Control of Guanylate and Adenylate Biosynthesis. J. Biol. Chem. *246*, 5812–5816.

Gatewood, M.L., and Jones, G.H. (2010). (p)ppGpp Inhibits Polynucleotide Phosphorylase from Streptomyces but Not from Escherichia coli and Increases the Stability of Bulk mRNA in Streptomyces coelicolor. J. Bacteriol. *192*, 4275–4280.

Gebetsberger, J., and Polacek, N. (2013). Slicing tRNAs to boost functional ncRNA diversity. RNA Biol. *10*, 1798–1806.

Gegenheimer, P., and Apirion, D. (1975). Escherichia coli ribosomal ribonucleic acids are not cut from an intact precursor molecule. J. Biol. Chem. *250*, 2407–2409.

Gendron, N., Putzer, H., and Grunberg-Manago, M. (1994). Expression of both Bacillus subtilis threonyl-tRNA synthetase genes is autogenously regulated. J. Bacteriol. *176*, 486–494.

Gentry, R.C., Childs, J.J., Gevorkyan, J., Gerasimova, Y.V., and Koculi, E. (2016). Time course of large ribosomal subunit assembly in E. coli cells overexpressing a helicase inactive DbpA protein. RNA *22*, 1055–1064.

Germain, E., Castro-Roa, D., Zenkin, N., and Gerdes, K. (2013). Molecular Mechanism of Bacterial Persistence by HipA. Mol. Cell *52*, 248–254.

Giegé, R., and Springer, M. (2016). Aminoacyl-tRNA Synthetases in the Bacterial World. EcoSal Plus *7*.

Giege, R., Sissler, M., and Florentz, C. (1998). Universal rules and idiosyncratic features in tRNA identity. Nucleic Acids Res. *26*, 5017–5035.

Gil, R., Silva, F.J., Peretó, J., and Moya, A. (2004). Determination of the Core of a Minimal Bacterial Gene Set. Microbiol. Mol. Biol. Rev. *68*, 518–537.

Gilet, L., DiChiara, J.M., Figaro, S., Bechhofer, D.H., and Condon, C. (2015). Small stable RNA maturation and turnover in Bacillus subtilis. Mol. Microbiol. *95*, 270–282.

Gobert, A., Gutmann, B., Taschner, A., Gößringer, M., Holzmann, J., Hartmann, R.K., Rossmanith, W., and Giegé, P. (2010). A single Arabidopsis organellar protein has RNase P activity. Nat. Struct. Mol. Biol. *17*, 740–744.

Gößringer, M., and Hartmann, R.K. (2007). Function of heterologous and truncated RNase P proteins in Bacillus subtilis. Mol. Microbiol. *66*, 801–813.

Goto, S., Kato, S., Kimura, T., Muto, A., and Himeno, H. (2011). RsgA releases RbfA from 30S ribosome during a late stage of ribosome biosynthesis. EMBO J. *30*, 104–114.

Gourse, R.L., Chen, A.Y., Gopalkrishnan, S., Sanchez-Vazquez, P., Myers, A., and Ross, W. (2018). Transcriptional Responses to ppGpp and DksA. Annu. Rev. Microbiol. *72*, 163–184.

Gropp, M., Strausz, Y., Gross, M., and Glaser, G. (2001). Regulation of Escherichia coli RelA Requires Oligomerization of the C-Terminal Domain. J. Bacteriol. *183*, 570–579.

Grosjean, H. (2013). Nucleic Acids Are Not Boring Long Polymers of Only Four Types of Nucleotides: A Guided Tour (Landes Bioscience).

Grundy, F.J., and Henkin, T.M. (1993). tRNA as a positive regulator of transcription antitermination in B. subtilis. Cell *74*, 475–482.

Guerrier-Takada, C., Gardiner, K., Marsh, T., Pace, N., and Altman, S. (1983). The RNA moiety of ribonuclease P is the catalytic subunit of the enzyme. Cell *35*, 849–857.

Guillier, M., Allemand, F., Dardel, F., Royer, C.A., Springer, M., and Chiaruttini, C. (2005). Double molecular mimicry in Escherichia coli: binding of ribosomal protein L20 to its two sites in mRNA is similar to its binding to 23S rRNA: Double ribosomal RNA-messenger RNA mimicry in E. coli. Mol. Microbiol. *56*, 1441–1456.

Gutmann, B., Gobert, A., and Giegé, P. (2012). PRORP proteins support RNase P activity in both organelles and the nucleus in Arabidopsis. Genes Dev. *26*, 1022–1027.

Hage, A.E., and Tollervey, D. (2004). A Surfeit of Factors: Why is Ribosome Assembly So Much More Complicated in Eukaryotes than Bacteria? RNA Biol. *1*, 9–14.

Hajnsdorf, E., and Kaberdin, V.R. (2018). RNA polyadenylation and its consequences in prokaryotes. Philos. Trans. R. Soc. B Biol. Sci.

Handke, L.D., Shivers, R.P., and Sonenshein, A.L. (2008). Interaction of Bacillus subtilis CodY with GTP. J. Bacteriol. *190*, 798–806.

Hartmann, R.K., Gößringer, M., Späth, B., Fischer, S., and Marchfelder, A. (2009). Chapter 8 The Making of tRNAs and More – RNase P and tRNase Z. In Progress in Molecular Biology and Translational Science, (Academic Press), pp. 319–368.

Haseltine, W.A., and Block, R. (1973). Synthesis of Guanosine Tetra- and Pentaphosphate Requires the Presence of a Codon-Specific, Uncharged Transfer Ribonucleic Acid in the Acceptor Site of Ribosomes. Proc. Natl. Acad. Sci. *70*, 1564–1568.

Hauryliuk, V., Atkinson, G.C., Murakami, K.S., Tenson, T., and Gerdes, K. (2015). Recent functional insights into the role of (p)ppGpp in bacterial physiology. Nat. Rev. Microbiol. *13*, 298–309.

Heath, R.J., Jackowski, S., and Rock, C.O. (1994). Guanosine tetraphosphate inhibition of fatty acid and phospholipid synthesis in Escherichia coli is relieved by overexpression of glycerol-3-phosphate acyltransferase (plsB). J. Biol. Chem. *269*, 26584–26590.

Henkin, T.M. (2002). Ribosomes, protein synthesis factors, and tRNA synthetases. In Bacillus Subtilis and Its Closest Relatives: From Genes to Cells, (Washington, DC: ASM Press), pp. 313–322.

Herskovitz, M.A., and Bechhofer, D.H. (2000). Endoribonuclease RNase III is essential in Bacillus subtilis. Mol. Microbiol. *38*, 1027–1033.

Holmes, K.L., and Culver, G.M. (2005). Analysis of Conformational Changes in 16S rRNA During the Course of 30S Subunit Assembly. J. Mol. Biol. *354*, 340–357.

Hori, H. (2014). Methylated nucleosides in tRNA and tRNA methyltransferases. Front. Genet. *5*.

Howard, M.J., Lim, W.H., Fierke, C.A., and Koutmos, M. (2012). Mitochondrial ribonuclease P structure provides insight into the evolution of catalytic strategies for precursor-tRNA 5′ processing. Proc. Natl. Acad. Sci. *109*, 16149–16154.

Hue, K.K., and Bechhofer, D.H. (1991). Effect of ermC leader region mutations on induced mRNA stability. J. Bacteriol. *173*, 3732–3740.

Ibba, M., and Söll, D. (2000). Aminoacyl-tRNA Synthesis. Annu. Rev. Biochem. *69*, 617–650.

Inoue, K., Alsina, J., Chen, J., and Inouye, M. (2003). Suppression of defective ribosome assembly in a rbfA deletion mutant by overexpression of Era, an essential GTPase in Escherichia coli. Mol. Microbiol. *48*, 1005–1016.

Iost, I., and Dreyfus, M. (2006). DEAD-box RNA helicases in Escherichia coli. Nucleic Acids Res. *34*, 4189–4197.

Iost, I., and Jain, C. (2019). A DEAD-box protein regulates ribosome assembly through control of ribosomal protein synthesis. Nucleic Acids Res.

Iost, I., Chabas, S., and Darfeuille, F. (2019). Maturation of atypical ribosomal RNA precursors in Helicobacter pylori. Nucleic Acids Res.

Irving, S.E., and Corrigan, R.M. (2018). Triggering the stringent response: signals responsible for activating (p)ppGpp synthesis in bacteria. Microbiology *164*, 268–276.

Ishimura, R., Nagy, G., Dotu, I., Zhou, H., Yang, X.-L., Schimmel, P., Senju, S., Nishimura, Y., Chuang, J.H., and Ackerman, S.L. (2014). Ribosome stalling induced by mutation of a CNS-specific tRNA causes neurodegeneration. Science *345*, 455.

Jacob, A.I., Köhrer, C., Davies, B.W., RajBhandary, U.L., and Walker, G.C. (2013). Conserved Bacterial RNase YbeY Plays Key Roles in 70S Ribosome Quality Control and 16S rRNA Maturation. Mol. Cell *49*, 427–438.

Jiang, X., and Belasco, J.G. (2004). Catalytic activation of multimeric RNase E and RNase G by 5′-monophosphorylated RNA. Proc. Natl. Acad. Sci. *101*, 9211–9216.

Jinks-Robertson, S., Gourse, R.L., and Nomura, M. (1983). Expression of rRNA and tRNA genes in Escherichia coli: Evidence for feedback regulation by products of rRNA operons. Cell *33*, 865–876.

Jomaa, A., Stewart, G., Mears, J.A., Kireeva, I., Brown, E.D., and Ortega, J. (2011). Cryo-electron microscopy structure of the 30S subunit in complex with the YjeQ biogenesis factor. RNA *17*, 2026–2038.

Kalman, M., Murphy, H., and Cashel, M. (1991). rhlB, a new Escherichia coli K-12 gene with an RNA helicase-like protein sequence motif, one of at least five such possible genes in a prokaryote. New Biol. *3*, 886–895.

Kanjee, U., Ogata, K., and Houry, W.A. (2012). Direct binding targets of the stringent response alarmone (p)ppGpp. Mol. Microbiol. *85*, 1029–1043.

Kaplan, R., and Apirion, D. (1975). Decay of ribosomal ribonucleic acid in Escherichia coli cells starved for various nutrients. J. Biol. Chem. *250*, 3174–3178.

Karbstein, K. (2013). Quality control mechanisms during ribosome maturation. Trends Cell Biol. *23*, 242–250.

Katz, A., Elgamal, S., Rajkovic, A., and Ibba, M. (2016). Non-canonical roles of tRNAs and tRNA mimics in bacterial cell biology. Mol. Microbiol. *101*, 545–558.

Khemici, V., Prados, J., Linder, P., and Redder, P. (2015). Decay-Initiating Endoribonucleolytic Cleavage by

RNase Y Is Kept under Tight Control via Sequence Preference and Sub-cellular Localisation. PLOS Genet. *11*, e1005577.

Kim, H.K., Fuchs, G., Wang, S., Wei, W., Zhang, Y., Park, H., Roy-Chaudhuri, B., Li, P., Xu, J., Chu, K., et al. (2017). A transfer-RNA-derived small RNA regulates ribosome biogenesis. Nature.

Kimura, S., and Waldor, M.K. (2019). The RNA degradosome promotes tRNA quality control through clearance of hypomodified tRNA. Proc. Natl. Acad. Sci. *116*, 1394–1403.

Kint, C., Verstraeten, N., Hofkens, J., Fauvart, M., and Michiels, J. (2014). Bacterial Obg proteins: GTPases at the nexus of protein and DNA synthesis. Crit. Rev. Microbiol. *40*, 207–224.

Klappenbach, J.A., Saxman, P.R., Cole, J.R., and Schmidt, T.M. (2001). rrndb: the Ribosomal RNA Operon Copy Number Database. Nucleic Acids Res. *29*, 181–184.

Klemm, B.P., Wu, N., Chen, Y., Liu, X., Kaitany, K.J., Howard, M.J., and Fierke, C.A. (2016). The Diversity of Ribonuclease P: Protein and RNA Catalysts with Analogous Biological Functions. Biomolecules *6*.

Koch, A.L., and Deppe, C.S. (1971). In vivo assay of protein synthesizing capacity of Escherichia coli from slowly growing chemostat cultures. J. Mol. Biol. *55*, 549–562.

Koh, C.S., and Sarin, L.P. (2018). Transfer RNA modification and infection – Implications for pathogenicity and host responses. Biochim. Biophys. Acta BBA - Gene Regul. Mech. *1861*, 419–432.

Komine, Y., Kitabatake, M., YOKOGAWAt, T., NISHIKAWAt, K., and Inokuchi, H. (1994). A tRNA-like structure is present in 10Sa RNA, a small stable RNA from Escherichia coli. Proc Natl Acad Sci USA 5.

Koo, B.-M., Kritikos, G., Farelli, J.D., Todor, H., Tong, K., Kimsey, H., Wapinski, I., Galardini, M., Cabal, A., Peters, J.M., et al. (2017). Construction and Analysis of Two Genome-Scale Deletion Libraries for Bacillus subtilis. Cell Syst. *4*, 291-305.e7.

Korch, S.B., Henderson, T.A., and Hill, T.M. (2003). Characterization of the hipA7 allele of Escherichia coli and evidence that high persistence is governed by (p)ppGpp synthesis: Persistence and (p)ppGpp synthesis in E. coli. Mol. Microbiol. *50*, 1199–1213.

Koslover, D.J., Callaghan, A.J., Marcaida, M.J., Garman, E.F., Martick, M., Scott, W.G., and Luisi, B.F. (2008). The Crystal Structure of the Escherichia coli RNase E Apoprotein and a Mechanism for RNA Degradation. Structure *16*, 1238–1244.

Krásný, L., and Gourse, R.L. (2004). An alternative strategy for bacterial ribosome synthesis: Bacillus subtilis rRNA transcription regulation. EMBO J. *23*, 4473–4483.

Krásný, L., Tišerová, H., Jonák, J., Rejman, D., and Šanderová, H. (2008). The identity of the transcription +1 position is crucial for changes in gene expression in response to amino acid starvation in *Bacillus subtilis*. Mol. Microbiol. *69*, 42–54.

Kriel, A., Bittner, A.N., Kim, S.H., Liu, K., Tehranchi, A.K., Zou, W.Y., Rendon, S., Chen, R., Tu, B.P., and Wang, J.D. (2012). Direct Regulation of GTP Homeostasis by (p)ppGpp: A Critical Component of Viability and Stress Resistance. Mol. Cell *48*, 231–241.

Kriel, A., Brinsmade, S.R., Tse, J.L., Tehranchi, A.K., Bittner, A.N., Sonenshein, A.L., and Wang, J.D. (2014). GTP Dysregulation in Bacillus subtilis Cells Lacking (p)ppGpp Results in Phenotypic Amino Acid Auxotrophy and Failure To Adapt to Nutrient Downshift and Regulate Biosynthesis Genes. J. Bacteriol. *196*, 189–201.

Kumar, P., Kuscu, C., and Dutta, A. (2016). Biogenesis and Function of Transfer RNA-Related Fragments (tRFs). Trends Biochem. Sci. *41*, 679–689.

Kurland, C.G., and Maaløe, O. (1962). Regulation of ribosomal and transfer RNA synthesis. J. Mol. Biol. *4*, 193–210.

Laalami, S., and Putzer, H. (2011). mRNA degradation and maturation in prokaryotes: the global players. Biomol. Concepts *2*, 491–506.

LaCava, J., Houseley, J., Saveanu, C., Petfalski, E., Thompson, E., Jacquier, A., and Tollervey, D. (2005). RNA Degradation by the Exosome Is Promoted by a Nuclear Polyadenylation Complex. Cell *121*, 713–724.

Lalaouna, D., Carrier, M.-C., Semsey, S., Brouard, J.-S., Wang, J., Wade, J.T., and Massé, E. (2015). A 3′ External Transcribed Spacer in a tRNA Transcript Acts as a Sponge for Small RNAs to Prevent Transcriptional Noise. Mol. Cell *58*, 393–405.

Lauber, M.A., Running, W.E., and Reilly, J.P. (2009). B. subtilis Ribosomal Proteins: Structural Homology and Post-Translational Modifications. J. Proteome Res. *8*, 4193–4206.

Lécrivain, A.-L., Rhun, A.L., Renault, T.T., Ahmed-Begrich, R., Hahnke, K., and Charpentier, E. (2018). In vivo 3′-to-5′ exoribonuclease targetomes of Streptococcus pyogenes. Proc. Natl. Acad. Sci. *115*, 11814–11819.

Lee, K., Bernstein, J.A., and Cohen, S.N. (2002). RNase G complementation of rne null mutation identifies functional interrelationships with RNase E in Escherichia coli. Mol. Microbiol. *43*, 1445–1456.

Lee, Y.S., Shibata, Y., Malhotra, A., and Dutta, A. (2009). A novel class of small RNAs: tRNA-derived RNA fragments (tRFs). Genes Dev. *23*, 2639–2649.

Lehnik-Habrink, M., Pförtner, H., Rempeters, L., Pietack, N., Herzberg, C., and Stülke, J. (2010). The RNA degradosome in Bacillus subtilis: identification of CshA as the major RNA helicase in the multiprotein complex. Mol. Microbiol. *77*, 958–971.

Lehnik-Habrink, M., Newman, J., Rothe, F.M., Solovyova, A.S., Rodrigues, C., Herzberg, C., Commichau, F.M., Lewis, R.J., and Stülke, J. (2011). RNase Y in Bacillus subtilis: a Natively Disordered Protein That Is the Functional Equivalent of RNase E from Escherichia coli. J. Bacteriol. *193*, 5431–5441.

Lehnik-Habrink, M., Lewis, R.J., Mäder, U., and Stülke, J. (2012). RNA degradation in Bacillus subtilis: an interplay of essential endo- and exoribonucleases. Mol. Microbiol. *84*, 1005–1017.

Lehnik-Habrink, M., Rempeters, L., Kovacs, A.T., Wrede, C., Baierlein, C., Krebber, H., Kuipers, O.P., and Stulke, J. (2013). DEAD-Box RNA Helicases in Bacillus subtilis Have Multiple Functions and Act Independently from Each Other. J. Bacteriol. *195*, 534–544.

Leipe, D.D., Wolf, Y.I., Koonin, E.V., and Aravind, L. (2002). Classification and evolution of P-loop GTPases and related ATPases11Edited by J. Thornton. J. Mol. Biol. *317*, 41–72.

Leong, V., Kent, M., Jomaa, A., and Ortega, J. (2013). Escherichia coli rimM and yjeQ null strains accumulate immature 30S subunits of similar structure and protein complement. RNA *19*, 789–802.

Li, S.J., and Cronan, J.E. (1993). Growth rate regulation of Escherichia coli acetyl coenzyme A carboxylase, which catalyzes the first committed step of lipid biosynthesis. J. Bacteriol. *175*, 332–340.

Li, Z., and Deutscher, M.P. (1996). Maturation Pathways for E. coli tRNA Precursors: A Random Multienzyme Process In Vivo. Cell *86*, 503–512.

Li, W., Bouveret, E., Zhang, Y., Liu, K., Wang, J.D., and Weisshaar, J.C. (2016). Effects of amino acid starvation on RelA diffusive behavior in live Escherichia coli. Mol. Microbiol. *99*, 571–585.

Li, Z., Pandit, S., and Deutscher, M.P. (1999a). RNase G (CafA protein) and RNase E are both required for the 5′ maturation of 16S ribosomal RNA. EMBO J. *18*, 2878–2885.

Li, Z., Pandit, S., and Deutscher, M.P. (1999b). Maturation of 23S ribosomal RNA requires the exoribonuclease RNase T. RNA *5*, 139–146.

Li, Z., Reimers, S., Pandit, S., and Deutscher, M.P. (2002). RNA quality control: degradation of defective transfer RNA. EMBO J. *21*, 1132–1138.

Liiv, A., Tenson, T., and Remme, J. (1996). Analysis of the Ribosome Large Subunit Assembly and 23 S rRNA Stabilityin Vivo. J. Mol. Biol. *263*, 396–410.

Lindahl, L. (1975). Intermediates and time kinetics of the in vivo assembly of Escherichia coli ribosomes. J. Mol. Biol. *92*, 15–37.

Linder, P., and Jankowsky, E. (2011). From unwinding to clamping — the DEAD box RNA helicase family. Nat. Rev. Mol. Cell Biol. *12*, 505–516.

Linder, P., Lemeille, S., and Redder, P. (2014). Transcriptome-Wide Analyses of 5′-Ends in RNase J Mutants of a Gram-Positive Pathogen Reveal a Role in RNA Maturation, Regulation and Degradation. PLOS Genet. *10*, e1004207.

Liu, M. (2004). Methylation of 23S rRNA nucleotide G745 is a secondary function of the RlmAI methyltransferase. RNA *10*, 1713–1720.

Liu, K., Myers, A.R., Pisithkul, T., Claas, K.R., Satyshur, K.A., Amador-Noguez, D., Keck, J.L., and Wang, J.D. (2015). Molecular Mechanism and Evolution of Guanylate Kinase Regulation by (p)ppGpp. Mol. Cell *57*, 735–749.

Loh, P.C., Morimoto, T., Matsuo, Y., Oshima, T., and Ogasawara, N. (2007). The GTP-binding protein YqeH participates in biogenesis of the 30S ribosome subunit in Bacillus subtilis. Genes Genet. Syst. *82*, 281–289.

Lopez, J.M., Dromerick, A., and Freese, E. (1981). Response of Guanosine 5′-Triphosphate Concentration to Nutritional Changes and Its Significance for Bacillus subtilis Sporulation. J. Bacteriol. *146*, 9.

Lorenz, C., Lünse, C.E., and Mörl, M. (2017). tRNA Modifications: Impact on Structure and Thermal Adaptation. Biomolecules *7*.

Loria, A., and Pan, T. (2000). The 3′ substrate determinants for the catalytic efficiency of the Bacillus subtilis RNase P holoenzyme suggest autolytic processing of the RNase P RNA in vivo. RNA *6*, 1413–1422.

Loveland, A.B., Bah, E., Madireddy, R., Zhang, Y., Brilot, A.F., Grigorieff, N., and Korostelev, A.A. (2016). Ribosome•RelA structures reveal the mechanism of stringent response activation. ELife *5*.

Lu, Q., and Inouye, M. (1998). The gene for 16S rRNA methyltransferase (ksgA) functions as a multicopy suppressor for a cold-sensitive mutant of era, an essential RAS-like GTP-binding protein in Escherichia coli. J. Bacteriol. *180*, 5243–5246.

Luciano, D.J., Vasilyev, N., Richards, J., Serganov, A., and Belasco, J.G. (2018). Importance of a diphosphorylated intermediate for RppH-dependent RNA degradation. RNA Biol. 1–4.

Luidalepp, H., Berger, S., Joss, O., Tenson, T., and Polacek, N. (2016). Ribosome Shut-Down by 16S rRNA

Fragmentation in Stationary-Phase Escherichia coli. J. Mol. Biol. *428*, 2237–2247.

Maciąg, M., Kochanowska, M., Łyżeń, R., Węgrzyn, G., and Szalewska-Pałasz, A. (2010). ppGpp inhibits the activity of Escherichia coli DnaG primase. Plasmid *63*, 61–67.

Mackie, G.A. (1998). Ribonuclease E is a 5J-end-dependent endonuclease. *395*, 6.

Mackie, G.A. (2013). RNase E: at the interface of bacterial RNA processing and decay. Nat. Rev. Microbiol. *11*, 45–57.

Madhugiri, R., and Evguenieva-Hackenberg, E. (2009). RNase J is involved in the 5'-end maturation of 16S rRNA and 23S rRNA in *Sinorhizobium meliloti*. FEBS Lett. *583*, 2339–2342.

Mangat, C.S., and Brown, E.D. (2008). Ribosome biogenesis; the KsgA protein throws a methyl-mediated switch in ribosome assembly. Mol. Microbiol. *70*, 1051–1053.

Marzi, S., Myasnikov, A.G., Serganov, A., Ehresmann, C., Romby, P., Yusupov, M., and Klaholz, B.P. (2007). Structured mRNAs Regulate Translation Initiation by Binding to the Platform of the Ribosome. Cell *130*, 1019–1031.

Mathy, N., Pellegrini, O., Serganov, A., Patel, D.J., Ehresmann, C., and Portier, C. (2004). Specific recognition of rpsO mRNA and 16S rRNA by Escherichia coli ribosomal protein S15 relies on both mimicry and site differentiation. Mol. Microbiol. 15.

Mathy, N., Bénard, L., Pellegrini, O., Daou, R., Wen, T., and Condon, C. (2007). 5'-to-3' Exoribonuclease Activity in Bacteria: Role of RNase J1 in rRNA Maturation and 5' Stability of mRNA. Cell *129*, 681–692.

McCann, K.L., and Baserga, S.J. (2013). Mysterious Ribosomopathies. Science *341*, 849–850.

McClain, W.H., Guerrier-Takada, C., and Altman, S. (1987). Model substrates for an RNA enzyme. Science *238*, 527–530.

Miller, O.L., Hamkalo, B.A., and Thomas, C.A. (1970). Visualization of Bacterial Genes in Action. Science *169*, 392–395.

Mittenhuber, G. (2001). Comparative genomics and evolution of genes encoding bacterial (p)ppGpp synthetases/hydrolases (the Rel, RelA and SpoT proteins). J. Mol. Microbiol. Biotechnol. *3*, 585–600.

Mizusawa, K., Masuda, S., and Ohta, H. (2008). Expression profiling of four RelA/SpoT-like proteins, homologues of bacterial stringent factors, in Arabidopsis thaliana. Planta *228*, 553–562.

Mohan, A., Whyte, S., Wang, X., Nashimoto, M., and Levinger, L. (1999). The 3' end CCA of mature tRNA is an antideterminant for eukaryotic 3'-tRNase. RNA *5*, 245–256.

Mohanty, B.K., and Kushner, S.R. (2000). Polynucleotide phosphorylase functions both as a 3'-5' exonuclease and a poly(A) polymerase in Escherichia coli. Proc. Natl. Acad. Sci. *97*, 11966–11971.

Mohanty, B.K., and Kushner, S.R. (2011). Bacterial/archaeal/organellar polyadenylation: Polyadenylation in bacteria and *Archaea*. Wiley Interdiscip. Rev. RNA *2*, 256–276.

Mohanty, B.K., Maples, V.F., and Kushner, S.R. (2012). Polyadenylation helps regulate functional tRNA levels in Escherichia coli. Nucleic Acids Res. *40*, 4589–4603.

Molle, V., Nakaura, Y., Shivers, R.P., Yamaguchi, H., Losick, R., Fujita, Y., and Sonenshein, A.L. (2003). Additional Targets of the Bacillus subtilis Global Regulator CodY Identified by Chromatin Immunoprecipitation and Genome-Wide Transcript Analysis. J. Bacteriol. *185*, 1911–1922.

Moreau, M., Lee, G.I., Wang, Y., Crane, B.R., and Klessig, D.F. (2008). AtNOS/AtNOA1 Is a Functional *Arabidopsis thaliana* cGTPase and Not a Nitric-oxide Synthase. J. Biol. Chem. *283*, 32957–32967.

Murray, D.K., and Bremer, H. (1996). Control of spoT-dependent ppGpp Synthesis and Degradation in Escherichia coli. J. Mol. Biol. *259*, 41–57.

My, L., Rekoske, B., Lemke, J.J., Viala, J.P., Gourse, R.L., and Bouveret, E. (2013). Transcription of the Escherichia coli Fatty Acid Synthesis Operon fabHDG Is Directly Activated by FadR and Inhibited by ppGpp. J. Bacteriol. *195*, 3784–3795.

Nakamura, A., Koide, Y., Miyazaki, H., Kitamura, A., Masaki, H., Beppu, T., and Uozumi, T. (1992). Gene cloning and characterization of a novel extracellular ribonuclease of Bacillus subtilis. Eur. J. Biochem. *209*, 121–127.

Nanamiya, H., and Kawamura, F. (2010). Towards an Elucidation of the Roles of the Ribosome during Different Growth Phases in *Bacillus subtilis*. Biosci. Biotechnol. Biochem. *74*, 451–461.

Nanamiya, H., Kasai, K., Nozawa, A., Yun, C.-S., Narisawa, T., Murakami, K., Natori, Y., Kawamura, F., and Tozawa, Y. (2008). Identification and functional analysis of novel (p)ppGpp synthetase genes in Bacillus subtilis. Mol. Microbiol. *67*, 291–304.

Nanamiya, H., Sato, M., Masuda, K., Sato, M., Wada, T., Suzuki, S., Natori, Y., Katano, M., Akanuma, G., and Kawamura, F. (2010). Bacillus subtilis mutants harbouring a single copy of the rRNA operon exhibit severe defects in growth and sporulation. Microbiology *156*, 2944–2952.

Narla, A., and Ebert, B.L. (2010). Ribosomopathies: human disorders of ribosome dysfunction. Blood *115*, 3196–3205.

Natori, Y., Tagami, K., Murakami, K., Yoshida, S., Tanigawa, O., Moh, Y., Masuda, K., Wada, T., Suzuki, S., Nanamiya, H., et al. (2009). Transcription Activity of Individual rrn Operons in Bacillus subtilis Mutants Deficient in (p)ppGpp Synthetase Genes, relA, yjbM, and ywaC. J. Bacteriol. *191*, 4555–4561.

Nedialkova, D.D., and Leidel, S.A. (2015). Optimization of Codon Translation Rates via tRNA Modifications Maintains Proteome Integrity. Cell *161*, 1606–1618.

Neidhardt, F.C., Ingraham, J.L., and Schaechter, M. (1994). Physiologie de la cellule bactérienne: une approche moléculaire (Masson).

Nesterchuk, M.V., Sergiev, P.V., and Dontsova, O.A. (2011). Posttranslational Modifications of Ribosomal Proteins in Escherichia coli. Acta Naturae *3*, 12.

Neumann, S., Petfalski, E., Brügger, B., Großhans, H., Wieland, F., Tollervey, D., and Hurt, E. (2003). Formation and nuclear export of tRNA, rRNA and mRNA is regulated by the ubiquitin ligase Rsp5p. EMBO Rep. *4*, 1156–1162.

Nickel, A.I., Wäber, N.B., Gößringer, M., Lechner, M., Linne, U., Toth, U., Rossmanith, W., and Hartmann, R.K. (2017). Minimal and RNA-free RNase P in Aquifex aeolicus. Proc. Natl. Acad. Sci. *114*, 11121–11126.

Nicolas, P., Mader, U., Dervyn, E., Rochat, T., Leduc, A., Pigeonneau, N., Bidnenko, E., Marchadier, E., Hoebeke, M., Aymerich, S., et al. (2012). Condition-Dependent Transcriptome Reveals High-Level Regulatory Architecture in Bacillus subtilis. Science *335*, 1103–1106.

Nierhaus, K.H. (1991). The assembly of prokaryotic ribosomes. Biochimie *73*, 739–755.

Nierhaus, K.H., and Dohme, F. (1974). Total Reconstitution of Functionally Active 50S Ribosomal Subunits from

Escherichia coli. Proc. Natl. Acad. Sci. *71*, 4713–4717.

Nissen, P., Hansen, J., Ban, N., Moore, P.B., and Steitz, T.A. (2000). The Structural Basis of Ribosome Activity in Peptide Bond Synthesis. Science *289*, 920–930.

Nomura, M., Gourse, R., and Baughman, G. (1984). Regulation of the synthesis of ribosomes and ribosomal components. Annu. Rev. Biochem. 45.

Nord, S., Bylund, G.O., Lövgren, J.M., and Wikström, P.M. (2009). The RimP Protein Is Important for Maturation of the 30S Ribosomal Subunit. J. Mol. Biol. *386*, 742–753.

O'Farrell, H.C. (2006). Recognition of a complex substrate by the KsgA/Dim1 family of enzymes has been conserved throughout evolution. RNA *12*, 725–733.

Oussenko, I.A., Sanchez, R., and Bechhofer, D.H. (2004). Bacillus subtilis YhcR, a High-Molecular-Weight, Nonspecific Endonuclease with a Unique Domain Structure. J. Bacteriol. *186*, 5376–5383.

Oussenko, I.A., Abe, T., Ujiie, H., Muto, A., and Bechhofer, D.H. (2005). Participation of 3'-to-5' Exoribonucleases in the Turnover of Bacillus subtilis mRNA. J BACTERIOL *187*, 10.

Pace, B., Stahl, D.A., and Pace, N.R. (1984). The catalytic element of a ribosomal RNA-processing complex. J. Biol. Chem. *259*, 11454–11458.

Pall, M.L. (1985). GTP: A Central Regulator of Cellular Anabolism. In Current Topics in Cellular Regulation, B.L. Horecker, and E.R. Stadtman, eds. (Academic Press), pp. 1–20.

Paul, B.J., Barker, M.M., Ross, W., Schneider, D.A., Webb, C., Foster, J.W., and Gourse, R.L. (2004). DksA: A Critical Component of the Transcription Initiation Machinery that Potentiates the Regulation of rRNA Promoters by ppGpp and the Initiating NTP. Cell *118*, 311–322.

Peck-Millert, K.A., and Altman, S. (1991). Kinetics of the Processing of the Precursor to 4.5 S RNA, a Naturally Occurring Substrate for RNase P from Escherichia coli. J. Mol. Biol. 5.

Pedersen, F.S., and Kjeldgaard, N.O. (1977). Analysis of the relA Gene Product of Escherichia coli. Eur. J. Biochem. *76*, 91–97.

Pellegrini, O., Li de la Sierra-Gallay, I., Piton, J., Gilet, L., and Condon, C. (2012). Activation of tRNA Maturation by Downstream Uracil Residues in B. subtilis. Structure *20*, 1769–1777.

Pesavento, C., and Hengge, R. (2009). Bacterial nucleotide-based second messengers. Curr. Opin. Microbiol. *12*, 170–176.

Pizarro-Cerdá, J., and Tedin, K. (2004). The bacterial signal molecule, ppGpp, regulates Salmonella virulence gene expression: ppGpp regulates Salmonella virulence gene expression. Mol. Microbiol. *52*, 1827–1844.

Podkovyrov, S.M., and Larson, T.J. (1996). Identification of Promoter and Stringent Regulation of Transcription of the fabH, fabD and fabG Genes Encoding Fatty Acid Biosynthetic Enzymes of Escherichia Coli. Nucleic Acids Res. *24*, 1747–1752.

Portier, C., Dondon, L., and Grunberg-Manago, M. (1990). Translational autocontrol of the Escherichia coli ribosomal protein S15. J. Mol. Biol. *211*, 407–414.

Potrykus, K., and Cashel, M. (2008). (p)ppGpp: Still Magical? Annu. Rev. Microbiol. *62*, 35–51.

Potrykus, K., Murphy, H., Philippe, N., and Cashel, M. (2011). ppGpp is the major source of growth rate control in E. coli: ppGpp and growth rate control. Environ. Microbiol. *13*, 563–575.

Proudfoot, N.J., Furger, A., and Dye, M.J. (2002). Integrating mRNA Processing with Transcription. Cell *108*, 501–512.

Proux, F., Dreyfus, M., and Iost, I. (2011). Identification of the sites of action of SrmB, a DEAD-box RNA helicase involved in Escherichia coli ribosome assembly: rRNA mutations that bypass SrmB requirement. Mol. Microbiol. *82*, 300–311.

Pulschen, A.A., Sastre, D.E., Machinandiarena, F., Asis, A.C., Albanesi, D., Mendoza, D. de, and Gueiros-Filho, F.J. (2017). The stringent response plays a key role in Bacillus subtilis survival of fatty acid starvation. Mol. Microbiol. *103*, 698–712.

Putzer, H., Brakhage, A.A., and Grunberg-Manago, M. (1990). Independent genes for two threonyl-tRNA synthetases in Bacillus subtilis. J. Bacteriol. *172*, 4593–4602.

Putzer, H., Laalami, S., Brakhage, A.A., Condon, C., and Grunberg-Manago, M. (1995). Aminoacyl-tRNA synthetase gene regulation in Bacillus subtilis: induction, repression and growth-rate regulation. Mol. Microbiol. *16*, 709–718.

Putzer, H., Condon, C., Brechemier-Baey, D., Brito, R., and Grunberg-Manago, M. (2002). Transfer RNA-mediated antitermination in vitro. Nucleic Acids Res. *30*, 3026–3033.

Py, B., Higgins, C.F., Krisch, H.M., and Carpousis, A.J. (1996). A DEAD-box RNA helicase in the Escherichia coli RNA degradosome. Nature *381*, 169.

Raina, M., and Ibba, M. (2014). tRNAs as regulators of biological processes. Front. Genet. *5*.

Randau, L., Schröder, I., and Söll, D. (2008). Life without RNase P. Nature *453*, 120–123.

Raynal, L.C., Krisch, H.M., and Carpousis, A.J. (1998). The Bacillus subtilis Nucleotidyltransferase Is a tRNA CCA-Adding Enzyme. J. Bacteriol. *180*, 6276–6282.

Razi, A., Britton, R.A., and Ortega, J. (2017a). The impact of recent improvements in cryo-electron microscopy technology on the understanding of bacterial ribosome assembly. Nucleic Acids Res. *45*, 1027–1040.

Razi, A., Guarné, A., and Ortega, J. (2017b). The cryo-EM structure of YjeQ bound to the 30S subunit suggests a fidelity checkpoint function for this protein in ribosome assembly. Proc. Natl. Acad. Sci. *114*, E3396–E3403.

Redder, P., Hausmann, S., Khemici, V., Yasrebi, H., and Linder, P. (2015). Bacterial versatility requires DEAD-box RNA helicases. FEMS Microbiol. Rev. *39*, 392–412.

Redko, Y., and Condon, C. (2009). Ribosomal protein L3 bound to 23S precursor rRNA stimulates its maturation by Mini-III ribonuclease. Mol. Microbiol. *71*, 1145–1154.

Redko, Y., and Condon, C. (2010). Maturation of 23S rRNA in Bacillus subtilis in the Absence of Mini-III. J. Bacteriol. *192*, 356–359.

Redko, Y., Li de la Sierra-Gallay, I., and Condon, C. (2007). When all's zed and done: the structure and function of RNase Z in prokaryotes. Nat. Rev. Microbiol. *5*, 278–286.

Redko, Y., Bechhofer, D.H., and Condon, C. (2008). Mini-III, an unusual member of the RNase III family of enzymes, catalyses 23S ribosomal RNA maturation in B. subtilis. Mol. Microbiol. *68*, 1096–1106.

Reiter, N.J., Osterman, A., Torres-Larios, A., Swinger, K.K., Pan, T., and Mondragón, A. (2010). Structure of a bacterial ribonuclease P holoenzyme in complex with tRNA. Nature *468*, 784–789.

Reuven, N.B., and Deutscher, M.P. (1993). Substitution of the 3' terminal adenosine residue of transfer RNA in

vivo. Proc. Natl. Acad. Sci. U. S. A. *90*, 4350–4353.

Rhaese, H.-J., Dichtelmüller, H., and Grade, R. (1975). Studies on the Control of Development. Eur. J. Biochem. *56*, 385–392.

Richards, J., and Belasco, J.G. (2019). Obstacles to Scanning by RNase E Govern Bacterial mRNA Lifetimes by Hindering Access to Distal Cleavage Sites. Mol. Cell *74*, 284-295.e5.

Richards, J., Liu, Q., Pellegrini, O., Celesnik, H., Yao, S., Bechhofer, D.H., Condon, C., and Belasco, J.G. (2011). An RNA Pyrophosphohydrolase Triggers 5'-Exonucleolytic Degradation of mRNA in Bacillus subtilis. Mol. Cell *43*, 940–949.

Romby, P., Moine, H., Lesage, P., Graffe, M., Dondon, J., Ebel, J.P., Grunberg-Manago, M., Ehresmann, B., Ehresmann, C., and Springer, M. (1990). The relation between catalytic activity and gene regulation in the case of E coli threonyl-tRNA synthetase. Biochimie *72*, 485–494.

Romby, P., Caillet, J., Ebel, C., Sacerdot, C., Graffe, M., Eyermann, F., Brunel, C., Moine, H., Ehresmann, C., Ehresmann, B., et al. (1996). The expression of E.coli threonyl-tRNA synthetase is regulated at the translational level by symmetrical operator-repressor interactions. EMBO J. *15*, 5976–5987.

Ronneau, S., and Hallez, R. (2019). Make and break the alarmone: regulation of (p)ppGpp synthetase/hydrolase enzymes in bacteria. FEMS Microbiol. Rev.

Rosenblum, J.S., Pemberton, L.F., and Blobel, G. (1997). A Nuclear Import Pathway for a Protein Involved in tRNA Maturation. J. Cell Biol. *139*, 1655–1661.

Ross, W., Vrentas, C.E., Sanchez-Vazquez, P., Gaal, T., and Gourse, R.L. (2013). The Magic Spot: A ppGpp Binding Site on E. coli RNA Polymerase Responsible for Regulation of Transcription Initiation. Mol. Cell *50*, 420–429.

Ross, W., Sanchez-Vazquez, P., Chen, A.Y., Lee, J.-H., Burgos, H.L., and Gourse, R.L. (2016). ppGpp Binding to a Site at the RNAP-DksA Interface Accounts for Its Dramatic Effects on Transcription Initiation during the Stringent Response. Mol. Cell *62*, 811–823.

Roy-Chaudhuri, B., Kirthi, N., and Culver, G.M. (2010). Appropriate maturation and folding of 16S rRNA during 30S subunit biogenesis are critical for translational fidelity. Proc. Natl. Acad. Sci. *107*, 4567–4572.

Ryals, J., Little, R., and Bremer, H. (1982). Control of rRNA and tRNA Syntheses in Escherichia coli by Guanosine Tetraphosphate. J BACTERIOL *151*, 8.

Sachla, A.J., and Helmann, J.D. (2019). A bacterial checkpoint protein for ribosome assembly moonlights as an essential metabolite-proofreading enzyme. Nat. Commun. *10*, 1526.

Sarubbi, E., Rudd, K.E., and Cashel, M. (1988). Basal ppGpp level adjustment shown by new spoT mutants affect steady state growth rates and rrnA ribosomal promoter regulation in Escherichia coli. Mol. Gen. Genet. MGG *213*, 214–222.

Sarubbi, E., Rudd, K.E., Xiao, H., Ikehara, K., Kalman, M., and Cashel, M. (1989). Characterization of the spoT gene of Escherichia coli. J. Biol. Chem. *264*, 15074–15082.

Sashital, D.G., Greeman, C.A., Lyumkis, D., Potter, C.S., Carragher, B., and Williamson, J.R. (2014). 11-- A combined quantitative mass spectrometry and electron microscopy analysis of ribosomal 30S subunit assembly in E. coli. ELife *3*, e04491.

Schaechter, M., Maaloe, O., and Kjeldgaard, N.O. (1958). Dependency on medium and temperature of cell size and chemical composition during balanced grown of Salmonella typhimurium. J. Gen. Microbiol. *19*, 592–606.

Schäferkordt, J., and Wagner, R. (2001). Effects of base change mutations within an Escherichia coli ribosomal RNA leader region on rRNA maturation and ribosome formation. Nucleic Acids Res. *29*, 3394–3403.

Schmalisch, M., Langbein, I., and Stülke, J. (2002). The general stress protein Ctc of Bacillus subtilis is a ribosomal protein. J. Mol. Microbiol. Biotechnol. *4*, 495–501.

Seif, E., and Altman, S. (2008). RNase P cleaves the adenine riboswitch and stabilizes pbuE mRNA in Bacillus subtilis. RNA N. Y. N *14*, 1237–1243.

Sergiev, P.V., Golovina, A.Y., Prokhorova, I.V., Sergeeva, O.V., Osterman, I.A., Nesterchuk, M.V., Burakovsky, D.E., Bogdanov, A.A., and Dontsova, O.A. (2011). Modifications of ribosomal RNA: From enzymes to function. In Ribosomes: Structure, Function, and Dynamics, M.V. Rodnina, W. Wintermeyer, and R. Green, eds. (Vienna: Springer Vienna), pp. 97–110.

Seyfzadeh, M., Keener, J., and Nomura, M. (1993). spoT-dependent accumulation of guanosine tetraphosphate in response to fatty acid starvation in Escherichia coli. Proc. Natl. Acad. Sci. *90*, 11004–11008.

Shahbabian, K., Jamalli, A., Zig, L., and Putzer, H. (2009). RNase Y, a novel endoribonuclease, initiates riboswitch turnover in Bacillus subtilis. EMBO J. *28*, 3523–3533.

Shajani, Z., Sykes, M.T., and Williamson, J.R. (2011). Assembly of Bacterial Ribosomes.

Sharma, M.R., Barat, C., Wilson, D.N., Booth, T.M., Kawazoe, M., Hori-Takemoto, C., Shirouzu, M., Yokoyama, S., Fucini, P., and Agrawal, R.K. (2005). Interaction of Era with the 30S Ribosomal Subunit: Implications for 30S Subunit Assembly. Mol. Cell *18*, 319–329.

Shcherbik, N., and Pestov, D.G. (2011). The ubiquitin ligase Rsp5 is required for ribosome stability in Saccharomyces cerevisiae. RNA *17*, 1422–1428.

Sherlock, M.E., Sudarsan, N., and Breaker, R.R. (2018). Riboswitches for the alarmone ppGpp expand the collection of RNA-based signaling systems. Proc. Natl. Acad. Sci. 201720406.

Shetty, S., and Varshney, U. (2016). An evolutionarily conserved element in initiator tRNAs prompts ultimate steps in ribosome maturation. Proc. Natl. Acad. Sci. *113*, E6126–E6134.

Shin, J.-H., and Helmann, J.D. (2016). Molecular logic of the Zur-regulated zinc deprivation response in *Bacillus subtilis*. Nat. Commun. *7*, 12612.

Shoji, S., Dambacher, C.M., Shajani, Z., Williamson, J.R., and Schultz, P.G. (2011). Systematic Chromosomal Deletion of Bacterial Ribosomal Protein Genes. J. Mol. Biol. *413*, 751–761.

Shyp, V., Tankov, S., Ermakov, A., Kudrin, P., English, B.P., Ehrenberg, M., Tenson, T., Elf, J., and Hauryliuk, V. (2012). Positive allosteric feedback regulation of the stringent response enzyme RelA by its product. EMBO Rep. *13*, 835–839.

Sierra-Gallay, I.L. de la, Mathy, N., Pellegrini, O., and Condon, C. (2006). Structure of the ubiquitous 3′ processing enzyme RNase Z bound to transfer RNA. Nat. Struct. Mol. Biol. *13*, 376.

Simonetti, A., Marzi, S., Jenner, L., Myasnikov, A., Romby, P., Yusupova, G., Klaholz, B.P., and Yusupov, M. (2008). A structural view of translation initiation in bacteria. Cell. Mol. Life Sci. *66*, 423.

Slagter-Jäger, J.G., Puzis, L., Gutgsell, N.S., Belfort, M., and Jain, C. (2007). Functional defects in transfer RNAs lead to the accumulation of ribosomal RNA precursors. RNA *13*, 597.

Sonenshein, A.L. (2005). CodY, a global regulator of stationary phase and virulence in Gram-positive bacteria. Curr. Opin. Microbiol. *8*, 203–207.

Springer, M., Plumbridge, J.A., Butler, J.S., Graffe, M., Dondon, J., Mayaux, J.F., Fayat, G., Lestienne, P., Blanquet, S., and Grunberg-Manago, M. (1985). Autogenous control of Escherichia coli threonyl-tRNA synthetase expression in vivo. J. Mol. Biol. *185*, 93–104.

Sprinzl, M., and Richter, D. (1976). Free 3'-OH Group of the Terminal Adenosine of the tRNA Molecule Is Essential for the Synthesis in vitro of Guanosine Tetraphosphate and Pentaphosphate in a Ribosomal System from Escherichia coli.

Sprinzl, M., Horn, C., Brown, M., Ioudovitch, A., and Steinberg, S. (1998). Compilation of tRNA sequences and sequences of tRNA genes. Nucleic Acids Res. *26*, 148–153.

Srivastava, A.K., and Schlessinger, D. (1990). Mechanism and Regulation of Bacterial Ribosomal Rna Processing. Annu. Rev. Microbiol. *44*, 105–129.

Stamminger, G., and Lazzarini, R.A. (1974). Altered metabolism of the guanosine tetraphosphate, ppGpp, in mutants of E. coli. Cell *1*, 85–90.

Steinchen, W., and Bange, G. (2016). The magic dance of the alarmones (p)ppGpp. Mol. Microbiol. *101*, 531–544.

Steinchen, W., Vogt, M.S., Altegoer, F., Giammarinaro, P.I., Horvatek, P., Wolz, C., and Bange, G. (2018). Structural and mechanistic divergence of the small (p)ppGpp synthetases RelP and RelQ. Sci. Rep. *8*, 2195.

Strahl, H., Turlan, C., Khalid, S., Bond, P.J., Kebalo, J.-M., Peyron, P., Poljak, L., Bouvier, M., Hamoen, L., Luisi, B.F., et al. (2015). Membrane Recognition and Dynamics of the RNA Degradosome. PLOS Genet. *11*, e1004961.

Sulthana, S., and Deutscher, M.P. (2013). Multiple Exoribonucleases Catalyze Maturation of the 3' Terminus of 16S rRNA. J. Biol. Chem. jbc.C113.459172.

Sulthana, S., Basturea, G.N., and Deutscher, M.P. (2016). Elucidation of pathways of ribosomal RNA degradation: an essential role for RNase E. RNA *22*, 1163–1171.

Sun, D., Lee, G., Lee, J.H., Kim, H.-Y., Rhee, H.-W., Park, S.-Y., Kim, K.-J., Kim, Y., Kim, B.Y., Hong, J.-I., et al. (2010). A metazoan ortholog of SpoT hydrolyzes ppGpp and functions in starvation responses. Nat. Struct. Mol. Biol. *17*, 1188–1194.

Svenningsen, S.L., Kongstad, M., Stenum, T.S., Muñoz-Gómez, A.J., and Sørensen, M.A. (2017). Transfer RNA is highly unstable during early amino acid starvation in Escherichia coli. Nucleic Acids Res. *45*, 793–804.

Tagami, K., Nanamiya, H., Kazo, Y., Maehashi, M., Suzuki, S., Namba, E., Hoshiya, M., Hanai, R., Tozawa, Y., Morimoto, T., et al. (2012). Expression of a small (p)ppGpp synthetase, YwaC, in the (p)ppGpp(0) mutant of Bacillus subtilis triggers YvyD-dependent dimerization of ribosome. MicrobiologyOpen *1*, 115–134.

Takahashi, K., Kasai, K., and Ochi, K. (2004). Identification of the bacterial alarmone guanosine 5'-diphosphate 3'-diphosphate (ppGpp) in plants. Proc. Natl. Acad. Sci. *101*, 4320–4324.

Talkington, M.W.T., Siuzdak, G., and Williamson, J.R. (2005). An assembly landscape for the 30S ribosomal

subunit. Nature *438*, 628–632.

Thurlow, B., Davis, J.H., Leong, V., F. Moraes, T., Williamson, J.R., and Ortega, J. (2016). Binding properties of YjeQ (RsgA), RbfA, RimM and Era to assembly intermediates of the 30S subunit. Nucleic Acids Res. gkw613.

Tomb, J.-F., White, O., Kerlavage, A.R., Clayton, R.A., Sutton, G.G., Fleischmann, R.D., Ketchum, K.A., Klenk, H.P., Gill, S., Dougherty, B.A., et al. (1997). The complete genome sequence of the gastric pathogen Helicobacter pylori. Nature *388*, 539.

Torres, M. (2001). Ribosomal protein S4 is a transcription factor with properties remarkably similar to NusA, a protein involved in both non-ribosomal and ribosomal RNA antitermination. EMBO J. *20*, 3811–3820.

Tozawa, Y., and Nomura, Y. (2011). Signalling by the global regulatory molecule ppGpp in bacteria and chloroplasts of land plants. Plant Biol. *13*, 699–709.

Tozawa, Y., Nozawa, A., Kanno, T., Narisawa, T., Masuda, S., Kasai, K., and Nanamiya, H. (2007). Calcium-activated (p)ppGpp Synthetase in Chloroplasts of Land Plants. J. Biol. Chem. *282*, 35536–35545.

Traub, P., and Nomura, M. (1968). Structure and function of E. coli ribosomes. V. Reconstitution of functionally active 30S ribosomal particles from RNA and proteins. Proc. Natl. Acad. Sci. U. S. A. *59*, 777–784.

Traxler, M.F., Summers, S.M., Nguyen, H.-T., Zacharia, V.M., Hightower, G.A., Smith, J.T., and Conway, T. (2008). The global, ppGpp-mediated stringent response to amino acid starvation in Escherichia coli. Mol. Microbiol. *68*, 1128–1148.

Trotta, C.R., Miao, F., Arn, E.A., Stevens, S.W., Ho, C.K., Rauhut, R., and Abelson, J.N. (1997). The Yeast tRNA Splicing Endonuclease: A Tetrameric Enzyme with Two Active Site Subunits Homologous to the Archaeal tRNA Endonucleases. Cell *89*, 849–858.

Trubetskoy, D., Proux, F., Allemand, F., Dreyfus, M., and Iost, I. (2009). SrmB, a DEAD-box helicase involved in Escherichia coli ribosome assembly, is specifically targeted to 23S rRNA in vivo. Nucleic Acids Res. *37*, 6540–6549.

Tu, C., Zhou, X., Tropea, J.E., Austin, B.P., Waugh, D.S., Court, D.L., and Ji, X. (2009). Structure of ERA in complex with the 3' end of 16S rRNA: Implications for ribosome biogenesis. Proc. Natl. Acad. Sci. *106*, 14843–14848.

Uicker, W.C., Schaefer, L., Koenigsknecht, M., and Britton, R.A. (2007). The Essential GTPase YqeH Is Required for Proper Ribosome Assembly in Bacillus subtilis. J. Bacteriol. *189*, 2926–2929.

Vercruysse, M., Köhrer, C., Shen, Y., Proulx, S., Ghosal, A., Davies, B.W., RajBhandary, U.L., and Walker, G.C. (2016). Identification of YbeY-Protein Interactions Involved in 16S rRNA Maturation and Stress Regulation in Escherichia coli. MBio *7*, e01785-16.

Vogel, U., and Jensen, K.F. (1995). Effects of the Antiterminator BoxA on Transcription Elongation Kinetics and ppGpp Inhibition of Transcription Elongation in Escherichia coli. J. Biol. Chem. *270*, 18335–18340.

Volta, V., Ceci, M., Emery, B., Bachi, A., Petfalski, E., Tollervey, D., Linder, P., Marchisio, P.C., Piatti, S., and Biffo, S. (2005). Sen34p depletion blocks tRNA splicing in vivo and delays rRNA processing. Biochem. Biophys. Res. Commun. *337*, 89–94.

Wagner, R. (2002). Regulation of ribosomal RNA synthesis in E. coli: effects of the global regulator guanosine tetraphosphate (ppGpp). J. Mol. Microbiol. Biotechnol. *4*, 331–340.

Wang, J.D., Sanders, G.M., and Grossman, A.D. (2007). Nutritional Control of Elongation of DNA Replication by

(p)ppGpp. Cell *128*, 865–875.

Weber, C., Hartig, A., Hartmann, R.K., and Rossmanith, W. (2014). Playing RNase P Evolution: Swapping the RNA Catalyst for a Protein Reveals Functional Uniformity of Highly Divergent Enzyme Forms. PLOS Genet. *10*, e1004506.

Wegscheid, B., Condon, C., and Hartmann, R.K. (2006). Type A and B RNase P RNAs are interchangeable in vivo despite substantial biophysical differences. EMBO Rep.

Weitzmann, C., Tumminia, S.J., Boublik, M., and Ofengand, J. (1991). A paradigm for local conformational control of fucntion in the ribosome: binding of ribosomal protein S19 to Escherichia coli 16S rRNA in the presence of S7 is required for methylation of m 2 G966 and blocks methylation of m 5 C967 by their respective methyltransferases. Nucleic Acids Res. *19*, 7089–7095.

Wen, T., Oussenko, I.A., Pellegrini, O., Bechhofer, D.H., and Condon, C. (2005). Ribonuclease PH plays a major role in the exonucleolytic maturation of CCA-containing tRNA precursors in Bacillus subtilis. Nucleic Acids Res. *33*, 3636–3643.

Wendrich, T.M., and Marahiel, M.A. (1997). Cloning and characterization of a relA / spoT homologue from Bacillus subtilis. Mol. Microbiol. *26*, 65–79.

Wendrich, T.M., Blaha, G., Wilson, D.N., Marahiel, M.A., and Nierhaus, K.H. (2002). Dissection of the Mechanism for the Stringent Factor RelA. Mol. Cell *10*, 779–788.

Willkomm, D.K., and Hartmann, R.K. (2007). An important piece of the RNase P jigsaw solved. Trends Biochem. Sci. *32*, 247–250.

Wilson, D.N., and Nierhaus, K.H. (2007). The Weird and Wonderful World of Bacterial Ribosome Regulation. Crit. Rev. Biochem. Mol. Biol. *42*, 187–219.

Winther, K.S., Roghanian, M., and Gerdes, K. (2018). Activation of the Stringent Response by Loading of RelA-tRNA Complexes at the Ribosomal A-Site. Mol. Cell *70*, 95-105.e4.

Woodson, S.A. (2008). RNA folding and ribosome assembly. Curr. Opin. Chem. Biol. *12*, 667–673.

Yang, X., and Ishiguro, E.E. (2001). Dimerization of the RelA protein of. *79*, 9.

Yoshida, H., and Wada, A. (2014). The 100S ribosome: ribosomal hibernation induced by stress: 100S ribosome. Wiley Interdiscip. Rev. RNA *5*, 723–732.

Zhang, Y., Zborníková, E., Rejman, D., and Gerdes, K. (2018). Novel (p)ppGpp Binding and Metabolizing Proteins ofEscherichia coli. MBio *9*.

Zundel, M.A., Basturea, G.N., and Deutscher, M.P. (2009). Initiation of ribosome degradation during starvation in Escherichia coli. RNA *15*, 977–983.

Zuo, Y., and Deutscher, M.P. (2001). Exoribonuclease superfamilies: structural analysis and phylogenetic distribution. Nucleic Acids Res. *29*, 1017–1026.

Zyskind, J.W., and Smith, D.W. (1992). DNA replication, the bacterial cell cycle, and cell growth. Cell *69*, 5–8.